University of Huddersfield Repository

Waterworth, Adelle

Quantitative characterisation of surface finishes on stainless steel sheet using 3D surface topography analysis

Original Citation

Waterworth, Adelle (2006) Quantitative characterisation of surface finishes on stainless steel sheet using 3D surface topography analysis. Doctoral thesis, University of Huddersfield.

This version is available at http://eprints.hud.ac.uk/id/eprint/385/

QUANTITATIVE CHARACTERISATION OF SURFACE FINISHES ON STAINLESS STEEL SHEET USING 3D SURFACE TOPOGRAPHY ANALYSIS

ADELLE WATERWORTH

A thesis submitted to the University of Huddersfield
in partial fulfilment of the requirements for
the degree of Doctor of Philosophy

May 2006

Abstract

The main aim of this project was to quantitatively characterise the developed surface topography of finishes on stainless steel sheet using three-dimensional surface analysis techniques.

At present surface topography is measured using (mainly) stylus profilometry and analysed with 2D parameters, such as R_a, R_q and R_z. These 2D measurements are not only unreliable due to a lack of standardised measurement methodology, but are also difficult to relate directly to the actual shape of the topography in 3 dimensions. They bear little direct relation to the functional properties of the surface of stainless steel, making them less useful than their 3D counterparts.

Initially it is crucial to ensure that the surface topography data collected is correct, accurate and relevant, by defining a measurement strategy. Models of the surface topography are developed encompassing the usual features of the topography and variations in the topography caused by production or 'defects'. The functional features are discussed and predicted relevant parameters are presented.

The protocol covers the selection of the correct measuring instrument based on the surface model and the size of the relevant functional features so that the desired lateral and vertical resolution and range is achievable. Measurement data is then analysed using Fast Fourier Transforms (FFTs) to separate the different frequencies within the spatial frequencies detected on the surface. The frequency of the important features shows up dominantly on a Power Spectral Density (PSD) plot and this is used to find the correct sampling interval to accurately reconstruct the 3D surface data. The correct instrument for further measurements is then selected using a Steadman diagram. Operational details of the measuring instruments available for this project are given and variables for these instruments are discussed. Finally, measurement method recommendations are made for each of the four finishes modelled.

Based on this surface characterisation an attempt is made to identify the 3D parameters that give a quantitative description of common stainless steel sheet finishes with respect to some aspects of their production and functional performance.

An investigation of the differences in manufacturing processes, gauge and grade of material is presented, providing an insight into the effect on topography of such divergences. The standardised 3D parameter set is examined to determine its sensitivity to common variations in the topography of the 2B finish and therefore their potential relevance.

A new data separation technique of the material probability curve for use on the 3D datasets establishes a cut-off (transition point) between the two main functionally relevant features of the 2B surface (plateaus and valleys) by finding the intersection of the asymptotes of a fitted conic section, giving a non subjective methodology to establish the section height. The standardised 3D parameters are then used on the separated data, with the aim of being more functionally relevant to the main surface studied.

Functional tests to rate capability of these parameters in the areas of optical appearance, lubricant retention and corrosion are carried out and the appropriate topography parameters are related to their performance.

Acknowledgements

Contents

List of figures

ix

xiii

List of tables

"Nothing exists until it is measured"

"An expert is a person who has made all the mistakes that can be made in a very narrow field"

Niels Henrik David Bohr
Physicist and Nobel Laureate

Chapter 1   Introduction

1.1. Introduction

As the usage of stainless steel increases there is a demand for better and improved variations, including different surface finishes which are optimised for service performance, for example appearance, cleansibility or lubricant retention and this has led to the introduction of a range of finishes (see table 2.1). Also, with the development of manufacturing routes, the surface characteristics of the product 'off the mill' may change and it is to be expected that variations in the processing history will influence both the appearance and the properties of the established finishes. These finishes are not normally subject to any quantitative specification, except possibly comments on relative 'dullness'. However, it is now accepted that the nature of the topography of a surface can have a significant influence on the efficiency and functional performance of the surface [1].

In virtually all applications it is becoming more important to reduce the variations in the topography of the common finishes, for example consistency of appearance for architecture applications where large areas of material are used. Sheet is usually formed into products using drawing and/or bending techniques (it is also employed as the most frequent starting point for a range of other surfaces either developed within the process route, i.e. roll patterning or coil polishing, or during and after fabrication as a result of shot and bead blasting, directional or non-directional mechanical polishing or electrochemical polishing). For many applications it is important that a specific surface finish is produced consistently and it would be advantageous to have a means of specifying and checking the surface properties by selecting parameters that are relevant to the end functions.

Since the growth and improvement of digital computers there have been significant changes in the way in which surfaces can be measured and viewed. Recently there have been attempts to standardise the numerous parameters that can be obtained from the various surface measurement methods and the procedures for their derivation are also the subject of standardisation.

1.2. Overall Aims and Objectives

1.2.1   Aims

The overall aim of this research project is to characterise quantitatively the developed surface topography of some widely used finishes on stainless steel sheet using three-dimensional surface analysis techniques. Based on this surface characterisation an attempt has been made to identify 3D parameters for quantitative description of stainless steel sheet with respect to some aspects of their functional performance.

1.2.2 Objectives

- Using the 3D techniques available, define a measurement strategy and protocol to effectively measure stainless steel sheet topography.
- Investigate the differences in topography across a range of grades and gauges of stainless steel using 3D topography parameters.
- Investigate the ability of 3D topography parameters to correlate with functional requirements of lubricant retention, optical appearance and corrosion.
- Develop a set of written procedures for industrial application to effectively characterise stainless steel sheet surface roughness.

1.3. Thesis Layout

1.3.1 Chapter 3 The 'Functional' Surfaces

The functional topographical features of four finishes are determined, with respect to the process/es by which they were made. A model of the surface topography is developed for WHB (white hot band), 2B, BA (bright annealed) and a unidirectional finish (brushed) encompassing the usual features of the topography and variations in the topography caused by production or 'defects'. The functional features are discussed and predicted relevant parameters are presented.

1.3.2 Chapter 4 Measurement Strategy

The measurement strategy has been designed to ensure correct, accurate and relevant collection of topography data. Feature identification is carried out based on the surface model and the average sizes of the features are found. The protocol covers the selection of the correct measuring instrument based on the surface model and the size of the relevant functional features. Operational details of the measuring instruments available for this project are given (Somicronic stylus instrument, Taylor Hobson Talysurf stylus instrument, Wyko NT2000 optical interferometer and DME AFM) and variables for these instruments are discussed. The strategy includes a statistical method of assessing how many measurements are needed for a surface, which is presented for the 2B finish. Finally, measurement method recommendations are made for each of the four finishes modelled in chapter 3.

1.3.3   Chapter 5 The Effects of Variations in Production

There is inherent variability in the surface topography produced due to differing process stages and grade of material. The desired thickness determines the number of passes through the rolling mill and the final finishing operation can be either skin-passing or tension levelling (this is source dependant, either Source 1 or 2, respectively). Results of the initial study into the topographical effect of variations in thickness, grade and source are presented and discussed.

1.3.4   Chapter 6 Optical Appearance

The available instrumentation is discussed and sample variation with respect to appearance is considered. The effect of rolling direction to appearance measurement direction, angle of appearance measurement and sample grade variation is studied and initial measurement trials are completed to assess the general optical properties of the 2B finish with regard to other finishes. The relationship of four optical descriptors to 3D topography parameters is presented and discussed.
Particular attention is paid to the 2B finish, being the principal product of Outukumpu, and a new method of analysing the data to separate the important features of the topography is developed.

1.3.5   Chapter 7 Lubricant Retention

A simplified method (based on drip tests) to assess the lubricant retention properties of topography is offered. The development of the technique includes proof of the equipment resolution and approach suitability for testing the 2B finish. Results are presented to show the relationship of 3D topography parameters to the ability of a surface to retain oil.

1.3.6   Chapter 8 Corrosion

In collaboration with Birmingham University several hand-polished unidirectional finishes and brushed production finishes were assessed and rated on their corrosion resistance. A new method was developed at Birmingham University, allowing faster evaluation than existing standard salt spray tests. Surface measurements were made in an effort to find the potential connection between certain surface characteristics and the susceptibility of a surface to pitting corrosion and the findings are presented and discussed.

1.3.7 Chapter 9 Summary of Discussions

A summary of the discussions from each chapter is given as a brief guide to the findings of the project. Comprehensive assessment of the 2B finish on stainless steel sheets is outlined. The overall significance of the results is discussed.

1.3.8 Chapter 10 Conclusion

A summary of the conclusions from each chapter is given and a set of 3D parameters for the characterisation of the 2B stainless steel finish is suggested. Conclusions are drawn, the perceived contributions to knowledge are identified and suggestions for further work made.

Chapter 2   Literature Survey

2.1. Summary of the Chapter

Initially the production of stainless steel is considered, with particular attention given to the effect of process stage on the development of surface topography. Common applications of stainless steels are discussed and the functional implications of their surface topographical characteristics are considered. (The work is set into context with work carried out to assess the behaviour of various surfaces in the areas of tribology, optical appearance and corrosion.)

A detailed review of surface topography measurement is presented with emphasis on 3D instrumentation capabilities. Popular data filtering techniques are considered prior to the discussion of the conventional methods of characterisation. Numerical methods such as parameterisation are presented alongside some of the new surface or application specific methods. The concepts involved in sampling theory are introduced to aid in the measurement protocol developed for stainless steel.

2.2. Stainless Steel

2.2.1   History

Harry Brearley made the first commercial cast of stainless steel in Sheffield in 1913. He was experimenting with alloys to produce steel for rifle barrels, which would not erode. He produced steel with 12.68% chromium and 0.24% carbon which, when he attempted to etch the surface with acid for inspection, was not affected. He had a local cutler make some knives using the new material that were not corroded by water or mild acids in food. These first stainless steels were difficult to work but they initiated the addition of a high content of chromium to promote corrosion resistance properties in steel.

Nowadays, stainless steel is categorised as having at least 10.5% chromium, although there are many other alloying agents used to enhance different properties of the material. The chromium in the steel combines with oxygen in the air to produce a thin, transparent, chrome-rich oxide on the surface, resisting oxidative corrosion. If this passive film is broken (by scratching) the layer will quickly reform and recover the exposed surface, as long as there is a supply of oxygen to it. Variances in the passive film are not detectable by topographical methods.

2.2.2   Composition/Grades

There are four main types of stainless steel, ferritic, martensitic, austenitic and duplex, each have different microstructures depending on their predominant metallurgical phase. The austenitic and ferritic steels account for approximately 95% of stainless steel production (70% austenitic, 25% ferritic [2]).

Martensitic stainless steels were the first to be developed for commercial use, as cutlery, and have a comparatively high carbon content of 0.1 – 1.2% with 12 – 18% chromium. They are used where high strength or hardness is required, as they can be heat treated to enhance these properties. They are magnetic but are, however difficult to weld and possess only moderate corrosion resistance compared to other types. Typical uses are knife blades, surgical instruments, pins and spindles and stressed engineering components. Heavily tempered, low carbon steels are used for oil and gas pipelines and for service at elevated temperatures.

An austenitic crystal structure is formed when sufficient amounts of austenite stabilising alloys such as nickel are added to the steel. By far the most common grades of stainless steel are austenitic steels, with basic compositions of around 18% chromium and 8% nickel. Austenitic stainless steels find widespread use for their excellent corrosion resistance, weldability and formability. They possess good strength properties at both high and especially low temperatures, are easy to clean and are therefore hygienic. Austenitic steels are non magnetic and can only be hardened by cold working. As the most commonly used type of stainless steel many applications are evident, in architecture, food and chemical processing, computer parts and most obviously kitchen sinks.

Ferritic stainless steels are low carbon stainless steels with 12 to 18% chromium. The corrosion resistance is dependant on the chromium content, with good resistance at 18%. Their formability is good, but not as good as the austenitic grades and weldability is poor. Ferritics are magnetic but hardening by heat treatment is not possible. Typical uses include automotive trim and exhausts and hot water tanks.

The nickel content of duplex stainless steels is balanced to give equal formation of ferrite and austenite in the final structure. They generally contain a relatively high amount of chromium, between 18 and 28% and have a moderate content of nickel, in the range 4.5 to 8%. Most duplex stainless steels also contain 2.5 to 4% molybdenum, which increases the corrosion resistance, especially to chloride ion attack. They also have superior resistance to stress corrosion cracking and a higher tensile and yield strength than both austenitic and ferritic grades (around twice as strong).

2.2.3   Stainless Steel Production (Figure 2.1)

The production of stainless steel begins in most cases with melting a charge of high-grade scrap steel and ferro alloys in an electric arc furnace. The molten metal is then tapped into a transfer ladle, where any slag is taken out. The contents of the ladle are then poured into a refining vessel (an argon/oxygen decarburisation vessel or AOD) where argon and oxygen are blown through the mix to greatly reduce the carbon level in the material before being further refined in a ladle arc furnace. Additional alloys are added here and the final correct chemical composition for the material is achieved. The molten metal is passed to a continuous caster, where it is solidified as it travels through the machine and cut into slabs or bloom. For sheet production slabs 1200 – 2000 mm wide are hot rolled, on a Steckel or 4-high mill, from around 200 mm thickness to coil of about 5 – 10 mm thickness. The hot rolled, coiled material is

annealed and descaled to produce 'white hot band', which is the starting point for most coil and sheet production.

The hot band coils are then softened through gas fired furnaces. After cooling in air, the outer scale is loosened via a process of fine shot blasting. The majority of the scale is then removed using a neutral electrolyte process.

Since many stainless steel products are made from thinner gauge material the hot band undergoes further reduction by cold rolling, usually in a Sendzimir mill (or 'Z' mill) which is capable of large reductions. This reduces the gauge and improves the strip geometry and surface finish.

For all of the designations there are two ways of achieving final gauge. Material can be 'single cycle' rolled, where the material is rolled close to its intended final gauge from hot band before being annealed, descaled and skin-passed or 'double cycle' rolled, for thinner products. This involves more than one cold rolling operation, where hot band is rolled, removed for intermediate annealing and descaling (to alleviate work hardening) and rolled for a second time (sometimes three cycles are required) to its final gauge before final annealing, descaling and skin-passing.
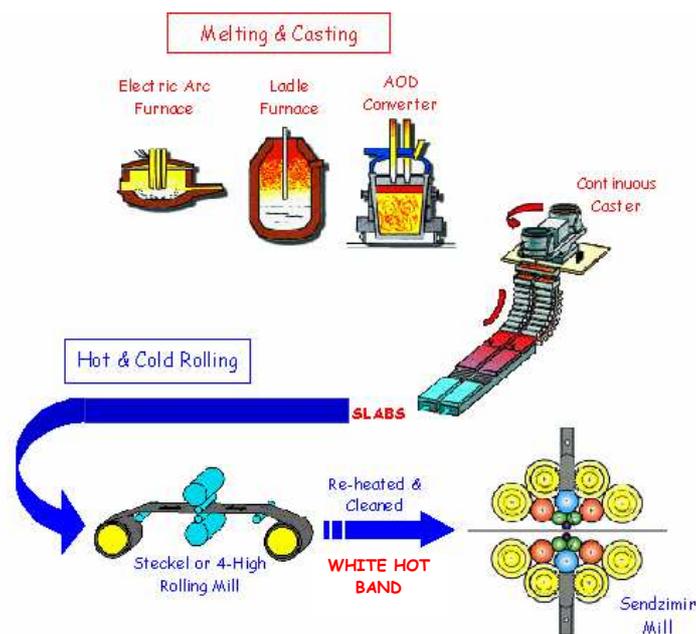
Figure 2.1: Stainless steel manufacturing process diagram to cold rolled strip stage

2.2.3.1   Production of Mill Finishes (Figure 2.2)

The cold rolled coil for a 2D or 2B finish from the Sendzimir mill is re-annealed (or softened) during which high temperature oxide film is produced on the surface. This second softening stage is required because when the stainless steel is rolled on the Sendzimir mill it becomes work hardened. If it were to be further rolled or be subject to a forming process, large forces would be required and the material may crack and fracture. Annealing the sheet produces a softer microstructure by the process of recovery and effectively brings some new undeformed

grains to the surface (recrystalisation). The nature of the annealing conditions influence the type of scale formed. If it is in an oxidising atmosphere or if the strip is cooled in air (as it is for white hot band, 2D and 2B finishes) a combination of mechanical scale loosening, for example shot blasting, and surface chemical or electrochemical attack is used.

Final eradication of the scale from cold rolled strip is achieved in an agitated acid bath, where the material is fed slowly through to ensure total cleansing. As this is accomplished the acid also has an increased effect on the grains of material at or near the surface. The selective chemical attack at the grain boundaries occurs because they are relatively high-energy sites in the crystal lattice.

The final control of shape and finish is performed in two ways. The material can be fed through a skin pass mill, which is a light but high-speed pass. It is not meant to greatly reduce the thickness of the sheet as this would again lead to a work hardened material, making the sheet unsuitable for further processing (i.e. drawing, bending and other forming). Coils may also be put through a tension levelling device, where the coil is lightly stretched, achieving similar results.

The 2R finish is developed by annealing the cold rolled material from the Sendzimir mill in a controlled, protective atmosphere of hydrogen and nitrogen, referred to as bright annealing. In this process the final oxide film is thin and protective so no further descaling treatment is required.
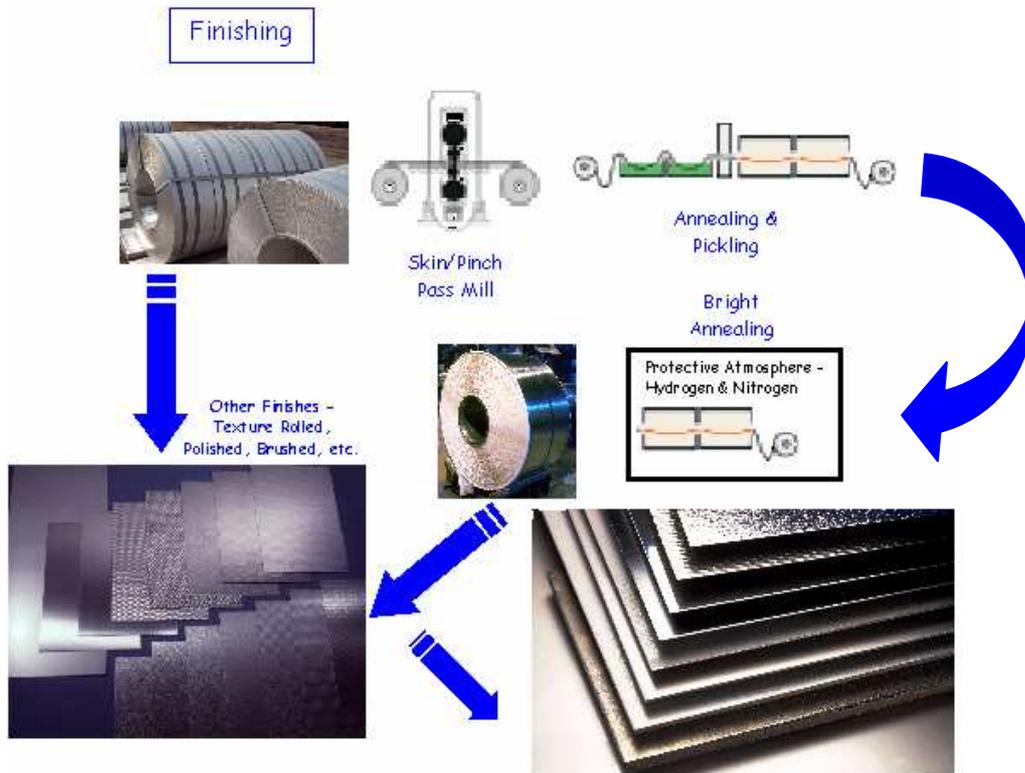
Figure 2.2: Stainless steel manufacturing process diagram to finishing stage

2.2.4 Surface Finish

2.2.4.1 Designation

The range of steel surface finishes encompassed by the designations 2D, 2B and 2R account for the greater part, by surface area, of stainless steel flat products. The definitions of these terms can be seen in table 2.1, adapted for use from BSEN 10088-2:1995 [3], with associated process routes.

Table 2.1: Definitions of designated finishes [3]

	Finish Name	Process route	Finish
Mill finishes	2D	Cold rolled, annealed and pickled	Matt with low reflectivity
	2B	Cold rolled, annealed, pickled, skin passed (or tension levelled)	Smooth but 'dull', pearly grey
	2R (Bright Annealed)	Cold rolled, bright annealed	Smooth and shiny
Derived finishes	Brushed	2B or 2R base finish with unidirectional brushing	Unidirectional, medium reflectivity
	Polished	2B or 2R base finish with unidirectional polishing	Sometimes called satin look, more glossy than brushed
	Peened	A 2B or 2R finish is peened with glass bead providing a hardened surface, which makes visible the annealing process to which the base metal was subject to in the manufacturing process.	The appearance is quite unusual
	Texture rolled	2B or 2R base finish is embossed with repetitive patterns stamped onto metal sheets.	Dependant on pattern
	Abraded	Base finish can be abraded using various materials and methods	Dependant on abrasive and method used

2.2.4.2 Applications

The finishes that are applied to stainless steel sheet have a number of functions, figure 2.3. The most obvious use of particular finishes is aesthetics. The popularity of stainless steel kitchen

appliances did not originate with its pleasing appearance, however, but from its resistance to food acid corrosion and its hygienic quality.

The corrosion resistant properties are inherent for stainless steel due to it self-repairing passive layer (figure 2.4) and the elimination of the need for coating or painting means no pits or scratches in the applied surface which would promote bacteria build-up. The 'mirror' finish was popular as it is very easy to clean; although more matt and brushed finishes are becoming increasingly desirable in the home because of the 'fingerprinting' nature of the smoother finish (the oil marks left by fingertips are far more visible on the mirror finish [4]). In the food and drink production industry much of the processing equipment is made from stainless steel, which has the additional benefit of ease of cleaning and does not impart any taste to the products.
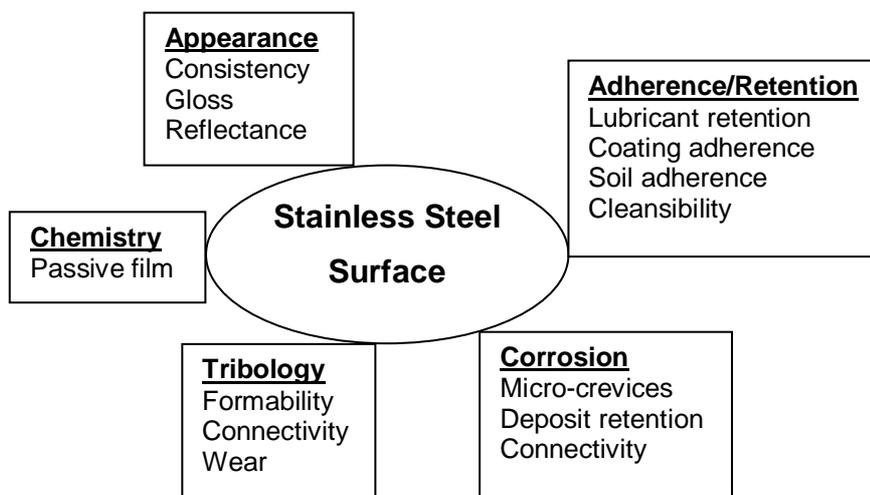
Figure 2.3: Common 'surface dependant' functions for stainless steel

The corrosion resistance and ease of cleaning also make stainless steel an excellent choice for public amenities like litterbins, ticket machines and lamp posts. Most grades are suitable for long-term outdoor use and combine good life-cycle costs with low maintenance costs, as dirt and graffiti can be washed off with water.
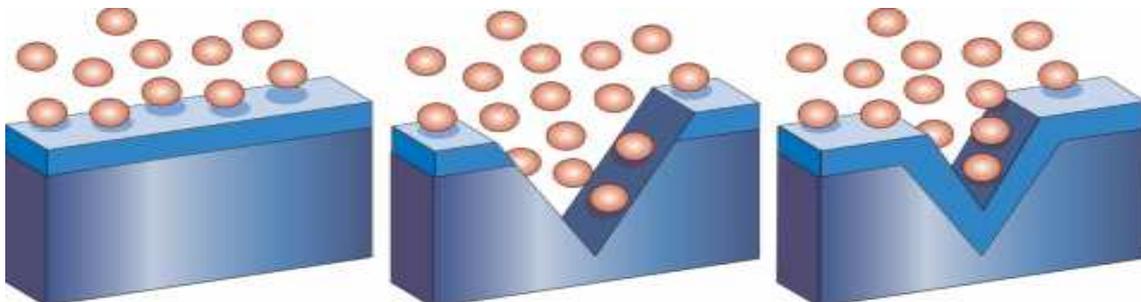
Figure 2.4: Self repairing passive layer on stainless steel [5]

Architecture is a growing market for stainless steel, in terms of surface finishes, for building cladding and in smaller amounts for things like lift interiors, doors and handrails. The mirror

finish is used for highly decorative effects, where as large areas are normally covered with the more matt or brushed finishes. A building clad in stainless steel would require great uniformity from the smooth mirror finish (which would disappear at certain aspects in sunlight), so it is more usual to see mill rolled, brushed, peened or texture pressed finishes where large areas are to be covered. Colours such as bronze effect and deep blues can be applied to the sheet prior to forming giving even more versatility.

The 2B finish is very popular in industrial applications, or when an 'industrial look' is desired and 2B and 2R are normally the raw material for further 'finishing' lines.

2.2.4.3   Origin of Micro-scale Surface Features in Mill Finishes

The surface finish of the final product depends on a number of factors within its process route, predominantly the final stages. The topography produced in the final stages is examined more closely in the determination of the surface features that are to be measured for the purpose of characterisation; this is carried out in further detail in chapters 3 and 4.

There is inherent variability in the surface topography produced due to differing process stages, grade of material and one-off variations known as 'defects'. Different process stages for the 2B finish occur in cold rolling, where the desired thickness determines the number of passes through the rolling mill and the final finishing operation can be either skin-passing or tension levelling, see figure 2.5 (this is source dependant, either Source 1 or 2, respectively). Other stages of the process route can produce discrepancies, like the 'greying' effect of over pickling or a general streaky appearance may be evident where variation existed in the white hot band. Variations due to the grade arise because of the individual properties of the materials and therefore slightly different reactions to the same processing operations. When all of these variables are the same, inconsistencies in the final finish can still occur. Roll imprints may be seen as a result of roll wear or lubrication problems and other faults such as scratching may be visible.
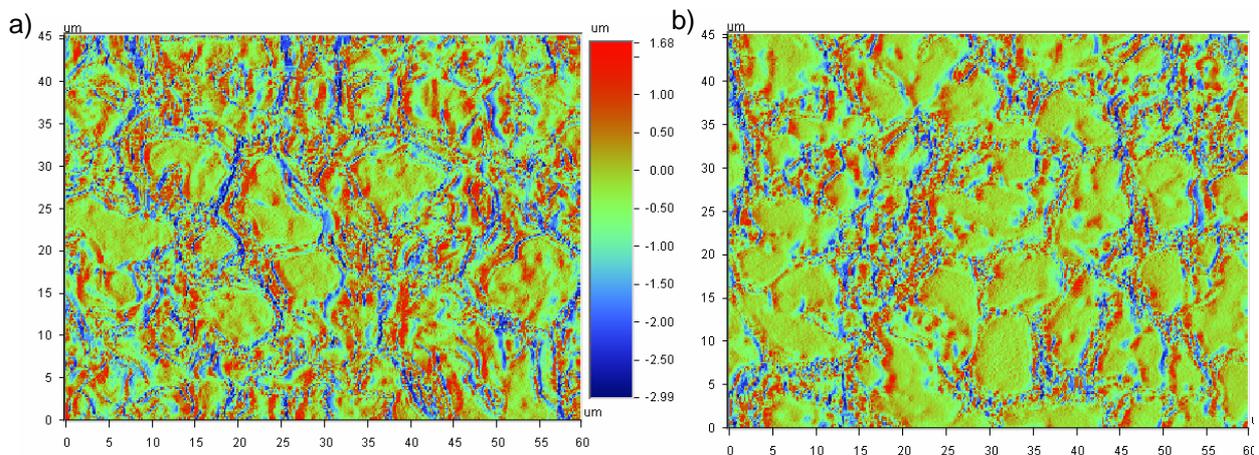
Figure 2.5: The effects of differing processes: Interferometer images of

a) skin passed 2B (Source 1) and

b) tension levelled 2B (Source 2)

2.3. Functional Surfaces

2.3.1   Introduction

A surface can be either functional or non-functional. Functional surfaces are those where the properties of the surface influence the performance of the component. A control loop was suggested by Stout & Davis [6], figure 2.6, showing the interdependence between the required functional behaviour of the surface, the manufacturing of it and the characterisation of its topography.

So if the function requires the surface to react in a certain manner the surface characteristics can be specified and a suitable manufacturing process chosen. This theory also works in the reverse direction; if a surface is manufactured by a particular process then given the necessary conditions the behaviour of the material may be predicted and controlled. Understanding the relationship between the surface features and component application can optimise the quality of functional surfaces.

Manufacturing

Characterisation

59.9

45.6 um
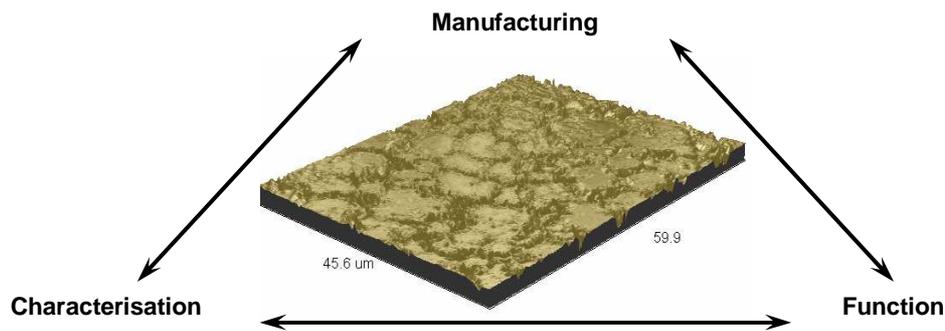
Function

Figure 2.6: Control loop showing interdependence between manufacture, characterisation and function [original from 6]

Surface interactions are affected by various properties and all must be considered for a full characterisation covering all functional aspects. The chemical composition of a surface affects such aspects as resistance to corrosion and chemical or biological adhesion. Residual stresses and other mechanical properties like hardness can affect the ability of a surface to deform in further forming or rolling operations. When all of these properties are stable the micro-scale surface topography of a surface can have an effect on appearance, lubricant retention (which is important for forming behaviour) and corrosion resistance. This project deals with the micro-scale surface topography in relation to functional aspects of stainless steel, as it is relatively easy to measure non-destructively, producing an ideal measurand.

2.3.2   Influence of Micro-topography

2.3.2.1   Effect of Micro-topography on Functionality

The understanding of the relationship between steel sheet topography and function is a vital part of product and process improvement. The way in which the surface topography of a component affects its ability to perform differs depending on the desired function. The major areas of previous study into metal surfaces have fallen into two categories; tribological concerns and appearance. Further separations within these main groups are possible, as seen in table 2.2, along with links where dual functions have been studied.

Table 2.2: Main areas of past research

Tribology	Appearance
Formability	Coatings
Wear	Painting
Surface wetting/Lubricant retention	Gloss
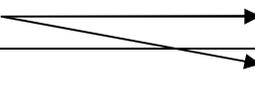
It has long been known that 'the smoother the better' approach to wear and sealing properties is not necessarily true. It has been found by many researchers [7, 8, and 9] that some surface roughness is desirable when using liquid lubricants, where valleys on the surface retain oil in the contact region. A certain roughness on auto body panels, for painting, is also required for the paint to adhere to the surface, although there is still optimisation work to find the best finish for final paint appearance, adherence of paint and amount of paint used [10].

In terms of stainless steel the grade chosen is obviously very important to achieve corrosion resistance in certain environments. Since the highly resistant grades are more costly initially, research into methods of improving the corrosion resistance of the standard grades, such as special surface finishes, better component design and cleaning regimes has become more crucial. In the past it was believed that smoother surfaces had better corrosion resistance, as they do not 'trap' contaminants and if outdoors are more easily 'cleaned' by rainwater. This may be true to some extent, although recent work has studied the effects of processing to final product design on corrosion resistance [11].

The effect of topography on the functionality of stainless steel surfaces in this project will be confined to three areas; appearance, lubricant retention and corrosion resistance. Further discussion of past research in these specific areas is given in the relevant sections of this chapter, 2.3.3 Optical Appearance, 2.3.4 Tribology and 2.3.5 Corrosion Resistance.

2.3.2.2   Effect of Production on Topography

The cause of failure of a work piece can be due to many factors and since scrapping components is not economical, the source should be identified with a view to elimination. Surface texture is the fingerprint of manufacture [6] and as such can be used as a control for production purposes. Changes in the process, whether they be intentional or not, effect the final finish of a component and if the features of surface topography can be traced to the point in the process where they were created the effect can be either controlled (for the engineering of surfaces for a specific function) or eliminated (for defects).

It is to be expected that variations in the processing history will influence both the appearance and the properties of the designated finishes (2D, 2B & 2R). For example, it is well established that the 2B R_a roughness value decreases with the degree of cold reduction from the hot band stage.

Firstly, features of the original hot band surface and those imprinted during its descaling that have endured the rolling operations may be retained. These can be in the form of defects in the sheet, like deep pits or heavy shot blast marks (used to clean the sheet); other shallower troughs may also be present as a result of hot rolling scale. At the white-hot band stage the surface is very rough and irregular.

The cold rolling process is not only used to reduce the gauge of the sheet but also to improve and consolidate the surface. The differences in methods and tribological conditions of cold rolling generate various surface characteristics, often the shallower pits present on the hot band surface are eliminated and the intermediate descaling (pickling) effects are minimised.

As mentioned previously, the next step depends on the finish required. After being rolled to the intended final gauge the material for 2D and 2B finishes is annealed again and must be descaling in an agitated acid bath.

This descaling method is highly influential to the surface and chemical attack on the metal substrate can be preferential, for example at grain boundaries in the recrystallised, annealed structures, giving rise to etching effects on the surface. It creates a 'matrix' of grain boundary valleys; figure 2.7, where the metal surface has been depleted of chromium during the oxidising process. Some of the grain boundaries are left intact so the remaining grain 'plateau' regions vary in size. This is the cold rolled, annealed and descaled surface that has a matt finish with low reflectivity, known as 2D (see table 2.1).

The plateau regions are relatively untouched at this stage, since they are the 'new' grains and so most have not been rolled. 'Skin passing', in a light but high-speed mill can enhance strip geometry and surface brightness. The skin pass, performed at the Sheffield site, does not alter the mechanical properties materially but it serves to reduce thickness and improve 'shape' tolerances and gives a final finish to the plateau regions. Being a light pass it does not totally smooth out the plateau regions but merely removes or flattens the higher asperities making the surface optically brighter. The skin pass also has a tensioning device, which helps to alleviate the effect of form and waviness created in the rolling process. The other method of brightening the surface, used at the Source 2 site, is to use a light tension device. The effect on the visible

appearance of the sheet is similar but has not been investigated in detail at a microscopic level. The surface is now designated as the 2B finish that has a 'pearly grey' appearance. Consequently there are two main features which distinguish the 2D and 2B surfaces, plateau regions and a pattern of valleys and to fully quantitatively characterise the surface every detail of these features must be measurable.
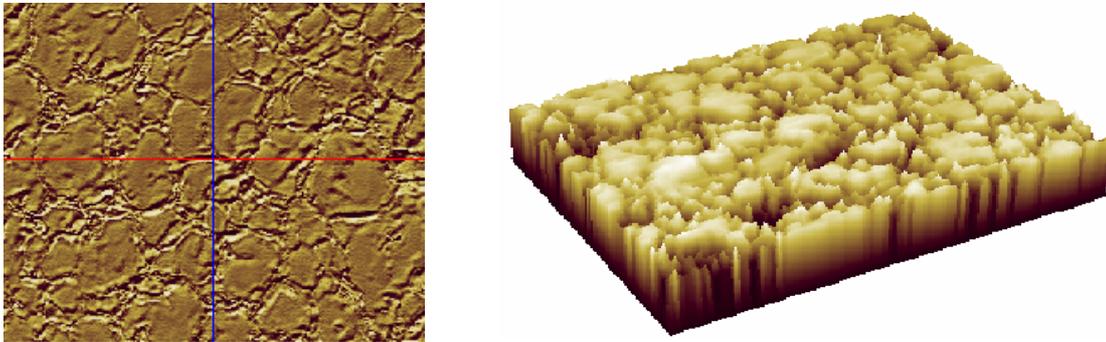
Figure 2.7: Interferometer images showing etched grain boundary valleys and plateau regions on 2B stainless steel

The annealing method for 2R material has a totally different effect on the surface. As no oxygen is present in the process no scale is formed and so no descaling is needed. The final product is highly reflective and bright with a mirror like finish.

These finishes are not normally subject to any quantitative specification, except possibly comments on relative 'dullness'. It is now accepted however that the nature of the topography of a surface can have a significant influence on the efficiency and functional performance of the sheet surface [1] and it is considered that a quantitative analysis of the surface is highly desirable if a deeper understanding of the surface function is to be gained.

2.3.3   Optical Appearance

The appearance of an object is influenced by many factors, the interaction of light with the surface, the direction of both light source and viewer, the objects' physical characteristics and subjective human perception. Generally a distinction is made between chromatic properties, like colour and geometric atributes, such as gloss, reflectance and haze. Instruments to measure these properties are also seperated into two groups, those that measure the physical properties of distributed light, like spectrophotometers and goniophotometers and psychophysical analysis instruments that give measurements that correlate with the human perception of light distribution, like colourometers and glossmeters [12].

2.3.3.1   Perception of Appearance

The appearance of a product is often used by consumers as a measure of the quality of the product and the materials it is made from. There is a psycological relationship [13] between

appearance and performance and durability. When given a choice between similar product function, a consumer will inevitably buy what looks best. Manufacturers of stainless steel products also realise the importance of uniformity of appearance, as variability in a group of the same products indicates to the end-user poor process or production control and therefore inferior quality.

How a material appears to the eye is dependant on the effect it has on light falling on it (the incident light). The light distribution can be characterised as either reflection or transmission and further divided into diffused and undiffused components. This gives four main types of light distribution, see figure 2.8, with most metals having a strong specular reflection property and a degree of diffuse reflection [14].

2.3.3.2   Instrumentation to Measure Reflectance

Instruments are separated into two groups, physical and psychophysical analysis types [14]. The appearance attributes of relevance for stainless steel are geometric rather than colour related and because of the nature of metals, only specular reflection meters are suitable for measuring the gloss, haze, specular reflectance and distinctness of image which are of interest. Generally known as glossmeters, the first commercial instrument was probably the Ingersoll Glarimeter developed in 1914 [15] for measurement of white paper gloss.

Modern glossmeters generally consist of two parts, the optical unit containing the light source, lenses and receptors and the readout unit which converts the electrical signals into meaningful instrument readings.

There are three common geometries, 20°, 60° and 85°, at which gloss (see table 2.3) can be measured (depending on the amount of gloss). This is to give better resolution for all surfaces, since a measurement at 20° on two low gloss surfaces would show little difference.
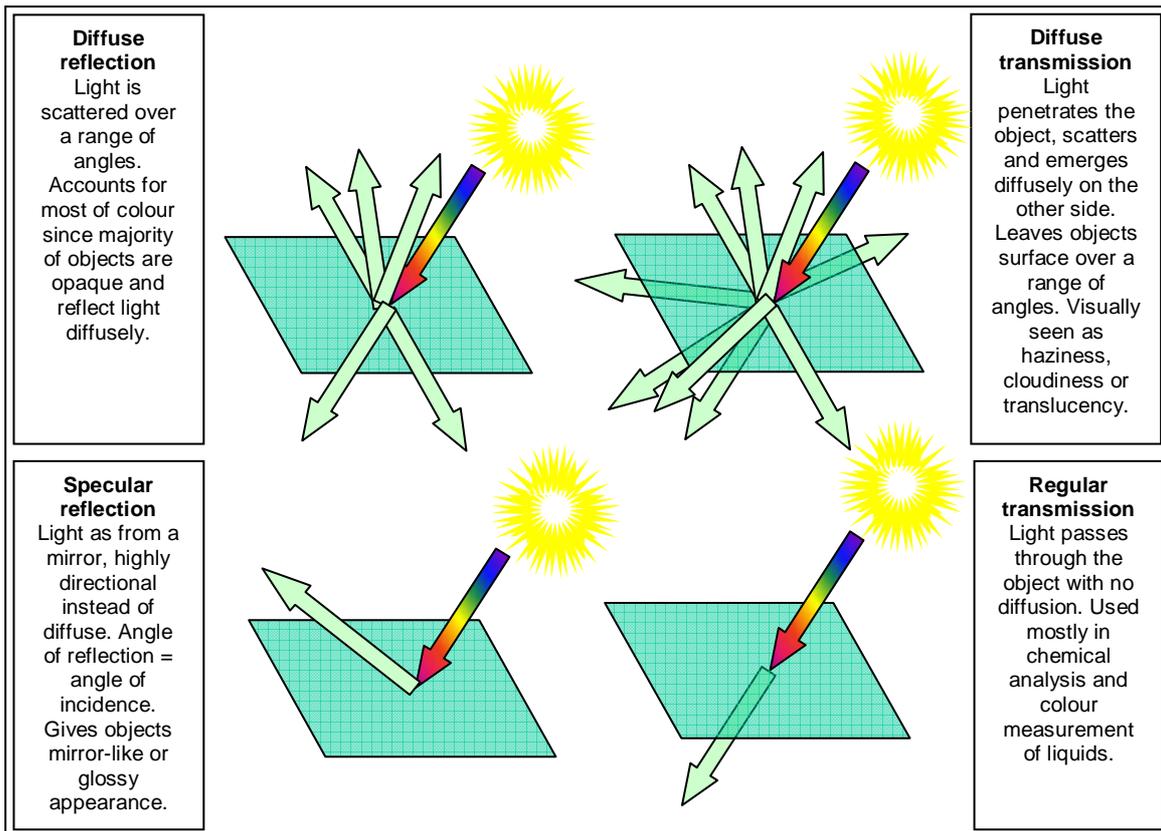
Figure 2.8: The four main types of light distribution

2.3.3.3   Parameters to Measure Reflectance

The perception of appearance can be thought of in many different ways and so parameters need to incorporate considerations for gloss, reflectivity, image clarity, degree of greyness or brightness and hue. Optical properties like these are considered on a nano-scale, Thomas has stated, [16], 'When surface irregularities are present at wavelengths comparable with those of visible light the appearance of the surface will alter, e.g. a painted surface such as a car body may appear dull instead of glossy (amplitude 0 – 10 nm)'.

Gloss (or specular gloss) is the general term for the attribute of 'shininess' of surface and it is a concept used to define sheet surface quality. In 1952 five kinds of reflection were defined [14], table 2.3, and it was generally accepted that an observer perceives not only the mirror image angle light but also components close to the specular angle.

Very smooth surfaces will have very high gloss values, as most of the incident light is reflected in the mirror image angle. Surface roughness will scatter the light, reflecting it at different angles to the mirror image, reducing these gloss values.

Table 2.3: Types of gloss [14]

Types of reflection	Characteristics
Specular gloss	Shininess, brilliance of highlights
Haze or absence of bloom	Halo or milky appearance near to reflected highlights
Distinctness of image	Sharpness of mirror image
Sheen	Gloss at grazing angles
Contrast gloss	Difference between specular and non specular areas

2.3.3.4   Sheet Metal Appearance

The appearance of sheet metals is governed by the extent of their reflection (diffuse and specular) as they do not possess transmission properties. They range in magnitude from the mirror-like (wholly specular reflection on a highly polished, flat surface) to the very matt (wholly diffuse reflection normally associated with rough finishes). Their optical properties depend mainly on their production method, although metal composition can have an effect (due to the materials reaction to the applied processing).

The appearance effects of production methods on stainless steel finishes are varied and it is possible to produce both matt and highly reflective surfaces (though the work involved deems this uneconomical). The mill and derived finishes (seen in table 2.1) can have distinctly different surface topographies, although their appearance may be very similar.

The key features that affect the optical properties of 2D and 2B surfaces can be deduced by comparing the production methods and end appearance of the two. The 2B finish is basically a skin passed 2D finish and as a result is much brighter than the matt 2D finish. Skin passing is used to enhance surface brightness and increase reflectivity by removing or consolidating the higher asperities present on the 2D finish. Optical properties of the studied surfaces are discussed in detail in chapter 6.

2.3.4   Tribology

2.3.4.1   Background

It is well known that, in forming operations, smooth surfaces are prone to scratching and galling as they friction weld easily to the forming die [17]. Surfaces with valleys allow lubricant to be held in the surface at the contact zone during forming, reducing friction and welding problems. Additionally these valleys act as debris traps, keeping contaminants away from the contacting surfaces [17, 18]. Wihlborg and Gunnerson [19] also found that friction is lower in surfaces with a large number of small isolated pockets. The development of a parameter to describe these

properties resulted in the use of the 'WC index' [20], which is discussed in section 2.4.5. It has been shown [21] (whilst studying aluminium sheets for stretch formed automotive panels) that it is important for friction and forming behaviour that surfaces possess both open and closed voids.

2.3.4.2   Functional Tests

Testing can be either practical, using the actual process and conditions of manufacture for a component, or experimental, where rigs are used to simulate the process and variables of manufacture can be changed and controlled. The effect of surface topography on tool friction properties was classically studied using a Draw Bead Simulation or 'DBS' tests [22], and variations of it, like the Bending Under Tension or 'BUT' test [23]. These can be used to analyse either the tool surface or the formed products' surface, both before and after testing and galling behaviour. A static oil retention test was developed by OCAS to study the effects during coiling or blanking [10]. A drip test can be used to study the lubricant retention and surface wetting properties of a finish.

Draw Bead Simulation (DBS)
Draw bead simulation or strip drawing tests have been used for many years to study the effects of friction, die and blank surface finish, draw speed, lubricant type and virtually every other variable in sheet product forming. Figure 2.9 is a schematic of a simple draw bead simulator. The sample is drawn through the stationary dies, with an indentation force applied. Lubricant can be applied to the sample before testing and the indentation and pull forces are measured during testing by strain gauges. The dies can be smooth to simulate rolling or can be roughened to study the effect of friction and the contact angle of the die can be changed.
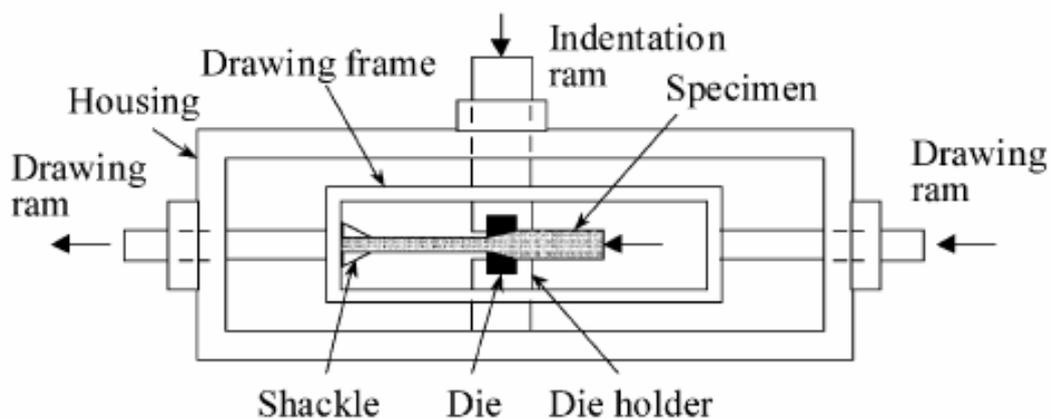
Figure 2.9: Schematic of a simple Draw Bead Simulation [22]

Bending Under Tension (BUT) Tests
The bending under tension rig, figure 2.10, is a variation of the draw bead simulator, sometimes referred to as a radial strip drawing rig which simulates the contact between the sheet and the

die radius in a drawing operation [24]. The sample sheet is stretched over a cylinder representing the die radius and is pulled whilst the force is monitored. By using a rolling cylinder sliding friction at the contact zone can be found in relation to the pulling force.
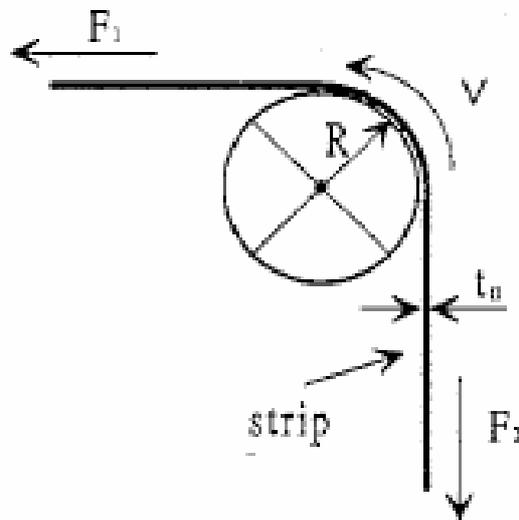
Figure 2.10: Bending Under Tension equipment [23]

Drip Tests

Film retention tests have been used traditionally for testing lubricant film retention properties, related to forming operations. It is a relatively straightforward method, whereby a shaped coupon of material, see figure 2.11, is coated with lubricant that is then left to run off the sample. The method of application of oil and the initial film thickness is made independent of the film retention properties, by allowing the sample to hang for a set time before weighing the sample for the first time. The film thickness at set time intervals (up to 2 weeks is the norm) can then be related to the lubricants film retention properties. There are variations of this method, chosen depending on the lubricant being tested and the availability of a roller press (giving a known initial film thickness), for the preferred method.

Similar methods can be used to test the lubricant retention properties of a surface, by varying the samples rather than the lubricant used. By controlling the amount of oil initially applied, then weighing the drips with respect to time, an indication of the surfaces ability to hold or distribute lubricant can be found.

The tribological property of lubricant retention is studied in further detail in Chapter 7.
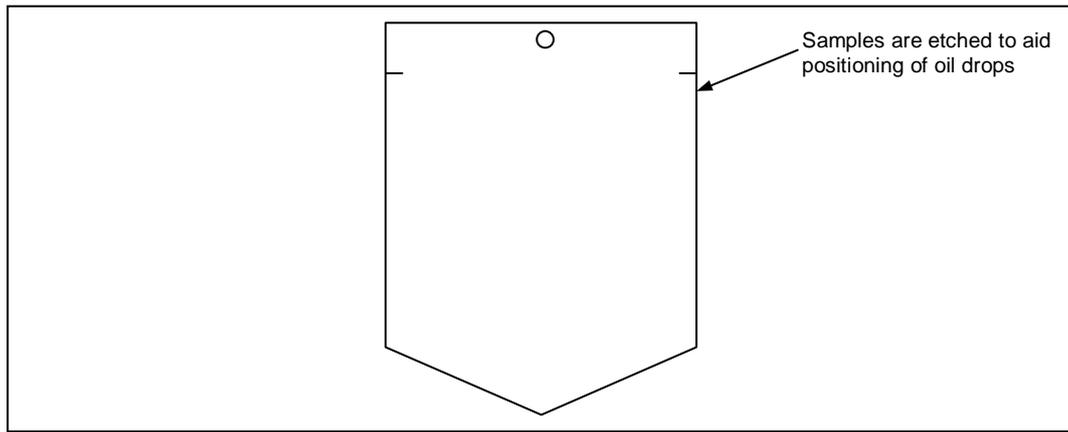
Figure 2.11: Shape of sample used for drip testing

2.3.5   Corrosion Resistance

2.3.5.1   Background

Corrosion can be defined as the chemical reaction or the electrochemical reaction of a material with its environment. For ferrous metals, it is usually referred to as atmospheric corrosion.

Oxidation is the direct chemical reaction between the material and oxygen. Oxidation can be a help or a hindrance. For instance, for stainless steel "corrosion" forms an oxidation layer giving strong retardation of additional corrosion through passivation (the passive film, see section 2.3.4.2).

Corrosion is another consideration that must be taken into account when selecting materials, either working alone with the environment, or working with other materials to perform a function. Since materials degrade, the rate and extent of this degradation must be controlled; some applications require more control than others. For instance, in the food industry, food processing equipment cannot tolerate even a minute amount of metal corrosion, particularly if metal ions or particles are released into the surrounding environment.

2.3.5.2   Corrosion Mechanisms of Stainless Steel

The corrosion resistance of austenitic stainless steel is the result of the passivating chromium oxide film that forms on its surface. To maintain the protective layer, a chromium content of at least 11% and a supply of oxygen are required. The film is self-repairing in air at room temperature but if not enough oxygen is present and the film is damaged corrosion will occur. Most stainless steels are susceptible to corrosion such as intergranular and stress corrosion, crevice corrosion and pitting. Grade 316L is commonly used for marine applications [25] due to its outstanding resistance to localised corrosion, however, the greatest shortcoming with this type of stainless steel is their vulnerability to pitting and/or crevice corrosion in the presence of chloride under static or stagnant conditions. The breakdown of the passive film on stainless steel occurs in the presence of chloride ions which subsequently results in the initiation of pits.

There are three identifiable phases to pitting of stainless steel. According to some research [26] pit nucleation in stainless steel is unstable since pit propagation is not always achieved. The nucleation current required dies continuously and most pit initiation events terminate. If the nucleation current is maintained and the pit survives then the pit growth is called metastable. Pitting only becomes stable when an effective barrier against diffusion is achieved and the nucleation current density is high enough. Stable pitting is a diffusion controlled reaction and the diffusion barrier is often related to pit depth [26].

2.3.5.3   Methods of Assessing Pitting Corrosion Susceptibility

Currently, a number of tests are used for ranking pitting susceptibility for different surface finishes, for example salt spray testing [27] and critical pitting temperature measurements [28]. However, these are relatively slow (up to a number of weeks). Common electrochemical testing methods include: Zero Resistance Ammeter (ZRA), Potentiostatic, Potentiodynamic and Galvanostatic. Two of these methods have been used within the scope of this project and are discussed in detail in chapter 8.

2.3.5.4   Relationship of Topography to Corrosion

B.Lee and C.Watanatham (Outukumpu UK Foundation for Research and Development students based at Birmingham University) have investigated pitting phenomena and localised corrosion behaviour with respect to variations in surface topography. Particular interest lies in the shape and relative depth of existing pits on plateaus or in valleys and whether certain topographies promote the initiation of pitting corrosion, crack initiation or the ease of release of an ion from a pit, as this directly effects the pitting corrosion susceptibility, see figure 2.13. It is thought that a combination of valley depth and aspect ratio (crevice acuity) parameters will be required for functional use.
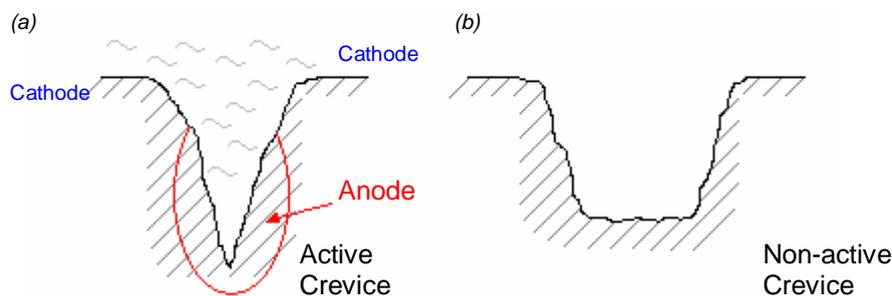
Figure 2.12: Pitting corrosion: attack on crevices – dependence on shape [reproduced from 8]

2.4. Surface Topography Measurement

2.4.1   Instrumentation

There is now an extensive range of 3D measuring equipment available for the engineer, metallurgist, biologist, etc. The techniques for the use of 3D instruments are also becoming far more defined and standardised but it can be difficult to choose the right method and equipment for a particular type of surface.

Some equipment can be easily eliminated from the choice based on the type of surface to be examined and the capabilities of the instrument. For example, a contacting stylus type instrument cannot be used to measure soft surfaces, due to the damage that the tip causes and surfaces with sharp peaks or valleys are distorted in relation to the geometry of the tip. Interferometry is not recommended for very rough finishes and the surfaces must possess a certain specular reflectance to be measured accurately.

Considering these problems there is a strong argument to suggest that before measuring commences the features that define or characterise the topography of the surface (the 'unit' features) must firstly be established.

2.4.1.1   Instrument Selection

There are many instruments that can be used for 3D surface measurements, making the selection of the right technique difficult. The most common classification of instrument types is into three groups, contact, non-contact and scanning probe microscopy, see figure 2.13.

By far the most widely used technique (in industry) is the 2D contacting stylus instrument. There are however, certain obvious limitations in this method and as a result other techniques are establishing themselves in a number of disciplines. The following section on instrument selection explains some of the options that are available with the advantages and disadvantages of each.

2.4.1.2   Stylus Instrument

The first stylus profilometers were developed in the 1930's. Work on the first transmission and scanning electron microscopes prompted their conception as an advance on the optical specular reflectance methods which, although a widely used method of areal measurement, presenting the root mean squares (RMS) roughness parameter, did not give quantitative height information or an image of the surface topography [6, 16]. Early stylus measurements were carried out by traversing the probe across the surface and recording the vertical movement of the lever. The major differences of these systems were in the logging of data, three common methods were magnification of an optical lever [29], a mirror/lever system recording the deflections of a light beam on photographic film [30] and mechanically amplifying the movement of the probe to scratch a smoked glass plate [31]. These gave a profile of the surface

topography with quantitative height information and were adequate for most isotropic engineering surfaces. It wasn't until about thirty years later that Williamson and Peklenik et al [32, 33], proposed three-dimensional measurement with the stylus instrument. This was realised by Sayles and Thomas [34] who, in 1976 added computer control to a 3D-stylus instrument. Many 3D systems are now commercially available and associated software has greatly improved. 2D systems are still used for profiling and in standards definition because of the speed and ease of measurement, which is not always true of 3D systems. The construction of the instruments is similar, but because of the nature of this project only the 3D assembly and features will be discussed.

Many authors [16, 34] have exhaustively discussed the mechanism of a 2D-stylus instrument and 3D systems are fairly similar in construction. The basic instrument consists of a stylus probe that is traversed across a surface, a pick-up, which is physically attached to the tip and converts the vertical movements into an electrical signal. This signal is then amplified and digitised to be processed by a computer, see figure 2.14. A linear variable differential transformer (LVDT) or an optical transducer are used in the pick-up mechanism and the translation stages are controlled by a gearbox driven by either a stepper motor, a DC motor or a linear motor regulated by a driving unit [35].

The pick-up arrangement sometimes includes a skid, which is either flat or has a large radius. The skid rests on the surface, usually in front of the stylus tip, following the macro surface or waviness of the topography, therefore acting as a high pass filter. Although skid-type stylus systems are less sensitive to external vibrations (making them more suitable for shop floor environments) they do not give a true measurement of the macro and micro surface topography and can cause distortion of the roughness profiles obtained, see figure 2.15 [36], particularly for surfaces with sudden steps.

With 2D methods a profile of the surface is obtained and the conventional method to realise the third dimension of movement to give an area map of the surface is the raster scan. A raster scan is a collection of parallel profile traces where each individual profile is displaced laterally a short distance from the previous one. All the profiles must be referenced to the same origin for the resulting areal plot to be a true raster scan. These 3D maps can then be displayed visually on a computer screen and/or used to calculate areal parametric descriptors. A radial scan is different as the profiles are taken with respect to radial angles and all traces have the same point of origin [37, 38]. This system is rarely used in current 3D data acquisition due to its difficulties in accurate physical realisation, amongst other things.

Stylus instruments are one of the oldest and probably the most popular methods of assessing surface topography and are therefore very well known and the measurement problems are now thoroughly investigated and documented [6, 8, 31, and 35]. Approved national and international standards exist for measurements using 2D stylus instruments, instilling confidence and ensuring consistency of measurements and results [16, 31]. Stylus systems also possess some element of self-cleaning, as the tip is traversed across the surface.

Correct measurement results however must take into account the effects of stylus load and tip geometry, figure 2.15. Although the load on the stylus is small (typically in the order of mN),

when it is transmitted to the surface via a very small area the resultant pressure is high and can damage the surface. In some cases asperities can be deformed plastically as well as elastically [31] and soft surfaces are therefore not measurable.

The data that is gained is distorted because of the effect of the tip geometry. It acts as a low pass filter, preventing asperities that are smaller than the radius of the tip being accurately resolved, see figure 2.15 [39]. Features like overhangs and pit hoods known generically as re-entrant features cannot be measured and may actually be damaged during measurement. The final drawback of stylus instruments for 3D work is time, measurement times are extremely high, a 4 x 4 mm area with a 1000 x 1000 point matrix may take as much as 3 hours to complete.

Other, unavoidable sources of errors are the conversion of the mechanical signal (given by the stylus tip) to the electrical signal (generated in the coils) and the conversion of this continuous, analogue signal to a digital one that is the computer input.
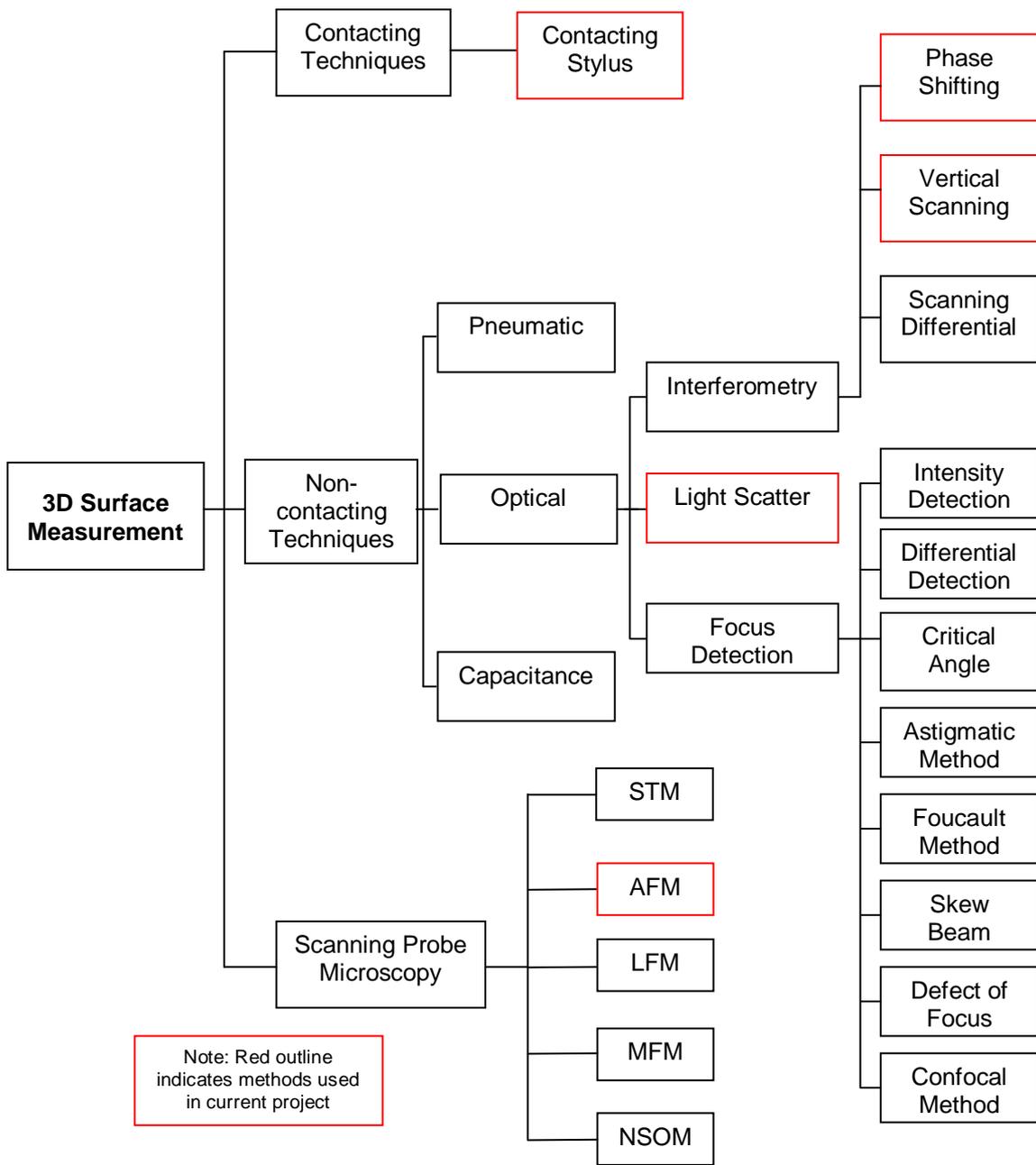
Figure 2.13: Classification of surface topography instruments based on the physical principles of measurement [35]

Figure 2.14: Schematic of a general stylus instrument with an inductive probe
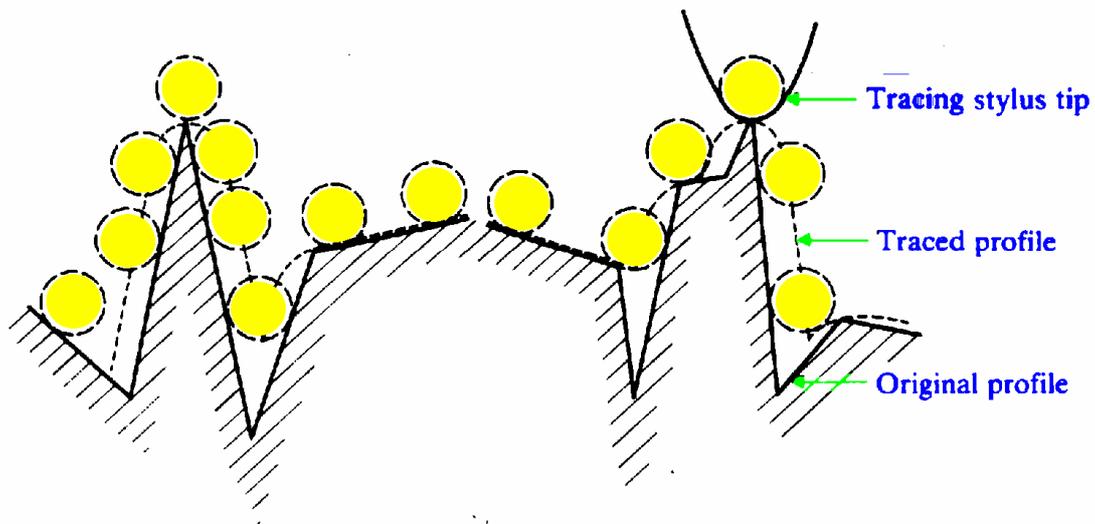
Figure 2.15: Effect of stylus tip radius on measurement results [39]

2.4.1.3   Interferometery

Until the 1970's optical interferometry could only be used for qualitative analysis and visualisation of surface topography. The technique was difficult and time consuming until developments in computing and electronics allowed complex analysis of optical fringe intensity and sophisticated graphics to be exploited.

There are two main approaches to interferometric measurement available in commercial instruments, phase shifting and vertical scanning (PSI & VSI). They both work on the same basic optical principles, but VSI was developed to measure the rougher surfaces which were not previously measurable using PSI.

The PSI system was developed by Bruning in 1977 and figure 2.16 shows a schematic diagram of a modern system. Filtered white light is passed through a beam splitter within the interferometer. Half of this incident beam is directed toward the specimen surface under examination and half to the reference surface, normally a very smooth mirror.

When the two wave fronts recombine and interfere they are collected by the charge coupled device (CCD) detector and an interference pattern or fringes are produced. Deviations in the pattern are actually deviations of phase between the two beams (either constructive or destructive) and can be related to height deviations between the test and reference surfaces (or more specifically height deviations of the test surface, since the reference has a known, near zero roughness). These interference phenomena can be collected and viewed as an interferogram. Quantitative height deviations are found by computer software that analyses the interferograms.

Phase shifting is enabled by driving the reference surface with a piezoelectric transducer (PZT). Once three or more interference patterns, for different axial positions of the reference surface, are measured the height distribution, h(x,y), for each coordinate pair, (x,y), can by found from the phase, Φ(x,y) by equation 2.1 [40].

$$h(x, y) = \frac{\lambda}{4\pi} \Phi(x, y)$$ *Equation 2.1*

The CCD detector is actually recording the intensity of the fringe pattern for the axial positions of the reference sample (I(x,y)) and equation 2.2 is used to find the phase Φ(x,y).

$$I(x, y) = A + B \cos[\Phi(x, y) + \alpha_i)$$ *Equation 2.2*

Where A = average intensity, B = constant and i = axial shift position, α = controlled phase angle

Most PSI systems at best detect phase differences of $\lambda/4$ [41] where λ is approximately 650nm, limiting the point-to-point range to around 150nm. For rougher surfaces visible white light is used, in VSI mode. Due to the short coherence length of unfiltered white light, interference happens over a very shallow depth of field (height band) for each focus plane. In this mode, instead of measuring the phase difference of the interference the CCD records the coherence, or degree of modulation of the fringes for different path lengths. By using the PZT to scan vertically above the test surface the modulation (fringe contrast) and therefore the intensity increases as the sample is brought into focus then decreases as it is translated past focus (figure 2.17) through the full depth of surface features. Frames of interference data are captured and a signal for each point on the surface is recorded. Algorithms are used to demodulate the envelope of this fringe signal and a vertical position corresponding to the peak of the interference signal (the point of best focus) is extracted for each point, see figure 2.18. The optical path difference is found for points across the surface and 3D roughness is deduced from these path differences.
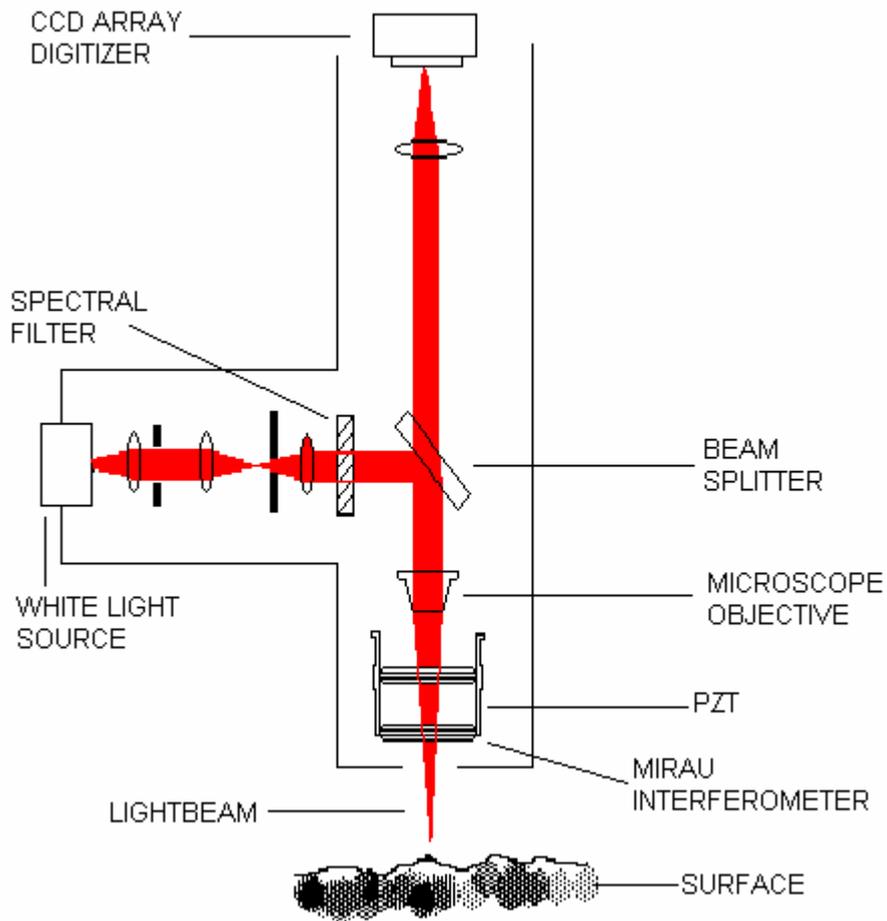
Figure 2.16: Schematic of a basic interferometer set-up (for Phase Shifting Interferometry, PSI)

The level of reconstruction of the topography is very accurate (with a quoted vertical resolution of approx 0.3nm for PSI and 3nm for VSI) and the measurement time is small, around a few seconds, after initial set-up time. Being non-contacting, both hard and soft materials can be measured without the risk of damage. The major limitation of these methods is that the test surface must reflect at least approximately 15% of the incident light to the detector and be optically homogeneous. This level of reflected light also affects the resolution of slopes on the surface, as angled light reflection may return insufficient intensity to the detector (around 15° is the limit) and higher slopes have been known to cause fringe ambiguities (near $\lambda/4$) [41].

Lateral and vertical resolutions are better than for a stylus instruments, but results are generally in good agreement. The vertical range is also limited, and so accurate measurement of surfaces with large amplitude features may not be possible. Re-entrant features cause problems for both stylus instruments and interferometers.

The point of maximum modulation is taken as the focal point for the surface being measured
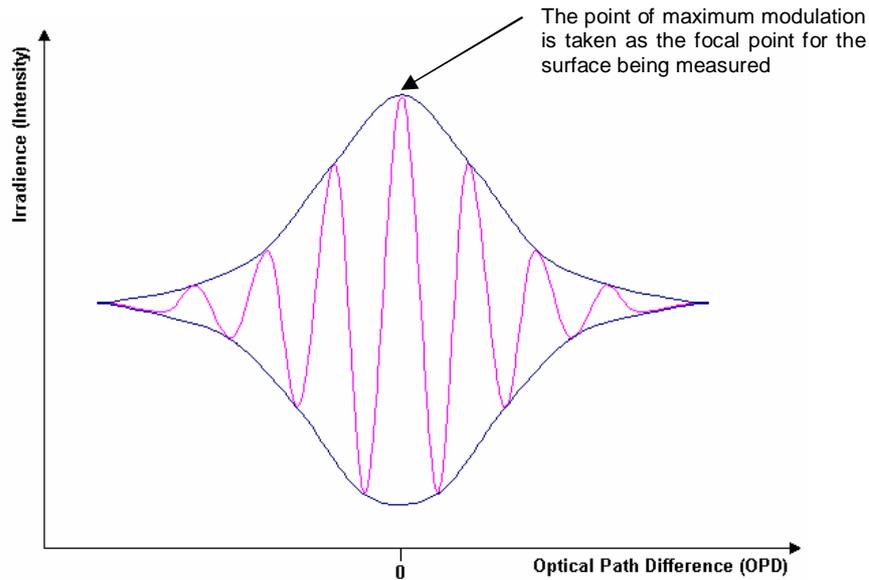
Figure 2.17: Intensity of light through optical path length showing maximum modulation point of focus [40]

I(z) → DC subtract → I'(z) → Square-law rectifier → Low pass filter → A(z) → Peak detector → Surface height
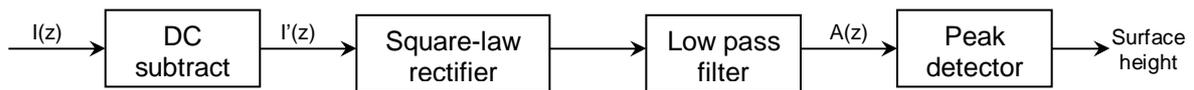
Figure 2.18: Fringe demodulation algorithm: deduction of 3D topography data from OPD

2.4.1.4   Atomic Force Microscope (AFM) [42, 43, 44]

The AFM was developed in 1986 by Binnig et al [45], and is a derivative of the Scanning Tunnelling Microscope (STM). The device is often likened to a stylus instrument on a smaller scale, as it utilises a scanning tip on a cantilever, see figure 2.19.

An AFM tip is approximately 10μm in length, in a tilted tetrahedron shape and the point is sharpened to less than 10nm in diameter. The tip can be made from a fractured diamond fragment or carbonaceous material (SiC or SiOi) via finely controlled micro-lithography or electron beam deposition and is attached to the free end of an aluminium or gold-coated silicon oxide cantilever of 100-200 μm in length.

There are three modes of measurement in atomic force microscopy, contacting, non-contacting and intermittent contacting. All of the modes rely on the response of the cantilever to the forces present when the tip moves close to the surface. The inter-atomic forces (repulsive) and the van der Waals forces (attractive) change as the distance between the sample surface and tip changes, see figure 2.20.
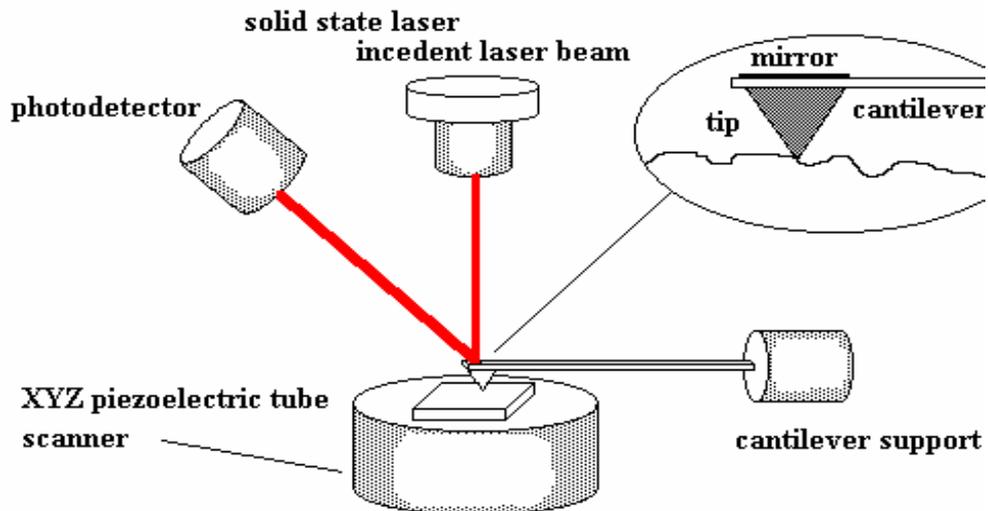
Figure 2.19: Representation of an Atomic Force Microscope

In contact AFM mode the tip makes soft "physical contact" with the sample. The cantilever has a low spring constant; lower than the effective spring constant holding the atoms of the sample together. As the scanner traces the tip across the sample the contact force causes the cantilever to bend to accommodate changes in topography.
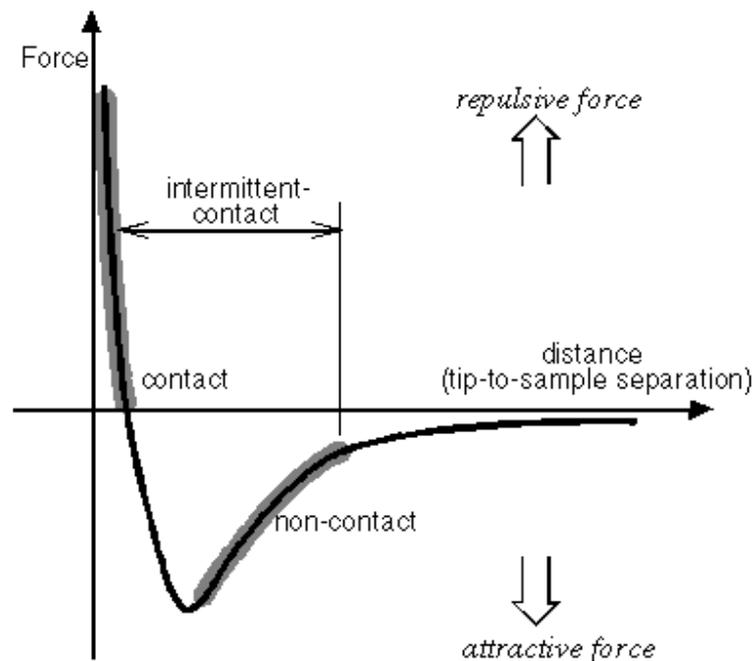
Figure 2.20: Interatomic force vs. distance curve: the effect of distance between atoms on the interatomic force [43]

In the contact regime, the cantilever is held less than a few nanometres from the sample surface, and the inter-atomic force between the cantilever and the sample is repulsive. This repulsive force balances almost any force that attempts to push the atoms closer together. This means that when the cantilever pushes the tip against the sample, the cantilever bends rather than forcing the tip atoms closer to the sample atoms. Even if a very stiff cantilever is used to

exert large forces on the sample, the inter-atomic separation between the tip and sample atoms does not decrease.

Currently most commercial systems detect the position of the cantilever with optical techniques. In the most common scheme, shown in figure 2.21, a laser beam bounces off the back of the cantilever onto a position-sensitive photo-detector (PSPD). As the cantilever bends, the position of the laser beam on the detector shifts. The PSPD itself can measure displacements of light as small as 1nm. The ratio of the path length between the cantilever and the detector to the length of the cantilever itself produces a mechanical amplification. As a result, the system can detect sub-nanometre vertical movement of the cantilever tip. Other methods of detecting cantilever deflection rely on optical interference, or even a scanning tunnelling microscope tip to read the cantilever deflection.
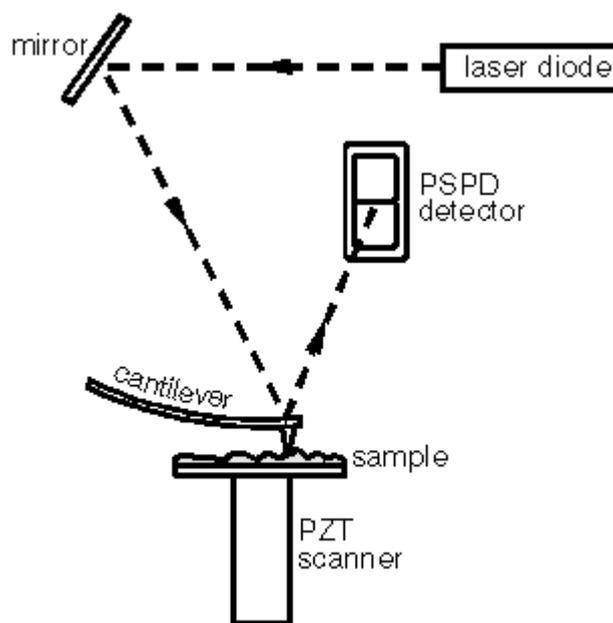
Figure 2.21: The beam-bounce detection scheme of an AFM [43]

Once the AFM has detected the cantilever deflection, it can generate the topographic data set by operating in one of two modes - constant-height or constant-force mode. In constant-height mode, the spatial variation of the cantilever deflection can be used directly to generate the topographic data set because the height of the scanner is fixed as it scans.

In constant-force mode, the deflection of the cantilever can be used as input to a feedback circuit that moves the scanner up and down in z, responding to the topography by keeping the cantilever deflection constant. In this case, the image is generated from the scanner's motion. With the cantilever deflection held constant, the total force applied to the sample is constant. Constant-force mode is generally preferred for most applications. Constant-height mode is often used for taking atomic-scale images of atomically flat surfaces, where the cantilever deflections and thus variations in applied force are small. Constant-height mode is also essential for recording real-time images of changing surfaces, where high scan speed is essential.

In "non-contact" atomic force microscopy an AFM cantilever is vibrated near the surface of a sample. The spacing between the tip and the sample is on the order of tens to hundreds of angstroms, see figure 2.20. This mode is desirable because it provides a means for measuring sample topography with little or no contact between the tip and the sample. The system vibrates a stiff cantilever near its resonant frequency (typically from 100 to 400 kHz) with an amplitude of a few tens of angstroms. It detects the changes in the resonant frequency or vibration amplitude as the tip comes nearer to the sample surface. The sensitivity of this detection scheme provides sub-angstrom vertical resolution in the image, as with contact AFM. The resonant frequency of a cantilever varies as the square root of its spring constant. In addition, the spring constant of the cantilever varies with the force gradient experienced by the cantilever. Finally, the force gradient, which is the derivative of the force versus distance curve shown in figure 2.20 changes with tip-to-sample separation. Thus, changes in the resonant frequency of a cantilever can be used as a measure of changes in the force gradient, which reflect changes in the tip-to-sample spacing, or sample topography.

In this mode, the system monitors the resonant frequency or vibrational amplitude of the cantilever and keeps it constant with the aid of a feedback system that moves the scanner up and down. By keeping the resonant frequency or amplitude constant, the system also keeps the average tip-to-sample distance constant.

Intermittent-contact atomic force microscopy is similar to the non-contact mode, except that the vibrating cantilever tip is brought closer to the sample so that at the bottom of its travel it just barely hits, or "taps" the sample, hence the usual term 'tapping mode'. The operating region is indicated on the force versus distance curve in figure 2.20. As for non-contact mode, the cantilever's oscillation amplitude changes in response to tip-to-sample spacing. An image representing surface topography is obtained by monitoring these changes.

Some samples are best handled using intermittent contact instead of contact or non-contact AFM. This is because the tip is less likely to damage the sample than in contact mode because it eliminates lateral forces (friction or drag) between the tip and the sample. In general, it has been found that 'tapping mode' is more effective for imaging larger scan sizes than non-contact mode. It has recently become an important AFM technique since it overcomes some of the limitations of both contact and non-contact AFM.

The measuring time for relative areas are slightly faster on the AFM compared to a stylus instrument but still much slower than on an interferometer. It can also be employed as a non-contact method and surfaces do not need to possess any specific optical or other properties. The AFM method is capable of resolving features that are theoretically atomic scale vertically and nanoscale laterally. However, the measurement range horizontally and vertically is limited, small areas and fairly smooth surfaces are most favourable when using this technique. Traceability is difficult to obtain using conventional techniques and standards are not yet available.

2.4.1.5   Scanning Electron Microscope (SEM)

The transmission electron microscope (TEM) was the first type of electron microscope (EM) to be developed in 1931 by Knoll and Ruska. The theoretical limit of magnification (approximately 1000 times) for light microscopes had been reached and development of EM's was driven by the desire of scientists to study the fine interior structure of organic cells. A light microscope with perfect lenses and illumination cannot distinguish details smaller than half the wavelength of light, for example half the wavelength of white light is approximately 0.275 microns (this is the theoretical interferometer level).

To 'see' smaller objects 'illumination' by accelerated electrons, with extremely short wavelengths was developed. For example, when pushed to their limits EM's can resolve the diameter of an atom. The first scanning electron microscope (SEM) was developed by von Ardenne in the early 1940's. All von Ardennes equipment and research was destroyed during the Second World War (approximately 1944) and further, commercial development was therefore delayed until, in 1947, Charles Oatley continued von Ardennes work, improving the 'scanning' capabilities of the instrument. The first commercial instruments became available in the mid sixties.

A stream of monochromatic electrons is produced in an electron gun and is condensed by the first condenser lens, see figure 2.22. Working in conjunction with the condenser aperture it reduces the number of high-angle electrons and limits the amount of current in the electron stream. The second condenser lens forms the stream into a fine thin, coherent beam, which then passes through an objective aperture, eliminating the remaining high-angle electrons. The beam then passes through the scan coils, where, by varying the voltage applied, a magnetic field deflects the beam in a grid pattern, producing the scanning motion. Before striking the sample, the beam passes through the objective lens, where it is focused on to the desired area of the specimen.

The whole column and sample chamber must always be at a vacuum when in use. This is due to the inability to produce a stable electron beam when gases are present. Transmission of the beam through the optics column may also be hindered by the presence of other molecules, which could react with the beam and form compounds or 'condensation' on the surface of the sample, obscuring detail.
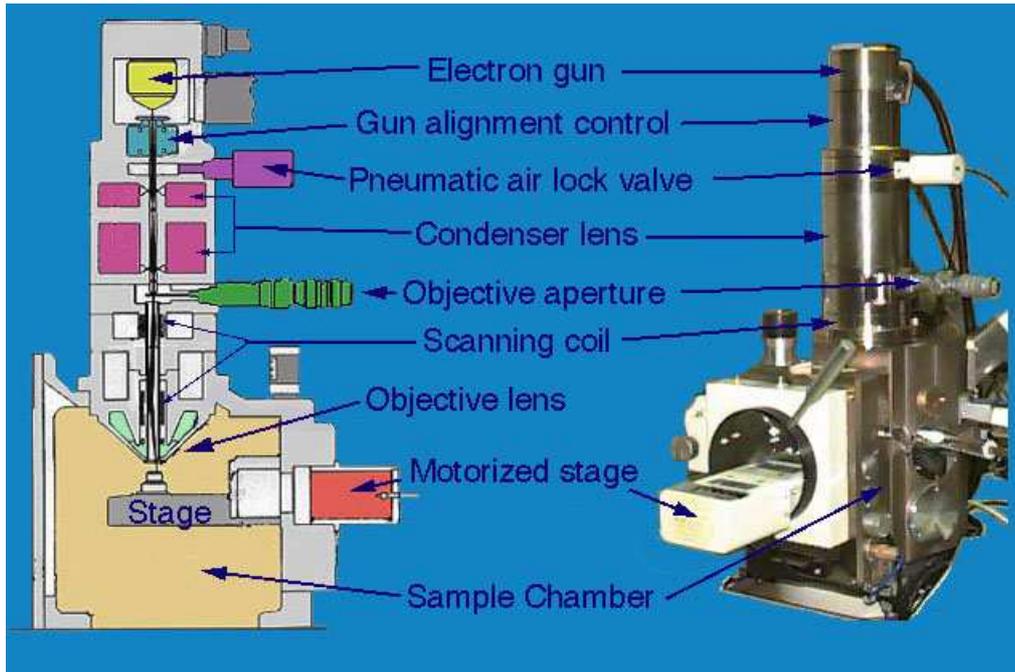
Figure 2.22: Basic Scanning Electron Microscope equipment [46]

As the beam strikes the sample, at each scan point, interaction occurs which is detected and analysed. The detectors basically count the number of interactions that occur and display them as a pixel on a cathode ray tube (CRT) where the intensity of the pixel is proportional to the number of interactions counted. The beam is moved to the next spot on the sample and the detection process is repeated throughout the scan. Separate detectors are used to 'count' different interactions, relating to various properties of the sample, see figure 2.23.

Only two of the interactions shown in figure 2.23 yield topographical information, primary backscattering and secondary electron emission. These are discussed in more detail below and further information on these and other interactions can be found in [46, 47].

There are two broad categories of electron scattering, elastic and inelastic. When an electron undergoes elastic scattering there is little or no change in its energy. There is a change in the electrons momentum and therefore in the direction of its velocity vector due to the relationship p = mv. Typically electrons are scattered at an angle of approximately 60 degrees, although 0 to 180 degrees is possible. Essentially Rutherford scattering, elastic scattering occurs due to interaction between the negative electron and the positive nucleus of an atom in the sample. When the scatter angle is such that the electron is directed back out of the sample, a backscattered electron, the backscatter detector collects it to give information about the sample composition (atomic number) and the topography.
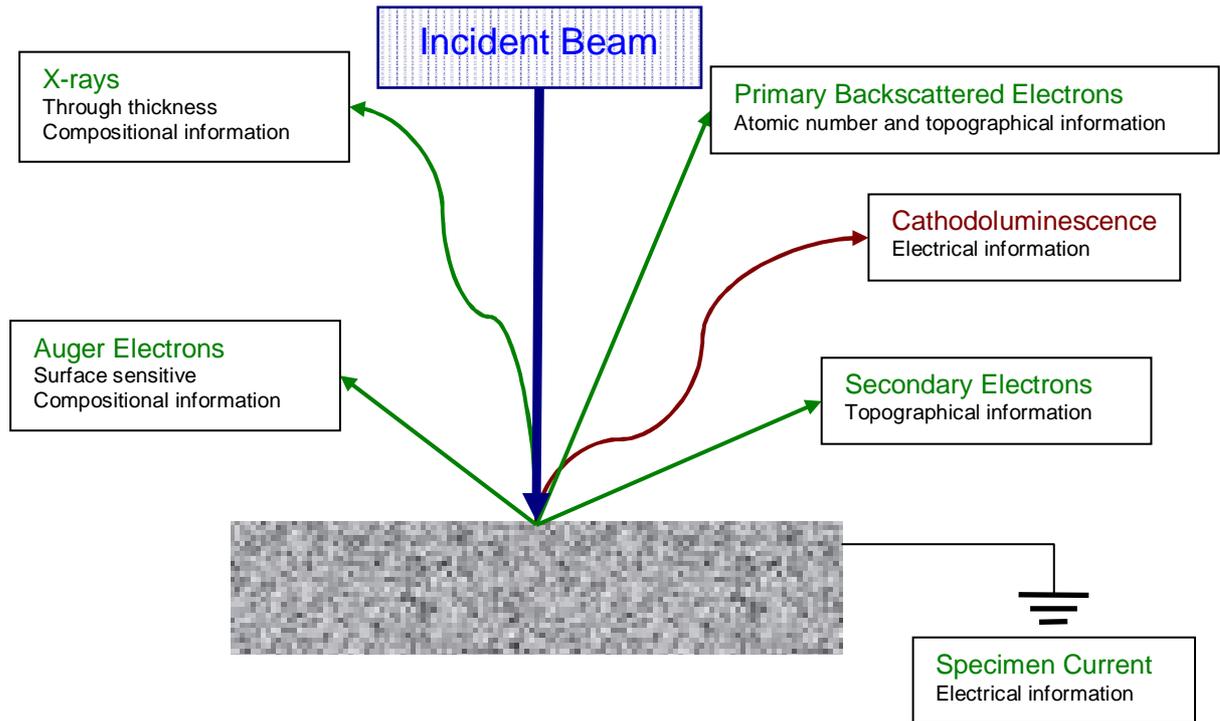
Figure 2.23: Interactions between electrons and sample in a scanning electron microscope

When inelastic scattering occurs there is a transfer of energy from the beam electron to the electrons surrounding atoms in the sample (excitation). The amount of energy transferred is dependant on the process that ensues, which could be phonon excitation, plasma excitation, secondary electron excitation, continuum X-ray generation or ionisation of inner shells, and can range from a fraction to many kilo electron volts. When secondary electron excitation happens electrons with a 'low' (<50eV) energy are emitted from the sample and are collected by the secondary electron detector and used to give topographical information of the surface.

The advantages of the SEM over light microscopes are clear, they have very much larger depth of field (therefore larger areas can be viewed) and far greater resolution is possible, but their main disadvantage is the sample limitation. Samples must be conductive and due to the use of a vacuum, live cell interaction cannot be studied using the SEM. For gaining topographical information of stainless steel samples the advantages in range and resolution are significant. The major disadvantage is the inability to measure in the third dimension, or depth of topographical features. For this reason the SEM is used qualitatively and as a lateral quantifier only, rather than as a primary surface measurement instrument.

2.4.1.6 Instrument Capabilities

It is clear that certain instruments have specific vertical and horizontal measurement ranges for which they are best suited. Additionally certain aspects of their physical attributes (probe size and geometry, transducer sensitivity, movement error scan length, datum, scale resolution etc.)

also define their window of performance. When comparing the performance of the different instruments however problems occur as to the criteria upon which comparisons should be made. A method for delineating the effective working range has been developed by Steadman [48].

The method is based around the limiting response of the instrument to sinusoidal surface perturbations. The limiting factors considered are the vertical range and resolution, the horizontal range and resolution, horizontal datum and probe size/geometry. This analysis results in a working amplitude wavelength space (A.W. space) for the given instrument. Figure 2.24 shows the construction of the Steadman diagram for an example instrument. The limitations of wavelength, height, curvature and slope are accounted for when drawing the bounding 'box'.

An amplitude-wavelength plot for common instruments is presented in figure 2.25. In this figure, the two axes represent the resolutions (towards the origin of the axes) and the ranges (away from the origin of the axes) of the instruments both in vertical and horizontal directions. Each block in the figure indicates the working area of an instrument. The lengths of two orthogonal lines drawn from any point, P, in the area gives an indication of the ratio of range to resolution, the longer the length, the bigger the ratio.
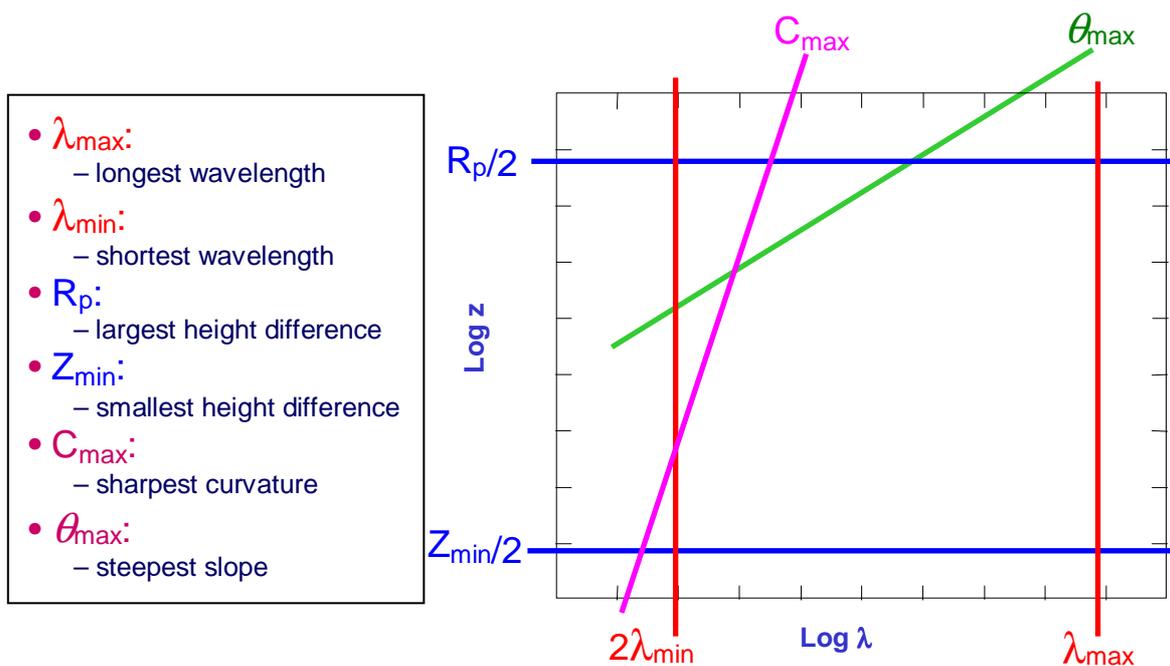
Figure 2.24: Construction of a Steadman diagram [49]

Figure 2.25 clearly shows that the specific working areas of the different instruments define an instrument's suitability for making a given measurement. The large working area of the stylus instruments illustrates its wide applicability. It should be noted that the STM/AFM systems have the highest resolution but limited range. Interferometric systems have high resolution but a greater range than the scanning microscopes.

The Steadman diagram has been modified to illustrate the ranges and resolutions of the instruments available for use in this project. It will be used to aid the selection of the correct

method for measuring stainless steel surfaces. But first it is necessary to investigate the geometry of the features of stainless steel topography, or in other words what ranges and resolutions are actually required to resolve the features of relevance on the surface.
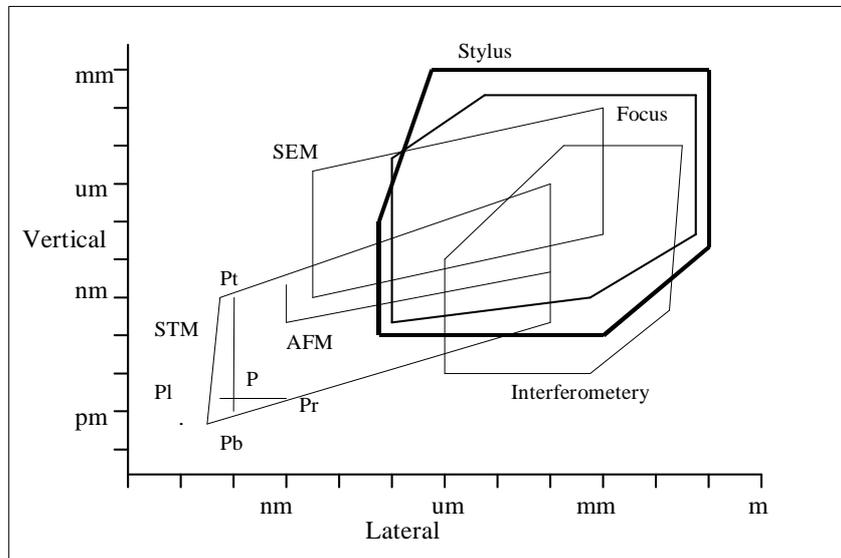
Figure 2.25: Amplitude wavelength plot of a range of 3D surface measurement instruments

2.4.2   Sampling the Surface Data

'Sampling is the process of defining the instantaneous points at which the data are to be observed' [50].

When a data signal is converted from analogue to digital, the signal must be sampled and quantised. Digital sampling is normally performed at equal intervals of time on a signal and it is this interval that is the important variable. If the interval is unnecessarily small, redundant data will be collected and the correlation of points would yield misleading results. If the interval is too large a phenomenon called aliasing will occur, where the high and low frequency components of the signal become confused. In terms of surface topography data however, the interval is spatial rather than time based.

The frequency of the features is needed to ensure that the demands of the Nyquist theorem [50] are met. The theorem states that for a periodic signal, the sampling interval should be smaller than half of the wavelength of the signal. If this theorem is not satisfied then aliasing will occur, as mentioned previously. This is the normal value of short wavelength limit for the sampling interval, but as stated, it is for periodic signals, which surface topography data cannot be assumed to be.

Firstly there are a number of methodologies to decide on the correct sampling interval required for a particular surface topography, measuring instrument or functional interest, but initially the important features of the surface must be identified. Obviously, it is desirable to measure the largest area possible, to get as many of the variations as possible. By increasing the area,

resolution is usually sacrificed, so there is a trade off between being able to measure at a high enough resolution to observe the critical features, see figure 2.26, and having a large enough sample area to include all the critical points. This issue of sampling interval for the surfaces used in the present study will be analysed in detail in later chapters.

Many researchers have studied the problem of optimising sampling intervals for several different surfaces and utilising a variety of instruments. In the main, studies have been confined to stylus measurements [51], using spectral analysis [52], linear interpolation [53], parameter variation [54], cumulative power spectra and deep valley analysis [55]. Stout et al [41] concluded that choosing optimal sampling intervals for practical applications was not a trivial affair and that experience is necessary. Further useful recommendations were made; in particular that setting the intervals in both orthogonal directions equal is acceptable for both isotropic and anisotropic surfaces. The issue of sampling interval for the surfaces used in the present study is analysed in detail in chapter 4.
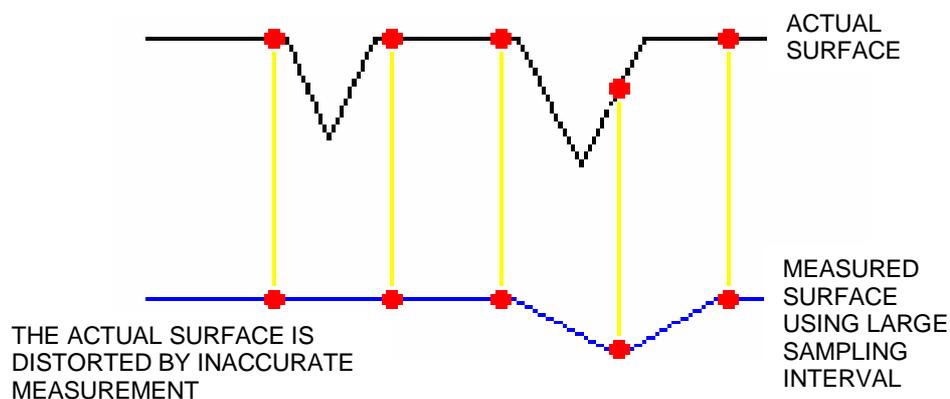
Figure 2.26: Aliasing: the effect of using a large sampling interval for surface measurements

2.4.3   Quantitative Characterisation of Surface Topography

In the past many common finishes have been defined in terms of a two-dimensional parameter value, i.e. R_a and R_q. It is now accepted that the difference in surface topographies with the same R_a value is too variable to be used as an acceptable functional characterisation tool, figure 2.27 [41]. R_a purely measures average surface heights; it takes no account of peak asymmetry or peak spacing. Since the growth and improvement of digital computers there have been significant changes in the way that surfaces can be measured and viewed. Three-dimensional techniques had always needed too much processing power to be commercially or computationally viable but the 1980's developments in computing changed this and from the 1980's 3D surface metrology instruments became increasingly widely available.
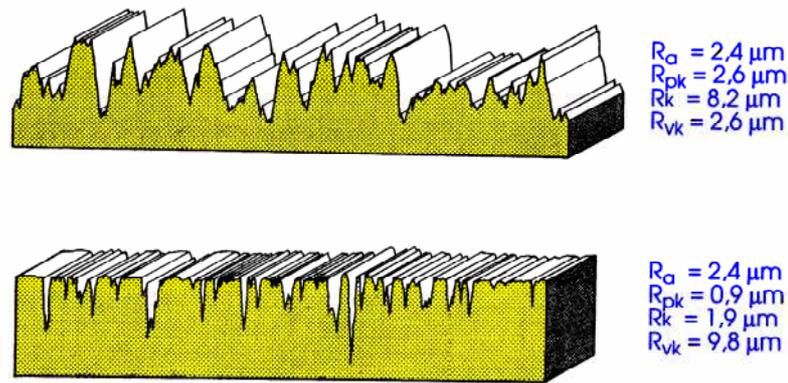
Figure 2.27: The ambiguity of 2D parameters: different surfaces, same R_a [39]

It is now accepted that the characteristics of a surface cannot be completely interpreted without three-dimensional information, as important features can be missed or misinterpreted using two-dimensional profiles and various models that have tried to study performance using these have failed. Pfestorf et al [56] studied two textured metal surfaces, laser and electron beam textured (EBT). Due to the deterministic properties of these finishes (patterned or structured), the common 2D parameters were deemed unsuitable for clear characterisation. Anamalay et al [57] deemed 2D profilometer measurements limited for surface feature recognition for machine wear characteristics and used instead a laser scanning confocal microscope, producing 3D data sets but still calculating 2D parameters (it is assumed that this was due to the non-standardisation of 3D parameters at the time). Sullivan et al [58] stated that 2D representation of 3D surfaces could be misleading and used a 3D surface analysis system to study the surface geometry with a view to estimating contact regions. For the detailed study (metal pipe joints) the authors show that 3D characterisation is essential for the prediction of joint performance.

There has been some previous work using 3D measurements for characterising the 2B finish [59] but a criticism of this investigation was due to a problem in the sampling conditions used (conditions were not chosen with reference to the important features of the surface but based on the limits of the instrument available). This is an area of 3D techniques that is becoming increasingly important as the shift from 2D continues. The influence of sampling on 3D measurements is more significant and the emphasis for this investigation is on devising the correct sampling methodology for the surface being measured.

It is also being suggested that the 'parameter rash' that occurred in 2D measurements [60] be avoided by standardising 3D parameters before the techniques have widespread use. This implies that before developing new parameters it is vital that original parameters are checked to ensure their functional significance before further 3D parameters are developed [35].

Further detail of 2D and 3D parameters is given in section 2.4.5 Characterisation.

2.4.4 Filtering

Measured topography data contains three major pieces of information – roughness, waviness and form. Surface roughness relates to the closely spaced, short wavelength features that are

left on the surface by the process of production, i.e. machining marks or, in the case of 2B stainless steel, plateau roughness and valleys. Waviness is the component of surface texture on which the roughness is super-imposed. In general, waviness refers to longer wavelength irregularities caused by vibrations or deflections in the machining or rolling process. The general shape of a surface is termed form and is not usually considered a part of surface texture. Roughness and waviness are super-imposed on the form, see figure 2.28, which is usually either purposely added to the component (the curve of a cylinder liner) or an undesirable deviation of shape resulting from insufficient rigidity of support in the production process (i.e. surface tensioning lost in rolling process).
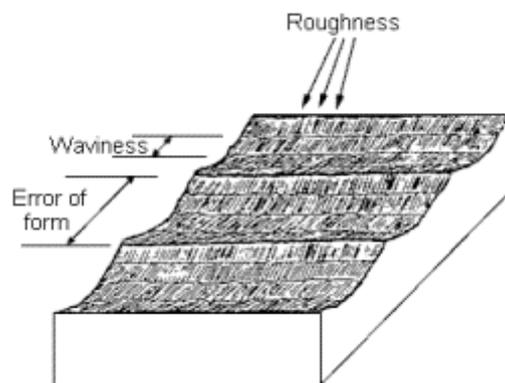
Figure 2.28: Roughness, waviness and form of surface topography data [16, 61]

In order to examine surface roughness the form and waviness components must be removed from the data set before analysis. Firstly, the reference datum for analysis and topography characterisation must be decided. Previous research [41] suggests that the least squares mean plane be used.

The least squares mean plane has a recognised mathematical definition, 'a plane such that the sum of the squares of asperity departures from this plane is a minimum'. A full discussion of its advantages compared to the other popular methods is given in [41]. The plane can be used as a levelling plane, to remove tilt from the data set. Further digital filtering can be employed to separate the components of waviness and roughness. There are many considerations when selecting filters, most importantly that they should be chosen with the application of the data in mind. There are numerous filters that have been developed or expanded for 3D characterisation [62].

Discussion here is limited to two of the most used digital filters, the Gaussian and the robust Gaussian. Stout et al [41] recommend the use of the Gaussian filter saying, 'The Gaussian filter is ideally suited for smoothing surfaces with rich features.' Surface roughness and waviness can be separated with no phase distortion in a single filtering procedure. It is essentially a low-pass filter. This method of filtering is strongly based on the assumption that the micro-geography of the surface is constructed of similar sinusoidal waveforms with various wavelengths, which most are not. This can result in significant topographical features being averaged out giving a distorted filtered surface for analysis. It is also not fully suited for nano-surface characterisation

unless it can be proven that the nano-surface itself obeys Gaussian distribution rules. These factors are the driving force behind current filtering research projects, allowing effective dominant feature separation. Multi-scalar functional surface filtering, nano-surface analysis and robust filtering techniques are being investigated. Some of the more relevant, new techniques include the robust Gaussian filter and 3-D envelope filters (part of the e-system [63]) and wavelet analysis.

Robust filters are currently being developed for use in the analysis of surfaces that have significant extreme data points. The special filter according to DIN 4776 [64] has in the past, filtered multi-processed surfaces like plateau honed cylinder bores, so called 'functionally stratified' surfaces. The influence of the outliers results in a filtered surface that is skewed and therefore is not subject to normal random error assumptions.

The Gaussian filter distorts the significant outliers, or pits, on the surface. The low weighting of the pit areas on the above surface by the robust Gaussian filter results in an accurate reconstruction of the surface after filtering. Figure 2.29 [62] clearly shows the difference between a standard Gaussian filter and the new robust Gaussian filter.

The newly developed robust Gaussian filters overcome the significant problems associated with the standard Gaussian filters:

➢ The effect of extreme data points (outliers) is reduced.
➢ The effects of edge distortions are largely eliminated thus allowing all of the measured data to be used in the surface characterisation.
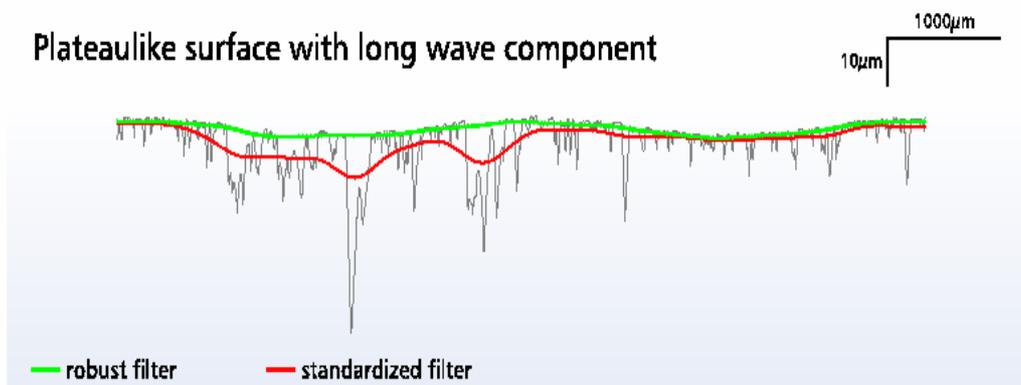
Figure 2.29: The difference between Standardised and Robust Gaussian filters

The principle of the rolling ball filter in 2-D, or envelope system is show in figure 2.30. This method is very functional as it is based on actual physical contact. In 2-D it is visualised as a circle, having a specific radius r or R, traced over the topography of the surface and contacting at certain points. The reference lines, or the filtering planes, are the loci of the rolling circles. Extended to 3-D with a rolling sphere on a plane, this method gives a useful functional simulation of contact. Development of these filters was part of the part of the EC project number 3374/1/0/170/90/2 [65].
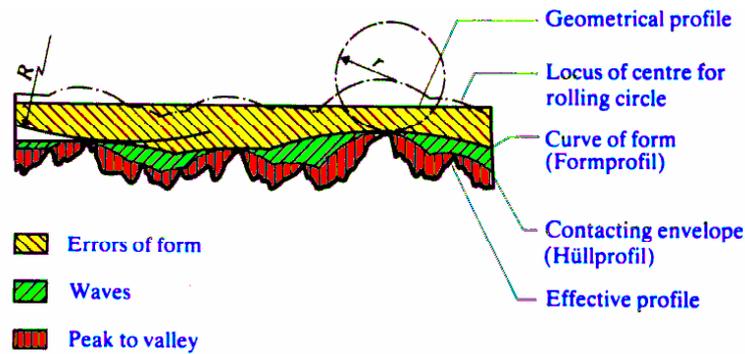
Figure 2.30: The effect of the Envelope system on surface topography data [49]

Wavelet analysis can be used to decompose a surface signal into the scale-space, without an assessment of frequency content of the original signal. In this case, the surface topography can be interrogated via a flexible transmission bank according to intended functional information that is required to be drawn from it. The roughness, waviness and form information involved in surface topography are separated and recovered respectively. The multi-scalar functionally relevant topographical features are identified and captured. The main difference between wavelet analysis and classical Fourier analysis is that Fourier analysis is a breakdown of a signal into a series of harmonic content, and then this space-based information is transferred into frequency-based information. The limitation of Fourier analysis is that it can only identify frequency events over space without any information about local position. Wavelet analysis can overcome this problem. In wavelet analysis, the space-based information is then transferred into scale-based information, which provides not only the frequency events of the original signal but also keeps their location properties completely identified. Another useful property is that there is no distortion of the data boundary. As a result, specific topographical features can be identified with very little or no prior frequency information. Due to this ability, wavelet analysis will become a very powerful tool in surface texture analysis in the future. It is possible that wavelet analysis will become a general surface filtering method and it will be used in primary roughness separation through to topography pattern recognition (paragraph from [66]). Currently, however, as development of these filters progresses, little proof of their success is available.

2.4.5 Characterisation

Surface characterisation can be achieved in several ways. Classification is usually made between methods by examining their scale dependency. Figure 2.31 shows some of the most popular methods for obtaining information about surface topography.

Currently, the finishes produced on stainless steel by cold rolling are not normally subject to any quantitative specification, except possibly comments (based on visual examination of reference samples) on relative 'dullness'. In the main they are visually inspected for defects and possibly mentally compared to the usual finish produced. Obviously, skilled and experienced personnel

do this and although it is reasonable to say if the finish is incorrect, the causes and effects of certain differences cannot be speculated on.
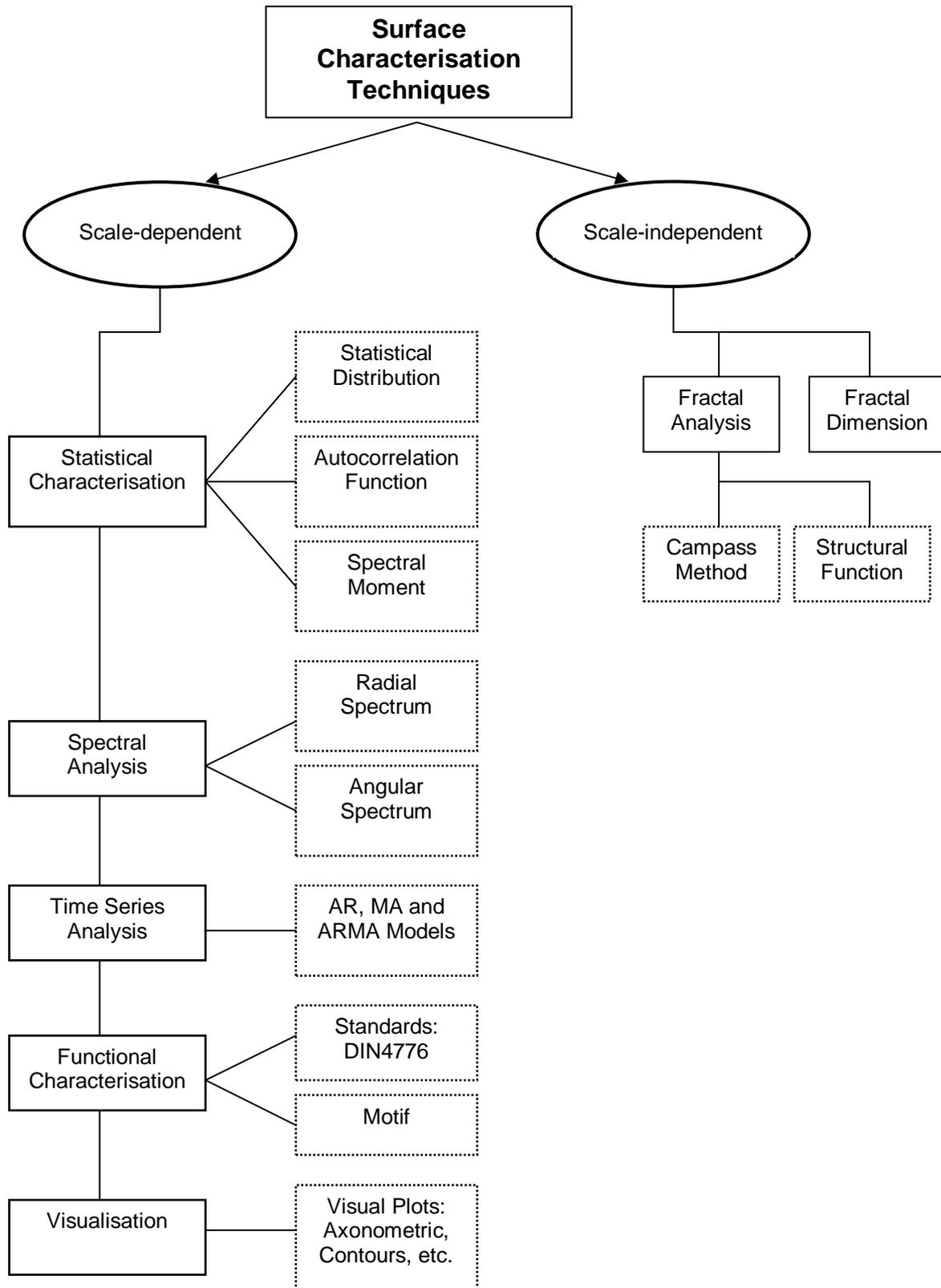
Figure 2.31: A classification of the popular surface characterisation techniques (adapted from [41])

Two-dimensional profiles have usually been analysed using statistical, spectral or time series analysis techniques. The latter two methods will not be discussed here, as they are deemed not relevant in this project. Further discussion of the methods can be found in [67 and 68].

The statistical parameters that refer to different parts of the signal from the instrument begin with different letters:

- **R** for roughness
- **W** for waviness
- **P** for the primary profile

Established 2-D statistical descriptors include R_a and R_q, etc., which are embedded in many standards. Historically, R_a, the arithmetic mean deviation of the assessed profile, was one of the first parameters used to quantify surface texture. Unfortunately, R_a may be misleading in that many surfaces with grossly different features may have the same R_a, but function quite differently.
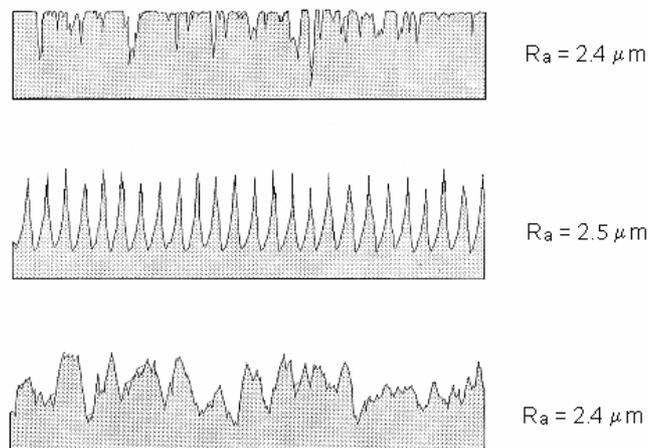
Figure 2.32: Three distinctly different profile shapes with similar R_a values

R_a only quantifies the "absolute" magnitude of the surface heights and is insensitive to the spatial distribution and z-direction of the surface heights (a deep valley will result in the same R_a value as a high peak). Despite its shortcomings, R_a is a good, simple monitor of changes during production of the surface. R_q, the standard deviation of the profile height distribution suffers from the same drawbacks as R_a, but is more sensitive to outlying features because of the squared term.

The two other common amplitude parameters are R_{sk}, skewness and R_{ku}, kurtosis (the second and third moments of the profile height distribution). The skewness, R_{sk} is a measure of the asymmetry of the profile about its mean line. Negative skew indicates a predominance of valleys, whilst positive skew is seen on surfaces with more peaks. When the surface texture is composed of non-normally (or non-Gaussian) distributed high peaks or deep valleys, the kurtosis, R_{ku} becomes very large (i.e. »3). When the surface is composed of a slowly varying, "rolling" hill type texture, the kurtosis will be less than 3. A kurtosis of ~3 indicates that the

surface distributions are Gaussian in nature. R_{ku} is a good indicator for when an otherwise Gaussian distributed surface may have some defects.

The typical spacing parameter is R_{sm} is the mean distance between peaks and there are two usual hybrid parameters, the average profile slope, Δa (the mean of the slopes of individual profile facets) and the root mean square profile slope, Δq. Other common 2D parameters are related to the bearing ratio curve and are known as the R_k parameters [70] and are described at the end of the characterisation section on page 49 and in table 2.5. For further details and equations of the common 2D parameters, refer to appendix 4.

A comprehensive survey of academic and industrial research trends on 3D parameters was carried out in 1992. This resulted in the modification of a draft proposal for 3-D parameters [41], based on a project supported by the Commission of the European Communities for which a primary set of 14 parameters was proposed. Further to this report, a modified 'field set' of parameters was finalised, and can be seen in table 2.4.

Some of the 3-D parameters have been extended from their 2D equivalents whilst others were specifically developed for use with 3-D topography data. The original recommendation was that all of these new parameters were denoted by an 'S' (for surface) instead of the conventional 'R' (for roughness) in their 2-D counterparts. Most of them are, but the new 'volume family' parameters are denoted by a 'V' (for volume). There are five parameters describing the amplitude properties, three describing the spatial properties, three hybrid parameters describing properties which are affected by either amplitude or spacing or both, a set of curve and related descriptors (including two curves) which include the five volume family parameters and three linear areal material ratio curve parameters, a group of slope and fractal functions and two other parameters, which have been included because of the popularity of their 2D counterparts. Detailed definitions of the most commonly used 3D parameters can be found in appendix 5 and further information in [35 and 41].

Table 2.4: Field set of 3-D parameters [65]

Family	Parameter name	Nomenclature and Units
Amplitude Parameters	Root mean square deviation	S_q (µm)
	Skewness	S_{sk}
	Kurtosis	S_{ku}
	Maximum peak height	S_p (µm)
	Maximum valley height	S_v (µm)
	Maximum height of texture surface	S_z (µm)
Spacing Parameters	Density of Summits	S_{ds} (1/mm^2)
	Fastest decay auto-correlation length	S_{al} (mm)
	Texture aspect ratio	S_{tr}
Hybrid Parameters	Arithmetic mean peak curvature	S_{sc} (1/µm)
	Root mean square slope of the assessed texture surface	$S_{\Delta q}$
	Developed interfacial area ratio	S_{dr} (%)
Curve and Related Parameters	Areal material ratio of the texture surface	S_{mr} (curve)
	Inverse areal material ratio of the texture surface	$S_{mr\%}$ (tp%)
	Areal material ratio curve of the texture surface	(curve)
	Linear areal material ratio curve parameters	S_k, S_{pk}, S_{vk}, (µm) S_{Mr1}, S_{Mr2} (%)
	Areal height amplitude curve	(curve related)
	Void volume	V_v (tp%)
	Material volume of the texture surface	V_{mp} (µm^3/mm^2)
	Core material volume of the textured surface	V_{mc} (µm^3/mm^2)
	Core void volume of the texture surface	V_{vc} (µm^3/mm^2)
	Valley void volume of the texture surface	V_{vv} (µm^3/mm^2)
Slope & Fractal Methods	Slope histogram	(histogram)
	Volume scale plot	S_{vs} (s) plot
	Fractal dimension	S_{fd}
Other Parameters	Texture direction of the texture surface	S_{td} (deg)
	Ten point height of surface	S_{5z} (µm)

Other 3-D parameters have been investigated since this set was devised. One of the most interesting (in the present context) is the Wihlborg-Crafoord index (WC_{index}) [20]. Wihlborg and Crafoord use the index to describe the frictional behaviour of a sheet and tool in a contact situation. It is defined as the number of isolated oil pockets ($NIOP_t$) multiplied by the border length of the lubricant area at the area fraction of contact ($BL\alpha$) and divided by the area fraction of contact (α); see equation 2.3. The index gives information about the degree to which the contact zones will be supplied with lubricant.

$$WC_{index} = \frac{NIOP_t \times BL_\alpha}{\alpha} \qquad \textit{Equation 2.3}$$

Where:

$NIOP_t$ = number of pockets required to achieve micro plasto hydrostatic lubrication (MPHSL)

$BL\alpha$= amount of possible sources for MPHSL to set in and

α= the amount of material supplied with lubricant by the two components

The total number of isolated oil pockets was used separately by Wihlborg and Crafoord [20]. A pocket is defined as having at least two connected data points that are located at a lower height in the topography than the evaluation height, which corresponds to the area fraction of contact. Their chosen truncation level in this case was 10nm, based on the size of the utilised lubricant molecules and the vertical resolution of the instrument used (Somicronic 3D, resolution 4nm). It is also stipulated that oil pockets should not have contact with the edges of the measurement, although no functional explanation is given.

The WC_{index} is used to describe the frictional behaviour, instead of simply the number of isolated oil pockets, as it gives a relationship between the density of oil pockets and the border length at contact, therefore including lubricant behaviour in the MPHSL regime (given by $NIOP_t$, [69]) with the micro plasto hydrodynamic lubrication (MPHDL) regime.

Visualisation methods are vitally important in 3-D surface analysis, far more than for 2-D profile analysis. In fact it is sometimes considered the only objective in using 3-D methods and is certainly accepted as the only adequate way to gain a full appreciation of a surface's topography. New computer technology has led to an increase in the use of visual techniques and the development of sophisticated hard and software means the methods are both powerful and flexible in the representation and manipulation of surface topography data.

Finally and perhaps most importantly for this project, there are various functional characterisation techniques to consider. The main methods are those outlined in DIN 4776 [70] and motif combination [41, 65 and 71].

The functional characterisation method proposed by Bodschwinna [72] and standardised in DIN 4776 was designed for use with highly stressed surfaces that are relatively flat on top and highly grooved or pored at the bottom. The standard defines a series of parameters, R_k, R_{pk}, R_{vk}, Mr1 and Mr2, collectively known as the R_k parameters. They are derived from the profile Abbott-Firestone curve (or Bearing Area curve) assigning them individual functional roles, see figure 2.32.
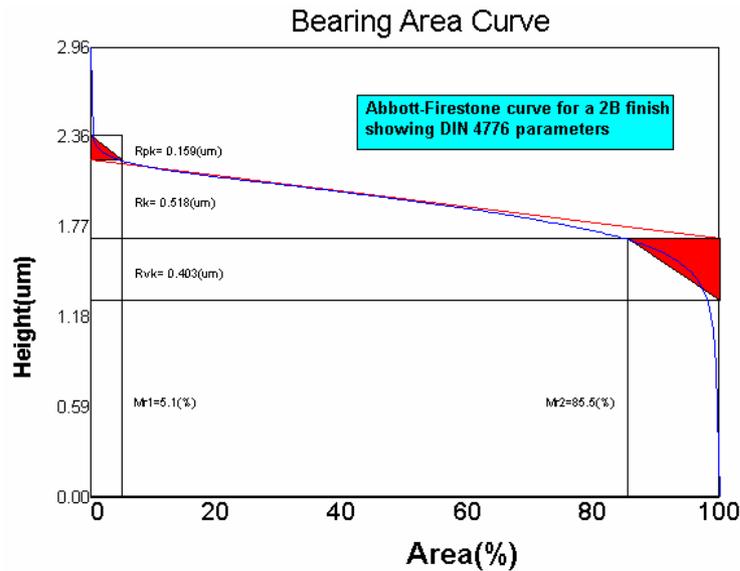
Figure 2.33: Graphical representation of the DIN 4776 parameters

Table 2.5 outlines the standard DIN 4776 parameters with a brief description of their functional significance. Care must be taken when analysing surfaces with these parameters as a double-step process, reducing the significant outliers has to be adopted for highly grooved surfaces before the Abbott-Firestone curve is calculated. This procedure is standardised in DIN 4776 [70].

Table 2.5: Description of DIN 4776 parameters (adapted from [41])

Notation	Name	Meaning	Function
R_k	The core roughness depth	Measures the height of the core material portion	Small R_k gives rise to a high mechanical resistance and high load carrying capacity during contacting operations
R_{pk}	The reduced peak height	Denotes the height of the profile peak projecting beyond the core profile	Small R_{pk} values mean a surface will have good running-in properties with respect to surface geometry
R_{vk}	The reduced valley depth	Denotes the proportion of profile valleys extending into the material below the core profile	Large R_{vk} values mean a surface has good oil retention properties
Mr1	Peak material ratio	Bearing area point	See figure 2.33
Mr2	Valley material ratio	Bearing area point	See figure 2.33

This characterisation method is easily extendable for use in 3-D surface metrology. However, the filtering requirements have not yet been standardised for this use. The reason for looking briefly at this technique in this project is its effectiveness in the analysis of surfaces with relatively flat tops and grooves, similar to the plateaus and valleys seen on the 2B surface.

The motif combination method is also useful for analysing data with significant outliers (the deep valleys). Motifs were first introduced in 1982 [73] with the definition: 'the motif is the part of a profile between two peaks'. The technique is essentially a pattern recognition exercise that was developed in the French automobile industry. Motif combination is reportedly a complementary approach to solving specific technical problems and useful for characterising non-Gaussian height distribution surfaces. The 2-D motif was established experimentally although Scott [71] has developed a general theory for the method. Taylor Hobson Ltd. is currently investigating the 3-D (or areal) motif combination procedure as part of the project EC number 3374/1/0/170/90/2. The most recent findings are detailed in [65], with background on motif combinations in 2-D in [41].

2.5. Overall Aims and Objectives

2.5.1 Aims

The overall aim of this research project is to characterise quantitatively the developed surface topography of some widely used finishes on stainless steel sheet using three-dimensional surface analysis techniques. Based on this surface characterisation an attempt has been made to identify 3D parameters for quantitative description of stainless steel sheet with respect to some aspects of their functional performance.

2.5.2 Objectives

Using the 3D techniques available, define a measurement strategy and protocol to effectively measure stainless steel sheet topography.

Investigate the differences in topography across a range of grades and gauges of stainless steel using 3D topography parameters.

Investigate the ability of 3D topography parameters to correlate with functional requirements of lubricant retention, optical appearance and corrosion.

Develop a set of written procedures for industrial application to effectively characterise stainless steel sheet surface roughness.

Chapter 3   The 'Functional' Surface Models

3.1. Summary of the Chapter

The functional topographical features of four finishes are determined, with respect to the process/es by which they were made. A model of the surface topography is developed for WHB (white hot band), 2B, BA (bright annealed) and a unidirectional finish (brushed) encompassing the usual features of the topography and variations in the topography caused by production or 'defects'. The functional features are discussed and predicted relevance is presented.

3.2. Introduction

In this chapter the functional, topographical features of four finishes, which are the subject of the present study, are discussed with respect to the processes by which they are manufactured. A model of the surface topography, based on initial inspection of the surface (by SEM and 3D techniques), is developed for WHB (white hot band), 2B, BA (bright annealed) and a unidirectional finish (brushed). The models encompass the usual features of the topography and variations in the topography caused by production 'defects'. The functional features are discussed and predicted relevant parameters are presented. Particular attention is paid to the 2B finish, being the principal product of Outukumpu.

3.3. White Hot Band (WHB)

3.3.1   Review of WHB Production

White hot band material is produced by hot rolling, annealing and descaling continuously cast slabs or bloom and is typically 5 – 10mm thick. During hot rolling, the length of the coil is increased as the gauge thickness is decreased. Bulk deformation of the material occurs, whereby many of the original surfaces' features are consolidated. Due to the heat used in this process and the following annealing, a thick, black, oxide scale is formed on the surface (this material is known as black hot band), which must be eradicated before cold rolling. The cleaning regime to yield the white hot band material is achieved by using aggressive shot blasting (loosening the scale) and finally acid pickling (eradication of the scale).

3.3.2   Model of the Surface Topography of a WHB Surface

A model of the typical surface topography of the white hot band material is determined by initial inspection of the surface with reference to the process by which it was developed. SEM images of the surface at different degrees of magnification show mainly severe shot blast damage. Shot blasting leaves a distinctive topography consisting of randomly spaced pits, which are created when the shot hits the surface. The size and shape of these pits is dependant on the type and size of shot used. Evidence of shot blasting with spherical shot can be seen on the white hot band surface using the interferometer, figure 3.1. Also evident on this surface are some small areas of rolled topography, where the rolls have made contact and the surface is 'smooth'. In these areas, viewed at higher magnification than the shot damage (figure 3.2), indications of the pickling process can be seen as the grain boundary regions have been removed (inter-granular attack). Rolling effects are not evident on the majority of the surface due to the production of the oxide scale during hot rolling which prevents the rolls from contacting the surface directly and the aggressive shot blasting marks are the most prominent features. Therefore the model is similar to that of a shot blast surface, with small plateaus of grains and the valleys created in pickling.
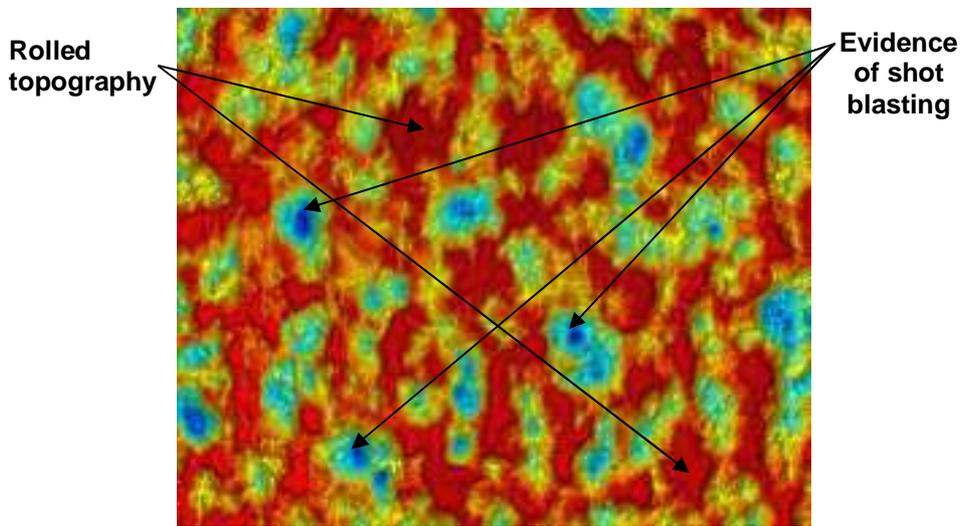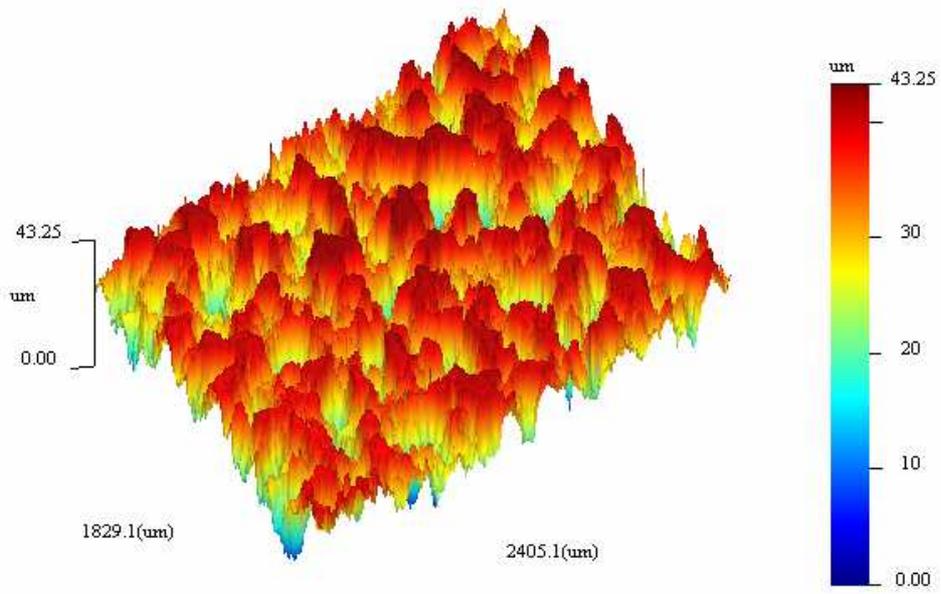
Figure 3.1: Axonometric and contour interferometer images of white hot band stainless steel topography
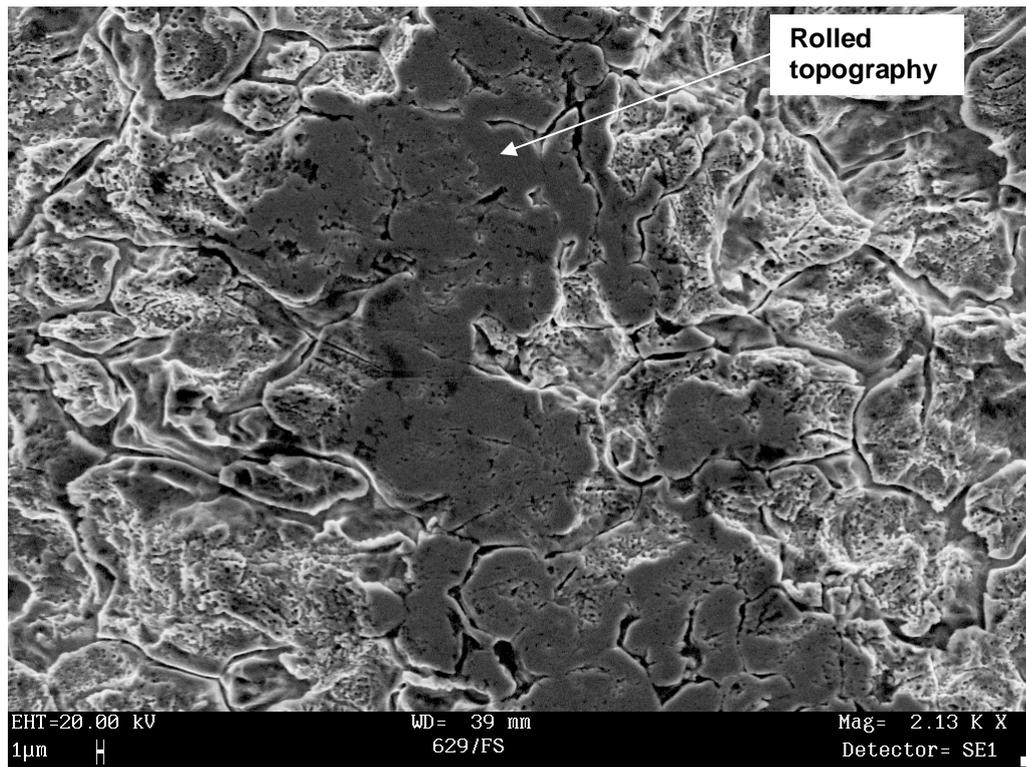
Figure 3.2: High magnification Scanning Electron Microscope image of white hot band stainless steel topography

3.3.3 Predicted Functional Relevance for WHB Features

The white hot band finish is used only as the raw product for further processing and therefore has limited functional relevance. The damage caused by shot blasting must be kept to a minimum to achieve good consolidation of the surface features in subsequent cold rolling operations, although evidence of remnant damage in other finishes is rare and the main features of interest are very deep, high aspect ratio pits on the surface that are difficult to consolidate.

3.4. 2B

3.4.1   Review of 2B Production

The 2B finish is produced by cold rolling the white hot band, producing coils that are of approximately final gauge, typically 0.7 – 5 mm thick. Cold rolling the coils also improves the surface finish, as asperities are flattened and pits consolidated, The coils are then annealed to alleviate work hardening, which forms another black oxide scale on the surface. The scale is removed by acid pickling only at this stage, since shot blasting would cause damage to the surface. The coils are then finished by skin passing or tension levelling.

3.4.2   Model of the Surface Topography of a 2B Finish

A model of the typical surface topography of 2B material is determined by initial inspection of the surface with reference to the process by which it was developed. SEM images of the surface at different degrees of magnification show that the original white hot band surface features are usually effectively consolidated during the cold rolling operation, figure 3.3. The pickling procedure creates a matrix of valleys, which tend to be approximately 'V' shaped. The valleys are located at the grain boundaries of the stainless steel, which are chromium rich. During pickling these grain boundaries are preferentially etched giving the network of valleys. The remaining surface grains that are unaffected by the pickling process are relatively flat and plateau-like due to the final finishing operation, although at higher magnifications (figure 3.4) micro roughness (particularly deep, small area pits remnant of the hot band surface) is evident on these plateaus. Therefore the model, figure 3.5, includes plateaus with micro roughness and a matrix of interconnecting valleys.

EHT=20.00 kV   WD= 19 mm   Mag= 1.99 K X
3μm ⊢   629/FS   Detector= SE1
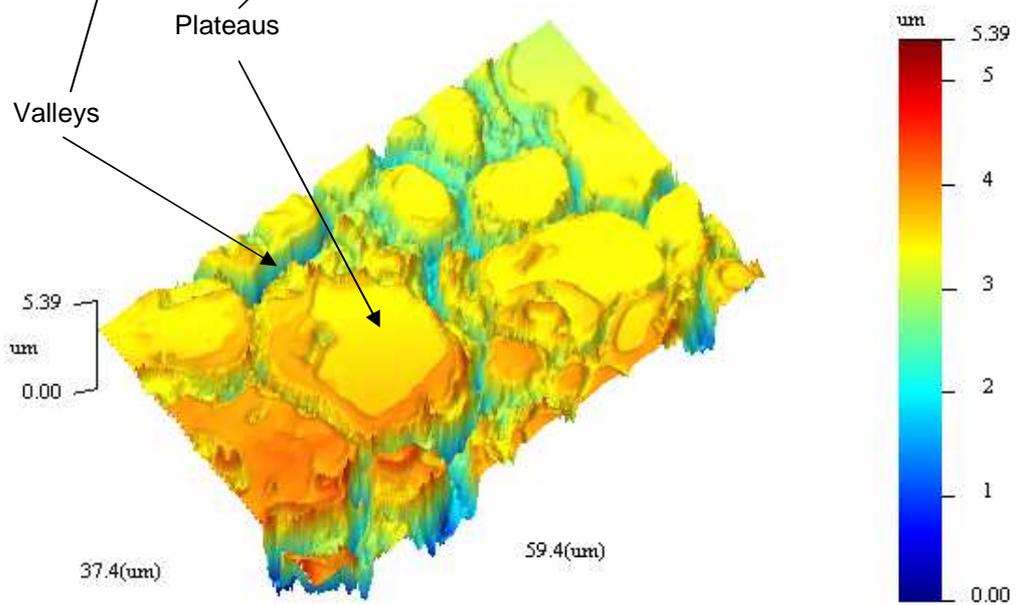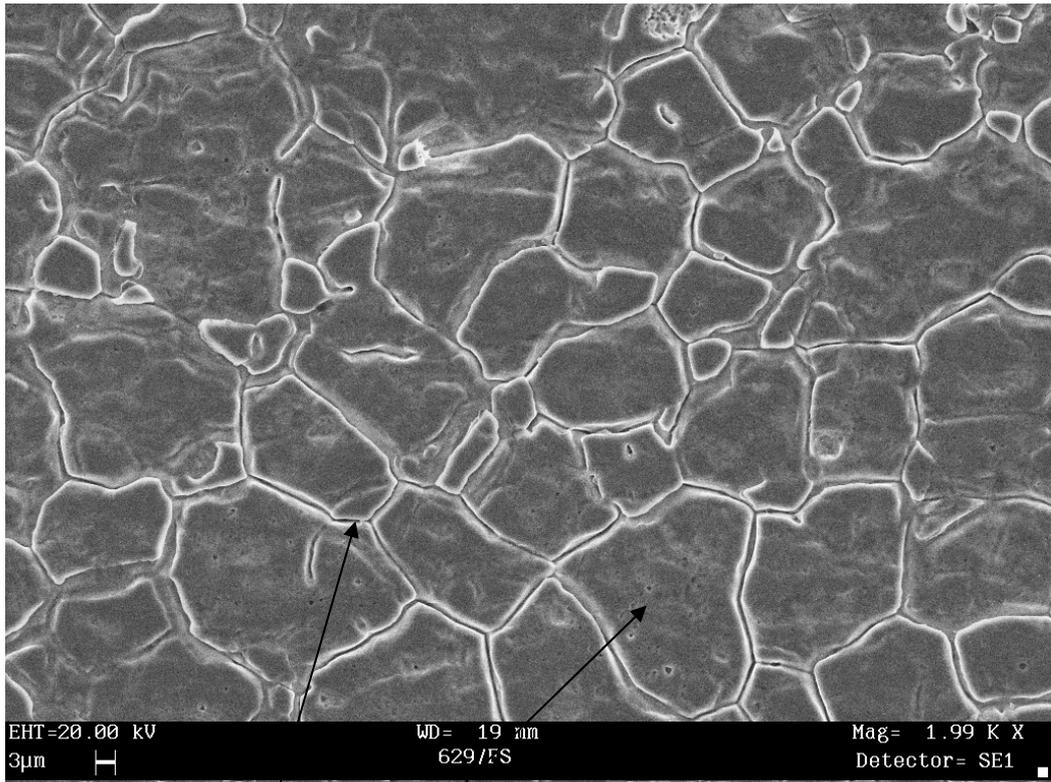
Plateaus

Valleys

Figure 3.3: SEM and interferometer images of 2B surface finish on stainless steel showing relatively flat plateaus and matrix of valleys
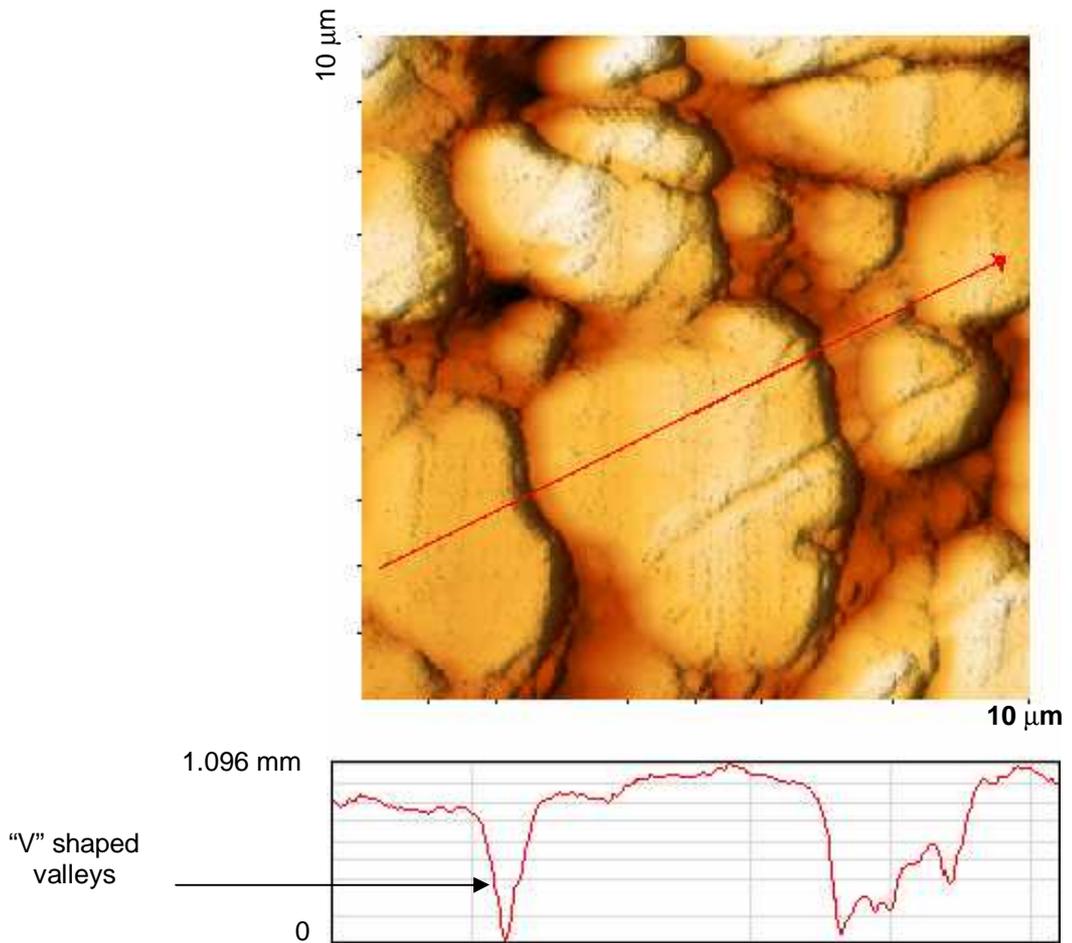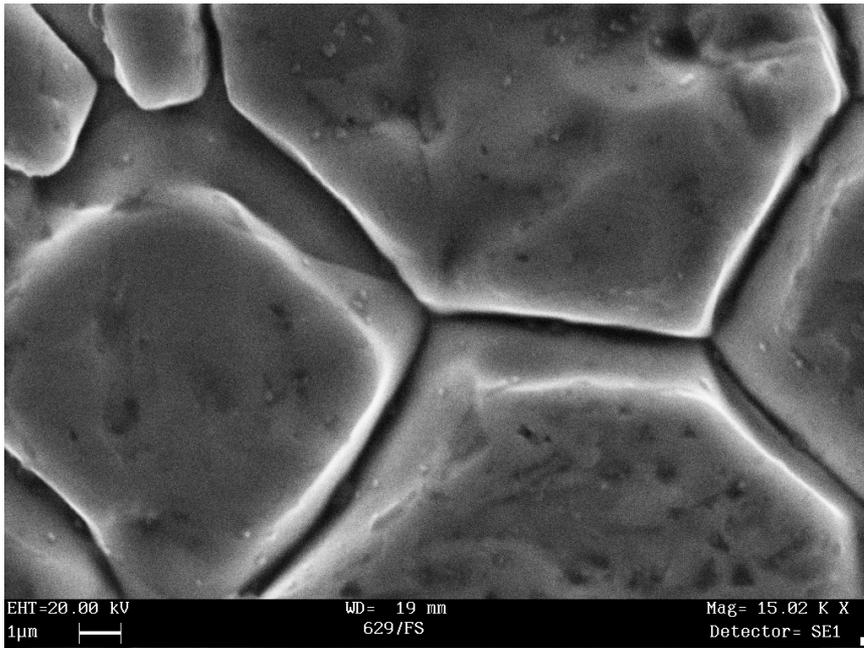
Figure 3.4: SEM and AFM images of a 2B surface finish on stainless steel showing plateau micro-roughness
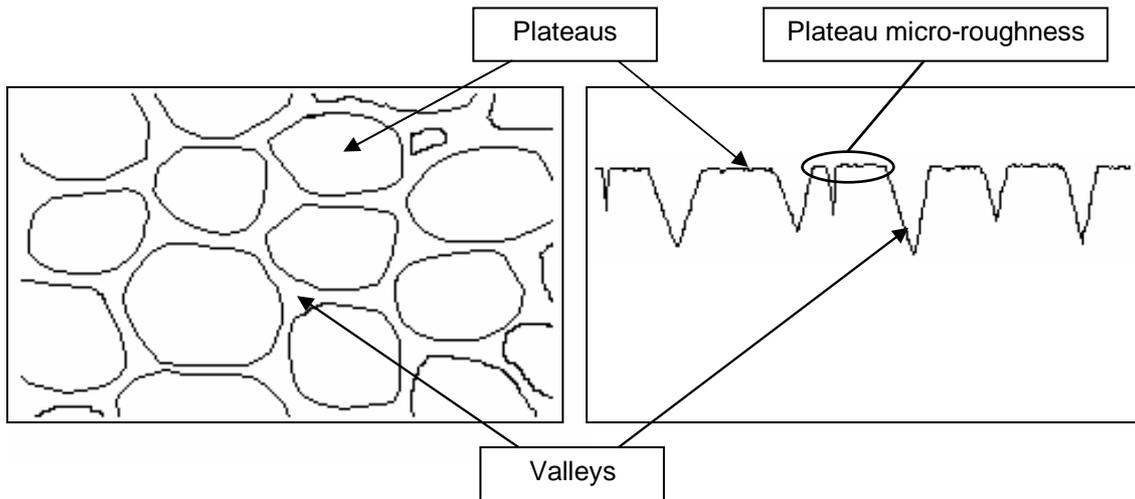
Figure 3.5: The developed model of the 2B surface finish

3.4.3   Predicted Functional Relevance for 2B Features

The 2B finish has been used in general industrial applications, like vessels and pipe work, for many years and is still the largest constituent of production for Outukumpu. It is not generally used in food or chemical processing as the valleys in its topography make it more difficult to clean than finishes like bright annealed. Due to its origins, the finish is often chosen for its appearance where an 'industrial look' is desired, in applications like street furniture and lift interiors, etc. The relatively smooth plateau regions give the finish its distinctive reflectance. The interconnecting valleys can aid the spread of lubricant in forming operations like the deep pressing used to make sinks.

3.5. BA

3.5.1 Review of BA Production

The BA finish is produced by cold rolling the white hot band, in the same way as for the 2B finish. The coils are then annealed in a controlled atmosphere where the final oxide film is thin and protective so no further descaling treatment is required. In this annealing method no scale is formed since no oxygen is present in the process and therefore descaling by pickling is not required.

3.5.2 Model of the Surface Topography of a BA Finish

A model of the typical surface topography of BA material is determined by initial inspection of the surface using an SEM and interferometer. The cold rolling procedure consolidates the majority of features from the white hot band surface topography and the controlled annealing procedure brings new grains to the surface by the process of recovery (recrystalisation). This means that the main features of the BA surface topography are those developed in the annealing process, although some remnant hot band features may be evident, figure 3.6a. The thermal effects of annealing in a controlled atmosphere produce a surface with a very smooth, mirror-like finish, with few visible features, figure 3.6b. At higher magnifications, some can be seen, figure 3.6a. The surface model is therefore almost flat, with occasional raised grain boundaries, figure 3.7.
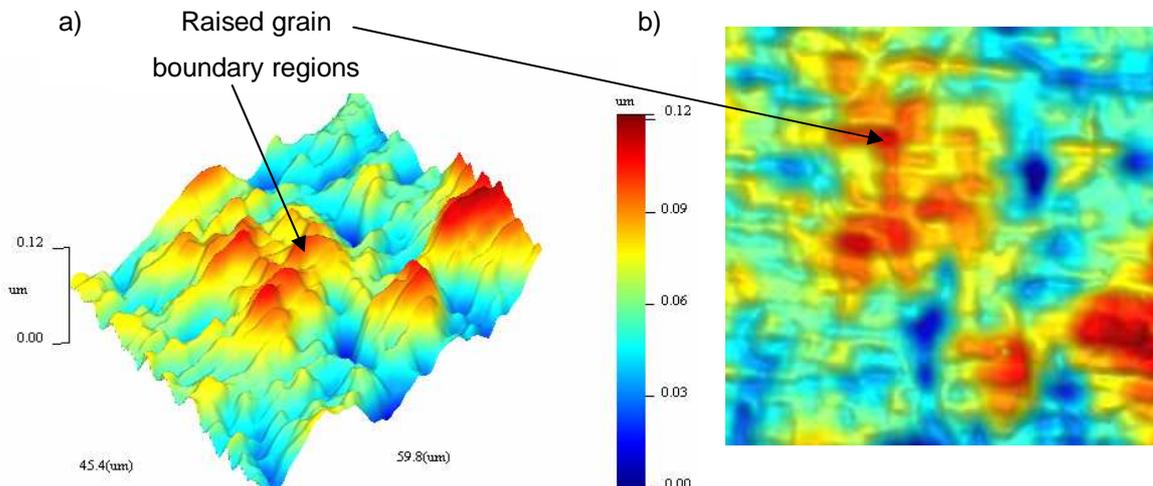
Figure 3.6: Interferometer images of the BA surface finish on stainless steel showing the effects of processing
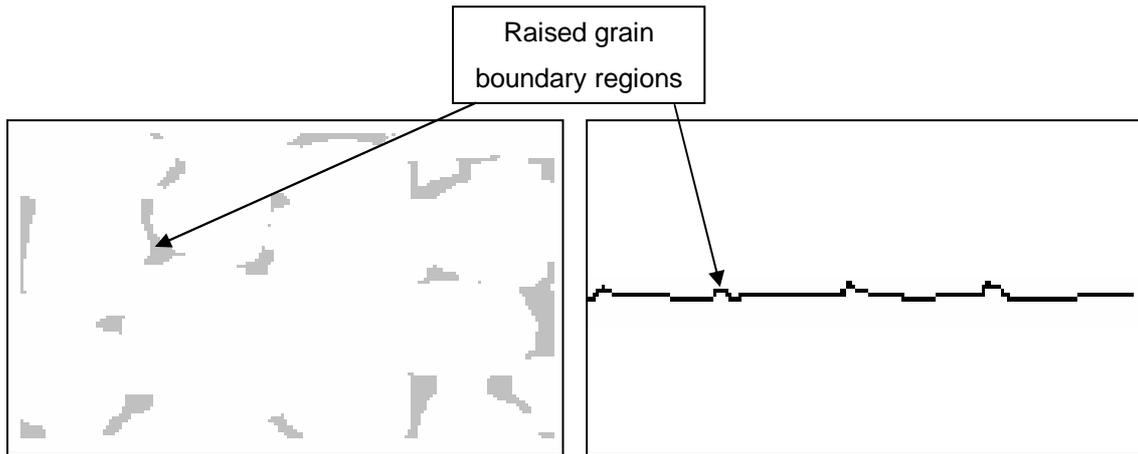
Figure 3.7: The developed model of the BA surface finish

3.5.3   Predicted Functional Relevance for BA Features

The BA finish is used where either cleanliness or appearance are important. The BA finish is hygienic and easy to clean because it does not have deep pits or valleys, where dirt could become trapped. It is however generally not used for large areas where appearance is important, as non-uniformity in the finish is obvious. The smooth topography is also prone to fingerprinting as the natural oils sit on the surface, rather than spreading into pits or valleys.

3.6. Unidirectional (Brushed)

3.6.1   Review of Brushed Finish Production

There is a range of standard unidirectional finishes available, but they are all commonly produced using either 2B of BA product as a precursor material. The final finish is normally produced using different types of brushes or grades of glass paper. In this instance we will consider the unidirectional finish produced by brushing on a 2B base.

3.6.2   Model of the Surface Topography of a Brushed Finish

A model of the typical brushed surface topography has been developed by studying SEM and interferometer images. The majority of the surface has unidirectional troughs and ridges, similar to those of a ground finish but on a smaller scale, figure 3.8. The troughs vary in size and depth and since there is no further processing, the ridges have rough edges. The brushing is soft and so the base 2B topography is also evident on the surface, particularly the etched grain boundaries, which are too deep to be affected by the bristles, figure 3.9. Therefore the model is mainly troughs and ridges with remnant 2B features seen aerially, figure 3.10.
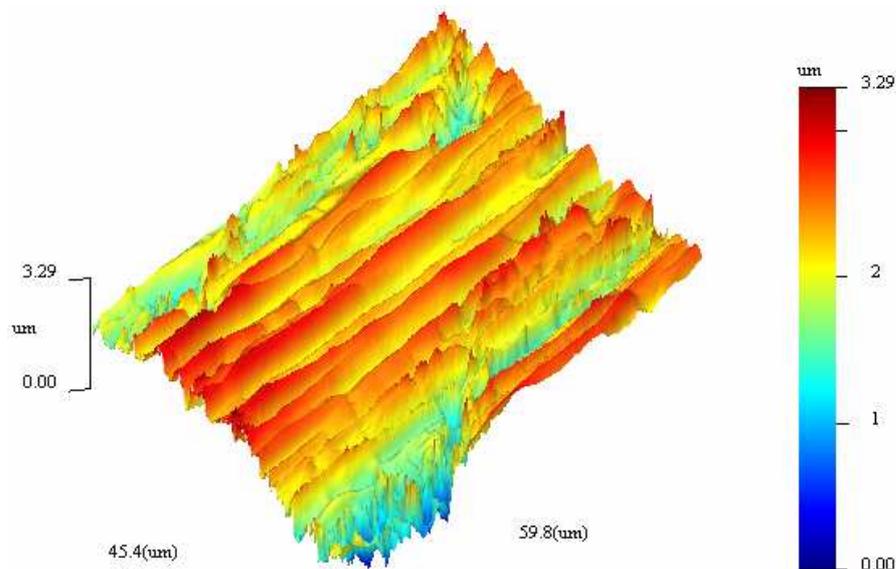
Figure 3.8: Interferometer image of a brushed finish on stainless steel showing unidirectional troughs and ridges
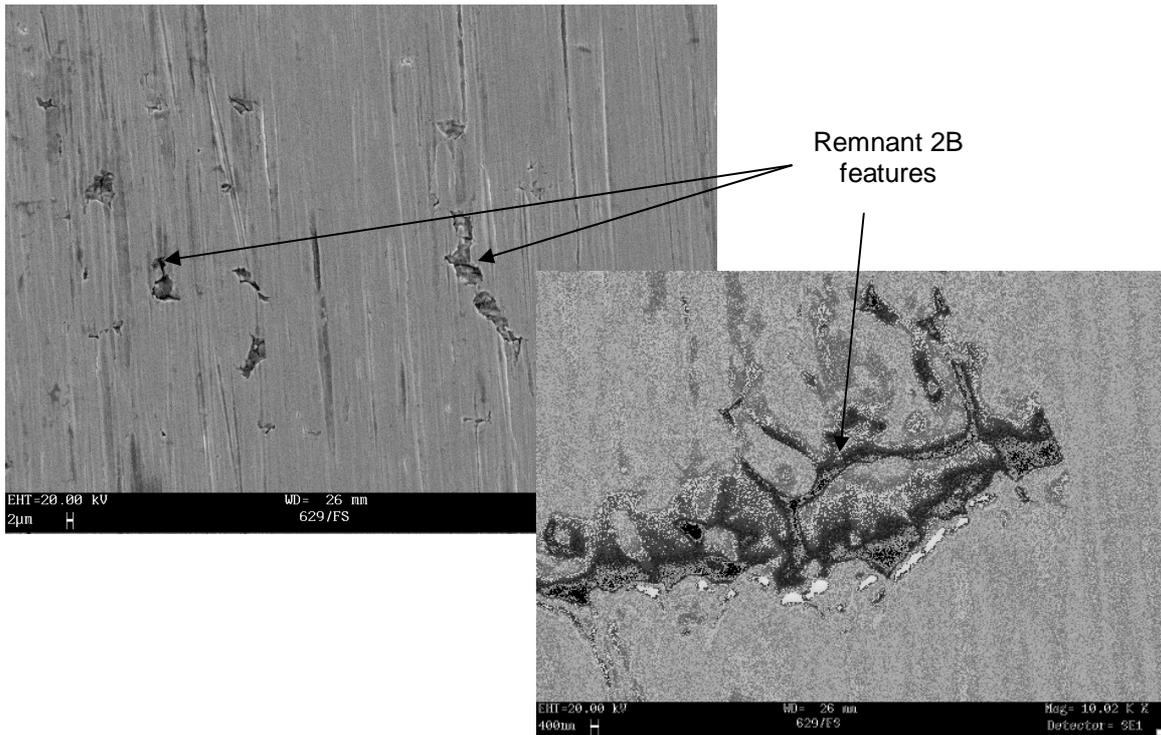
Figure 3.9: SEM images of a brushed surface showing remnant 2B features
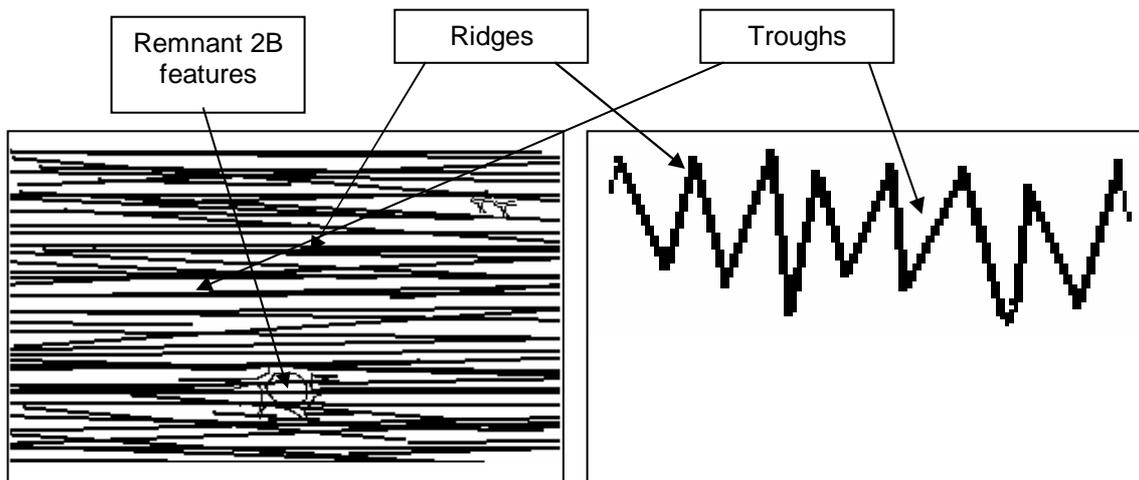
Figure 3.10: The developed model of a brushed surface finish

3.6.3 Predicted Functional Relevance for Brushed Features

The main function of brushed finishes is aesthetics, although they are also popular in areas like kitchens due to their ease of cleaning. Brushed finishes are ideal for covering larger areas as minor variations in the finish are only seen if they impair the directionality, i.e. if they are perpendicular to the rolling direction.

3.7. Conclusions

This chapter has presented a series of models of the primary production surfaces produced by the sponsoring company, Outukumpu. The models provide a basis for further study of functional performance with respect to surface topography and give a foundation for drawing functional and metrological hypotheses for the following chapters.

Chapter 4   Measurement Strategy

4.1. Summary of the Chapter

The measurement strategy has been designed to ensure correct, accurate and relevant collection of topography data. Feature identification is carried out based on the surface model and the average sizes of the features are found. The protocol covers the selection of the correct measuring instrument based on the surface model and the size of the relevant functional features. Operational details of the measuring instruments available for this project are given (Somicronic stylus instrument, Taylor Hobson Talysurf stylus instrument, Wyko NT2000 optical interferometer and DME AFM) and variables for these instruments are discussed. The strategy includes a statistical method of assessing how many measurements are needed for a surface, which is presented for the 2B finish. Finally measurement method recommendations are made for each of the four finishes modelled in chapter 3.

4.2. Introduction

The 'usefulness' of measured data used to quantify surface texture is dependant on several factors:

  ➤ The quality of the measured data and the confidence level and repeatability of the parameters calculated from it.
  ➤ The repeatability of one measured data set (or set of parameters) to another.
  ➤ The ability to relate the measured features to their point of production or to their post process functionality.

In an effort to avoid producing data that is of little use to the project a measurement strategy is needed to address these issues. In addition, the developed measurement strategy can also be applied by the sponsoring company to their wider range of surface finishes. Firstly a protocol is defined, covering sample preparation and instrument selection. Secondly general instrument and measurement variables are presented, enabling a full strategy of measurement to be defined for each of the common finishes encountered by the sponsoring company.

4.3. Protocol

4.3.1   Sample Preparation

Obviously to aid in all of the issues of quality, repeatability and functional usefulness, the samples initial conditions must be free from external influences. This can be achieved by obtaining a good, undamaged sample of material (the sample must be of a suitable size for an SEM chamber, i.e. not bigger than about 100 mm square, depending on the instrument). Following this it is essential to clean the sample with a polishing cloth and solvent to remove any oil and using compressed air to blow away any pieces of loose dirt or contaminants.

4.3.2   Feature Identification

Firstly, to ensure that the measured data has a direct relationship to the process area or function of interest, qualitative identification of the dominant features of the topography that will affect them must take place. It is suggested that an instrument with a large range of area resolutions is utilised, such as an optical or scanning electron microscope.

Obviously, it is also desirable to measure the largest area possible; to get as many of the topographical variations as possible, but the importance of resolution is greater. Utilising an SEM to view the surface and analyse the features at different magnifications is the best option. Any significant features found should relate to the point in the production process where they were created. This initial analysis and feature identification has been carried out in chapter 3, where models of the topography of the common finishes have been developed.

The images should then be manipulated to include at least 10 features of interest on one view. A method of meshing the images obtained can be used as a manual assessment of the dimensions of the features of interest, a similar the procedure of ASTM E112-96e1 [75] is recommended. The average and minimum sizes of the features from at least 5 images should be calculated. In a general production environment this procedure need only be carried out on a few occasions in order to establish models of the surfaces to be tested or when new finishes are being developed. For example the 2B finish average grain size dimensions results from this type of analysis.

4.3.3   Instrument Selection

An instrument should be selected on the basis that the desired lateral and vertical resolution and range is achievable. In terms of the lateral and vertical resolution and range the Nyquist theorem states that for a periodic signal, the sampling interval should be smaller than half of the wavelength of the signal. Therefore, for a minimum features size of x μm, the first suggested sampling interval is x/2 μm.

The sample should then be measured and a frequency spectrum analysis carried out on at least 10 measured areas. This involves using FFTs (Fast Fourier Transforms) to separate the

different frequencies within the spatial frequencies detected on the surface. The frequency of the important features should show up dominantly on a Power Spectral Density (PSD) plot and this is used to find the correct sampling interval to accurately reconstruct the 3D surface data.

4.3.3.1   Frequency Spectrum Analysis Method

On a PSD plot, the high frequency limit that relates to the initial estimate of sampling interval from the SEM analysis (see equation 4.1) should be selected. This value should then be entered and the inverse FFT run, to show a reconstruction of the surface at this limiting frequency. If an unacceptable difference in the reconstructed surface is observed, a new high frequency limit must be sought.

The surface should be measured using an instrument with a higher lateral resolution and the maps used to re-run the frequency spectrum analysis. At least 10 maps should be used and the high frequency limit that relates to the new sampling interval obtained. The inverse FFT should again be run on these maps and the reconstructed surfaces analysed. There should be a good reconstruction at this level of resolution, if there is not then a further instrument, with a higher lateral resolution must be sought. If the reconstructions are 'good' then the high frequency limit should be reduced in intervals or by visual examination of the PSD plot, until a minimum high frequency limit and therefore a maximum sampling interval is found.

$$\text{Sampling interval} = \frac{1}{2 \times \text{frequency}} \qquad \textit{Equation 4.1}$$

Re-arranged as:

$$\text{High frequency limit} = \frac{1}{2 \times \text{sampling interval}}$$

Based on the sampling interval found by the frequency spectrum analysis the instrument for further measurements can be selected using a Steadman diagram [48] (an amplitude/wavelength plot, figure 2.27) or a table of instrument capabilities, see table 4.1.

Once chosen, other variables of the instrument can be investigated with relation to a particular surface to optimise the measurement conditions. Common measurement variables for the instruments available for this project are presented in the following section.

Table 4.1: Instrument Capabilities

Instrument	Type/Mode	Measurement Area	Lateral Resolution	Vertical Range	Vertical Resolution
Stylus	Somicronic	80 x 80 mm	2 µm to 58 µm	±3 mm	6 nm
Stylus	Taylor Hobson Ltd – Talysurf series 2 PGI	50 x 90 mm	1.25 µm to	±5 mm	4 nm
Optical Interferometer	Wyko NT2000 PSI mode	45 x 60 to 3700 x 4900 µm	160 nm to 15.5 µm	160 nm	0.3 nm
Optical Interferometer	Wyko NT2000 VSI mode	45 x 60 to 3700 x 4900 µm	160 nm to 15.5 µm	Overall = ±300 µm Pixel to pixel = 600 nm	3 nm
AFM	Veeco DI Dimension 3100	230 nm sq to 40 µm sq	0.2 nm to 2.5 µm	10 nm	0.1 nm

4.4. Measurement Variables (excluding area size and resolution)

4.4.1   Stylus Instrument

There are very few controllable variables when considering stylus measurements, providing that the same instrument is used. Tip load is typically low, 75 mg and should be relatively constant so the main variable is tip size, which would have a major effect on the measurement results if changed between measurements (see section 2.4).

4.4.2   Interferometry

When using an interferometer to measure surface topography there are a number of 'user defined' factors, which must be carefully selected to allow correct, quality, repeatable measurements.

4.4.2.1   Mode

There are commonly two modes in which to operate on current interferometers; PSI and VSI (see 2.4.1.3 Interferometry). The limiting factor for these modes is the actual surface roughness; PSI is only capable of measuring point-to-point roughness differences of up to about 150 nm. For rougher surfaces, VSI must be employed. Determining the mode to be used is only difficult if the surface measured initially in one mode is near to this limit. When this occurs, it is advisable to measure the surface with an instrument capable of higher resolutions, to determine the point-to-point range and proceed to use the appropriate interferometer mode.

4.4.2.2   Modulation Threshold

The standard description of modulation threshold is: 'It determines the signal-to-noise level for which a given pixel is considered "valid".' [40]. To optimise sampling conditions for a particular surface this description and its actual effect(s) on the measured data must be investigated so that an accurate threshold value can be established.

As the interferometer scans through focus at evenly spaced intervals it captures frames of interference data. An interference signal for each point on the surface is recorded. In vertical scanning mode the software uses an algorithm to process fringe modulation data from the intensity signal, which is then used to calculate the corresponding surface heights.

In VSI mode the irradiance signal is sampled at fixed intervals as the optical path difference is varied by a continuous translation of the vertical axis through focus. Since white light has a short coherence length the interference fringes are present over only a short depth for each focus position with the best contrast fringe occurring at best focus. The fringe contrast, or modulation, increases as the sample is translated into focus, reaches a peak (for a single point)

at best focus and then falls as the sample is translated past focus. The system measures the degree of fringe modulation (or coherence). Effectively any readings below the modulation threshold are discarded. If the surface has low reflectivity or the roughness scatters the reflected light, the difference between the modulation threshold and the signal noise is less distinct. In this case the user can select a lower modulation threshold. This has the effect of recording more surface data but can allow signal noise to be recorded as surface data. Increasing the modulation threshold has the effect of reducing the level of noise recorded, but less surface data is also registered and much of the surface is considered as 'bad data'. Consequently a balance should be sought between recording 'bad data' and 'signal noise'. To some extent small amounts of bad data can be compensated for by software interpolation techniques but an upper limit of acceptance should be set (see next section).

The correct modulation threshold must be determined for each individual surface, as the effects vary dependant on topography. A number of measurements should be taken over a range of modulations thresholds and a parameter variation analysis performed. An alternative approach could be to define the modulation threshold for a given percentage of bad data, e.g. 75%. Since the effects need to be related to the particular surface topography, no general rules are presented here, results for the examined surfaces are presented in the following sections.

4.4.2.3   % Bad Data

During measurements data that falls outside the modulation threshold, or where the scan length is too short (i.e. deep pits), or where the intensity of returned light is not sufficient, is returned as immeasurable, or bad data. This can be restored using software algorithms based on interpolation techniques and quoted as a percentage of the total pixels. A decision must be made on the allowable % bad data, as it is not advisable to rely on the 'data restore' facilities of the software, especially for large areas of immeasurable data (data restore relies on the data which is collected to 'interpolate', giving the 'expected' surface topography). Judgement and experience is required where surface topographies present this problem and results variability should be carefully examined. Levels of 40% bad data as being acceptable are applied in some industrial applications; however 20 - 25% bad data would be a more acceptable figure for laboratory work.

4.4.3   AFM

The variables associated with AFM measuring are mode and tip type. In general AFMs operate in three possible modes; contact, intermittent contact (or tapping) and non-contact. Differences between these modes are described in section 2.4.1.4 Atomic Force Microscopes. The choice of mode is dependant on the capability of the instrument and the sample material and topography. Presently, contact mode is rarely used except for vary smooth surfaces, as tip damage can occur due to the high pressure between tip and sample. Non-contact mode is obviously desirable for softer samples although intermittent contact mode has been found to be

more reliable for larger area scans and relatively rough surfaces as encountered in the steel sheet industry.

4.4.4 Number of Measurements per Sample

Repeatability of results is affected by inherent variance in surface topography and can be achieved by ensuring that enough of the surface has been measured. The number of measurements required per sample is dependant on both the measurement method (instrument) and the surface topography.

Confidence in the results obtained can be achieved by carrying out a statistical variance test of relevant surface parameters. Obviously 'relevance' is related to the process and function of surfaces and therefore is presented with respect to each examined surface in the following sections. The statistical analysis is achieved by simply plotting variance of parameters from an increasing number of measurements (averaging) and accepting the number of measurements that gives a variation in the parameters of less than 10% for 3D measurements [76] and 16% [17] for profile measurements.

4.4.5 Parameter Selection

Parameters should be selected for their functional relevance to the surface topography. Obviously, this varies from surface to surface and cannot be generalised (hence the diversity of the 3D field set, section 2.4.5 Characterisation). Discussion of expected parameter correlations for the 2B stainless steel surface finish and their functionality is given in section 4.5.1.4.

4.5. Examples

4.5.1   Recommended Measurement Method for a 2B Finish

Initially the important features of the surface must be identified. To decide on the critical sampling interval work has been carried out in chapter 3 to establish the major features of the 2B finish. By viewing a range of 2B product surfaces using a scanning electron microscope the features of the surface were recognised as plateau regions and a network of interconnecting valleys. The SEM images reveal that the plateaus and valleys are of various sizes and the plateau regions are not totally smooth but have a micro surface roughness in the form of small pits and shallow 'troughs' (relative to the deeper valleys). The small features must be resolvable using the chosen sampling interval and the average and minimum dimensions of both the plateaus and valleys are also needed.

4.5.1.1   Protocol for a 2B Finish

Measure the features: A scanning electron microscope (SEM) was employed to show the areal geometry of the surface features and images, figure 4.1, were collected from different samples, in several areas and at varying degrees of magnification. The images were manually examined and analysis based on methods in ASTM E112 [75] used to collect the data in table 4.2.

Table 4.2: Data collected from SEM study for a 2B finish

	Average	Maximum	Minimum
Plateau Diameter (µm)	9.1	12.3	4.5
Valley Width (µm)	0.7	1	0.4
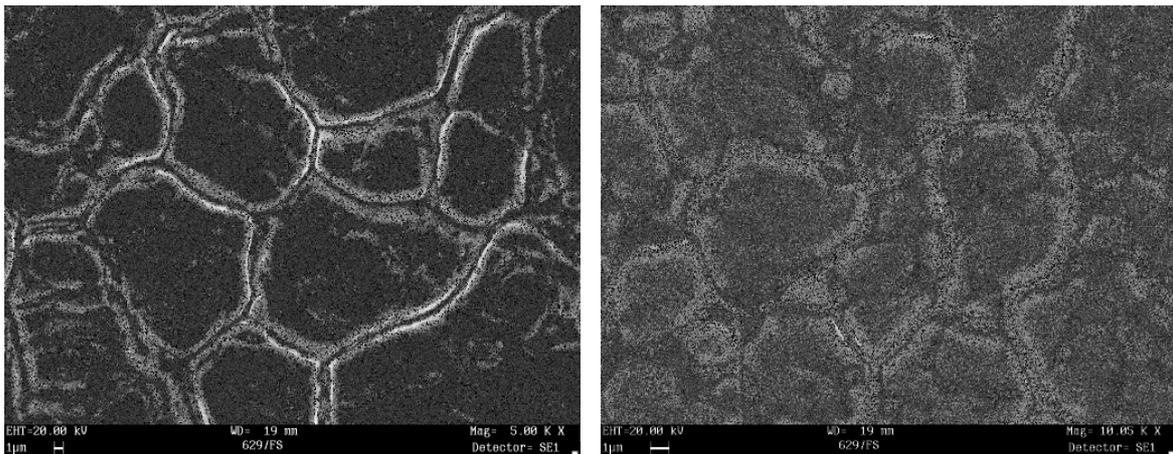
Figure 4.1: SEM images showing plateaus and valleys on 2B at x5k & x10k magnifications

Meet the demands of the Nyquist theorem: The initial estimate of required sampling interval for 2B finish was calculated, based on the Nyquist theorem. The smallest feature on the surface

is the minimum valley width, 400 nm, so the initial estimate of sampling interval is half this, 200 nm.

Chose a suitable instrument: After using a Steadman diagram an optical interferometer was chosen (Wyko NT2000 in VSI mode) and surface data files were studied. The surfaces were measured with a lateral sampling interval of 160 nm.

Run frequency spectrum analysis: Frequency spectrum analysis (using Fast Fourier Transforms) was used to determine the frequencies of the surface features. The frequency of the valleys of a 2B surface showed up dominantly on a Power Spectral Density (PSD) plot and this was used to find the correct sampling interval to accurately reconstruct the 3D surface data. Firstly surface data files from the Wyko NT2000 interferometer in VSI mode were studied. The surfaces were measured with a lateral interval of 160 nm. From these 3D maps the PSD plot was created for many 2D profiles, using a real time FFT, right-hand graph of figure 4.2. It can be seen that the important frequencies lie below about 1500 mm^{-1}. This equates to a required sampling interval of approximately 330 nm. The actual reconstructed surface at this interval can be viewed by entering a high frequency limit at this level and running an inverse FFT (the reconstructed surface is the blue line on the left profile image in figure 4.2; the red line is the actual measured surface).

The estimation of sampling interval from the SEM study of 200 nm relates to a frequency of 2500 mm^{-1} and the actual minimum measurement interval of 160 nm for the Wyko NT2000 interferometer in VSI mode relates to a frequency of 3125 mm^{-1}. The reconstructed surfaces at these intervals reveal a very high correlation with the original measured surface, see figure 4.3.

These figures were checked by using the same frequency spectrum analysis on higher resolution surface maps measured on an Atomic Force Microscope, AFM. The lateral sampling interval for the AFM measurements was approximately 40 nm (10 μm x 10 μm area). In this case the important frequencies lie below 2000 mm^{-1} (an interval of 250 nm) and the initial estimate of a suitable frequency of 1500 mm^{-1} is too low to accurately reconstruct the surface data, see figure 4.4.

The results of the practical and mathematical analyses on the determination of sampling interval are very similar. From the SEM investigations a 200 nm interval is suggested. Using the frequency spectrum analysis, a frequency of 2000 mm^{-1} is suggested to accurately reconstruct the surface data, equating to an interval of 250 nm.

Re-select a suitable instrument: The Wyko NT2000 interferometer in VSI mode at 100 times magnification has a sampling interval of 160 nm, indicating its suitability for measuring the 2B surface.
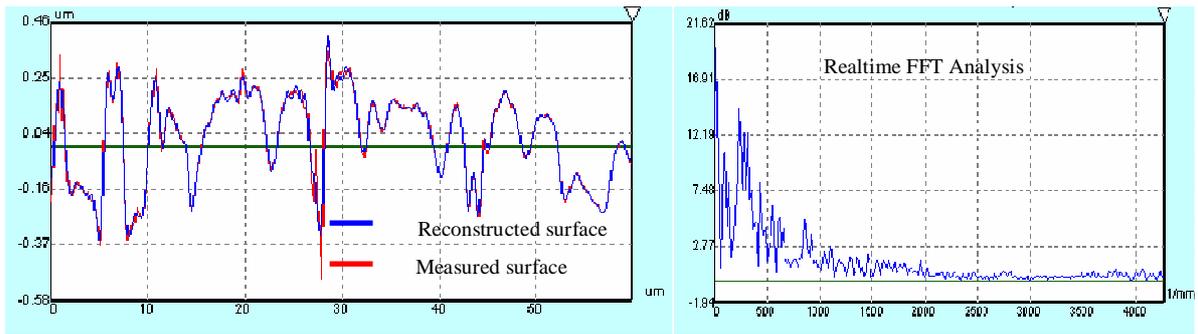
Figure 4.2: Profile of surface with reconstruction at high frequency limit of 1500 mm⁻¹ and PSD plot for surface frequencies
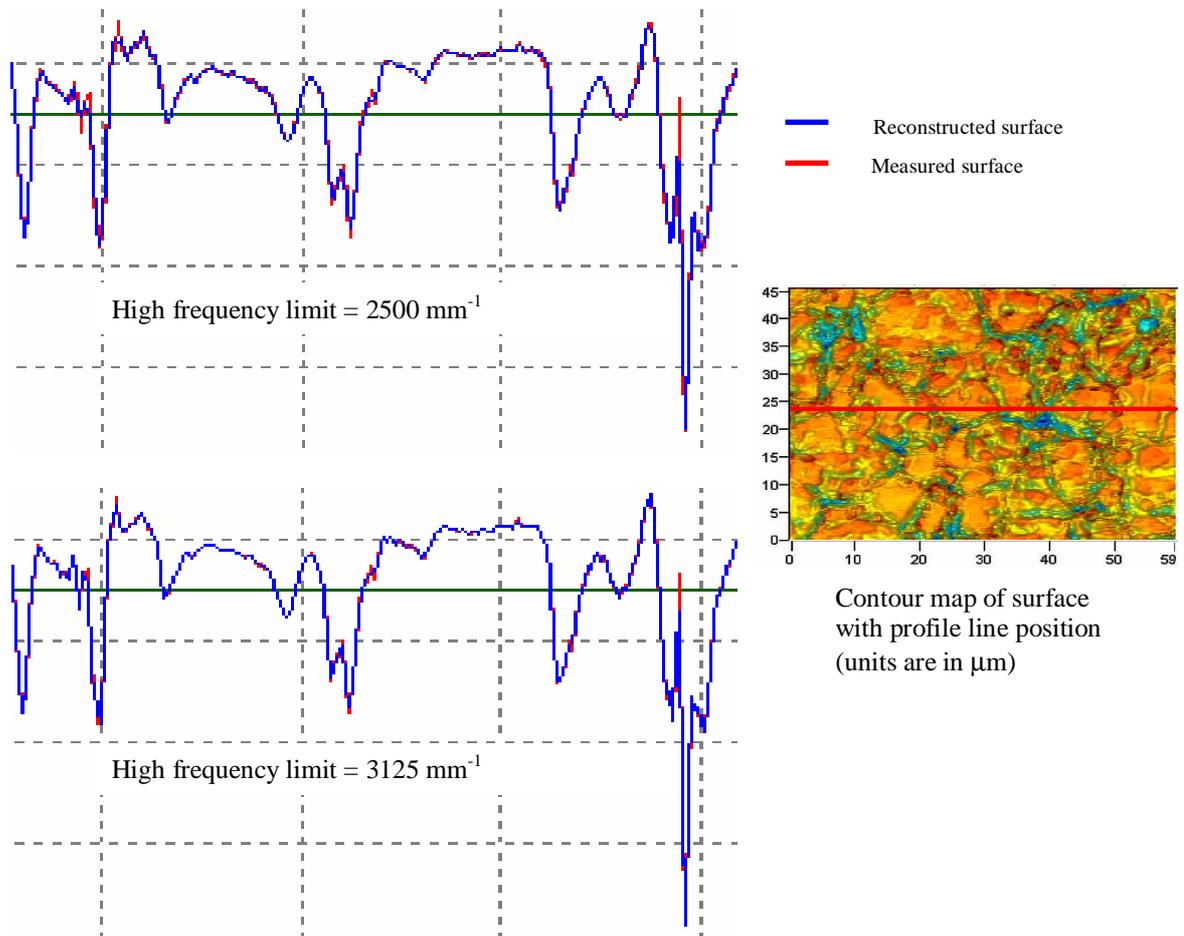
Figure 4.3: The reconstructed surfaces at frequencies of 2500 mm⁻¹ and 3125 mm⁻¹ with contour map showing area used
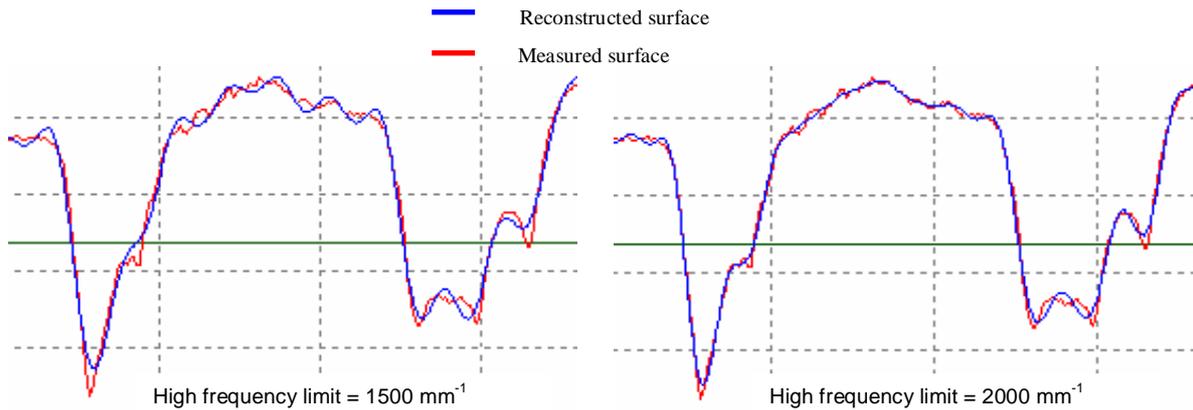
Figure 4.4: Comparison of frequency limits and effect on accuracy of profile reconstruction

4.5.1.2   Measurement Variables for a 2B Finish

Modulation Threshold [77] (also see appendix 1)

As discussed in section 4.3.2.2 the system in VSI mode measures the degree of fringe modulation (or coherence) and effectively any readings below the modulation threshold are discarded as bad data. If the threshold is raised to avoid using any bad points more and more data is lost and the image becomes very broken. Eventually using the data restore facility introduces problems when many points are missing. By decreasing the modulation threshold, less data points are ignored and there are many points included in the analysis but decreasing it too far means that very poor signal noise data is considered in analysis. This can have severe effects on the characterisation of the 2B sheet steel.
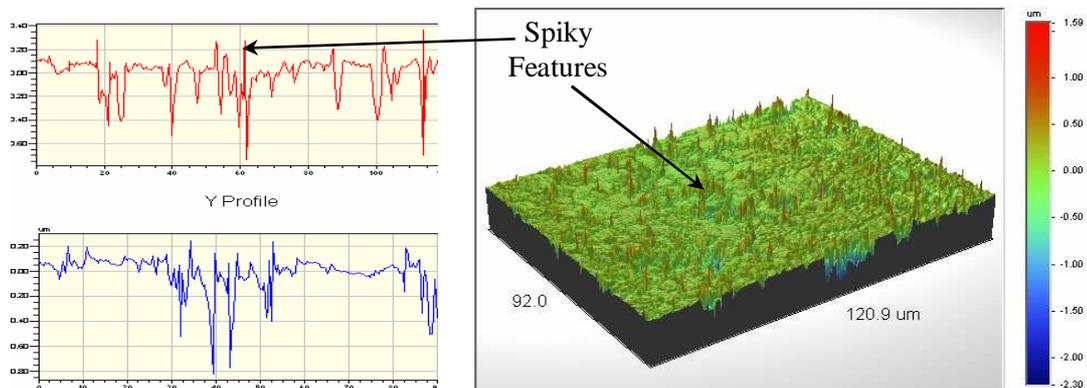
Figure 4.5: 2D profile and axonometric plot showing plateaus,
boundaries and spiky features

The images in figure 4.5 show, as expected, plateau regions with valleys between. They also show spikes in the valleys that protrude above the level of the plateaus. These spikes originate from the optical artefacts associated with the rapid slope changes from pixel to pixel in the valley zones. The limit of detection is based upon a pixel-to-pixel height difference of $\lambda/4$ and the slope limit depends on this and the chosen magnification. SEM analysis would seem to confirm the fact that the spikes are artefacts and not "real", figure 4.1.

A study was carried out to address this problem, determining a suitable modulation threshold. Areas of 121 μm x 92 μm and later, 60 μm x 45 μm (magnifications of 50 and 100 times respectively) were measured on the surface of a sheet of stainless steel with a 2B finish using a Wyko NT2000 optical interferometer. The modulation threshold was varied from 0% to 20% with 5 data sets obtained for each threshold value at the x50 magnification and 15 for the x100 (hence the larger error bars). The parameters were calculated and averaged for each modulation threshold. The original 'Birmingham 14' [41] set parameters were calculated in the initial study at 50 times magnification, whereas the new field set [65] parameters were calculated for the further study at 100 times magnification, hence there are some differences in the actual parameters used. The error bars on figures 4.6 – 4.10 are all half a standard deviation of the sample set.

The average parameter values were plotted against the modulation threshold and all the graphs were examined to determine which parameters correctly showed the effects of a variation in threshold value. Certain parameters were deemed to be of greater interest due to their specificity for the function of the sheet, i.e. analysing plateaus and valleys.

As can be seen in figures 4.6 to 4.8 the functional volume parameters have a distinctive relationship with the modulation threshold. The parameters decrease with an increase in threshold value but they 'describe' different effects.

S_m, the material volume, figure 4.6, decreases from 7634 $\mu m^3/mm^2$ at 0% to 5623 $\mu m^3/mm^2$ at 20%. This is believed to be because at lower threshold values many optical spikes are present in the analysis, which adds to material volume whilst not actually being real. As the threshold is increased fewer spikes are included in the analysis and so the effect is an apparent decrease in material volume. The results also show an unexplained rise in S_m at 2.5% modulation, up to 8841 $\mu m^3/mm^2$ before the decrease. This anomaly may be due to a combination of things but is most probably influenced by small spikes being omitted from the calculation and the data points being replaced by points that give a higher material volume, resulting from the interpolation algorithms.
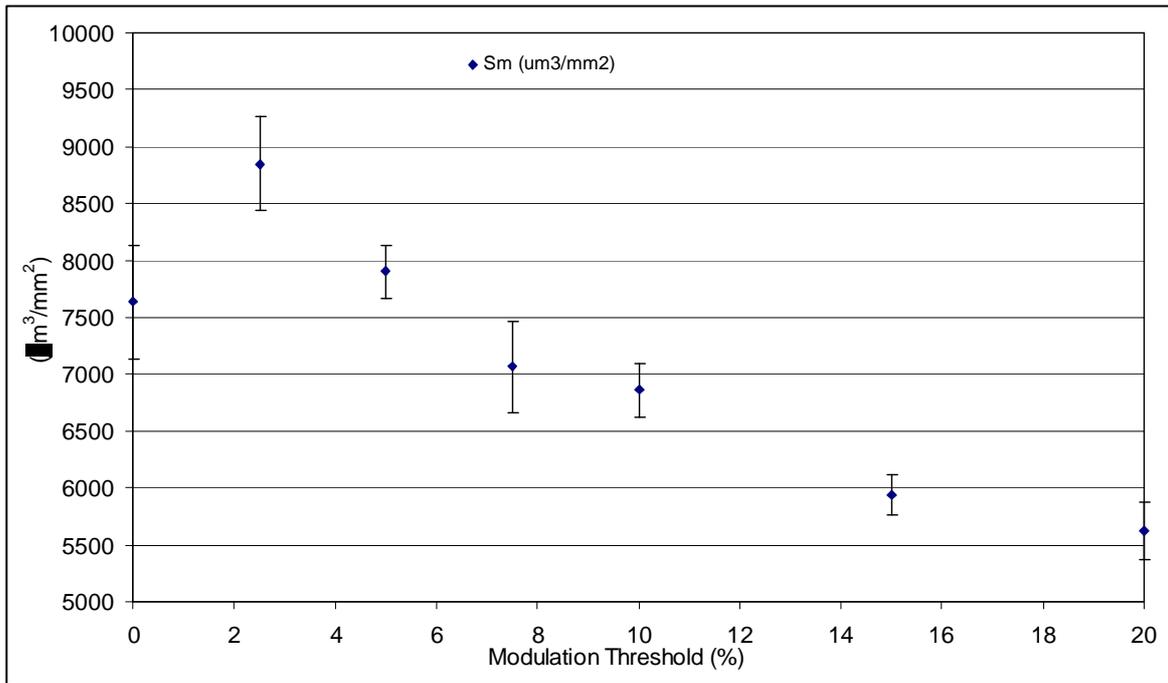
Figure 4.6: Graph of S_m (Material Volume) against Modulation Threshold (for x50 mag.)
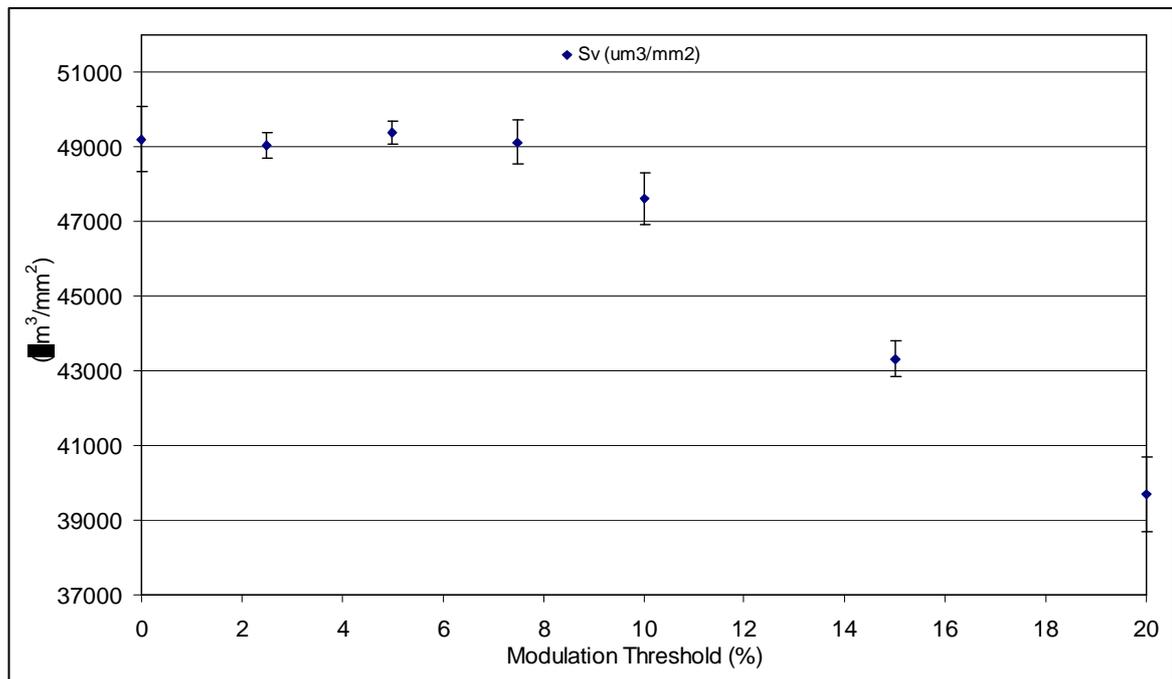
Figure 4.7: Graph of S_v (Valley Void Volume) against Modulation Threshold (for x50 mag.)

S_v, the valley void volume, also decreases, from 49206 $\mu m^3/mm^2$ to 39680 $\mu m^3/mm^2$, figure 4.7. However, this parameter stays fairly stable between 0% and 7.5% modulation before it begins to decline. It is believed that the omission of optical spikes in the analysis has no effect on the valley void volume as the data points are replaced with values outside this range. As the modulation threshold is increased it is possible that good valley data is omitted, so decreasing

the apparent void volume. A gradual decrease was observed for V_{vv}, the volume of voids in the valleys (figure 4.8), which is the most similar parameter in the new field set to S_v (numbers are different due to differences in analysis zones). This shows that the omission of optical spikes in the analysis does not seem to have an effect on the valley zone; rather that exclusion of good valley data decreases the apparent volume of voids.
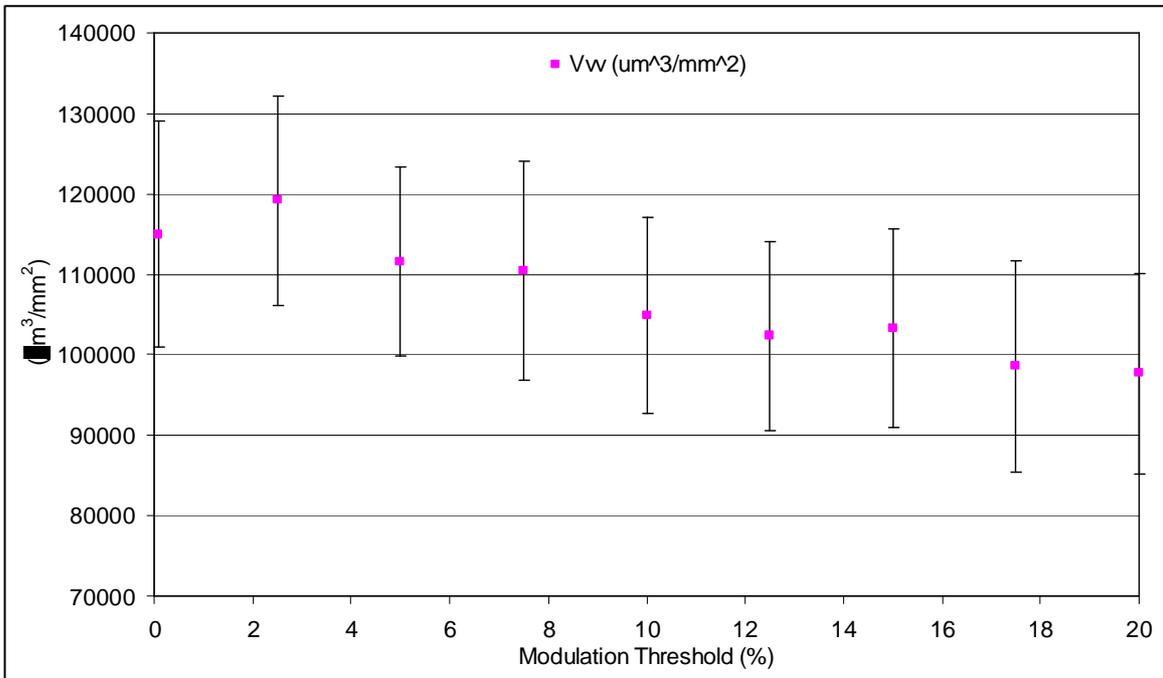
Figure 4.8: Graph of V_{vv} (Volume of Voids in the Valley Zone) against Modulation Threshold (for x100 mag.)

The amplitude group of parameters also displayed a link to the modulation threshold. From figure 4.9, it can be seen that S_z, the Ten Point Height and S_q, the Root Mean Square Deviation of the surface both decrease.

The decrease in both can be attributed to the fact that as the threshold value is increased there are fewer optical spikes included in the calculations. This will obviously cause a greater decrease in S_z (as seen), as it is calculated from only ten points, some of which will inevitably be optical spikes of large amplitude (see figure 4.5). The decrease in S_q can also be attributed to the fact that there are less high spikes and deep valleys, reducing the deviation from the surface mean height. Also the deepest valleys may become missing data as the threshold rises past 5 or 7.5%. The initial stability of the parameters, between 0% and 2.5%, could indicate that the noise level of a signal is, on average, higher at 2.5%.
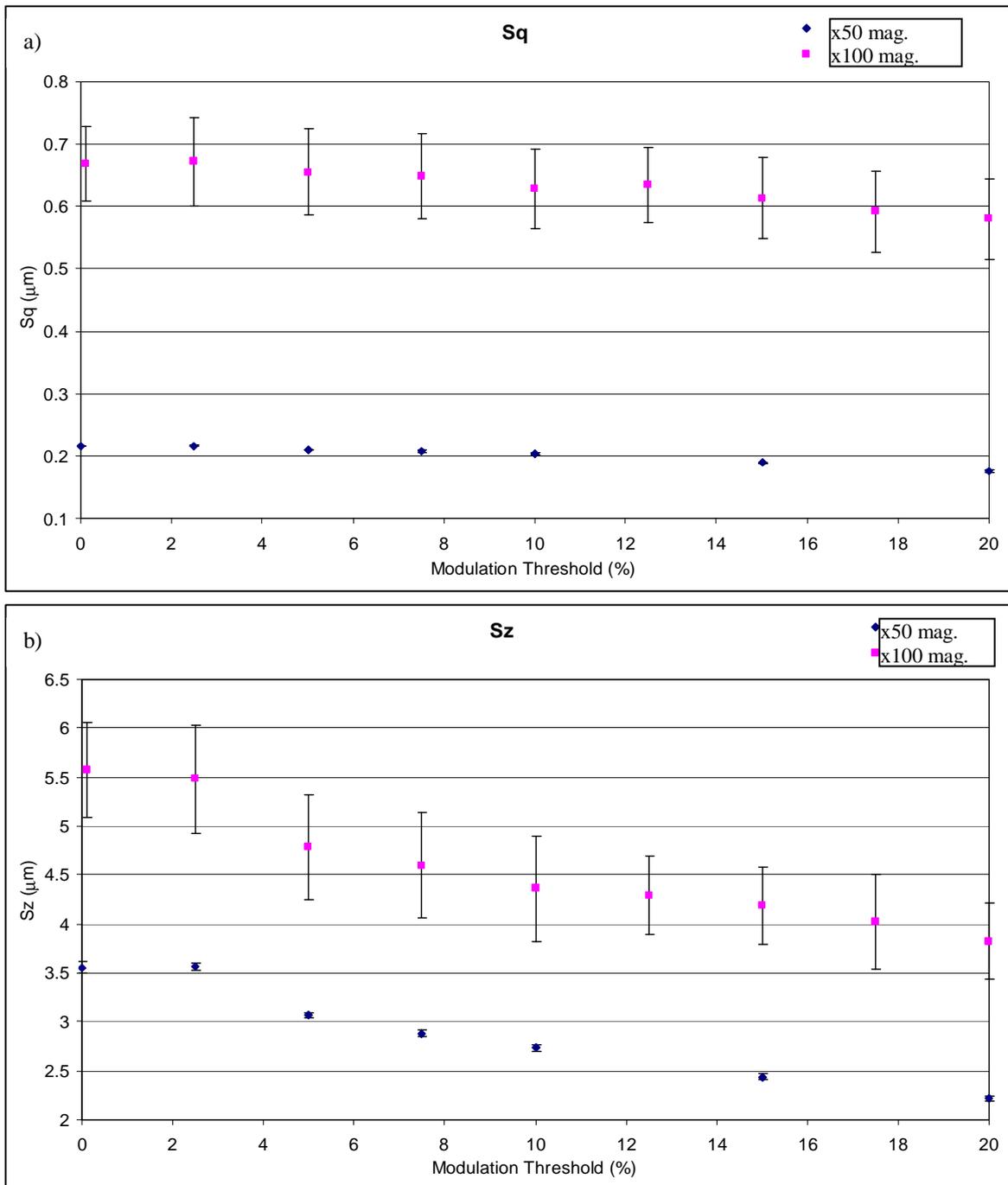
Figure 4.9: Graphs of (a) S_q, Root Mean Square Deviation and (b) S_z, Ten Point Height, against Modulation Threshold (for x50 and x100 mags.)

The other two parameters in the amplitude group are S_{sk} and S_{ku}, the skewness and kurtosis of the surface respectively (not shown graphically). The skewness is a measure of the symmetry of the amplitude distribution of the data and therefore of the surface deviations about the mean plane. The graph of skewness against modulation threshold is difficult to interpret on its own since the mean plane will vary for each threshold value. It does however show the value to be negative, indicating pits or troughs (Gaussian surface, $S_{sk} = 0$). The kurtosis is a measure of the peakedness or flatness of the amplitude distribution relative to a normal distribution. For a

standard normal distribution the S_{ku} value is 3 (a Gaussian surface), a kurtosis value greater than 3 shows a distribution has a sharp peak around the mean, declining rapidly with heavy tails (a centrally distributed surface with a few outliers) and a value less than 3 shows a flat topped distribution (a more uniform distribution, indicating a surface with less extreme deviations from the mean plane). The values of S_{ku} for the 2B surface lie above 3, indicating that it has a central distribution with outliers (the valleys and optical spikes). It decreases with increasing modulation threshold, as expected, due to the omission of the sharp optical spiky features.

The only other parameter to be considered is $S_{\Delta q}$, the root-mean square slope of the surface, from the hybrid family. Figure 4.10 shows a decrease in $S_{\Delta q}$ with an increase in the modulation threshold, apart from the area between 0% and 2.5%, which is relatively unchanged. The decrease indicates that the average slopes of the asperities and valley 'walls' is falling, or the surface is becoming smoother (this parameter is often useful to detect wear on a surface). This is attributed to the fact that the optical spikes, with very 'sharp' sloped edges are being omitted. The area between 0% and 2.5% modulation threshold is stable and so the justification given previously (noise level) looks to be correct.

It is evident from this work that there is a definite relationship between the parameters (and measured surface) and the modulation threshold. The results also show that the presence of optical spikes affects the analysis of data in a major way. Parameters that rely on extremes are greatly influenced, as are the functional parameter set, which do also rely on extremes but to a lesser extent.

Before being able to accurately characterise the surface of 2B steel it is necessary to eliminate any variation due to 'spiky features' that do not exist in reality. This project goes some way to describing the basic effects of varying the modulation threshold but more work on the influence of data restore facilities maybe required for other surfaces (see following section on % bad data). The average noise level of a signal is apparently around 2.5% as found by these results. Good stability of parameters is seen between 2.5% and 7.5%, so the standard 5% modulation threshold can be used.
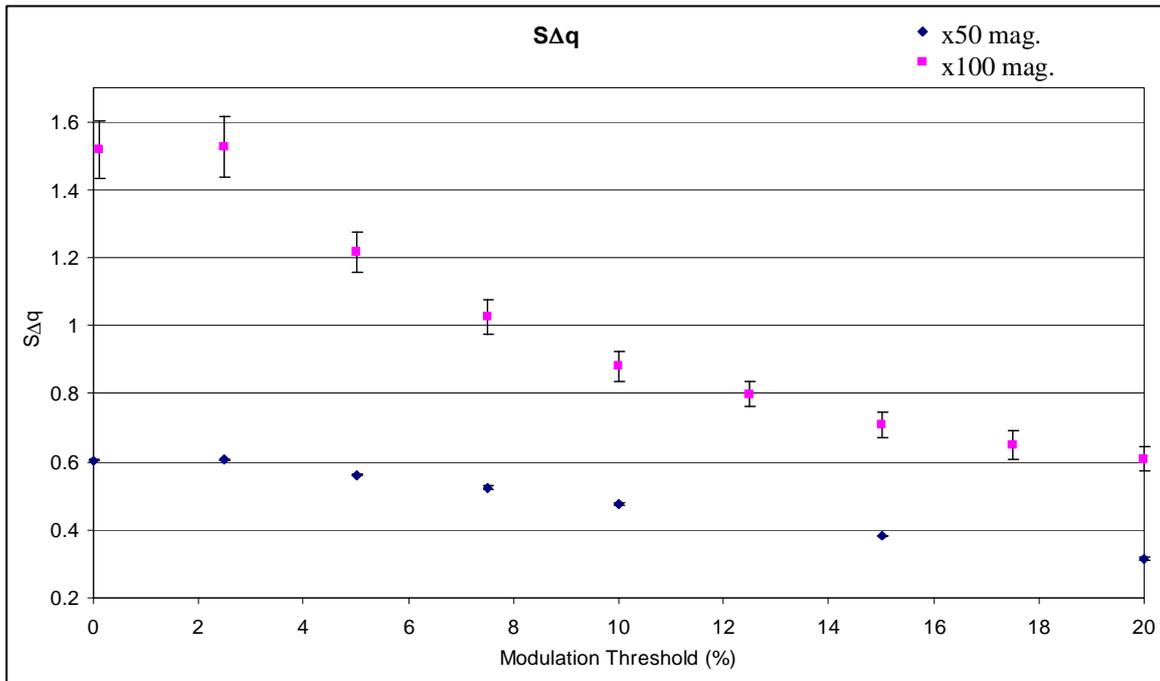
Figure 4.10: Graph of $S_{\Delta q}$ (Root Mean Square Slope of the surface in $\mu m/\mu m$) against Modulation Threshold (for x50 and x100 mags.)

<u>% Bad data</u>

As discussed in section 4.3.2.3, a decision must be made on the allowable % of bad data for measurements. The 20% maximum was initially accepted, although during the course of the study of modulation threshold, it was discovered that the 2B surface gave good intensity of returned light and so a maximum of only about 10% was reached (at 20% modulation). A figure of 15% maximum bad data was adopted for subsequent measurements.

4.5.1.3 Number of Measurements per 2B Sample

Repeatability of results is affected by inherent variance in surface topography and can be achieved by ensuring that enough of the surface has been measured. The number of measurements required per sample is dependant on both the measurement method (instrument) and the surface topography.

Confidence in the results obtained can be achieved by carrying out a statistical T-test of relevant surface parameters. The statistical analysis is achieved by simply plotting the percentage confidence interval for each parameter from an increasing number of measurements and accepting the number of measurements that gives a variation in the parameters of less than 10% for 3D measurements and 16% for profile measurements.

Thirty measurements were made of a random 2B sample and the statistical analysis carried out. Figure 4.11 shows the graphs of several relevant parameter variations against the number of measurements used. Every parameter plotted had a % confidence of less than +- 10% for 12 or less measurements, except S_m, which initially went to +- 9% confidence for only 4 measurements but then rose above the level to finally settle after 19 measurements.

A factor of 'safety' was added to the necessary 12 measurements and the average parameters of 15 measurements will be used for the remainder of this project.
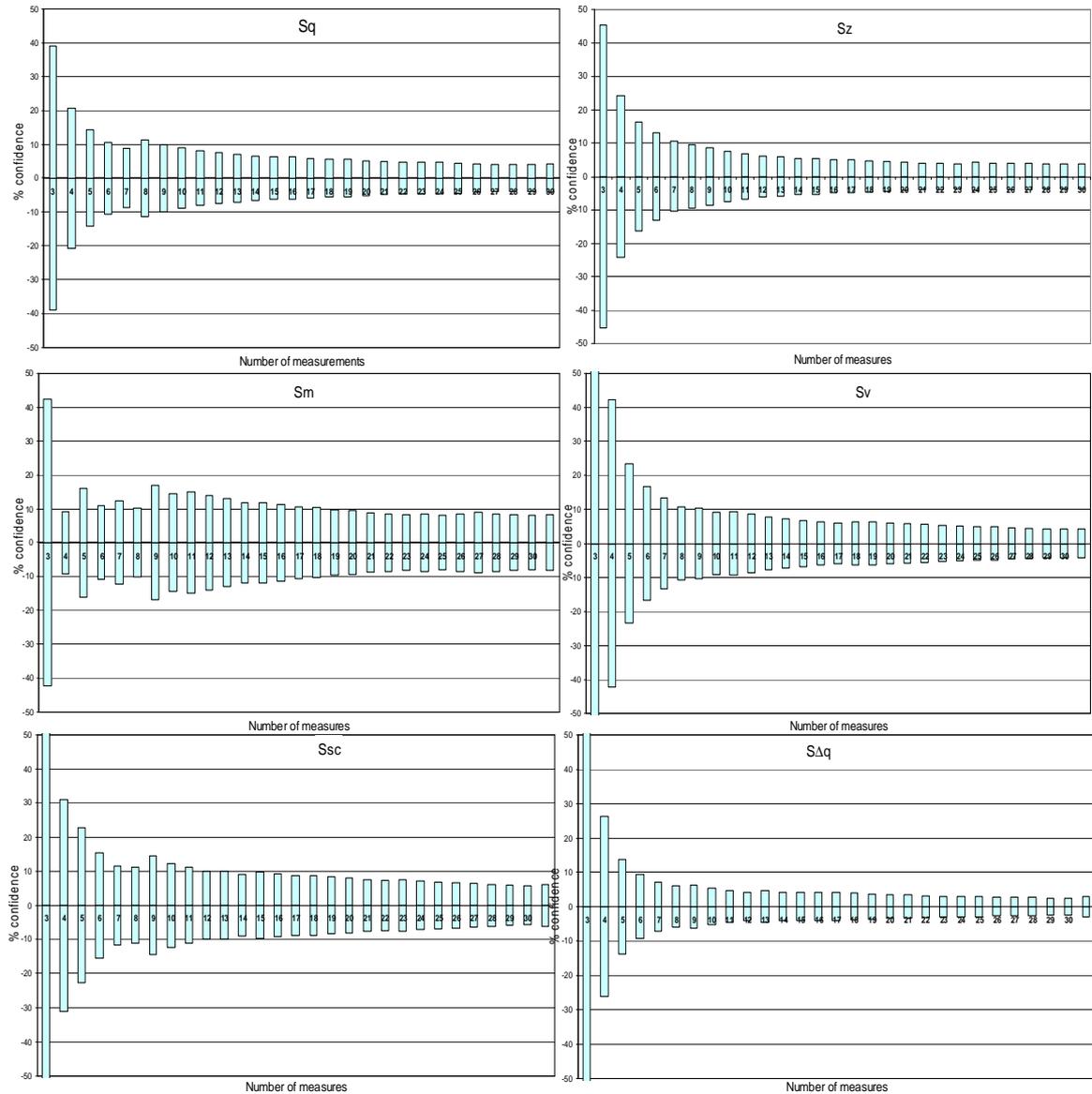
Figure 4.11: Graphs showing the variations of parameter values against number of measurements used

4.5.1.4   Parameters Selection

It is important for all finishes that the parameters chosen to describe the surface features are relevant to functionality. Table 4.3 shows the 3D parameter set with corresponding potential relationships to production and/or functionality.

The amplitude family should have consistent values for repeated measurements of the 2B surface (provided that the sampling interval and area sizes are the same) and so changes in the amplitude parameter values will be an indication of surface changes due to production and may

relate to functionality. S_{5z} is an extreme parameter, the average height of the five highest peaks and five deepest valleys or pits. Since the surface topography contains few large peaks it is the depth of the valleys that will have a major influence on variations in this parameter.

Table 4.3: 3D parameters set with potential relationships

● High   ◑ Moderate   ○ Low

Amplitude						Spacing			Hybrid		
S_q	S_{sk}	S_{ku}	S_p	S_v	S_z	S_{ds}	S_{al}	S_{tr}	S_{sc}	$S_{\Delta q}$	S_{dr}
●	●	●	◑	◑	●	◑	○	○	◑	◑	◑

Curve and Volume									Fractal	Others	
S_{mr}	S_k	S_{pk}	S_{vk}	V_v	V_{mp}	V_{mc}	V_{vc}	V_{vv}	S_{fd}	S_{td}	S_{5z}
◑	○	◑	◑	○	●	◑	◑	●	◑	○	●

The value of S_{sk} for a 2B finish is large and negative, as it has outliers, the valleys and good bearing properties, because of the relatively flat plateau regions. The value of S_{ku} is very large, which is also due to the outliers (valleys). These two parameters should be used in conjunction with each other to identify surfaces which have relatively flat tops and deep valleys, like 2B and plateau honed, from other surface topographies with similar values for the other parameters.

The spatial and hybrid families are not particularly useful for functionally characterising the 2B surface, as it has no particular texture or lay, although they may be useful to show small changes when considering optical properties.

Absolute values for volumes are calculated using the functional volume family of parameters and these should have strong relationships to the lubrication retention properties of the surface.

4.5.2   Recommended Measurement Method for a Brushed Finish

Initially the important features of the surface must be identified. By viewing a range of brushed product surfaces using a scanning electron microscope the features of the surface were recognised as unidirectional ridges and troughs. The SEM images reveal that the ridges have rough edges and some remnant 2B finish can be seen in the troughs. The smallest features must be resolvable using the chosen sampling interval so the average and minimum dimensions of the ridges, troughs and remnant 2B must be found.

4.5.2.1   Protocol for a Brushed Finish

Measure the features: A scanning electron microscope (SEM) was employed to show the areal geometry of the surface features and images as in figure 4.12 were collected from different

samples, in several areas and at varying degrees of magnification. The images were manually examined and the data in table 4.4 gathered.

Table 4.4: Data collected from SEM study for a brushed finish

	Average	Maximum	Minimum
Ridge Width (μm)	450	1100	200
Trough Width (μm)	550	1300	200
Remnant 2B features (μm)	450	600	350

Meet the demands of the Nyquist theorem: The initial estimate of required sampling interval for a brushed finish was calculated, based on the Nyquist theorem. The smallest feature on the surface is the minimum trough width, 200 nm, so the initial estimate of sampling interval is 100 nm.

Chose a suitable instrument: After using a Steadman diagram an optical interferometer was chosen (Wyko NT2000 in VSI mode) and surface data files were studied. The surfaces were measured with a lateral sampling interval of 160 nm.
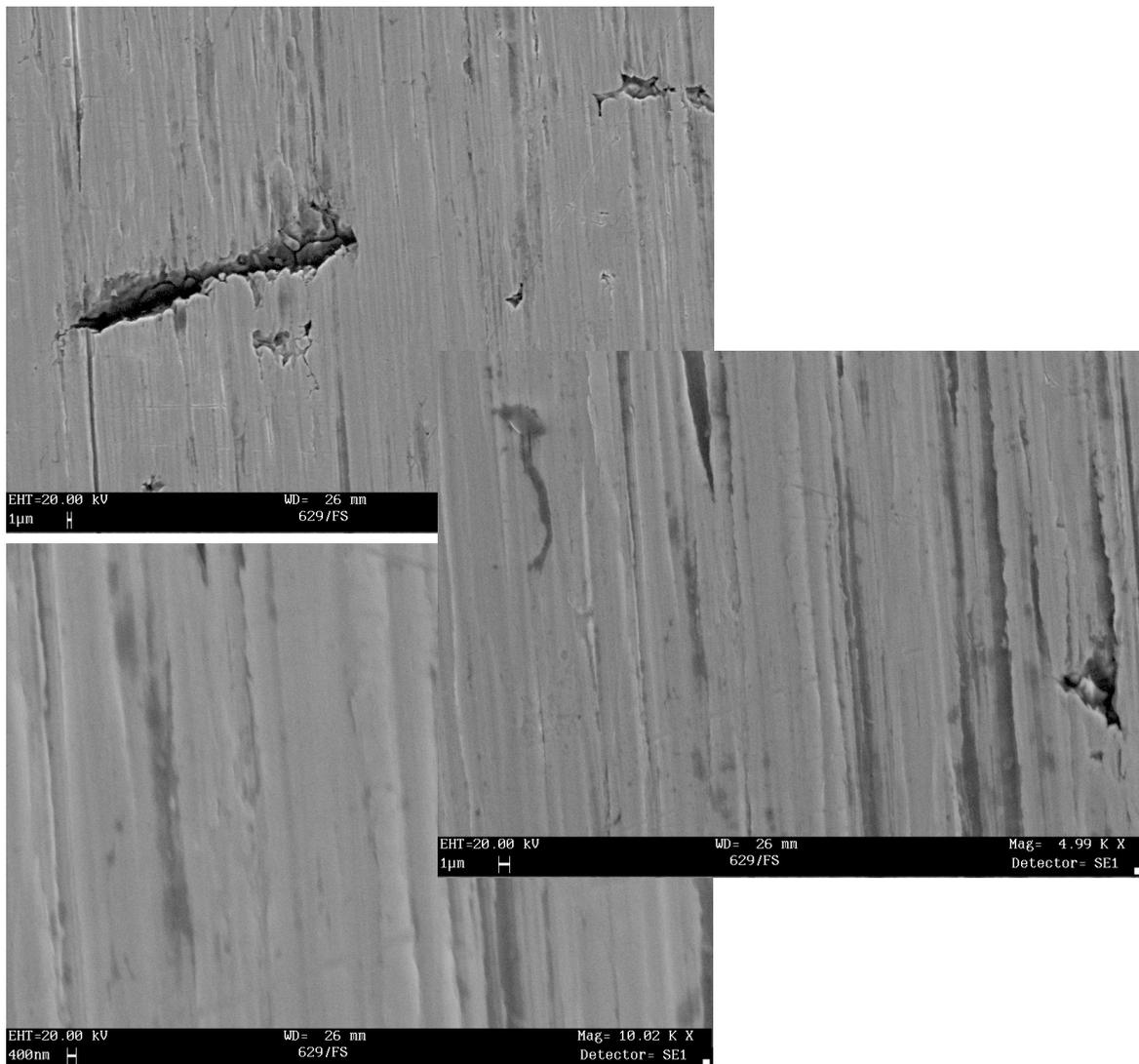
Figure 4.12: SEM images of a brushed surface finish showing ridges, troughs and remnant 2B features at x2k, x5k & x10k magnifications

Run frequency spectrum analysis: Frequency spectrum analysis (using Fast Fourier Transforms) has again been used to determine the frequencies of the surface features. The surfaces were measured with a lateral interval of 160 nm. From the 3D maps the PSD plot was created for many 2D profiles, using a real time FFT. The estimation of sampling interval from the SEM study of 100 nm relates to a frequency of 5000 mm^{-1} and the actual minimum measurement interval of 160 nm for the Wyko NT2000 interferometer in VSI mode relates to a frequency of 3125 mm^{-1}. The reconstructed surfaces at these intervals reveal a very high correlation with the original measured surface. In fact for a brushed surface, a frequency of 2500 mm^{-1}, equating to an interval of 200 nm, almost perfectly reconstructs the surface profiles, figure 4.13.
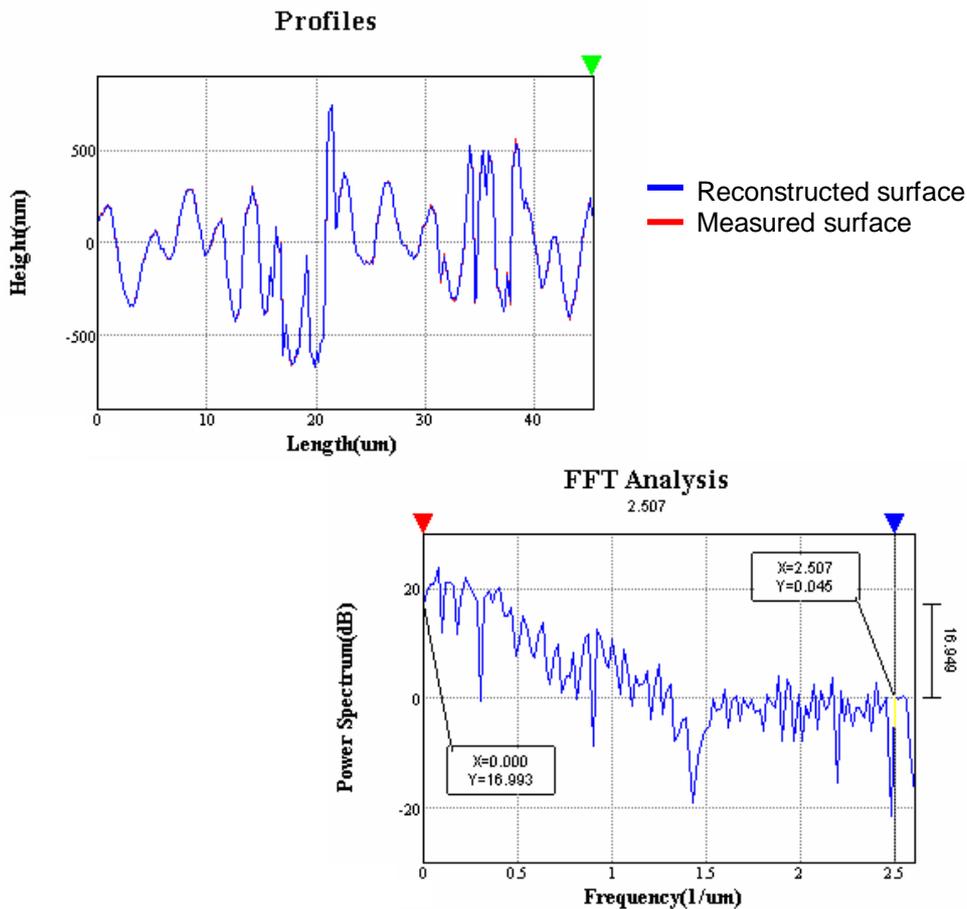
Figure 4.13: Profile reconstruction after FFT analysis showing good reconstruction
(a) Reconstructed surface
(b) FFT analysis

The results of the practical and mathematical analyses on the determination of sampling interval are similar. From the SEM investigations a 100 nm interval is suggested. Using the frequency spectrum analysis, a frequency of 2500 mm^{-1} is suggested to accurately reconstruct the surface data, equating to an interval of 200 nm.

Re-select a suitable instrument: The Wyko NT2000 interferometer in VSI mode at 100 times magnification has a sampling interval of 160 nm, indicating its suitability for measuring the brushed surface.

4.5.3   Recommended Measurement Method for a WHB Surface

Initially the important features of the surface must be identified. By viewing the white hot band surface using a scanning electron microscope and an interferometer the features of the surface were recognised as shot blast marks, deep valleys created by pickling and isolated high-aspect ratio pits. The smallest features must be resolvable using the chosen sampling interval so the average and minimum dimensions of the shot marks, valleys and pits must be found.

4.5.3.1   Protocol for a WHB Surface

Measure the features: A scanning electron microscope (SEM) was employed to show the areal geometry of the valley and pit features and an interferometer was used to determine the width of shot marks on the surface. Images as in figure 4.14 were collected from different samples, in several areas. The images were manually examined and the data in table 4.5 gathered.

Meet the demands of the Nyquist theorem: The initial estimate of required sampling interval for a brushed finish was calculated, based on the Nyquist theorem. The smallest feature on the surface is the minimum pit width, 250 nm, so the initial estimate of sampling interval is 125 nm.

Table 4.5: Data collected from SEM study for WHB surface

	Average	Maximum	Minimum
Shot Marks Width (μm)	200	300	100
Valley Width (μm)	1.25	2.5	0.5
Isolated Pits Width (μm)	0.5	1	0.25
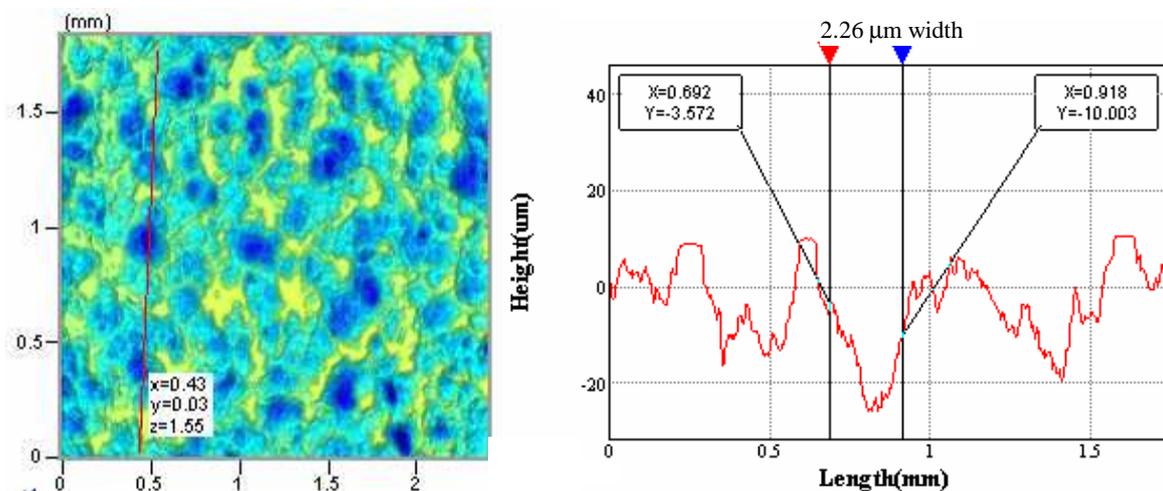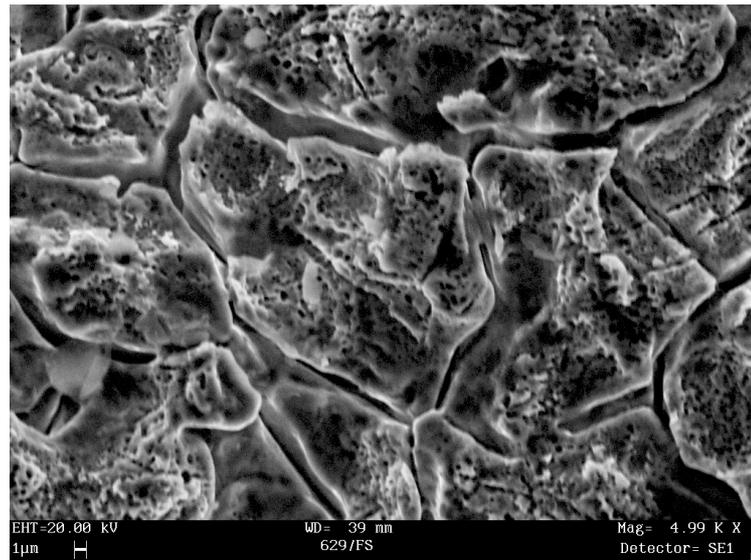
Figure 4.14: SEM and interferometer images of a white hot band surface showing size of shot mark features

Chose a suitable instrument: Although an optical interferometer (Wyko NT2000 in VSI mode at 100 times magnification) can achieve a lateral sampling interval of 160 nm, the area measured would be approximately 50 μm x 100 μm, meaning no shot marks would be fully represented. Considering that the 'function' of the white hot band is to be consolidated into the smoother rolled surfaces and that it is most common to see remnant shot marks as 'defects' on these surfaces, it is important that the shot marks are measured.

Therefore the initial suggestion is to measure the pits and valleys using the interferometer in VSI mode at 100 times magnification and to measure the shot marks using the same instrument but at only 2.5 or 5 times magnification (approximately 2 μm and 3.5 μm lateral resolution with areas of 0.9 mm x 1.2 mm and 1.8 mm x 2.4 mm, respectively). The same lateral resolution can also be achieved on most stylus instruments; however there is a huge time benefit with using an optical interferometer. In reality, when attempting to measure the white hot band using the interferometer in VSI mode at 100 times magnification, the surface proved too 'dark', i.e. not

enough light was returned to the instrument from the surface. Figure 4.15 shows the profile reconstruction of a white hot band surface (measured with a lateral interval of 2 μm) with high frequency limits of 250 mm^{-1} and 143 mm^{-1} (relating to 2 μm and 3.5 μm sampling intervals respectively). Good reconstruction is achieved with both limits, although the 250 mm^{-1}, or 2 μm sampling interval is recommended as it accurately reconstructs the fine details.
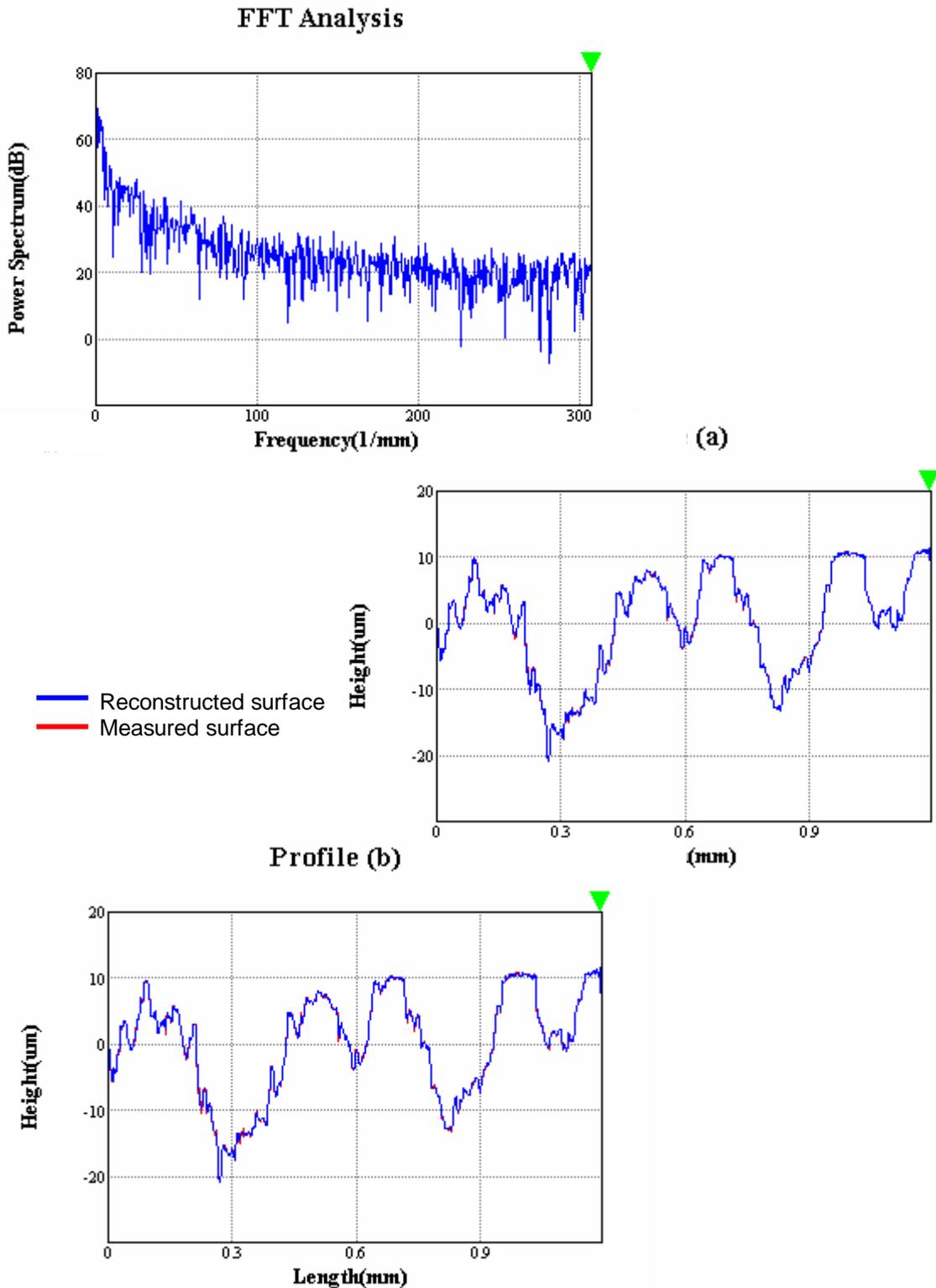
Figure 4.15: FFT analysis and profile reconstructions for high frequency limits showing good agreement at (a) 250 mm^{-1} and (b) 143 mm^{-1}

4.6. Conclusion

This chapter has presented a generalised measurement strategy, to aid the selection of measurement and instrument selection for any surface topography. The strategy and its protocol have then been demonstrated using three common surface finishes produced by the sponsoring company. The results of these examples will be used in the remainder of this project, ensuring the quality of measurements and functionality of calculated parameters. Further, it is suggested that the approach described could be used as a general guide for surface metrology of different surfaces.

A flow chart of the generalised protocol is presented in figure 4.16 to aid in the visualisation of the steps involved for the sponsoring company.

Identify important
surface features

Plateau regions and a network of
interconnecting valleys

Measure the features

A scanning electron microscope (SEM) was
employed to depict the areal geometry of the
surface features. Images were manually
examined and analysis used to collect the
data in table 4.2.

Meet Nyquist
theorem

FIRST ESTIMATE OF
SAMPLING INTERVAL

The smallest feature on the surface is the
minimum valley width, 400nm, so the
initial estimate of sampling interval is half
this, 200nm.

Chose a suitable
instrument

Non-contacting optical interferometer (Wyko
NT 2000 in VSI mode)

Measure surface –
at least 10 maps

Can

The frequency of the valleys of a
2B surface show up dominantly on
a PSD plot

The significant frequencies were
checked using higher resolution
surface maps measured on an
Atomic Force Microscope, AFM.
The lateral sampling interval for the
AFM measurements was
approximately 40nm. From this the
suggested high frequency limit is
2000mm^{-1}.

Run frequency
spectrum analysis on
maps and get PSD
plot

The Wyko minimum interval of 160nm relates to a
frequency of 3125mm^{-1}. The reconstructed surfaces
at these intervals reveal a very high correlation with
the original measured surface.

Can't

Increase
estimate of
high
frequency
limit

Select high
frequency limit and
reconstruct surface
by running inverse
FFT

SECOND ESTIMATE OF
SAMPLING INTERVAL

THIRD ESTIMATE OF
SAMPLING INTERVAL

Measure surface with an
instrument with a higher
lateral resolution

NO

Is the
reconstruction
good?

YES

Use equation 1 to
calculate related
sampling interval from
high frequency limit

The results of the practical and mathematical analyses on the
determination of sampling interval are very similar. From the
SEM investigations a 200nm interval is suggested. Using the
frequency spectrum analysis, a frequency of 2000mm^{-1} is
recommended, equating to an interval of 250nm.

Select a suitable instrument using
table and set all other instrument
variables to suit the surface

THE WYKO INTERFEROMETER AT **100** TIMES MAGNIFICATION HAS A
SAMPLING INTERVAL OF **160nm,** INDICATING ITS SUITABILITY FOR
MEASURING THE **2B** SURFACE.

Figure 4.16: Flow chart of test protocol (red boxes show 2B finish results, section 4.4.1)

Chapter 5   The Effects of Variations in Production

5.1. Summary of the Chapter

There is inherent variability in the surface topography produced due to differing process stages and grade of material. The desired thickness determines the number of passes through the rolling mill and the final finishing operation can be either skin-passing or tension levelling (this is source dependant, either Source 1 or 2, respectively). The main aim of this chapter is to investigate the effect that normal production variations have on the surface topography of stainless steel. This is achieved by comparing the relevant measured 3D surface topography parameters and relating the differences to variations in the samples' production, including:

- Variation in nominal thickness of samples
- Variations in grade of material (316 and 304 grades) and actual, measured thickness
- Variation in source of material and therefore in the final process step (skin passing or tension levelling)

In addition to the above production variations, the micro hardness of the different grades and sources is presented, in an attempt to fully understand the issues.

5.2. Introduction

Surface texture is the fingerprint of manufacture [6] and as such can be used as a control for production purposes. Changes in the process, whether they are intentional or not, effect the final finish of a component and if the features of surface topography can be traced to the point in the process where they were created the effects can be either controlled (for the engineering of surfaces for a specific function) or eliminated (for defects).

5.3. Known Effects of Production on Topography of 2B Finish (review)

The surface finish of the final product depends on a number of factors within its process route, but predominantly it is the final stages that dominate the final topography.

The cold rolling process is not only used to reduce the gauge of the sheet but also to improve and consolidate the surface. The differences in methods and tribological conditions of cold rolling generate various surface characteristics, often the shallow pits present on the hot band surface are eliminated and the intermediate descaling (pickling) effects are minimised.

After being rolled to the intended final gauge the material for 2B finishes is annealed again and must be descaling in an agitated acid bath.

This descaling method is highly influential to the final surface and chemical attack on the metal substrate can be preferential, for example at grain boundaries in the recrystallised, annealed structures, giving rise to etching effects on the surface. The process creates the 'matrix' of grain boundary valleys, discussed previously in Chapter 2. Some of the grain boundaries are left intact so the remaining grain 'plateau' regions vary in size. The skin pass, performed at the Source 1 site, does not alter the mechanical properties but it serves to reduce thickness and improve 'shape' tolerances and gives a final finish to the plateau regions. Being a light pass it does not totally smooth out the plateau regions but merely removes or flattens the higher asperities. The skin pass process route includes a tensioning device, which helps to alleviate the effect of form and waviness created in the rolling process. The parallel method of brightening the surface, used at the Source 2 site, is to use a light tension device. Both processes result in very similar surface topographies.

Consequently there are two main features that distinguish both of the 2B surfaces, plateau regions and a pattern of interconnecting valleys.

5.4. Sample/Production Variations

There is inherent variability in the surface topography produced due to differing process stages, grade of material and one-off variations known as 'defects'. Different process stages for the 2B finish occur in cold rolling, where the desired thickness determines the number of passes through the rolling mill and the final finishing operation can be either skin-passing or tension levelling (this is source dependant, either Source 1 or 2, respectively). Other stages of the process route can produce discrepancies, like the 'greying' effect of over pickling or a general streaky appearance may be evident where variation existed in the white hot band. Variations due to the grade arise because of the individual properties of the materials and therefore slightly different reactions to the same processing operations. When all of these variables are the same, inconsistencies in the final finish can still occur. Variation across the length and width of the sheet are unintentional but can occur due to wear of rolls and differences in the spread of lubrication. Roll imprints may be seen as a result of roll wear or lubrication problems and other faults such as scoring may be visible. Since the aim of this study is to investigate normal production variables, samples have been taken from the middle sections of the strip and

although the 15 measurements are taken randomly within the sample area, faults or defects are avoided.

5.5. Measurement Method

The measurement strategy (Chapter 4) was followed for this study. For the 2B finish, samples were measured using the Wyko NT2000 interferometer in VSI mode at 100 times magnification. Fifteen measurements were taken on each sample and the parameter results averaged to give stable results [17].

5.6. Results

Results are given in the form of graphs with parameters against thickness. All error bars are $\pm$ ½ standard deviations of the 15 measurements taken. Correlation was measured using the linear least squares method.

General observations:
The value of S_{sk} for a 2B finish is large and negative, due to the presence of valleys and plateaus. The value of S_{ku} is very large, which is also due to the outliers (valleys) effecting the height distribution. These two parameters are normally used in conjunction with each other to identify surfaces which have relatively flat tops and deep valleys, such as 2B and plateau honed.

The spatial and hybrid families are not particularly useful for characterising the differences in the basic 2B surface, as the texture or lay is very similar for all grades.

5.6.1   Results for Nominal Thickness Variation

The first 'set' of figures (5.1 to 5.6) shows the simplest separation of the samples, by their nominal thickness only. All the major grades studied are included and their source is not distinguished.

S_q (Root Mean Square Deviation) decreases with decreasing thickness, as expected, figure 5.1. This mirrors the result found using the R_a values in 2 dimensions (appendix 2), meaning that the overall roughness of the surface is reduced, or the thinner gauges have a smoother finish.
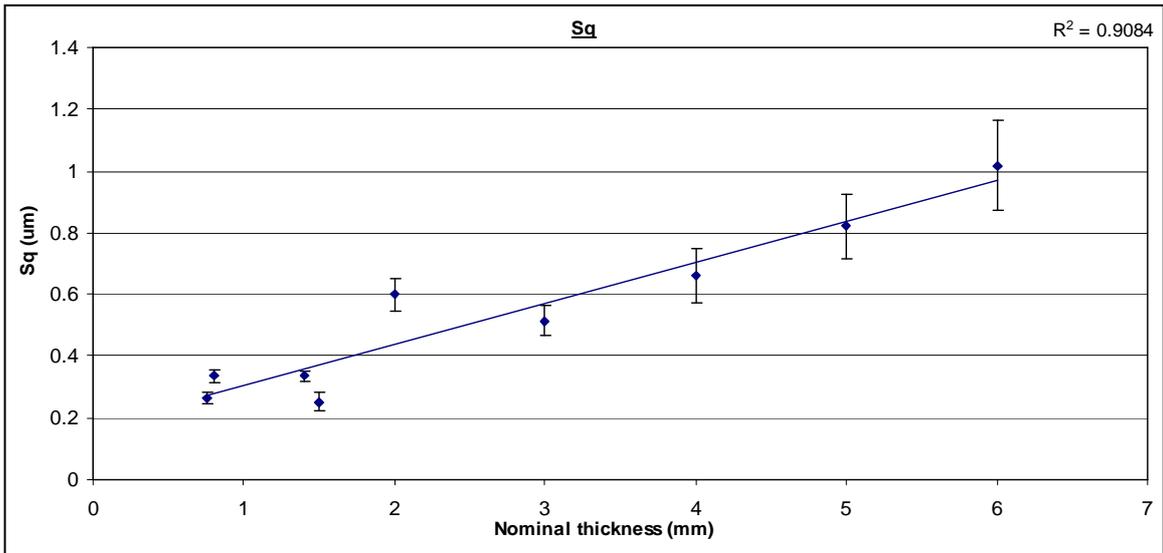
Figure 5.1: Graph of S_q (Root Mean Square Deviation) against nominal thickness for all grades
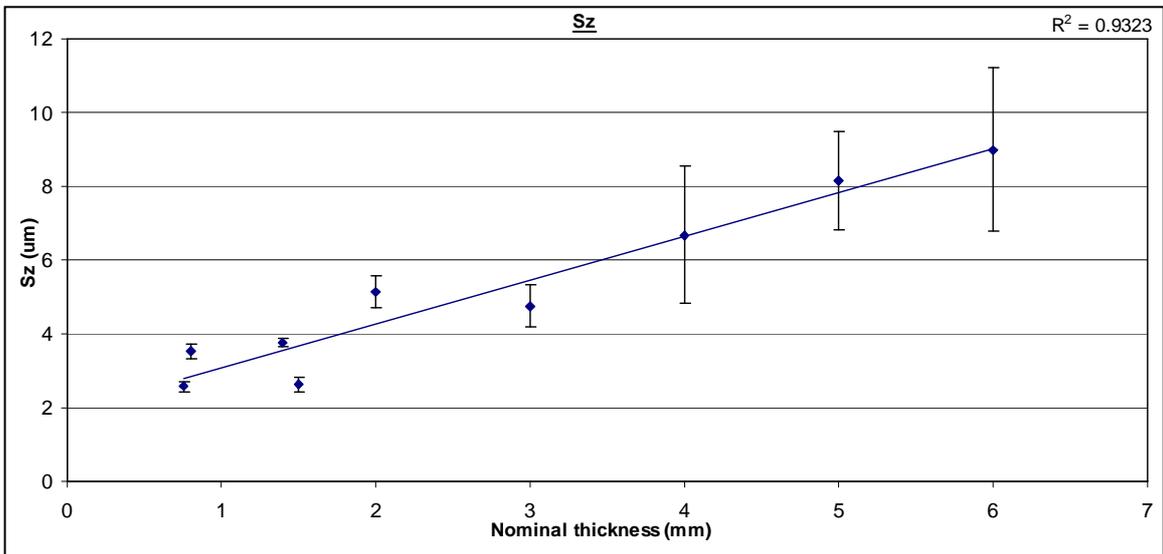
Figure 5.2: Graph of S_z (Maximum Height of Texture surface) against nominal thickness for all grades

S_z (Maximum Height of Texture surface, formerly named St) follows a similar trend to S_q, as does S_v (Maximum Valley Depth of Texture surface), figures 5.2 and 5.3. These two extreme parameters give an insight into the overall change as the material gets thinner. It is not only the plateau areas that are smoothed; the valley depths are also reduced.
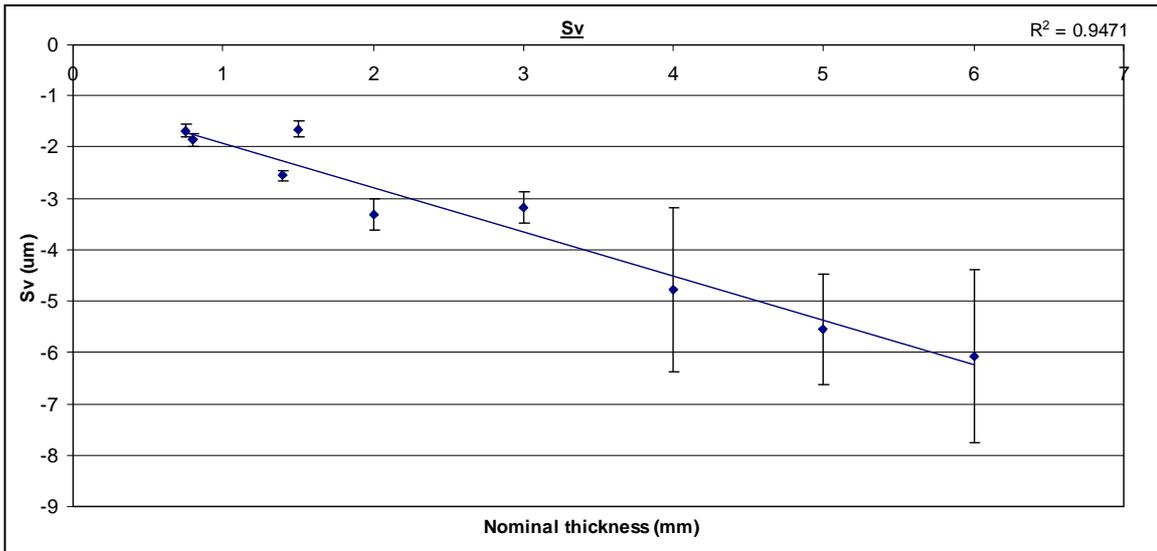
Figure 5.3: Graph of S_v (Maximum Valley Height) against nominal thickness for all grades

The more functional parameters are those derived from the bearing curve and the related family (formerly the volume family). The relationship between these four parameters is very interesting, see figure 5.4. All four show a steady decrease with reduced thickness. The trend that they follow is very alike and this implies that, although the scale of the topography is getting smaller, the shape of the features on the surface and their relationship to each other is unchanged. This aspect is represented in figure 5.5, using profiles from the thinnest and thickest Source 2 samples.
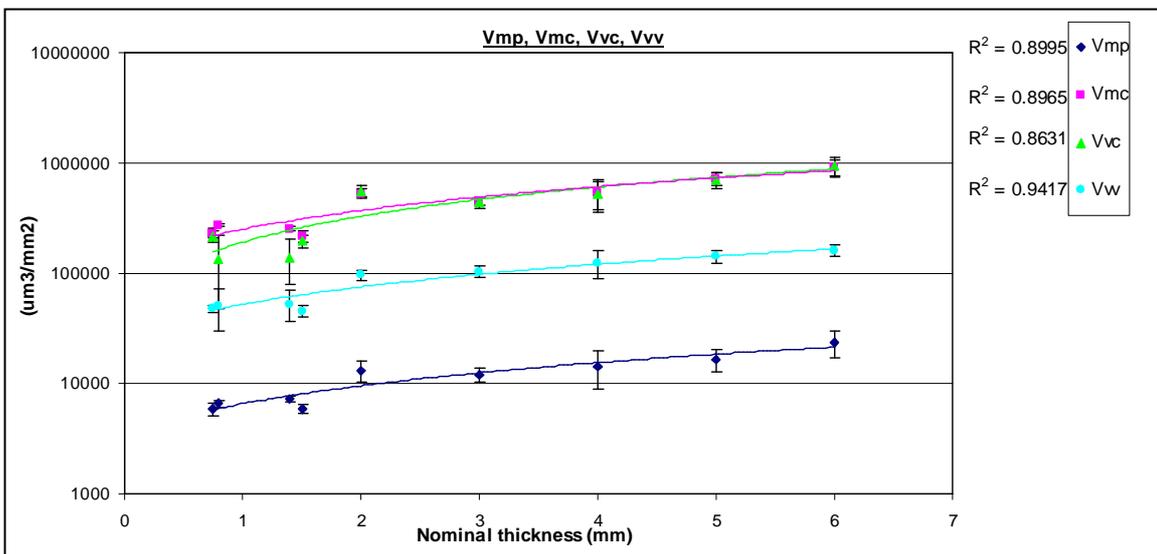
Figure 5.4: Graph of functional volume parameters against nominal thickness for all grades
(note: the trend line on this graph is curved due to the use of a logarithmic scale on the y-axis)

Figure 5.4 gives an indication that there are very few peaks left on the surface and that valleys dominate (much higher values for V_{vv} than for V_{mp}).

The V_{mc} and V_{vc} parameters are very close in value to each other. This shows that within the core area of the material the material and voids are of approximately the same volume.

2mm thick sample from Avesta (304L)   **6mm thick sample from Avesta (304L)**
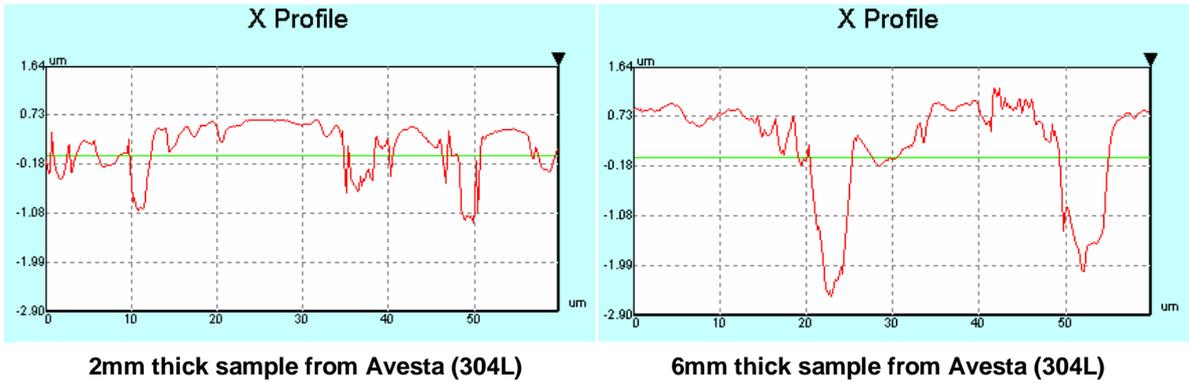
Figure 5.5: Profiles of the thickest and thinnest samples from Source 2

The extreme parameter S_{5z} (Ten Point Height of the surface) is calculated using only the ten highest points of the topography, figure 5.6. This is material that would be expected to be consolidated in the rolling processes. Hence, those samples that have had a greater degree of cold rolling (the thinner samples) have the lowest values of S_{5z}.
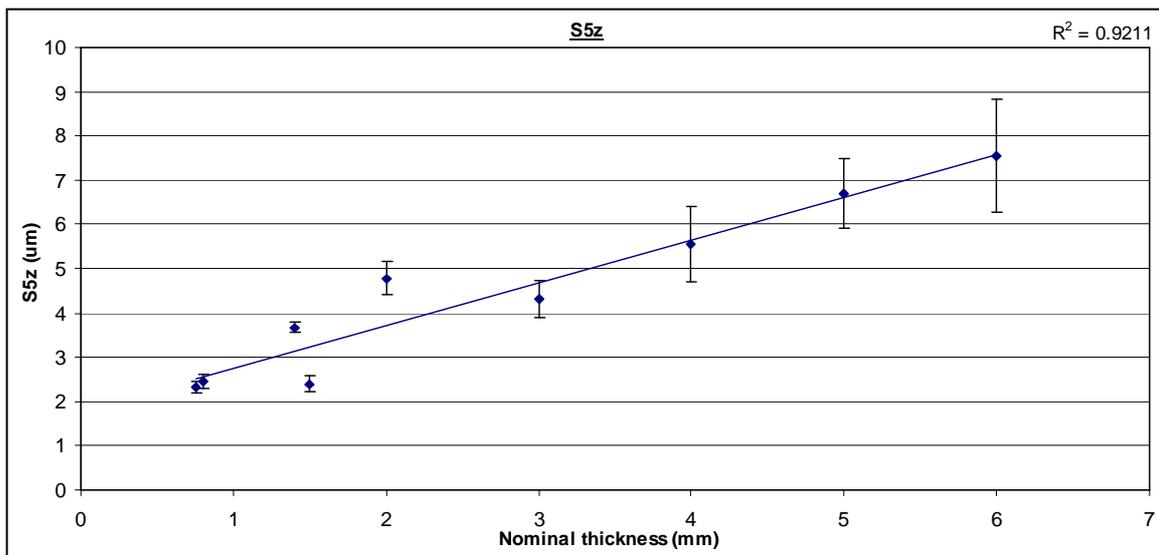
Figure 5.6: Graph of S_{5z} (Ten Point Height of surface) against nominal thickness for all grades

S_a (the Arithmetic Average Roughness), figure 5.7 shows a very similar trend to S_q (figure 5.1), as would be expected due to their similarity. It is given for completeness, since its 2D counterpart, R_a, is one of the most commonly used surface quality parameters in the industry.
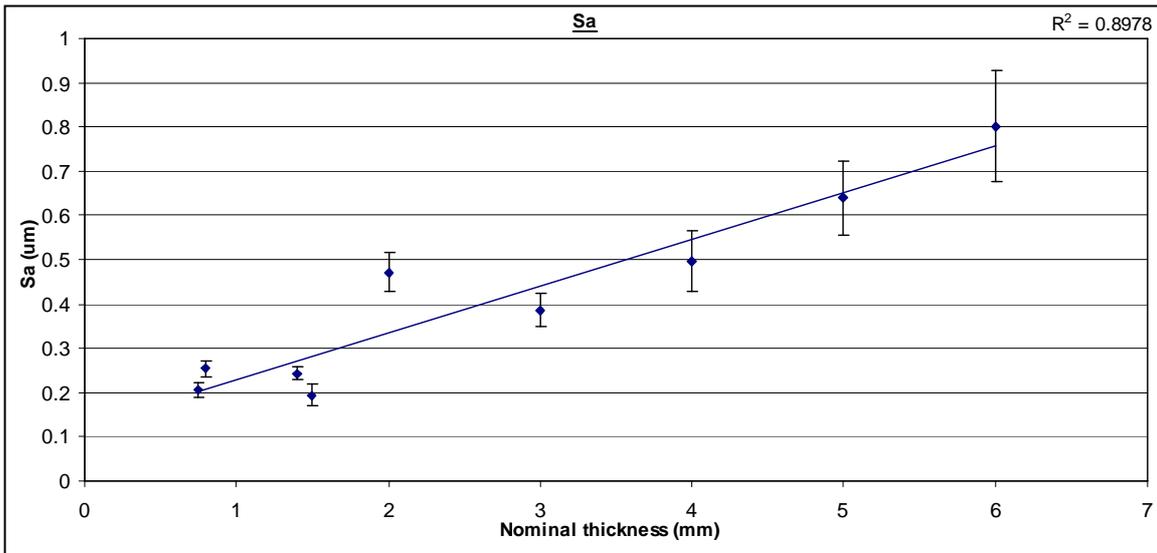
Figure 5.7: Graph of S_a (Arithmetic Average Roughness) against nominal thickness for all grades

5.6.2 Results for Grade Variation

Parameters that showed good correlation with grade alterations are: S_q, S_z & S_v from the amplitude family, V_{mp}, V_{mc}, V_{vc} & V_{vv} from the volume family and S_{5z} & S_a (others).

The variation in results between the different material specifications is shown in the second set of graphs (5.8 to 5.14). The two main grades studied are 304 and 316, which are the highest production grades by Outukumpu. The actual material thickness is used, rather than the nominal thickness, for accuracy. The variation in results between the different material specifications revealed that similar trends to those found without grade separation were present. S_q (Root Mean Square Deviation) decreases with decreasing thickness for both 304 and 316 grades, figure 5.8. Using the trend line as a guide, it can be noted that, on average, 304 materials have slightly higher surface roughness than 316 materials of the same thickness.
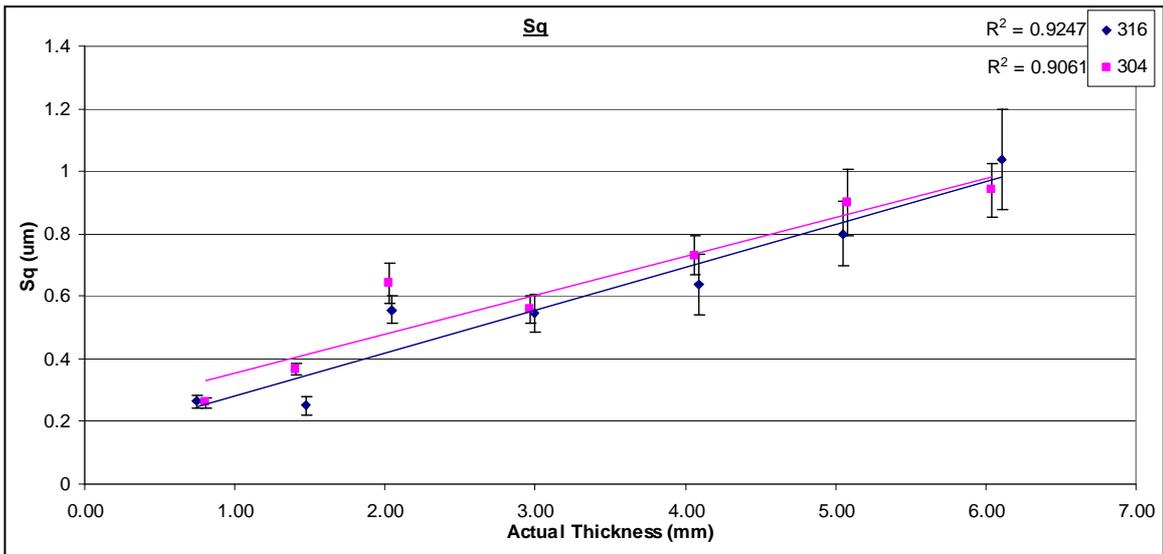
Figure 5.8: Graph of S_q (Root Mean Square Deviation) against actual measured thickness for 316 and 304 grades

Being extreme parameters, S_z and S_v do not show the trend found for S_q, that 304 is generally slightly rougher than 316, figures 5.9 and 5.10. This is almost certainly due to the fact that outliers influence them. It is interesting to notice that the 316 materials error bars and therefore the spread of the data is much greater than that of 304 materials. This may indicate that 316 is more difficult to consolidate, as the spread is highest toward the thicker samples (i.e. those with least rolling to consolidate outlying features). This is considered further in section 5.7, where the hardness of the main grades is investigated.
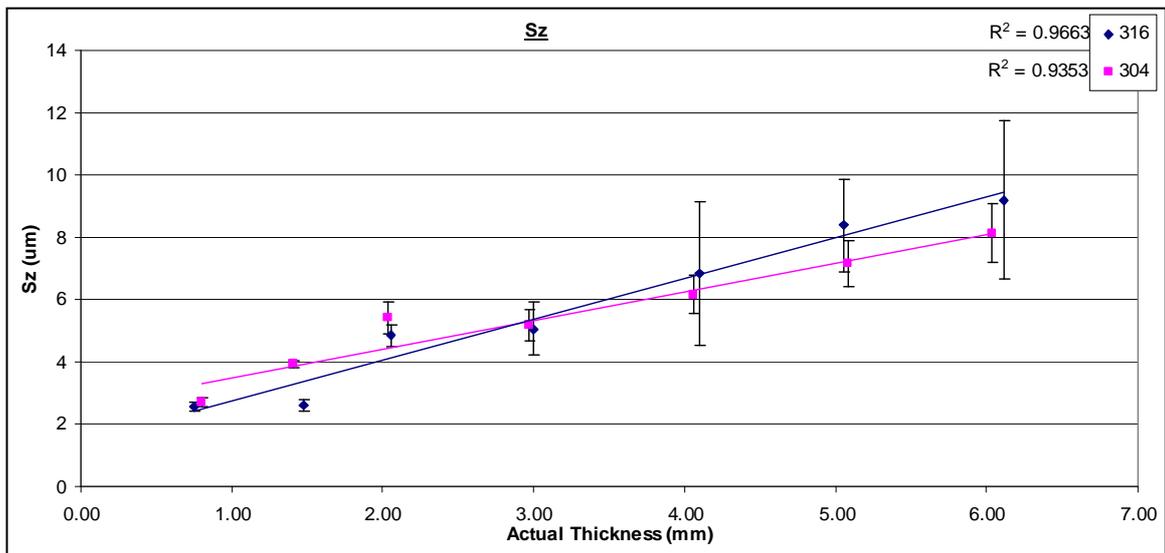
Figure 5.9: Graph of S_z (Maximum Height of Texture surface) against actual measured thickness for 316 and 304 grades

97
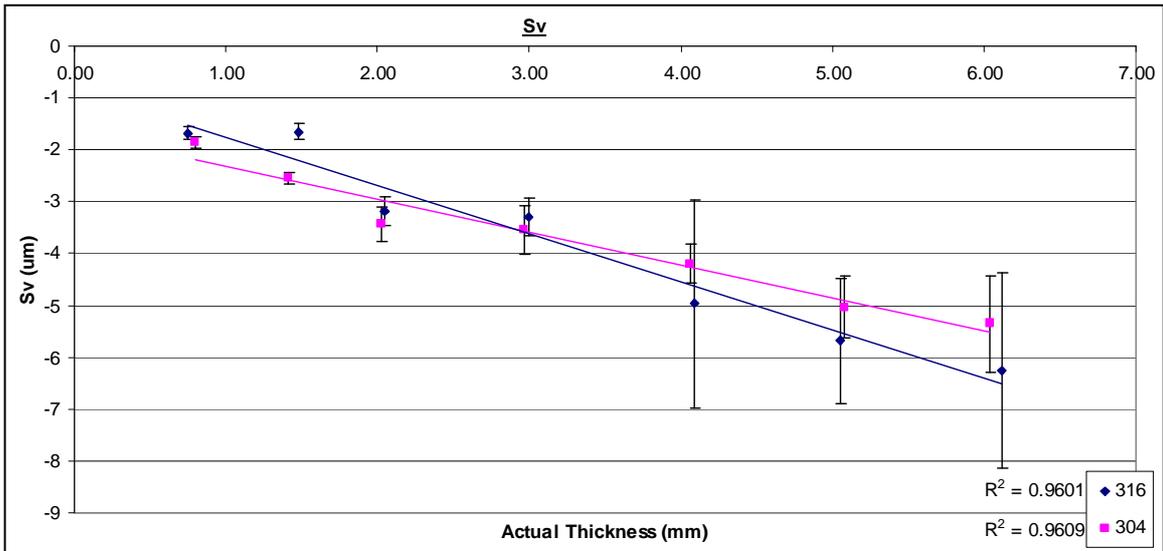
Figure 5.10: Graph of S_v (Maximum Valley Height) against actual measured thickness for 316 and 304 grades

The functional set of parameters (V_{mp}, V_{mc}, V_{vc} and V_{vv}), figures 5.11 and 5.12, again follow similar trends to figure 5.4. Note that the data has been separated over two graphs and does not use a log scale on y (as previously). This is simply for clarity.

Again, it should be noted that, with the exception of V_{vv}, values for 304 materials are slightly higher than for 316 materials. The fact the V_{mp} is larger for 304, yet S_z is not, could indicate that the peaks on 304 material are not necessarily high but do take up more volume (possibly 'squashed' peaks).
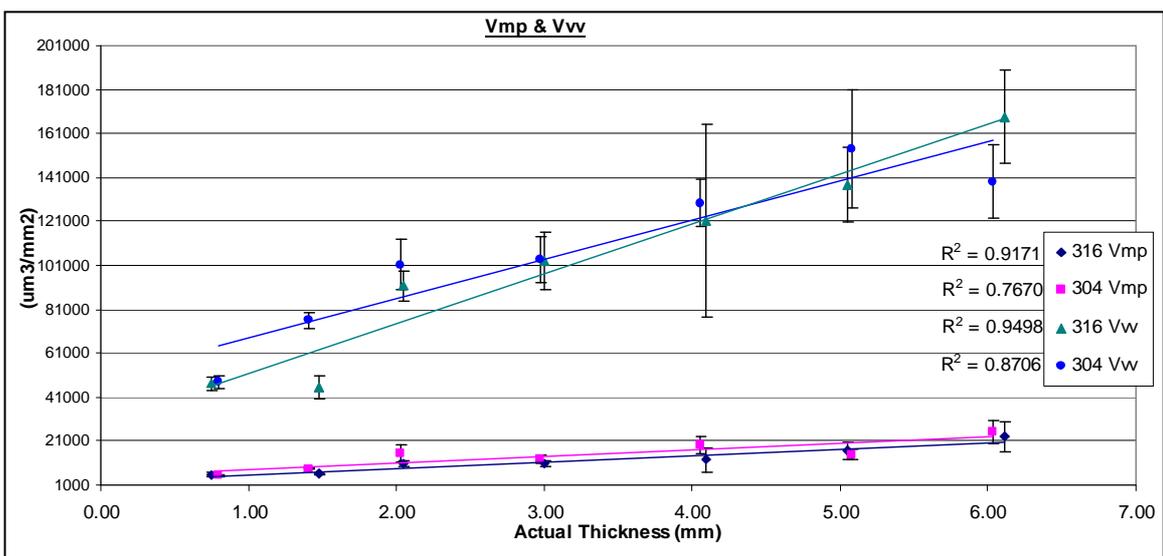
Figure 5.11: Graph of functional volume parameters, V_{mp} (Material Volume of the Texture surface) and V_{vv} (Valley Void Volume of the Texture surface) against actual measured thickness for 316 and 304 grades
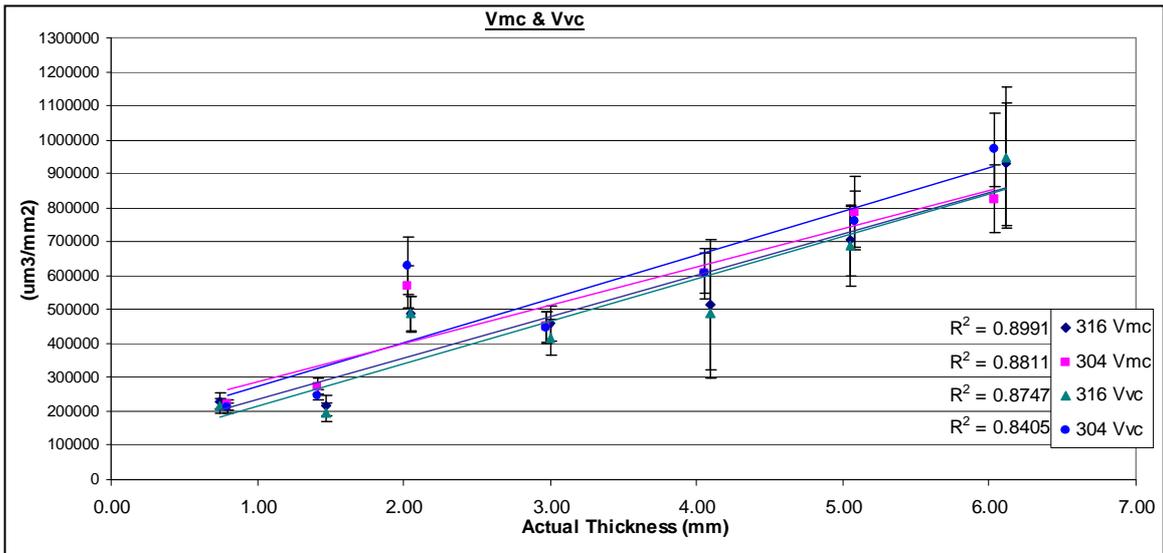
Figure 5.12: Graph of functional volume parameters, V_{mc} (Core Material Volume of the Texture surface) and V_{vc} (Core Void Volume of the Texture surface) against actual measured thickness for 316 and 304 grades
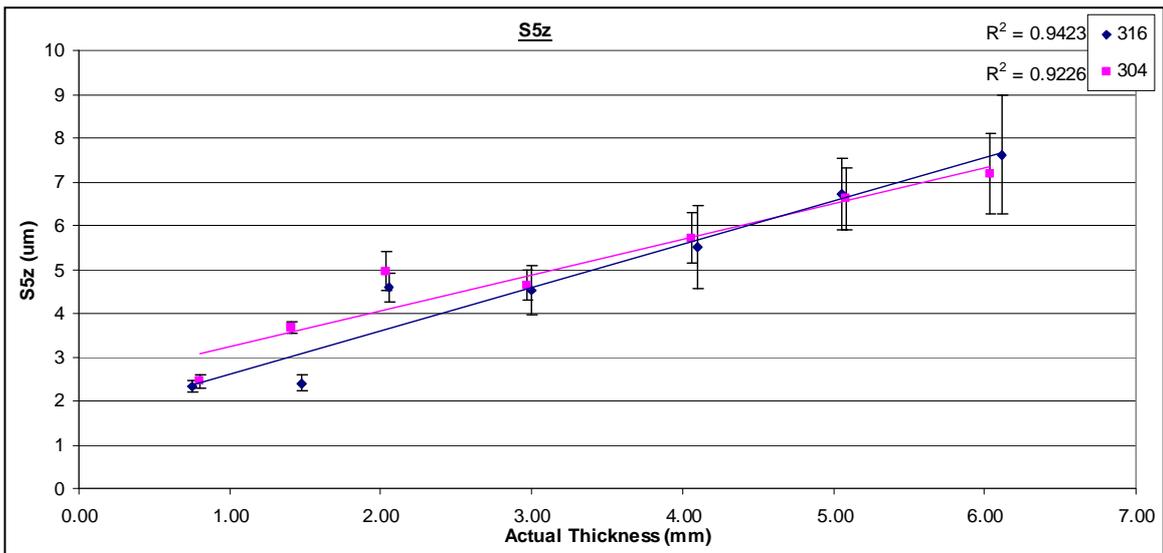
Figure 5.13: Graph of S_{5z} (Ten Point Height of surface) against actual measured thickness for 316 and 304 grades

Figure 5.13, S_{5z}, reiterates the results of figure 5.6 and has a similar trend.

Figure 5.14, S_a, is similar to the result of figure 5.7, as expected and is shown only for completeness.
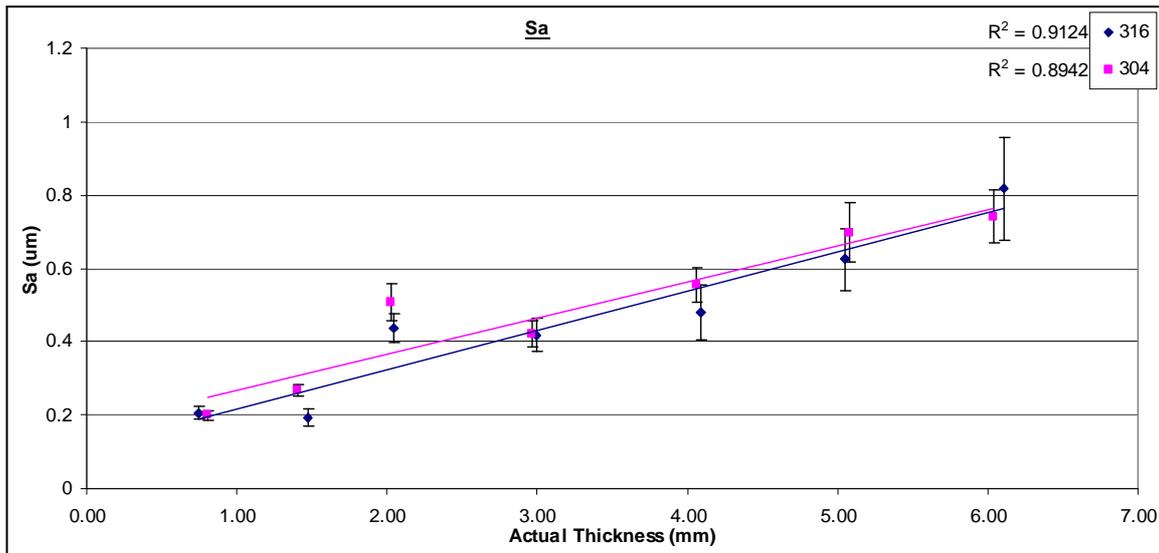
Figure 5.14: Graph of S_a (Arithmetic Average Roughness) against actual measured thickness for 316 and 304 grades

5.6.3   Discussion of Results for Grade Separation

The most obvious result of the separation of grades is that, in general, 304 grade materials are slightly rougher, on average than 316 materials of the same thickness. The extent of this slight difference is clarified below studying the average values for 316 and 304 materials of all thicknesses. As can be seen in table 5.1 below, with the exception of S_z, all amplitude related parameter values for 304 grade materials are higher than for 316 grades.

Table 5.1: Average parameters for 316 and 304 grade materials

Parameter	Average 316	Average 304
S_q	0.585	0.628
S_z	5.653	5.531
S_v	-3.817	-3.712
S_{5z}	4.811	5.035
S_a	0.454	0.484

The fact that S_q and S_a values are higher implies that the 304 materials have slightly higher average roughness. However, the difference between the S_z and S_v parameters shows that the 316 grade materials have a greater range of topography heights (both higher peaks and deeper valleys). Since this may have been due to the slightly higher range of thicknesses, table 5.2 shows average parameters only for nominal thicknesses between 2 and 6 mm where the same trends were seen. It is also evident in the data that the spread of results (the standard deviation – see error bars on graphs) is larger for the 316 materials.

Parameter	Average 316	Average 304
S_q	0.716	0.754
S_z	6.872	6.414
S_v	-4.677	-4.316
S_{5z}	5.791	5.824
S_a	0.555	0.584

Changes in topography across the width of strip are apparently caused by variations in rolling pressure and lubrication distribution. It was hoped that further samples from within the process route could be obtained to track the changes in surface topography at each stage of production. This would give a better insight into the way that the final finish is developed and how adjustments in the production may affect the outcome but is, in reality, very difficult to accomplish in large-scale production such as this and as a result have not formed part of this study.

The other major variation in the sample set is the final process method used. This can either be skin-passing or tension levelling (this is source dependant, either Source 1 or 2, respectively).

Due to the limited number of samples and the processing capabilities of the different manufacturing sites, there is only one comparable pair of samples of the same thickness (3 mm) that come from different sources. Therefore the analysis of the differences in topography caused by the final processing operation is based on the trends found for Source 1 and 2 samples.

Figures 5.15 to 5.21 show the results of analysis with separation based on source and thickness using all the grades available in the study.
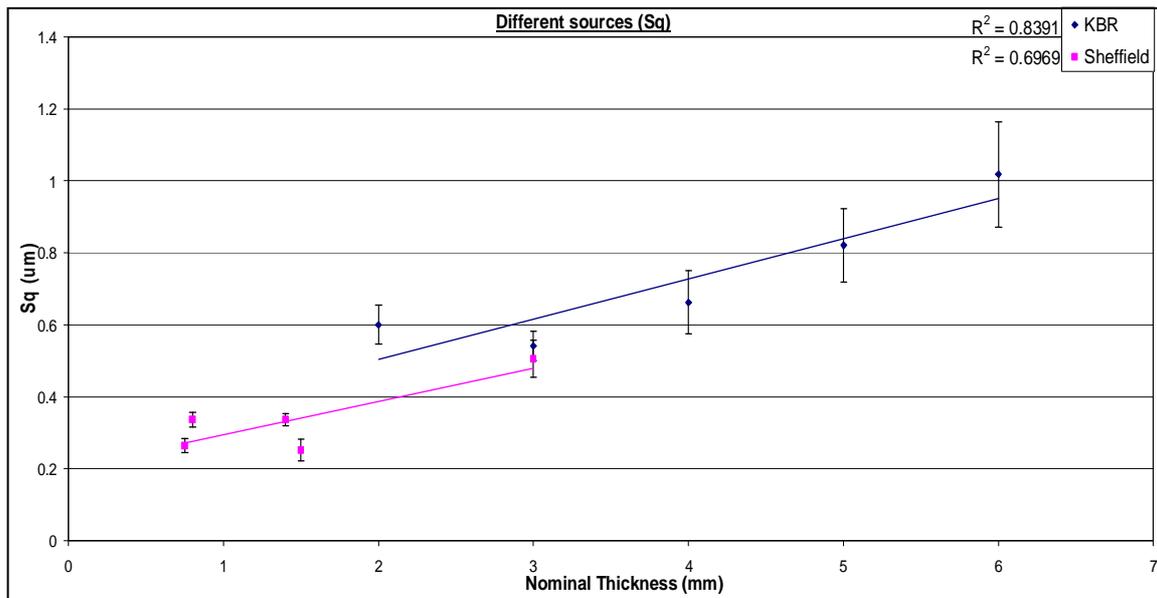
Figure 5.15: Graph of S_q (Root Mean Square Deviation) against nominal thickness for different sources
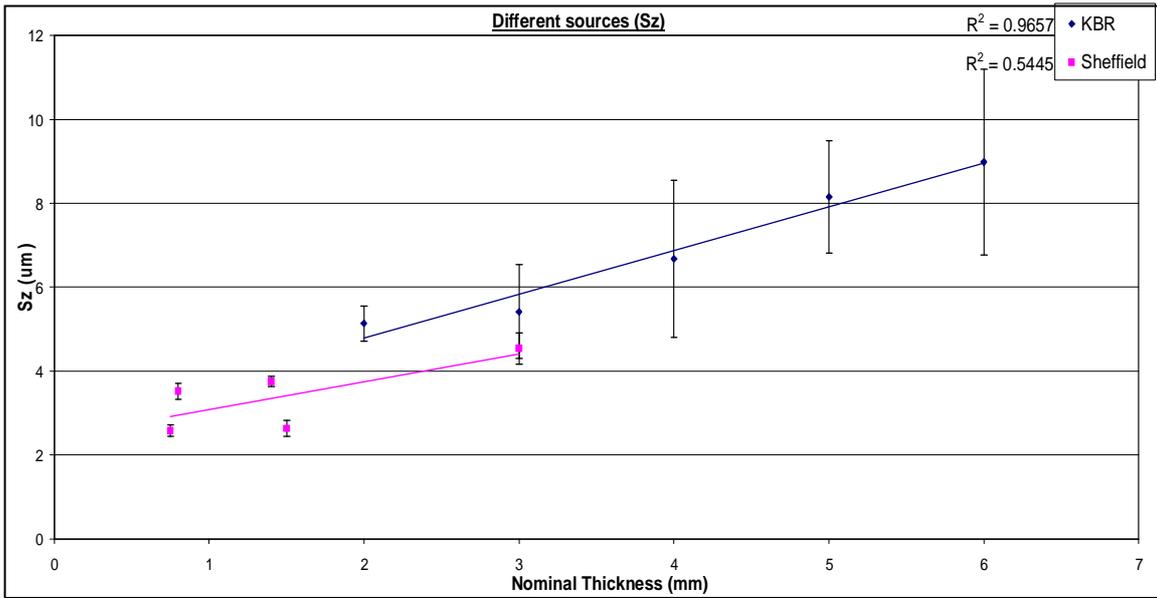
Figure 5.16: Graph of S_z (Maximum Height of Texture surface) against nominal thickness for different sources
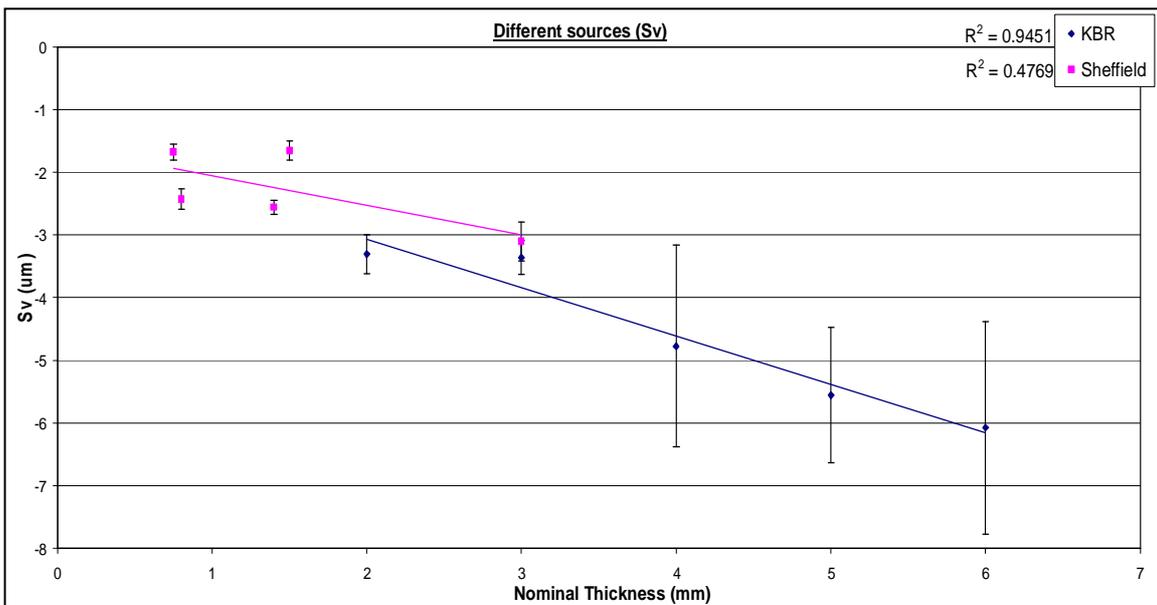
Figure 5.17: Graph of S_v (Maximum Valley Height) against nominal thickness for different sources
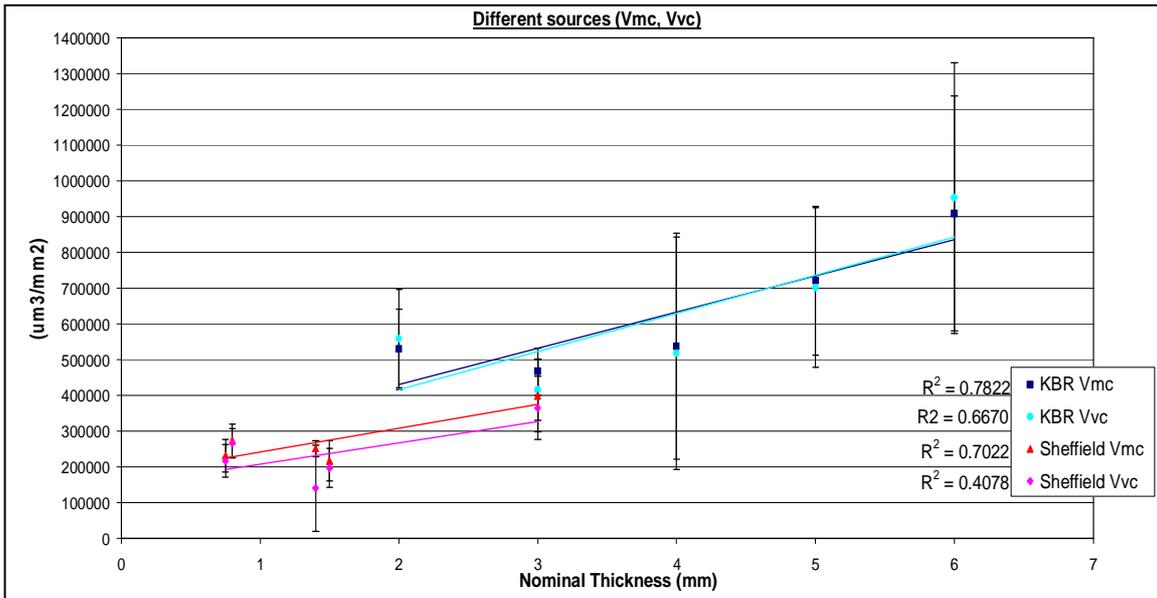
Figure 5.18: Graph of functional volume parameters, V_{mp} (Material Volume of the Texture surface) and V_{vv} (Valley Void Volume of the Texture surface) against nominal thickness for different sources
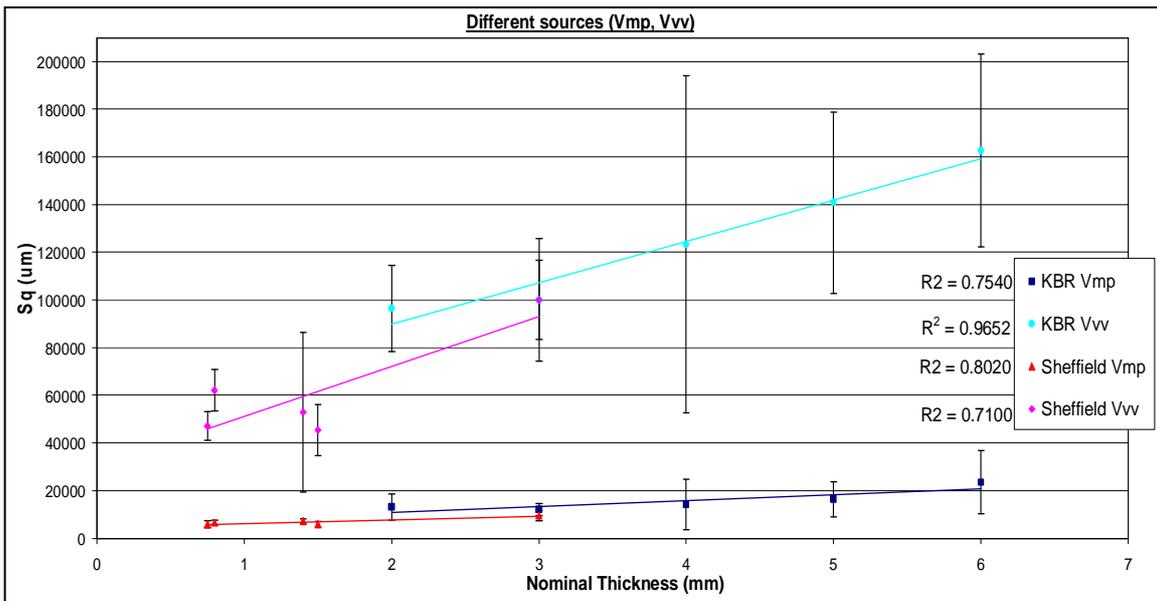
Figure 5.19: Graph of functional volume parameters, V_{mc} (Core Material Volume of the Texture surface) and V_{vc} (Core Void Volume of the Texture surface) against nominal thickness for different sources
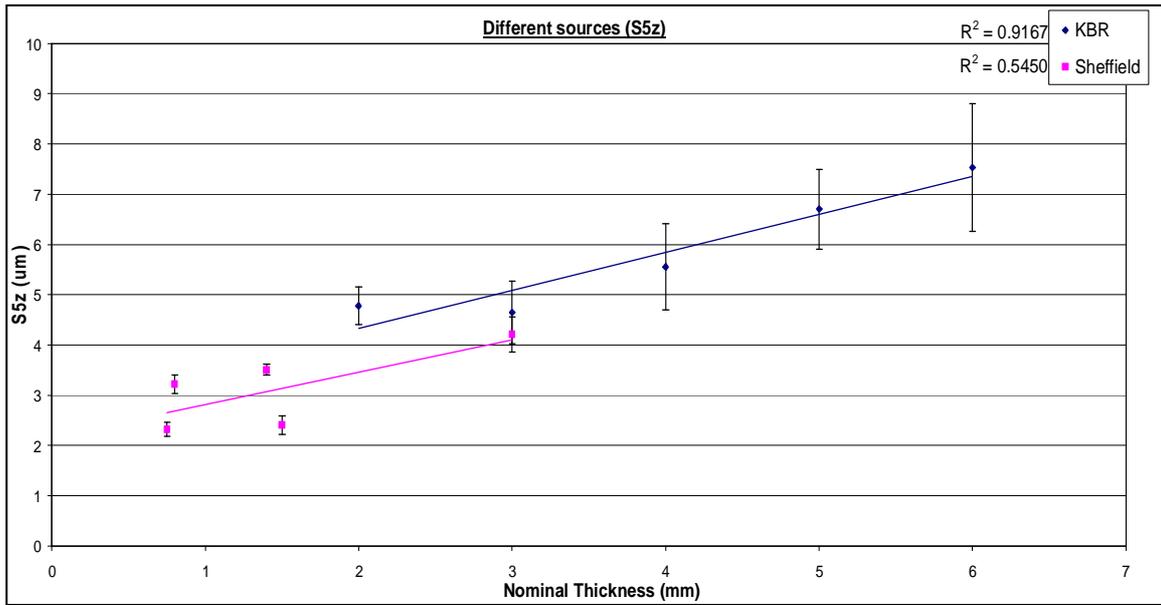
Figure 5.20: Graph of S_{5z} (Ten Point Height of surface) against nominal thickness for different sources
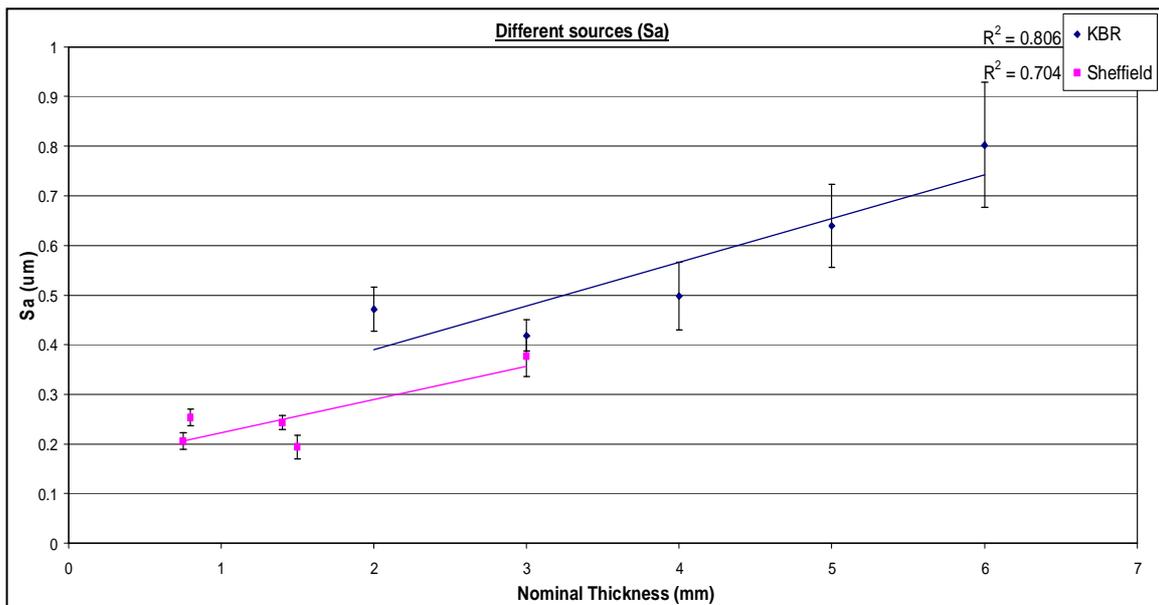
Figure 5.21: Graph of S_a (Arithmetic Average Roughness) against nominal thickness for different sources

In all the graphs the Source 1 samples have smaller values of parameters than those of Source 2 samples in general and this is more obvious when looking at materials of the same thickness (for both 316 and 304 grades). This is most apparent on the extreme parameters (S_z and S_{5z}, figures 5.16 and 5.20). The difference in processing of the samples is now apparent, the skin-pass method of final finishing (used on Source 1 samples) gives a smoother and more consolidated topography, having better defined edges than those that have undergone tension stretching (used on Source 2 samples), see figure 5.22.

3mm Source 2 sample (304L)　　　　**3mm Source 1 sample (304L)**
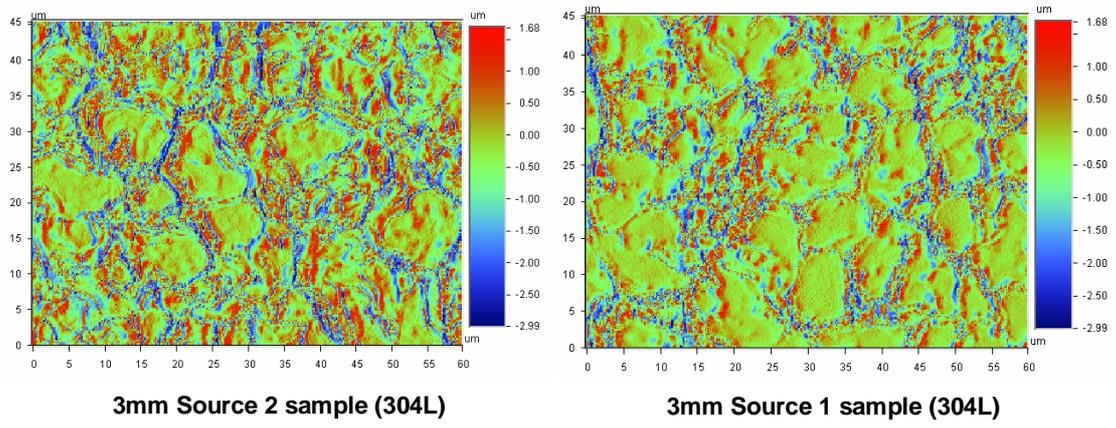
Figure 5.22: Contour map showing surface topography differences between sources

5.7. Hardness Investigation

To further the understanding of the results found for differences in topography for the two main production grades, 304 and 316, their bulk hardness and microhardness (surface hardness) were tested.

The results for Vickers hardness of the bulk of the materials are shown in figure 5.23 (error bars are too small to show). They are plotted against the actual gauge of the samples tested and separated, distinguishing between the different grades (304 and 316) and the two production sites (Sources 1and 2).

As expected, there is only minimal difference in bulk hardness properties between the two production methods. Also, the difference caused by gauge variation is small (<40HV between the thickest and thinnest samples). This is believed to be due to the bulk properties stemming mainly from the properties of the original hot band material. The effects of rolling and pickling do not affect the bulk hardness properties. However there is a small but distinct difference between the 304 and 316 grades bulk properties, whereby 304 grade material is marginally harder than 316.
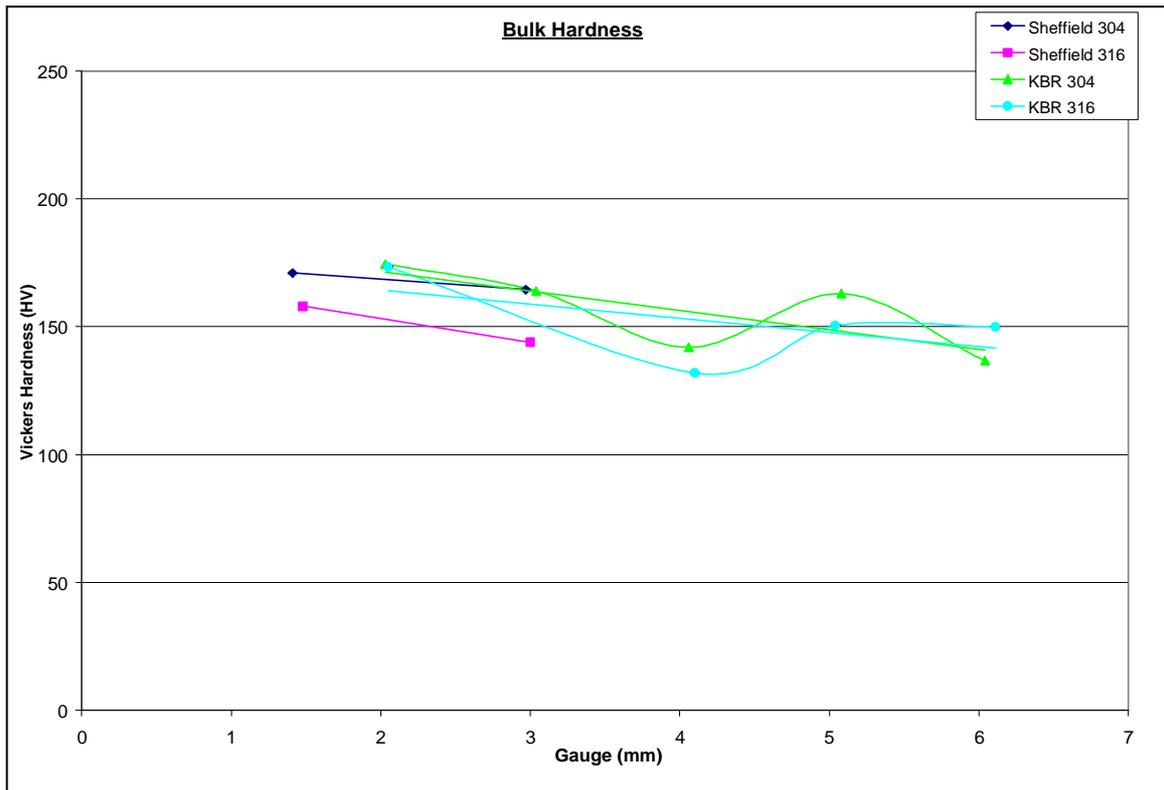
Figure 5.23: Vickers Bulk Hardness against gauge thickness for sources 1 and 2

To further this study, the micro-hardness (or surface hardness) has also been tested. The results, figure 5.24, show that there is only a small magnitude of difference between the two grades of material from the Source 2 site; however, the difference in surface hardness properties between the grades from the Source 1 site is more noticeable. This would imply that

the skin pass method of finishing used in production at Source 1 gives more distinction between the grades, whereas the tensioning device used in Source 2 production does not.

The difference in surface hardness properties between the two production sites is also more noticeable for the 316 grades. This result implies that the Source 2 production method makes the surface of the 316 material harder than the Source 1 method of skin passing.

Additionally, a greater range of surface hardness's can be seen across the different gauges. The thicker samples have a marginally softer surface, implying that the rolling operation to bring the sheet to gauge has the effect of hardening the surface.
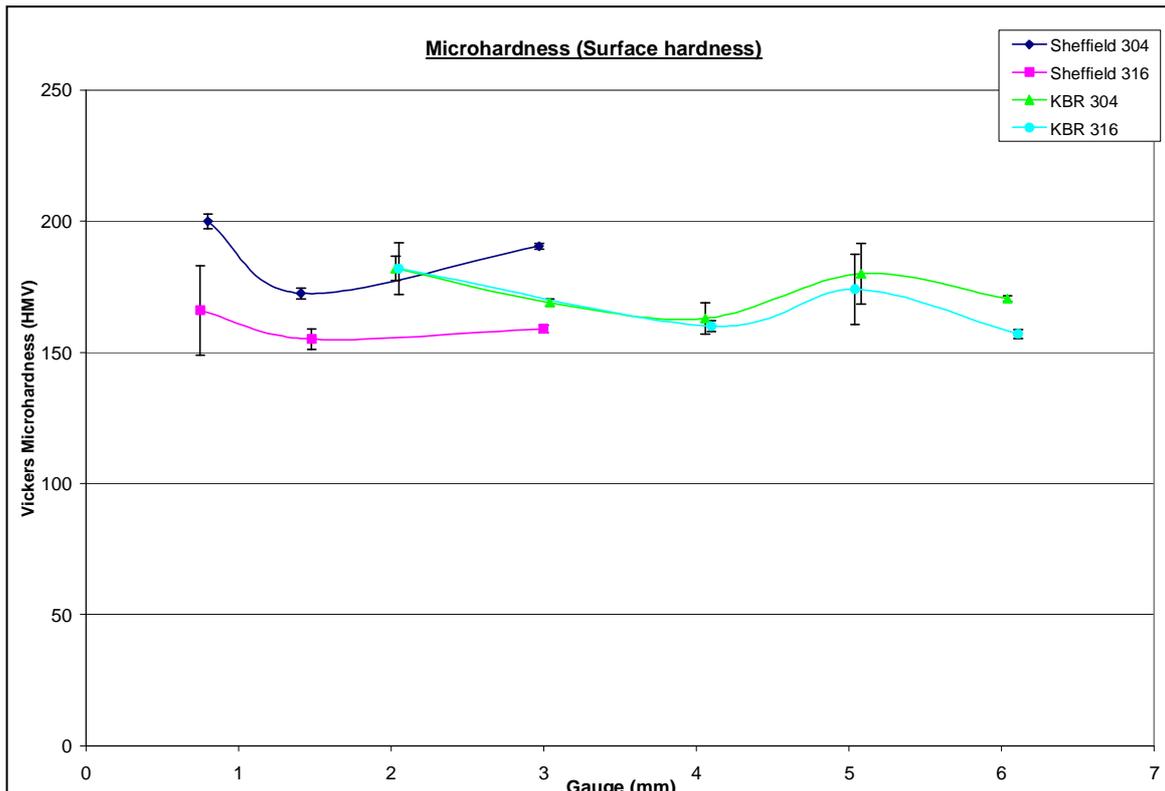
Figure 5.24: Vickers Microhardness against gauge thickness for sources 1 and 2 (error bars based on ½ standard deviation of measurements)

5.7.1   Summary of Hardness Investigation

The main findings of this investigation are:

> ➤ The bulk hardness of 304 grade samples is marginally greater than 316 grades.
> ➤ The surface hardness of 304 samples produced at Source 1 is greater than the 316 grade.
> ➤ The thicker samples have a marginally softer surface.

5.8. Conclusions

The general relationship between surface roughness and gauge has expanded into an in-depth examination of what is happening to the features of the surface during cold rolling and how differences in grade and process can affect the development of features.

> ➢ The thinner gauges have a smoother finish.
> ➢ Although the scale of the topography is getting smaller, the shape of the features on the surface and their relationship to each other is unchanged.
> ➢ There are very few peaks left on the surface and the valleys dominate the topography.
> ➢ Within the core area of the material, the material and voids are of approximately the same volume.
> ➢ On average, 304 materials have slightly higher surface roughness than 316 materials of the same thickness.
> ➢ The spread of the data for 316 grade materials is much greater than that of 304 grade materials.
> ➢ The peaks on 304 grade materials are not necessarily higher but do take up more volume than those on 316 grade materials.
> ➢ The skin pass method of final finishing (used on Source 1 samples) gives a smoother and more consolidated topography, having better defined edges than those that have undergone tension stretching (used on Source 2 samples).

Chapter 6   Optical Appearance

6.1. Summary of the Chapter

The available instrumentation is discussed and sample variation with respect to appearance is considered. The effect of rolling direction to appearance, measurement direction (in respect to the rolling direction of the sample), angle of the measurement, sample thickness and grade variation are studied and initial measurement trials are completed to assess the general optical properties of the 2B finish with regard to other finishes. The relationship of four optical descriptors to 3D topography parameters, including the use of a new analysis method, are presented and discussed.

6.2. Introduction

The appearance of a product is often used by consumers as a measure of the quality of the product and the materials it is made from. There is a psychological relationship between appearance and performance and durability [13]. When given a choice between similar product function, a consumer will inevitably buy what looks best, despite having no other evidence to back up this view.

The appearance of an object is influenced by many factors, the interaction of light with the surface, the direction of both light source and viewer, the objects physical characteristics, optical properties and subjective human perception. As previously mentioned, stainless steel finishes are not normally quantitatively assessed. Inspection of the surface appearance is carried out by the human eye and the colour and general look is commented on. Phrases like 'dullness', 'greyness', 'pearly' and 'matt' are used, which clearly gives rise to variations in perception across inspectors, especially where the product is supplied from multiple manufacturing sites. The result of this inspection is a simple statement of whether the product looks good or bad (pass or fail criteria).

Manufacturers of stainless steel products realise the importance of uniformity of appearance, as variability in a group of the same products indicates to the end-user poor process or production control and therefore inferior quality. Companies are consequently working towards a more quantitative assessment method. The ability to link the surface topography features to numerical optical property characteristics will yield not only a better understanding of the effects of topography on appearance but also enable manufacturers to quantify their pass/fail criteria and remove the subjectivity of human perception and eventually increase consumer confidence.

6.3. Method of Assessing Appearance

As discussed in section 2.4.3.2 Instrumentation to measure reflectance, instruments are seperated into two groups, physical and psychophysical analysis types [14]. The appearance attributes of interest for this project are geometric rather than colour related and because of the nature of stainless steel, only specular reflection meters are suitable for measuring the gloss, haze, specular reflectance and distinctness of image. The instrument used for this project was a Panaspect appearance meter (a type of glossmeter), see figure 6.1, providing the following four optical parameters (equations given are for 60°illu mination angle):

Gloss (Gls). This is the percentage of light reflected from the sample at the specular angle, when compared to that from a perfect mirror and is responsible for reflected highlights and shiny or lustrous appearance.

$$Gls = 100 \times \frac{\sum Ir_{sample}(60° \pm 0.9°)}{\sum Ir_{s \tan dard}(60° \pm 0.9°)}$$

Equation 6.1

Specular Reflectance (Rs) is the proportion of the total emitted light that is reflected from the sample to the specular angle rather than diffused either side.

$$Rs = 100 \times \frac{\sum Ir_{sample}(60° \pm 0.1°)}{\sum Ir_{s \tan dard}(60° \pm 0.1°)}$$

Equation 6.2

Haze (Hz) is the percentage of light reflected from the sample at a range of angles compared to that reflected from a perfect mirror and gives the milky or cloudy appearance next to the reflected highlights.

$$Haze = 100 \times \frac{\sum Ir_{sample}((58°to59°) + (61°to62°))}{Gls_{s \tan dard (Blackglass)}}$$

Equation 6.3

Distinctness of image (DOI) is a measure of the ratio of light that is reflected from the sample over a limited range either side of the specular angle and can be considered as a sharpness of an image reflected from the surface.

$$DOI = 100 \times 1 - (\frac{\sum Ir_{sample}((59.4°to59.6°) + (60.4°to60.6°))}{2 \times \sum Ir_{sample}(60° \pm 0.1°)}$$

Equation 6.4
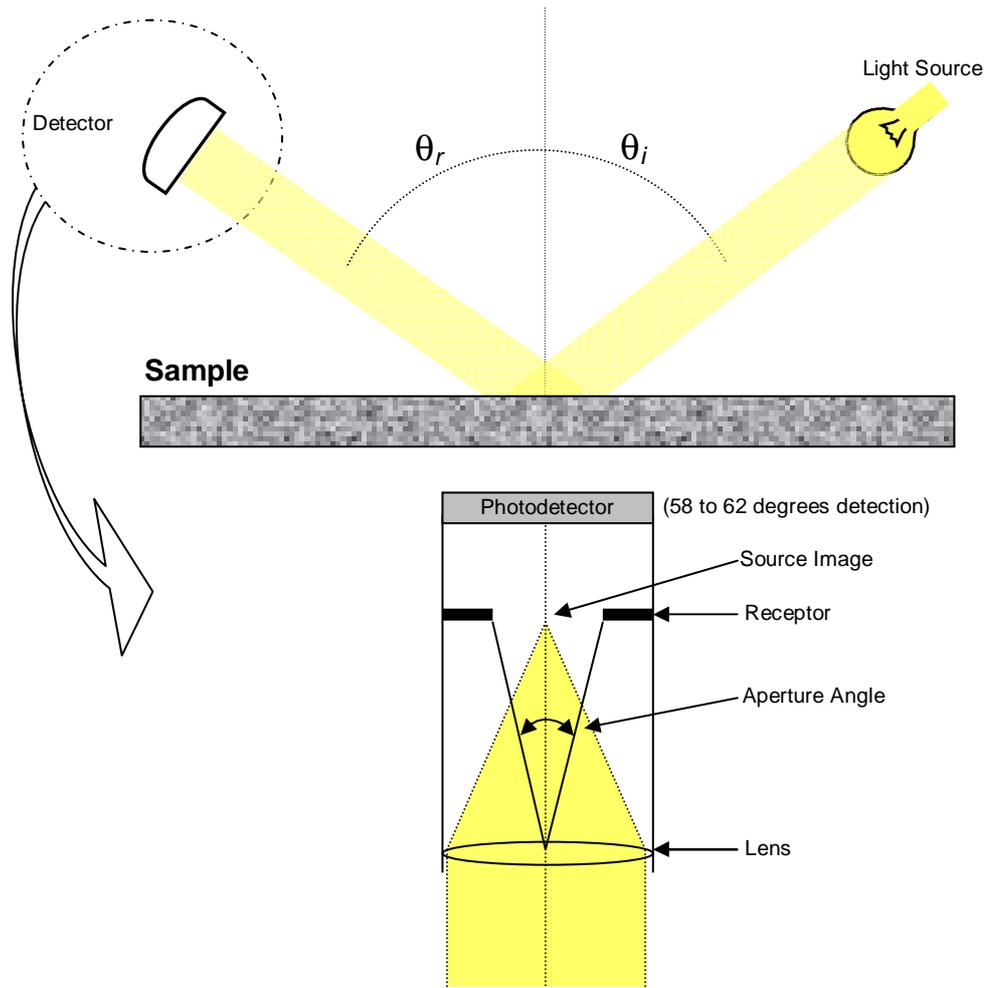
Figure 6.1: Panaspect Appearance Meter

The above definitions of the parameters are given by the instrument manufacturers, based on the method of measurement and calculation algorithms and hence, there maybe a slight variation from other manufacturers terminology.

6.4. Relationship of Topography to Appearance

The appearance of sheet metals is governed by the extent of their reflection (diffuse and specular) as they do not possess transmission properties. They range in magnitude from the mirror-like (wholly specular reflection on a highly polished, flat surface) to the very matt (wholly diffuse reflection normally associated with rough finishes). Their optical properties depend mainly on their production method, although metal composition can have an effect (due to the materials reaction to the applied processing).

The appearance effects of production methods on stainless steel finishes are varied and it is possible to produce both matt and highly reflective surfaces (though the work involved deems this uneconomical). The mill and derived finishes (seen in table 2.1) can result in distinctly different surface topographies, although their visual appearance may be very similar.

The features that affect the optical properties of stainless steel sheet can be deduced by comparing the production methods and end appearance of 2D and 2B surfaces. The 2D finish is matt with low reflectivity. As discussed previously skin passing enhances surface brightness. It is the only difference in the process between 2D and 2B, wherein it removes or flattens the higher asperities of the 2D surface to give the 2B surface which is of similar colour but much brighter and more reflective. So the deduction is that plateau roughness and, conceivably, the area covered by valleys dictates the reflectivity and brightness of the 2B surface.

Although it is clear how the surface topography of the 2B finish is developed during manufacture (section 2.4.2.2 Effect of Production on Topography), there is currently no method to quantify its visual appearance.

6.5. Direction and Angle of Measurement

Appearance measurements of gloss (Gls), specular reflectance (Rs), haze (Hz) and distinctness of image (DOI) were made at two angles (20 and 60 degrees to the horizontal) and longitudinally and transversely to the rolling direction on each surface.

This gives four variations for each sample, 20° transversely (20T), 60° transversely (60T), 20° longitudinally (20L) and 60° longitudinally (60L).

6.6. Initial Measurements

The initial investigation carried out involved samples with very different surface finishes (on stainless steel). This was used firstly to assess the ability of the glossmeter to detect large differences in gloss and also to give preliminary, average values of the four optical descriptors for the 2B surface (gloss, specular reflectance, haze and distinctness of image). The four different stainless steel surface finishes studied were: 2B, bright annealed (2R), superbrushed and Hyclad (a new finish produced by peening a 2B finish).

The glossmeter readings were taken at two angles, 20 and 60 and longitudinally and transversely to the rolling direction on each sample (shown as L20, L60, T20 and T60 lines on the graphs). Sampling for all finishes was carried out in accordance with the test protocol (Chapter 4).

6.6.1   Results for 4 Finishes

Figure 6.2 shows a graph of gloss against S_q (Root Mean Square Deviation) for the four different stainless steel surface finishes. From this graph, the effect of rolling direction on the optical properties looks minimal, with the angle of measurement being more influential, except for on the superbrushed finish, where it is expected that rolling direction would be important due to the very anisotropic nature of the surface. It is also obvious that the gloss of the 2B surface is far lower than that of the bright annealed, which is normally described as "mirror like". In general it can be said that the higher the average roughness, the lower the gloss.
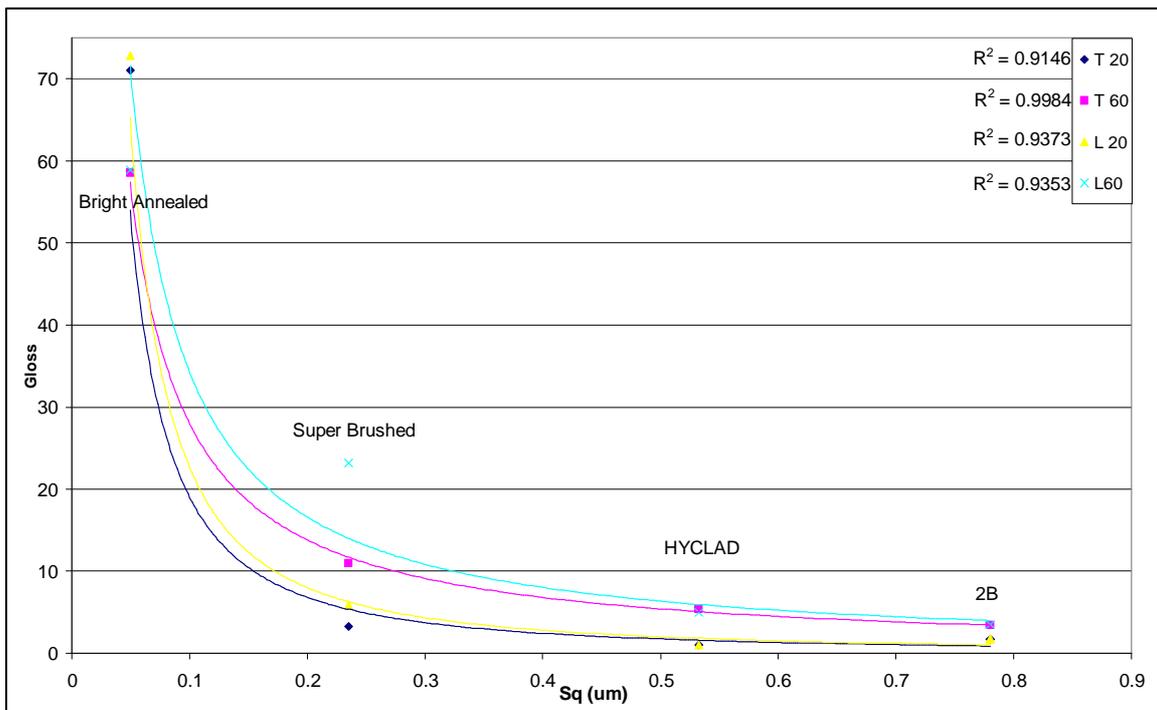
Figure 6.2: Graph of Gloss (Gls) against S_q (Root Mean Square Deviation)

Figure 6.3 shows a graph of specular reflectance (Rs) against S_q (Root Mean Square Deviation). The Rs of bright annealed is so much higher than for the other 3 finishes, it is difficult to see the relationships between them without separating the graphs.
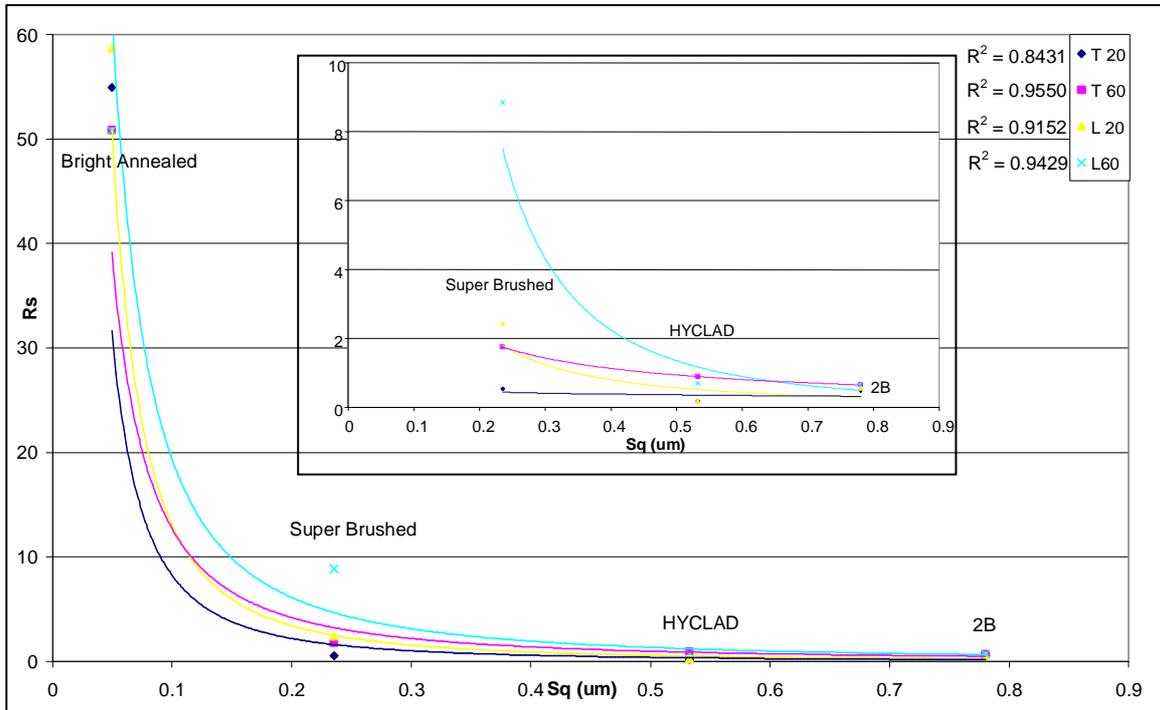
Figure 6.3: Graph of Specular Reflectance (Rs) against S_q (Root Mean Square Deviation)

It can be seen that the Rs of the superbrushed finish is heavily dependant on the rolling direction and the angle of measurement, again, this is due to the directional nature of the finish. The 2B finish again has lower values of Rs than the others alongside a higher average roughness. In general it can be seen that the higher the average roughness, the lower the specular reflectance.

Figures 6.4 and 6.5 show that haze and DOI do not clearly distinguish between the 4 main finishes and have little relationship to the average roughness of a surface.
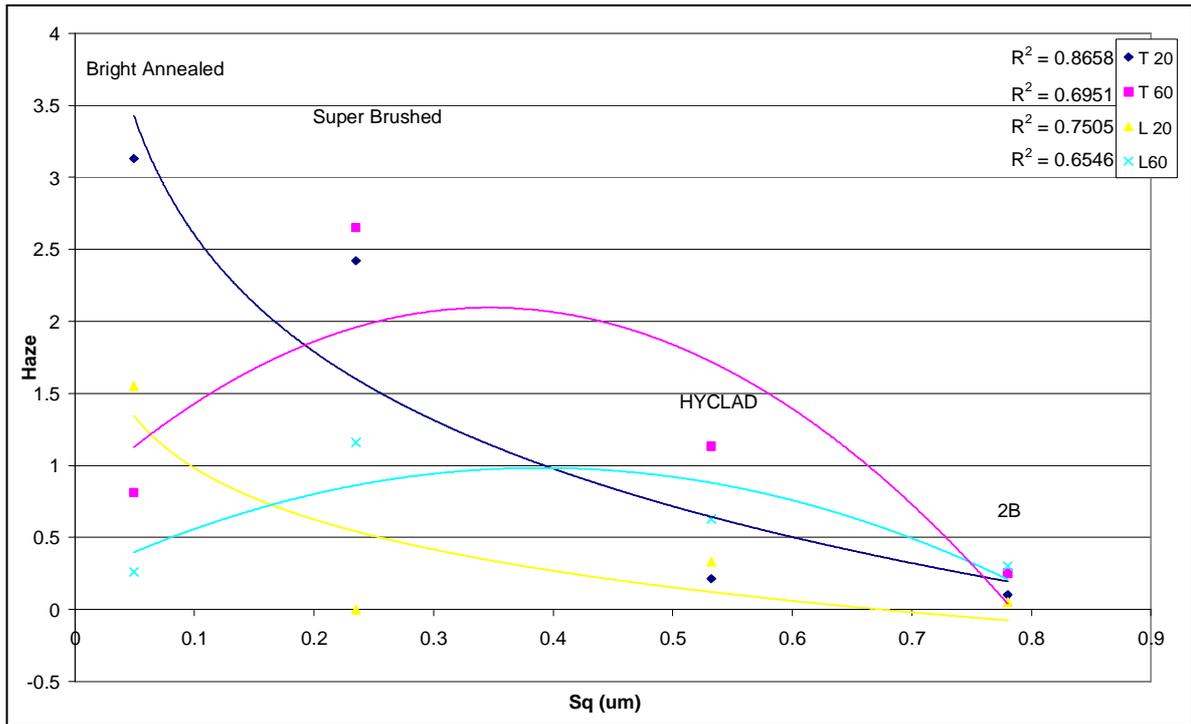
Figure 6.4: Graph of Haze (Hz) against S_q (Root Mean Square Deviation)
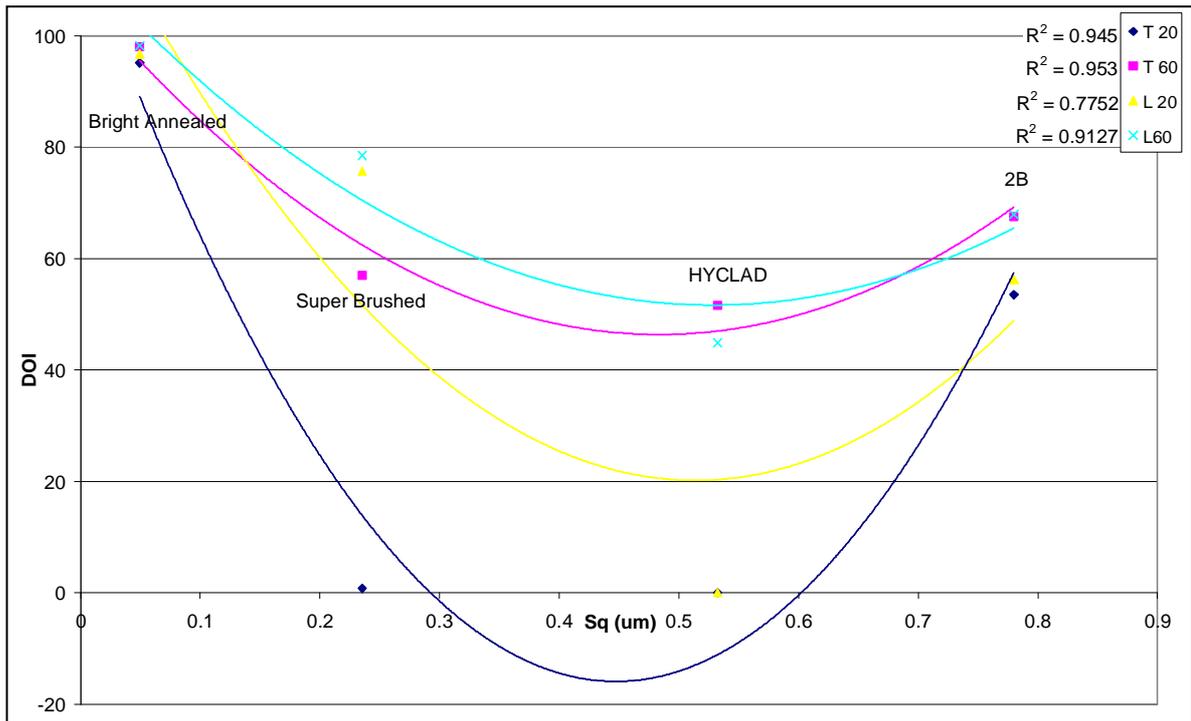
Figure 6.5: Graph of distinctness of image (DOI) against S_q (Root Mean Square Deviation)

115

6.7. Parameter Assessment

6.7.1   Results for the 2B Finish

The following results show the correlation of the appearance parameters to the 3D surface parameters of the 2B finish.

In past research it has been found that smooth surfaces reflect most of the incident light into the zero order, the specular direction, giving high values for Gls, Rs and DOI and diffract only a small amount of light either side of the zero order, giving low haze (Hz) readings.

In general, specular reflectance and gloss were the only appearance parameters that followed any trend with distinctness of image and especially haze being very irrational (selection shown in appendix 3).

Sampling for all finishes was carried out in accordance with the test protocol (Chapter 4). Error bars are ½ standard deviation of set. Trend lines are of exponential form.

As expected, the Arithmetic Mean Peak Curvature (S_{sc}) had a high trend correlation to gloss and specular reflectance, figures 6.6 and 6.7, although with error bars added to the graphs, little information can be construed, except between the highest and lowest values of S_{sc}.
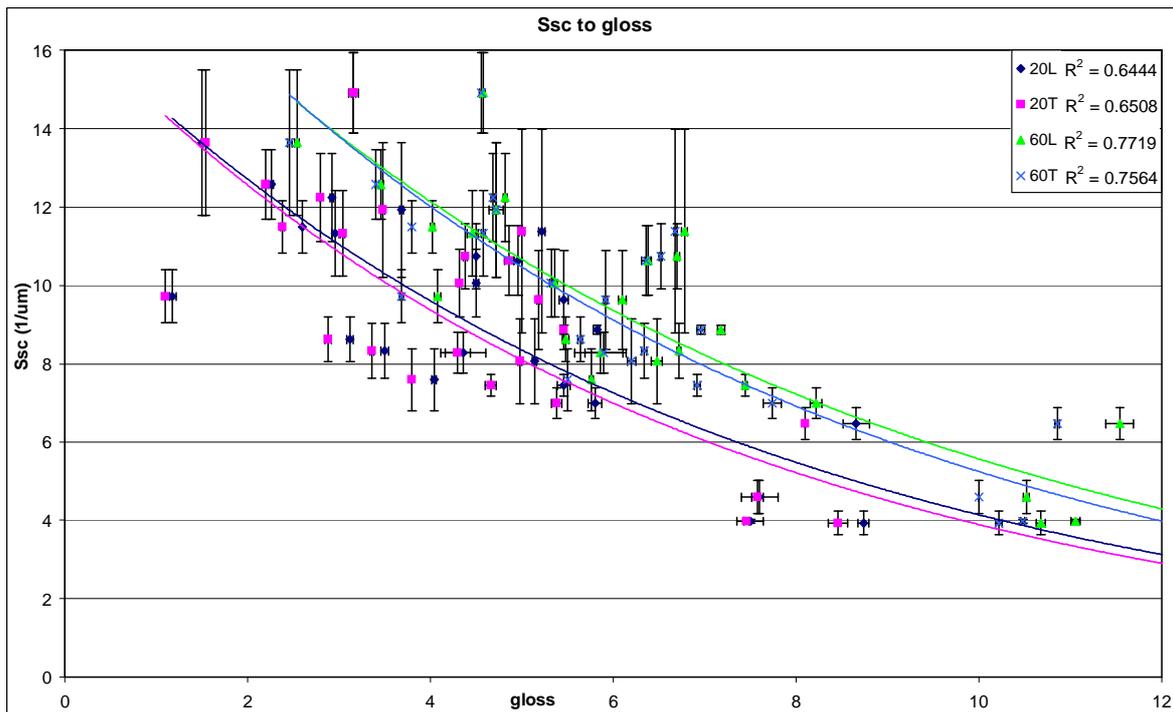
Figure 6.6: Graph of Average S_{sc} (Arithmetic Mean Peak Curvature) against Average Gloss (Gls)
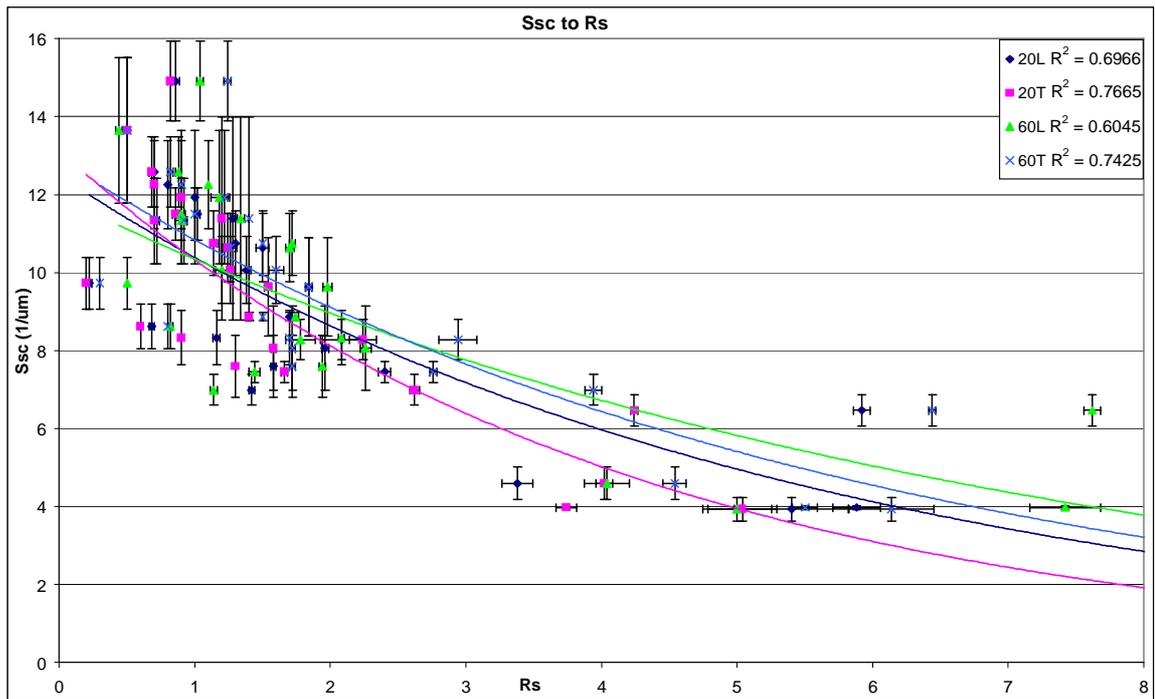
Figure 6.7: Graph of Average S_{sc} (Arithmetic Mean Peak Curvature) against Average Specular Reflectance
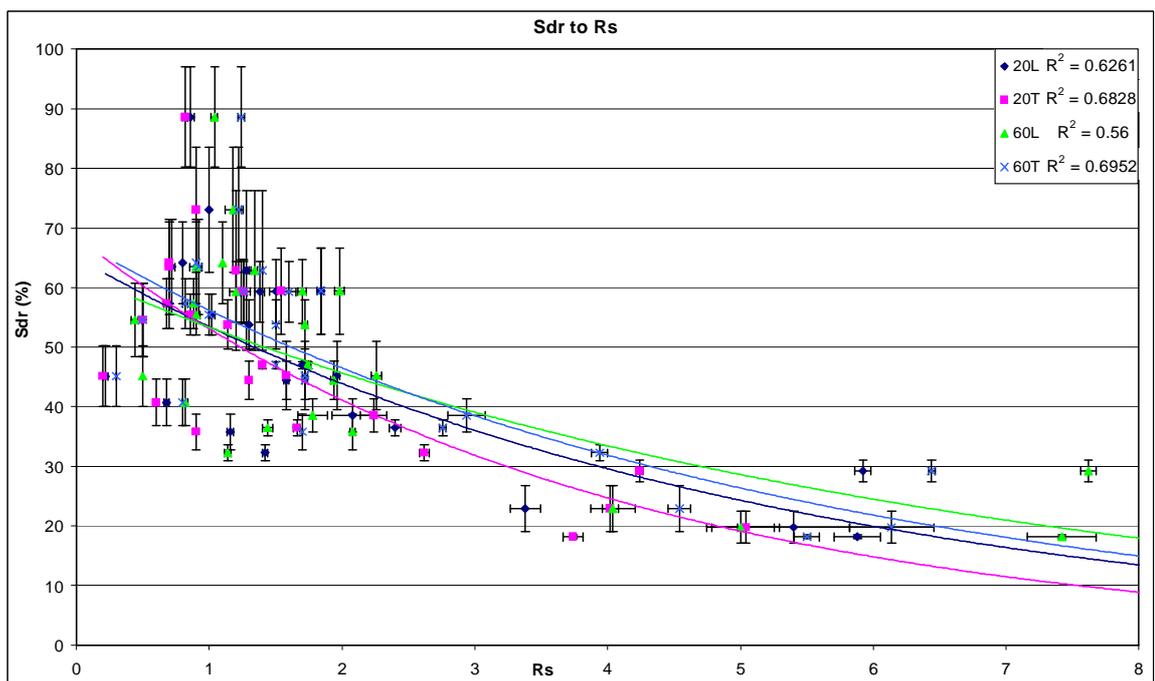
Figure 6.8: Graph of Average S_{dr} (Developed Interfacial Area Ratio) against Average Specular Reflectance

The Developed Interfacial Area Ratio (S_{dr}) also showed a high trend correlation to specular reflectance, figure 6.8. Again, the large error bars at the higher end of the S_{dr} values make it difficult to deduce any meaningful information.

6.8. Development of Data Truncation Method

6.8.1   Introduction

It has been hypothesised that by studying the relationship between the topography (and process) variations of different surfaces and their appearance that the plateau data is, in the main, responsible for the aspects of appearance (see section 6.4), whereas the valley data would be related to lubricant retention and tribological properties. However, it is not discounted that the valley data may have an effect on the optical appearance of a surface and consequently the effects of each need to be studied.

A novel method of separating the plateau and valley data has been developed to yield more functionally relevant topography parameter results for the 2B surface. The hypothesis would suggest that the new parameters are expected to correlate as shown in table 6.1.

Table 6.1: Hypothesised relationship between new parameters and appearance characteristics

● High   ◑ Moderate   ○ Low

		Function	Appearance	
	Feature of Interest	**Parameter**	**Reflectance/DOI**	**Gloss**
Plateaus	Average roughness	S_q of top data	●	●
	Height of asperities	S_z of top data	◑	◑
	Number of asperities	S_{ds} of top data	●	◑
	Slope	$S_{\Delta q}$ of top data	◑	◑
	Curvature	S_{sc} of top data	◑	◑
	Size	Possible using edge detection	●	◑
	Size distribution	As above	●	◑
	No. of isolated oil pockets	Pattern recognition/related to WC	◑	◑
	Aspect of pits	Further Study Required	◑	○
Valleys	Max. Depth	S_t	○	◑
	Av. Max. depth	S_{vm}	○	◑
	Av. Depth	Further Study Required	○	◑
	Slope of walls	Further Study Required	◑	◑
	Wall roughness	Further Study Required	◑	◑
Both	Area fraction ratio	From bearing area curve (Further Study Required)	●	●

6.8.2 Derivation of the Method

A method has been sought to separate the data on the 2B surface into the plateau and valley regions. The bearing area curve has been used in the past to visualise the different functional parts of a surface, see figure 6.9. The data regions can be easily approximated visually, but a routine for calculating the point of transition from plateaus to valleys is needed to ensure uniformity.
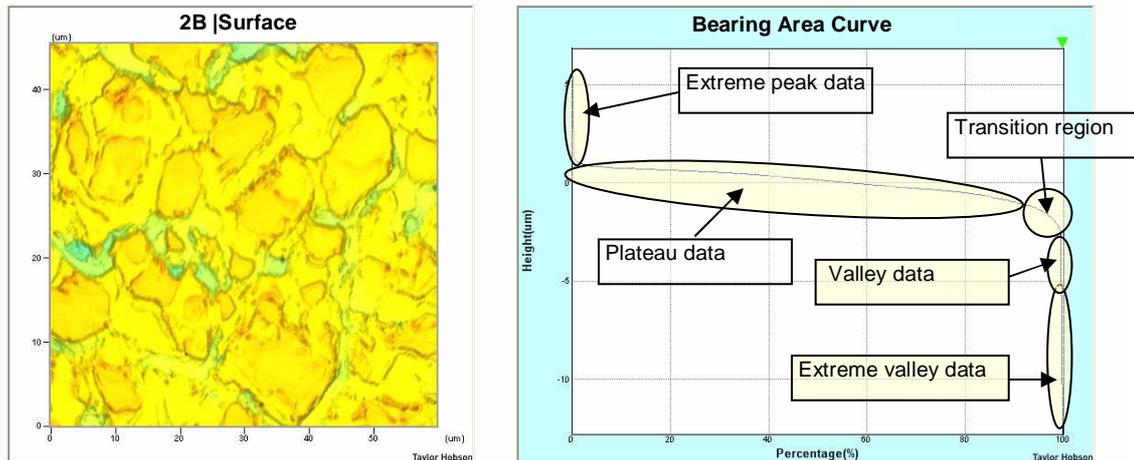
Figure 6.9: Bearing Area curve of 2B surface showing main data regions

The seperation of data for stratified surfaces into functionally relevant sections has been carried out (for profiles) in the GPS standard, EN ISO 13565-3:2000 [78]. This standard gives the method for identifying and calculating the percentages of the 5 main regions on stratified surfaces, plateaus, valleys, outlying peaks and valleys and the region at the transition between plateaus and valleys, see figure 6.10.

This standardised method for calculating the transition point between plateaus and valleys on stratified surfaces has been modified to be used with the 3D data sets of the 2B finish.
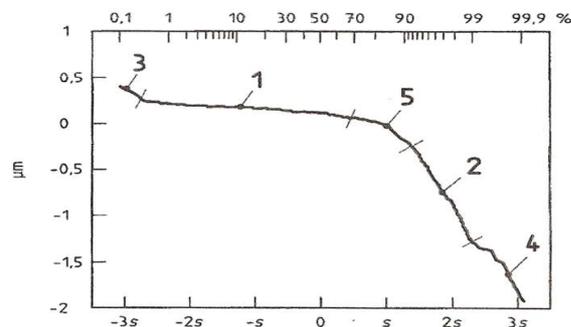
Key

1   Plateau region
2   Valley region
3   Debris or outlying peaks in the data (profile)
4   Deep scratches or outlying valleys in the data (profile)
5   Unstable region (curvature) introduced at the plateau to valley transition point based on the combination of two distributions

Figure 6.10: Material Probability curve showing 5 main regions (taken from [78])

6.8.3   Basic Method in Matlab™

1) Plot the bearing area (Abbott-Firestone) curve, of % probability against height of data and find the nearest fit polynomial curve to this data.
2) Express the % probability axis in standard deviations, giving the material probability curve (as seen in EN ISO 13565-3:2000 [78]).
3) Fit a conic section to this curve and rotate and translate to give a centre of zero and find the asymptotes of the conic section.
4) When re-rotated and translated to the original orientation, the transition point is given at the intersection of the asymptotes of the conic section, see figure 6.11.
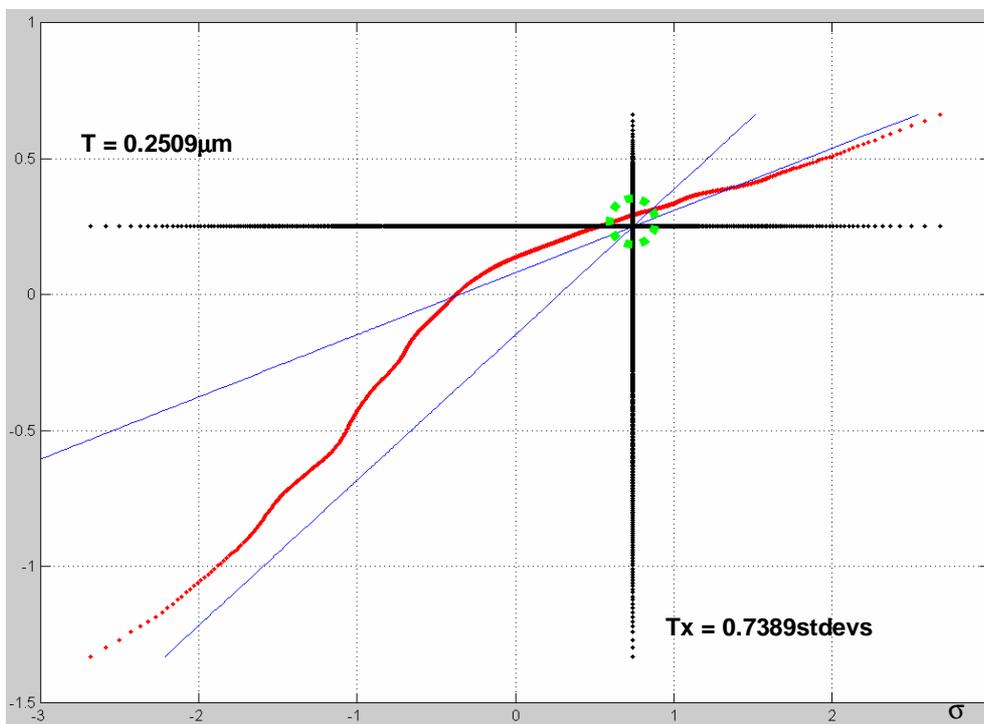
Figure 6.11: Transition point on Material Probability curve

All these calculations are carried out in MatLab™ code, and the graphs viewed on the graphical user interface (GUI), see figure 6.12. Based on this transition point the surface is sectioned at the transition point giving a non subjective methodology of establishing the section height.
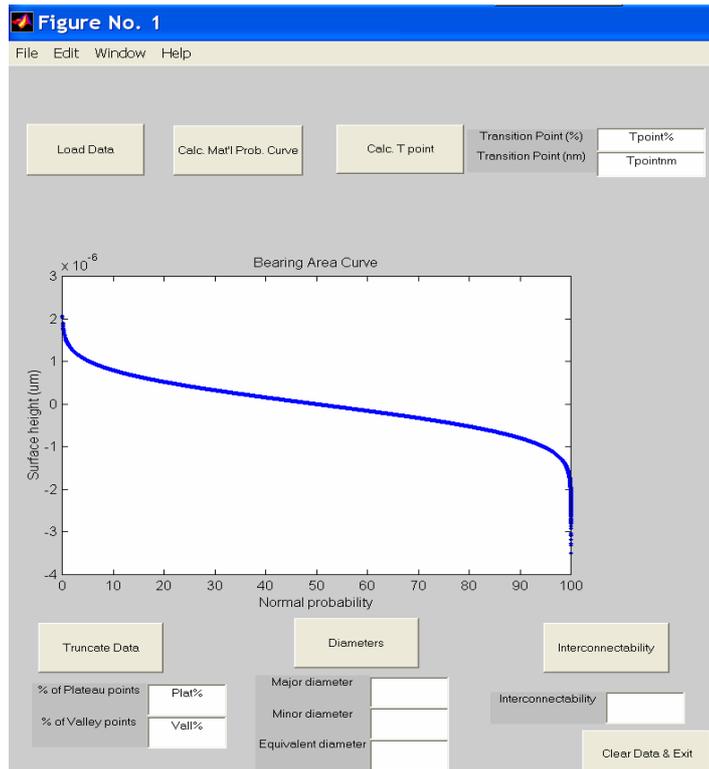
Figure 6.12: MatLab™ GUI

Further processing is carried out in the SurfStand software (used to calculate the 3D parameters previously). The y-axis transition, in micrometers is given as the separation height, and the two data sets are treated separately to recalculate 'plateau' and 'valley' parameters, see figure 6.13. Some of these parameters are expected to have a better correlation with the appearance data due to increased functional relevance.

1)

2)
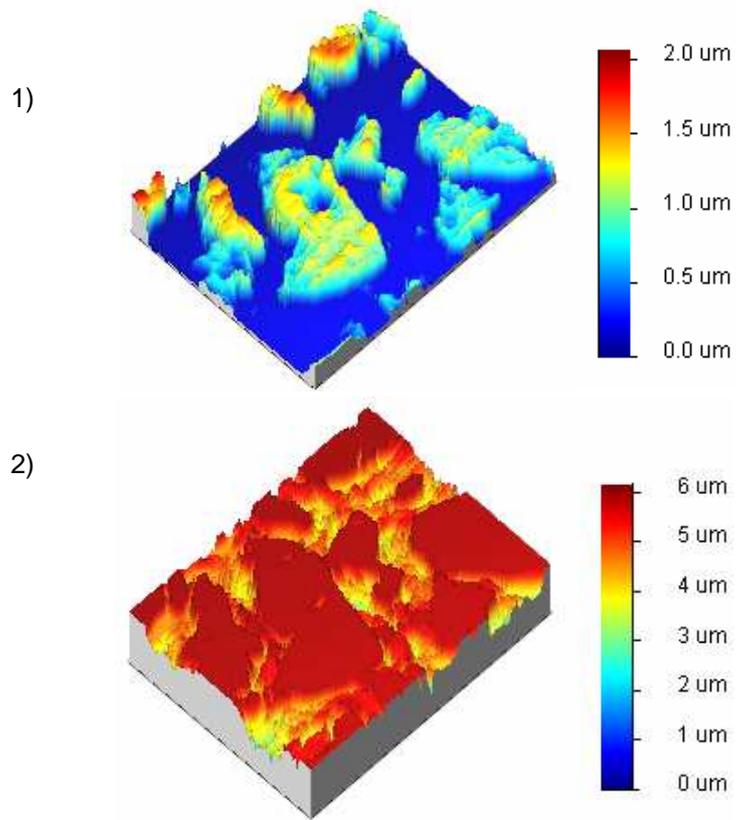
Figure 6.13: 2B data separated into 1) plateaus and 2) valleys in SurfStand software

6.9. Parameter Assessment

6.9.1   Results

The following results show the correlation of the appearance parameters to the 3D surface parameters of the separated plateau and valleys features of the 2B finish.

Sampling for all finishes was carried out in accordance with the test protocol (Chapter 4). Error bars are ½ standard deviation of set. Trend lines are of exponential form. It was decided that this investigation would use only the results for the 60° glossmeter measurements since it is accepted as the universal standard for measuring gloss, since 20° is normally only used for surfaces with high gloss values, above about 60 (2B is around 0 to 20).

Stemming from an investigation into the differences between the 2B and 2D processing methods, it was expected that the Root Mean Square Deviation of the surface (S_q) and other general roughness parameters (which are not extreme data dependant) like S_a, S_p and S_{5z} (to some extent) would also have a high correlation to gloss, specular reflectance and distinctness of image. Previously, when the whole of the data was analysed, these simple relationships were not found. However, when the average roughness of the plateau data (S_q plateaus) alone was used, there was a good correlation to specular reflectance, figure 6.14. Additionally, a relationship was found between the S_a of the plateaus and specular reflectance, figure 6.15.
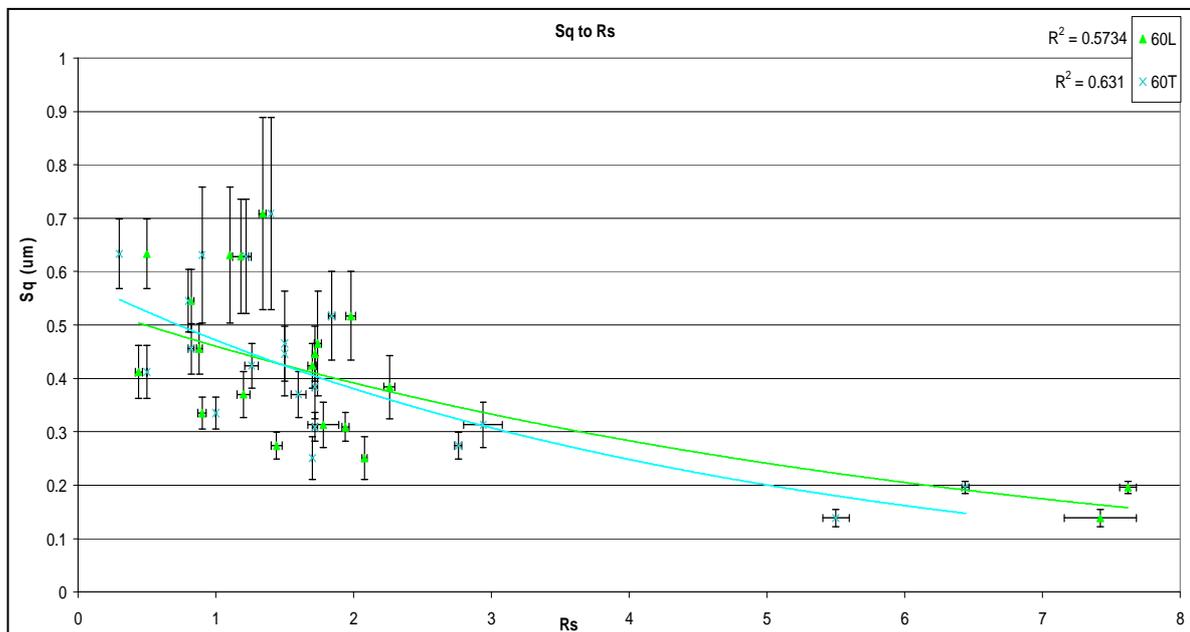
Figure 6.14: Graph of S_q (Root Mean Square Deviation) of plateau data against Specular Reflectance (Rs)
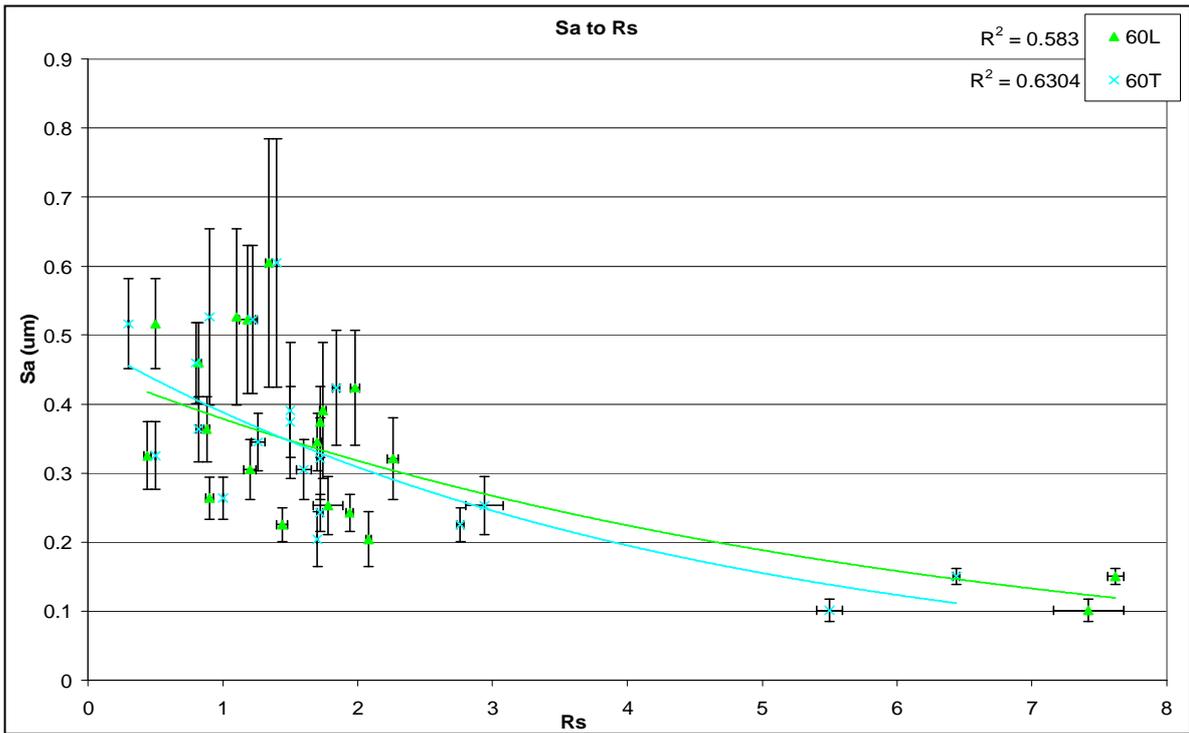
Figure 6.15: Graph of S_a (Arithmetic Average Roughness) of plateau data against Specular Reflectance (Rs)

A relationship was found previously (figure 6.6 and 6.7) between S_{sc} and Gls and Rs, similar relationships were found for these parameters of the separated plateau data figures 6.16 and 6.17.
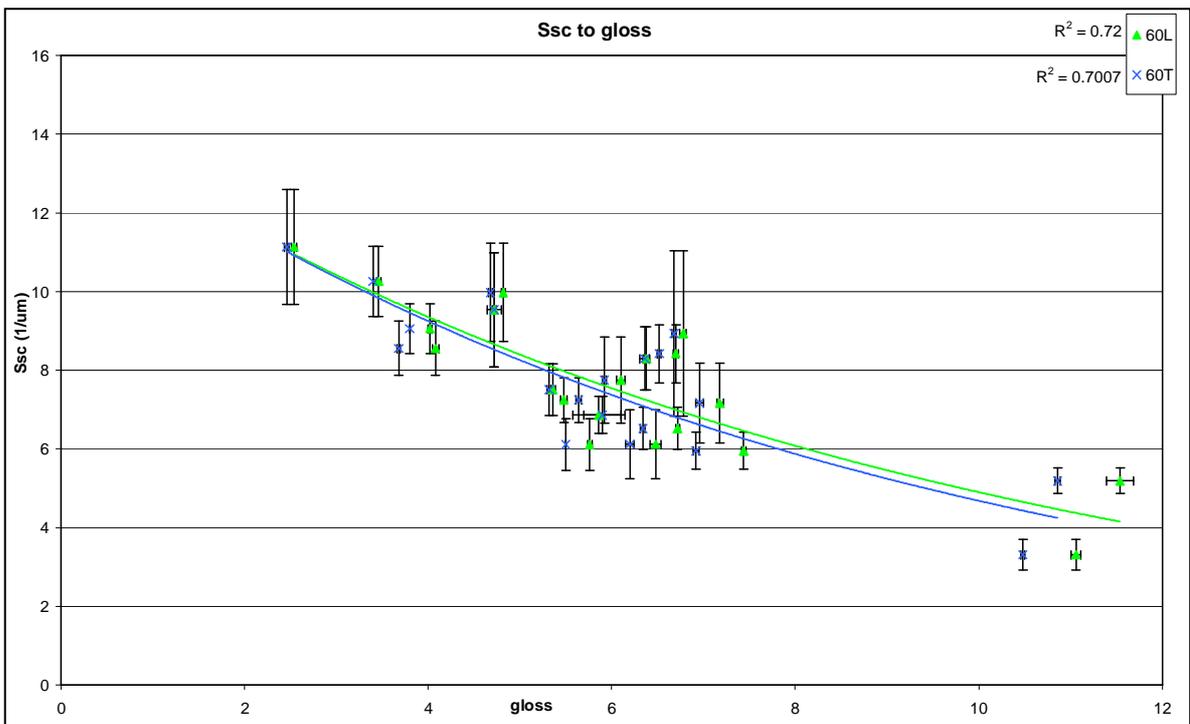
Figure 6.16: Graph of S_{sc} (Arithmetic Mean Peak Curvature) of plateau data against Gloss (Gls)
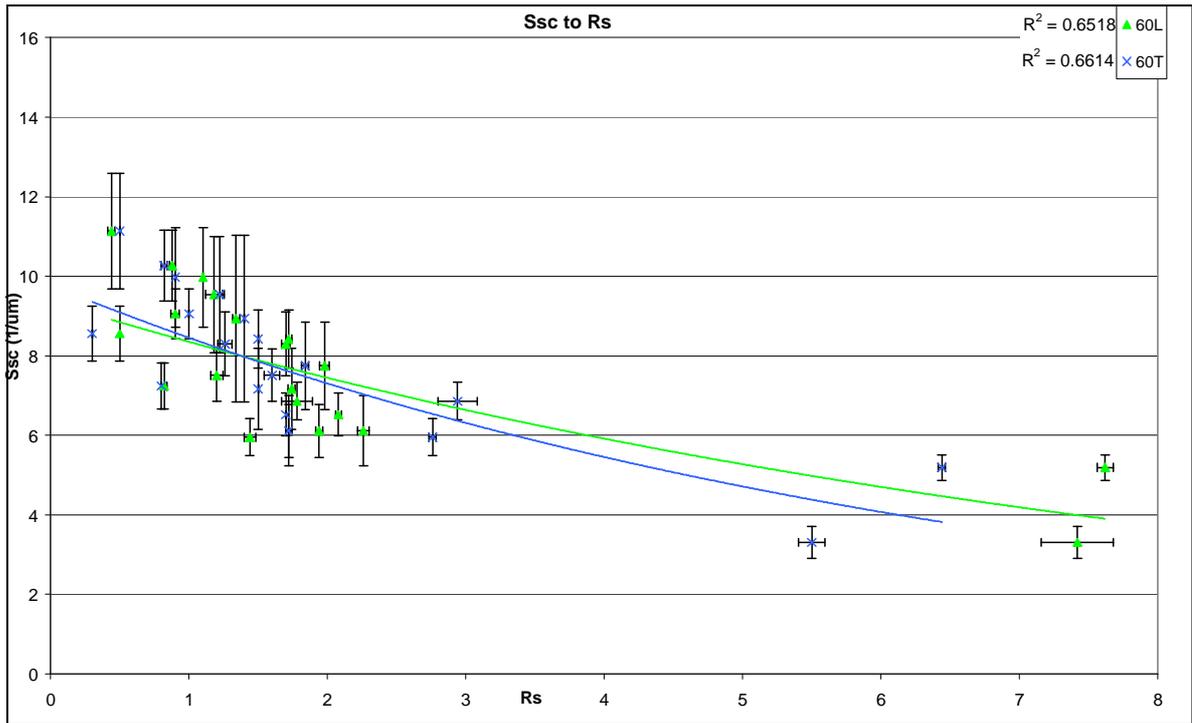
Figure 6.17: Graph of S_{sc} (Arithmetic Mean Peak Curvature) of plateau data against Specular Reflectance (Rs)

It was also expected that $S_{\Delta q}$ (Root Mean Square Slope of the surface) would give strong correlations to Gls, Rs and DOI, as found by Cao et al [79], since smaller slopes indicate smoother surfaces, but this result was not found when all of the surface topography data was analysed. When the data was separated, the $S_{\Delta q}$ value of the plateau data did have a strong relationship with the Gls and Rs values, see figures 6.18 and 6.19.
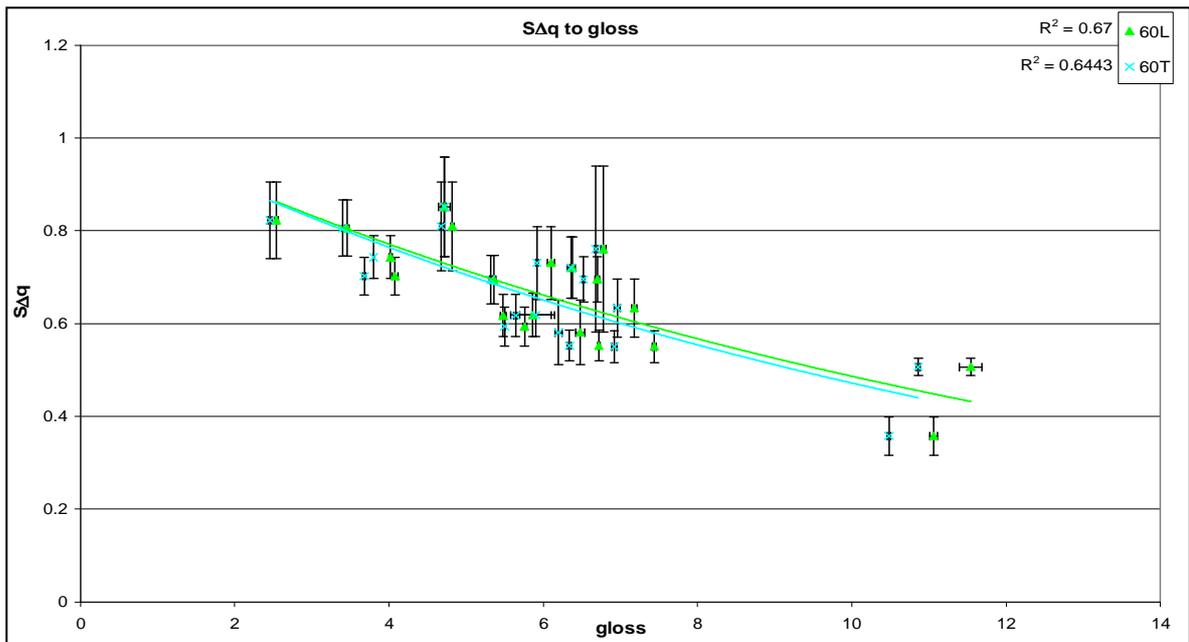
Figure 6.18: Graph of $S_{\Delta q}$ (Root Mean Square Slope of the surface) of plateau data against Gloss (Gls)
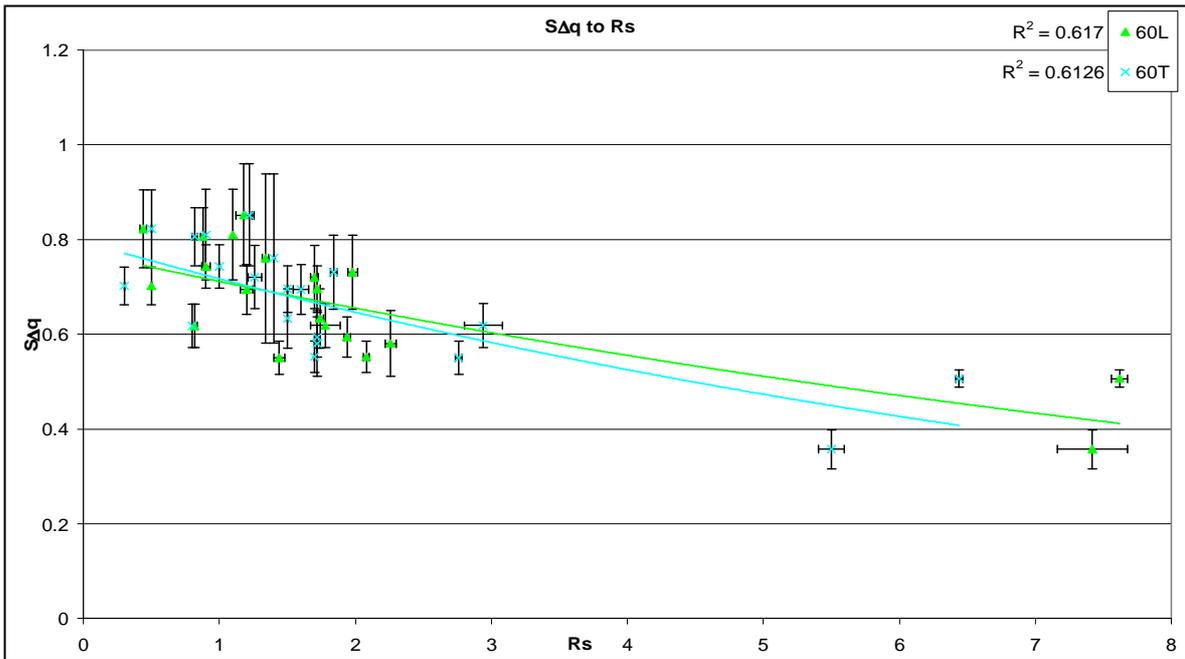
Figure 6.19: Graph of $S_{\Delta q}$ (Root Mean Square Slope of the surface) of plateau data against Specular Reflectance (Rs)

Parameters in the spatial family set are only likely to have a correlation to appearance information for surfaces with a well defined direction or lay, although a high density of summits on the surface (S_{ds}), if the summits were sizable, would be expected to have an effect on Rs, Hz and DOI. No correlation has been found relating any of these appearance parameters to S_{ds} of the plateau data; although figure 6.20 shows that there is a relationship between Rs and S_{ds} of the valleys.

Additionally, a correlation between the S_a (Average Roughness) of only the valley data was found, figure 6.21.
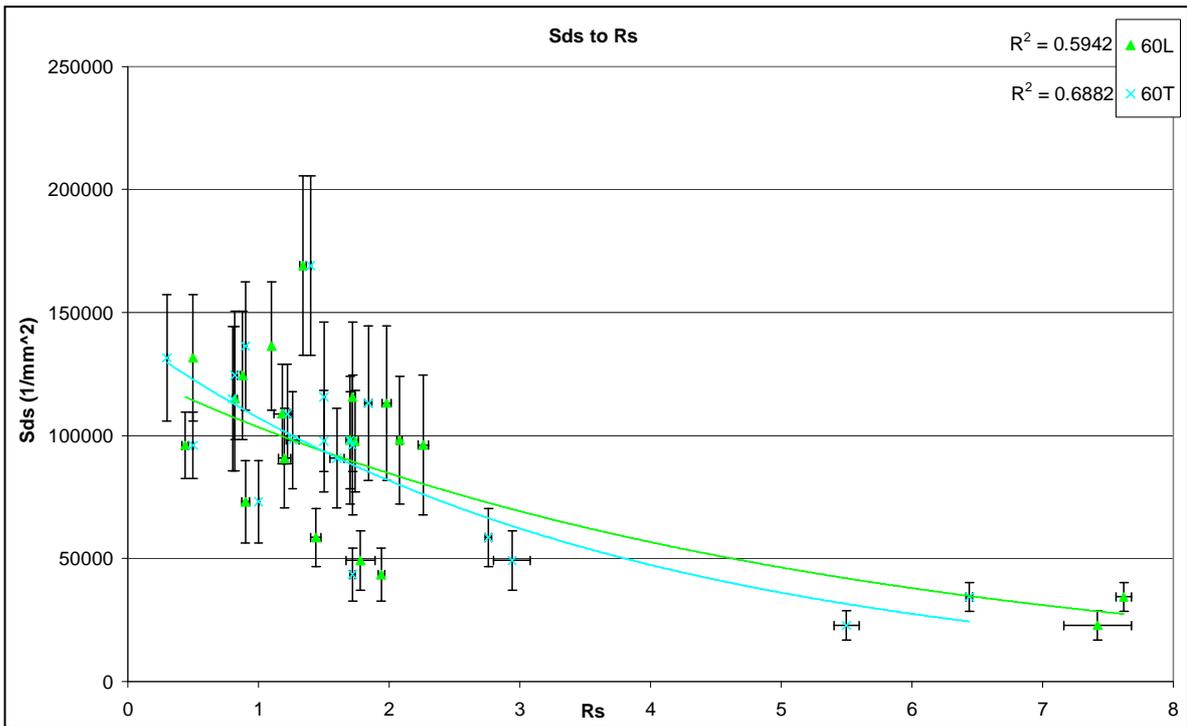
Figure 6.20: Graph of S_{ds} (Density of Summits) of the valleys against Specular Reflectance (Rs)
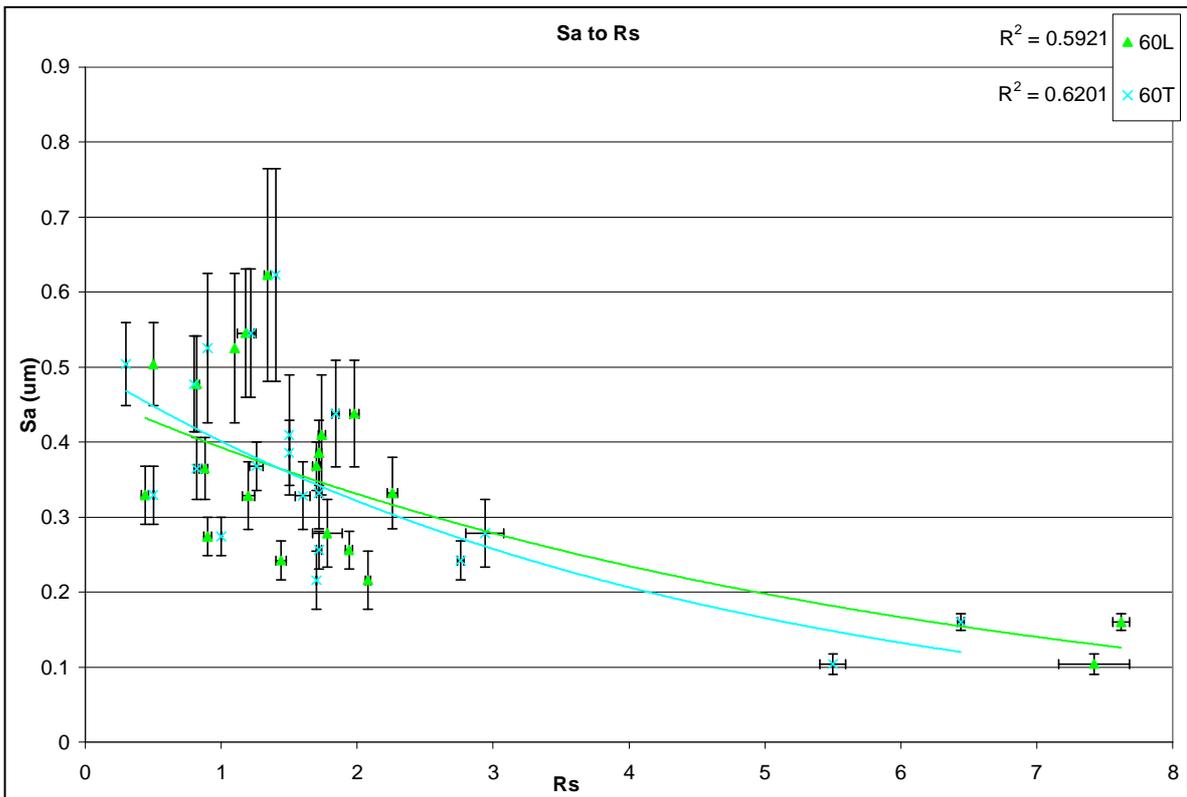
Figure 6.21: Graph of S_a (Arithmetic Average Roughness) of the valleys against Specular

Reflectance (Rs)

6.10. Discussion

The initial trials were used to confirm the instruments suitability for measuring the 2B finish. These compared four of the main production finishes leading to the conclusion that the Panaspect glossmeter was capable of measuring the relatively low optical properties of the 2B surface. Further to this study a wide range of 2B finish samples were measured in an attempt to correlate the optical properties with the 3D topography parameters. Correlations were only found between the Arithmetic Mean Peak Curvature, S_{sc} (to gloss and specular reflectance) and the Developed Interfacial Area Ratio, S_{dr} (to specular reflectance only). It was then hypothesised that better correlations would be found if the data was separated into the two functional areas of plateaus and valleys.

It was expected that the S_q (Root Mean Square Deviation) of the whole surface topography would correlate to Gls and Rs, since it has long been believed that rougher surfaces have lower values of these optical properties. This relationship was not found until the data was separated, then the S_q of the plateau data correlated to specular reflectance. This indicates that the S_q of the whole surface is heavily influenced by the valleys on the surface and the specular reflectance is influenced mostly by the microroughness of the plateaus. This may be due to light entering the valleys not returning to the detectors and therefore no correlation is evident.

The same reasoning can be applied to the finding of a relationship between the S_a (Average Roughness) of the plateaus to specular reflectance, although in this case, the S_a of the valleys was also found to correlate. Since S_a is an amplitude based parameter, this implies that as the valley depth increases, the specular reflectance decreases. It is theorised that deeper valleys will "absorb" light rather than reflect it back to the detector.

In general the results agree with the perception, as the average roughness of the surface is increased so the specular reflectance decreases. This is not found in relation to gloss. This may be due to the relatively low gloss of all the surfaces measured. It may have been evident if a higher measurement angle was used in the glossmeter (85° is suggested for low gloss surfaces).

S_{sc} (Arithmetic Mean Peak Curvature) is related to the radius of curvature, whereby a large radius of curvature implies lower peaks which results in smaller S_{sc} values. More lower peaks are found on smother surfaces and hence the S_{sc} of the plateaus areas relate more closely to the gloss and specular reflectance, where as the S_{sc} increases, the Gls and Rs decrease. This is in general agreement with the theory, where the light is being scattered more by a surface with high S_{sc}.

As $S_{\Delta q}$ (Root Mean Square Slope of the surface) of the plateaus increased the gloss and specular reflectance decreased as expected, since smaller slopes are found on smoother surfaces or as the slope of the surface is increased, more light is diffusely scattered meaning less light is returned to the detector along the specular angle.

Parameters in the spatial family set are only likely to have a correlation to appearance information for surfaces with a well defined direction or lay, although a high density of summits on the surface, if the summits were sizable, would be expected to have an effect on Rs, Hz and

DOI. No correlation has been found relating any of these appearance parameters to S_{ds} (Density of Summits) of the plateau data, although there is a relationship between Rs and S_{ds} of the valleys, as the density of summits in the valleys increases, the specular reflectance decreases. This is a complex relationship, since summits in the valleys are found where the etching of the grain boundaries has left peaks within the valleys, see figure 6.22. It may indicate that these summits have an influence of whether the light is reflected back to the detector, i.e. if the topography of the valley bottoms is unaffected by summits (smoother) then it is more likely that the light will be reflected back at the specular angle and not diffused by summits.

6.11. Conclusions

➤ The direction of the measurement does not have a significant effect on the optical parameters.

➤ The angle of measurement does have a significant effect on the optical parmeters, a 60° orientation is suggested for the 2B finish.

➤ The glossmeter is a suitable instrument to measure two of the optical parameters of the 2B finish, gloss and specular reflectance. The haze and DOI cannot be accurately determined using this arrangement.

➤ The results are in general agreement with past research which established that smoother surfaces have higher gloss and specular reflectance.

➤ The gloss of the 2B surface can be related to its curvature and slope, whereby an increase in either gives a decrease in the gloss.

➤ The specular reflectance of the 2B surface is influenced by both the plateau and valley data regions.

➤ The specular reflectance of the 2B surface can be related to the average roughness, curvature and slope of the platau data.

➤ The specular reflectance of the 2B surface can be related to the average roughness and density of summits within the valley areas.

Table 6.2: Suggested parameter set for optical specification

	Surface Parameter	
Optical Parameter	Plateaus	Valleys
Gloss	S_{sc}	
	$S_{\Delta q}$	
	S_q	S_{ds}
Specular reflectance	S_a	S_a
	S_{sc}	
	$S_{\Delta q}$	

Chapter 7   Lubricant Retention

7.1. Summary of the chapter

A simplified method (based on drip tests) to assess the lubricant retention properties of topography is presented. The development of the technique includes proof of the equipment resolution and approach suitability for testing the 2B finish. Results show the relationship of 3D topography parameters to the ability of a surface to retain oil.

7.2. Introduction

For tribological concerns such as how much lubricant the surface can retain or the extent of tool friction in forming operations surface features are critical. In some instances, for example on plateau-honed surfaces for cylinder bores, it is important that the surface valleys possess a certain amount of interconnectability (so that oil can be distributed around the whole of the surface area) and have a specific lubricant reservoir volume [6, 7]. The size, density and slopes of asperities on the surface can also affect tool friction and galling behaviour and the volume of closed pockets has been cited as a critical factor in calculating work piece friction in drawing [80].

As discussed in chapter 2, section 2.4.4.2, there are two common testing methods of forming behaviour, a Draw Bead Simulation or 'DBS' tests [22] and the Bending Under Tension or 'BUT' test [23]. These can be used to analyse either the tool surface or the formed products' surface, both before and after testing and thus analyse the galling behaviour. A static oil retention test was developed by OCAS to study the effects during coiling or blanking [10]. A drip test can be used to study lubricant retention, although it has been found that for low quantities of oil this type of test may not be suitable. In the present work the effects of sheet topography on the lubricant retention properties has been studied, for a number of different finishes and variations of the 2B finish, using a modified drip test.

7.3. Drip Tests

To test the lubricant retention properties of a surface a known amount of oil is initially applied and then the drips are weighed with respect to time giving an indication of the surfaces ability to retain lubricant.

A simplified drip tests method has been devised in the present study, based on the available equipment [10]. The methodology involved dripping a given amount of oil on to the drip test sheets (figure 7.1) over a set time period (2 minutes). The sheet was then suspended from a balance and the mass change of the sheet plus the remaining oil was recorded as a function of time.
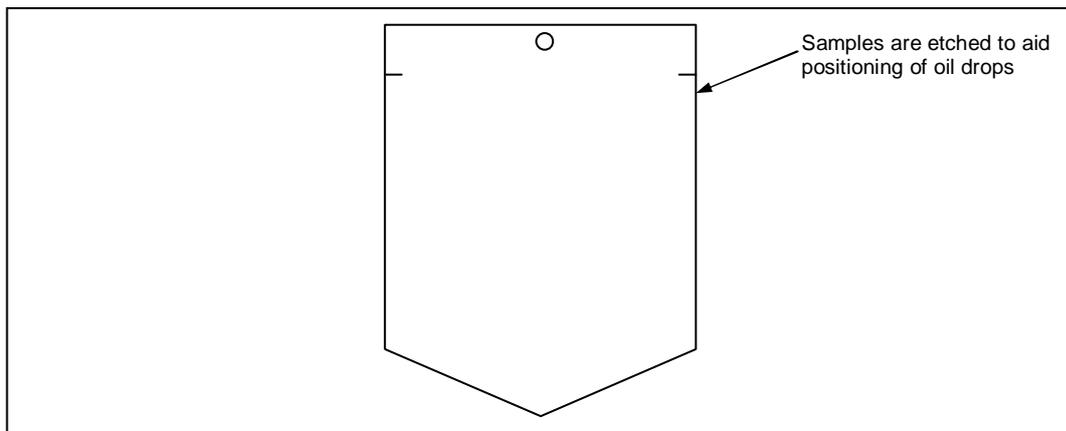
Figure 7.1: Shape of the sample for drip testing

The balances are standard enclosed flat pan chemical balances, with a mass capacity of 125g. The first few tests were carried out by lying the sample plus oil on the pan and weighing, then tilting the drip sheet (outside the balance enclosure) at approximately 90° allowing the tip of the sheet to touch absorbent paper. After the set time (every 10s for first 2 mins) the sheet is laid horizontally on the pan again and weighed.

There were several problems with this method. Including many variables the major problem arose when heavier sheets were tested. A 0.75mm gauge sheet weighed about 80 to 90g with oil added. The next thickest sheet (2mm) is more than twice this weight, therefore exceeding the mass capacity of the balance. A new method with fewer variables was devised, using a rig to hang the sheets above the flat pan balance, see figure 7.2. The weight of oil that has dripped off the sheet is recorded with respect to time, with no need for absorbent paper to be used.

In the modified methodology, a known mass of oil is added (dripped from a burette). This is done over a period of around 2 minutes, as before and the sheet is kept as horizontal as possible throughout. The sheet is then hooked on to the rig, still horizontal and turned to the vertical position as a clock records the elapsed time. This final movement was carried out quickly and must ensure that any swinging of the sheet is eliminated.

The recorded results are the mass of the initial oil added and the mass of oil that has dripped off at time intervals of 10s.
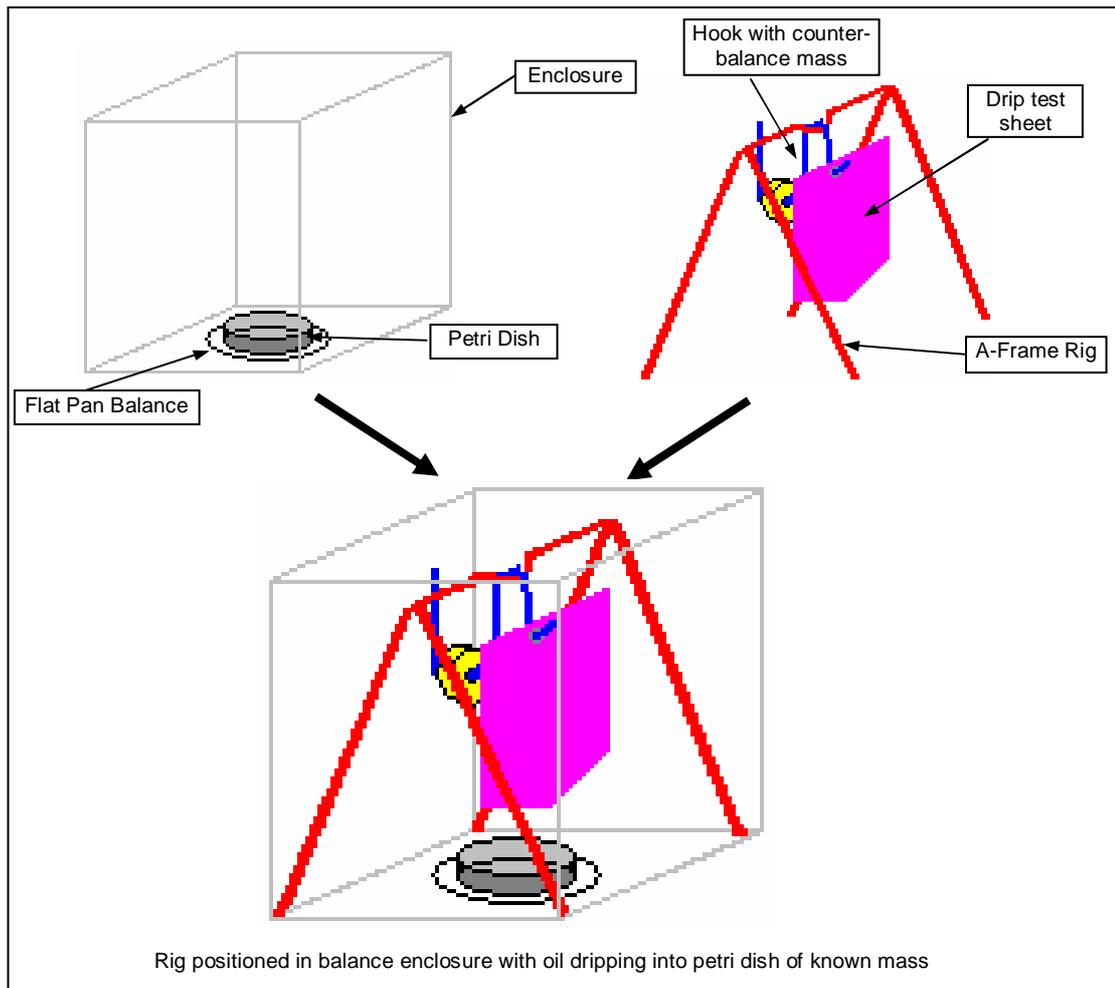
Figure 7.2: New Rig set-up for drip testing

A percentage of oil retained (compared to the mass of oil originally applied) is calculated using equation 7.1.

$$\% \, retained = 100 \times (\frac{m_i - m_{oil}}{m_i})$$

Where m_{oil} = mass of oil that has dripped off at time x (g)

m_i = Initial mass of oil (g)

7.4. Initial Trials

The initial results are presented below in the form of graphs (all trend lines are based on power series).

To decide on the initial amount of oil to use, an optimisation study was carried out, this also gave the % error in repeatability of the method. The sensitivity of the method was then checked by comparing two different finishes.

7.4.1   Results

7.4.1.1   Optimisation of Method

The optimisation study was carried out using a sample of 0.75mm gauge 2B 316 stainless steel. The initial amount of oil applied was varied and the test was repeated 5 times. The average error in repeatability of the test was calculated and the best result, with 25 drops of oil (figure 7.3) chosen. The ±4.8% error was used as the standard error of the percentage of oil retained in further studies.
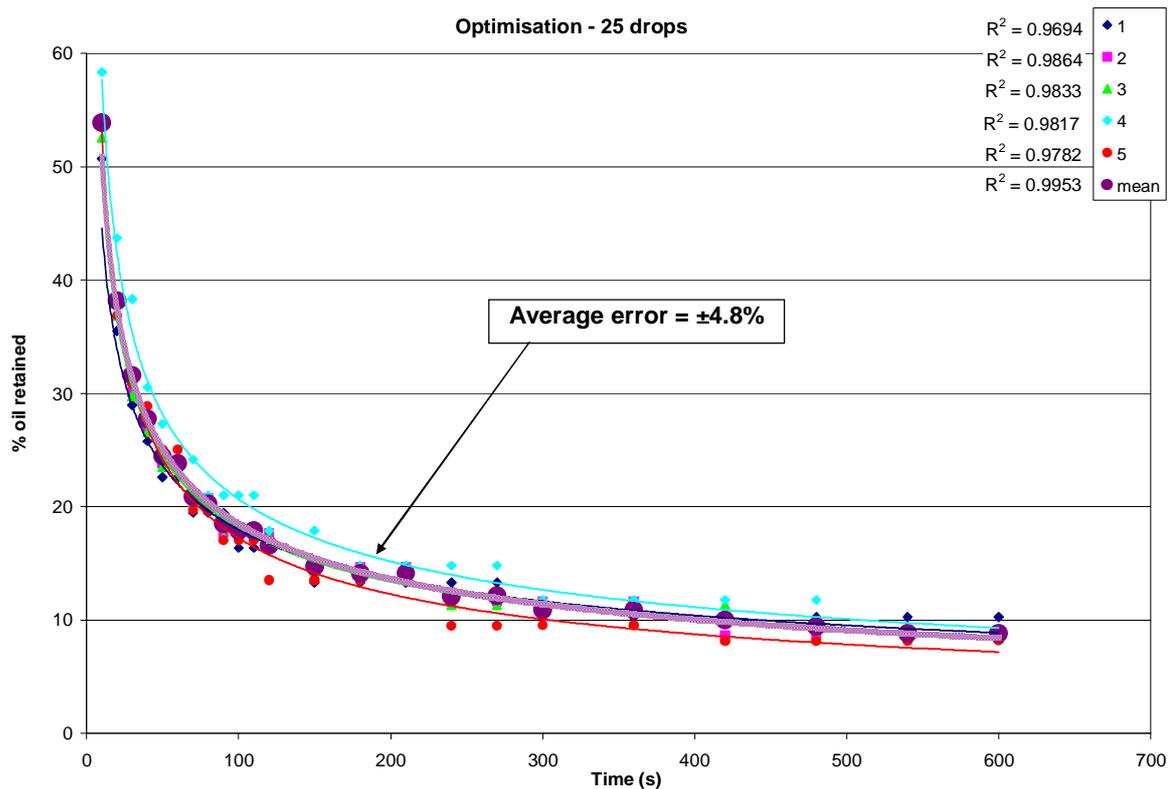
Figure 7.3: Graph showing repeatability of test with 25 drops of oil applied

7.4.1.2   Sensitivity of Method

Figure 7.4 shows the initial results from tests to check the sensitivity of the measurements. Sheets of 2B finish and BA finish both of 0.75mm gauge, were tested five times. The repeatability error of ±4.8% (taken from the optimisation study) is represented on the graph by error bars. None of these error bars cross, suggesting that we can be confident that the series are distinct data sets, outside the degree of repeatability error.
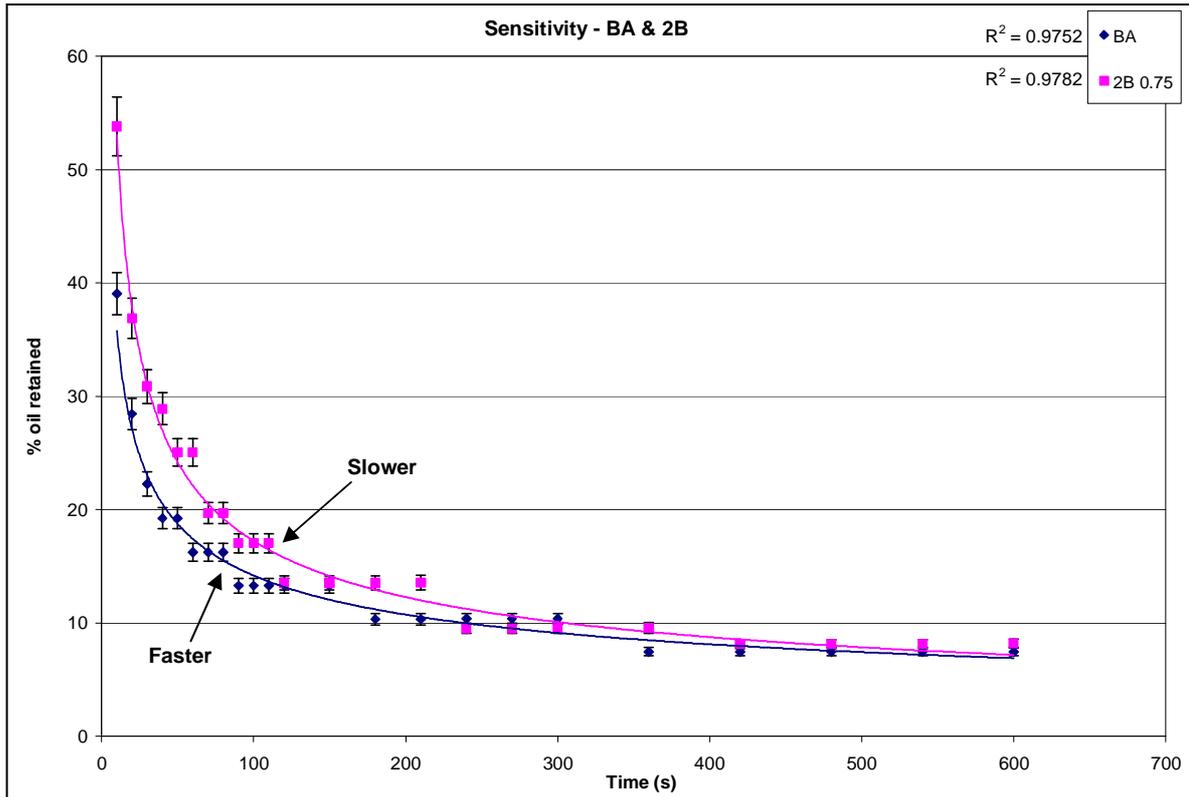
Figure 7.4: Graph showing the sensitivity of the test using the 2B and BA finishes

7.4.1.3   Initial Conclusions Concerning the Methodology

The conclusion of the optimisation was that more oil gave better repeatability of results but that 30 drops of oil (approximately 0.7g) was too much for the size of the sample area, causing run-off at the edges whilst still being applied. Therefore all subsequent tests were carried out with 25 drops of oil applied.

The conclusion from the comparison of 2B and BA samples is that the test is sensitive enough to detect differences in the topographies of the samples. Also, as expected, the bright annealed surface has a faster run-off of oil than the 2B surface.

7.5. 2B Trials

7.5.1   Study of Methodology

Figure 7.5 shows the variation of four different gauges of a 2B finish. In general this indicates that the thinner gauge samples have a faster run off than the thicker gauges. Below around 80 seconds the error bars on the graph interfere, meaning this data is not as clear. This may be because in the initial stages, the amount of oil dripped off is very rapid – it is simply surface runoff of excess oil and does not closely relate to the differences in the samples.
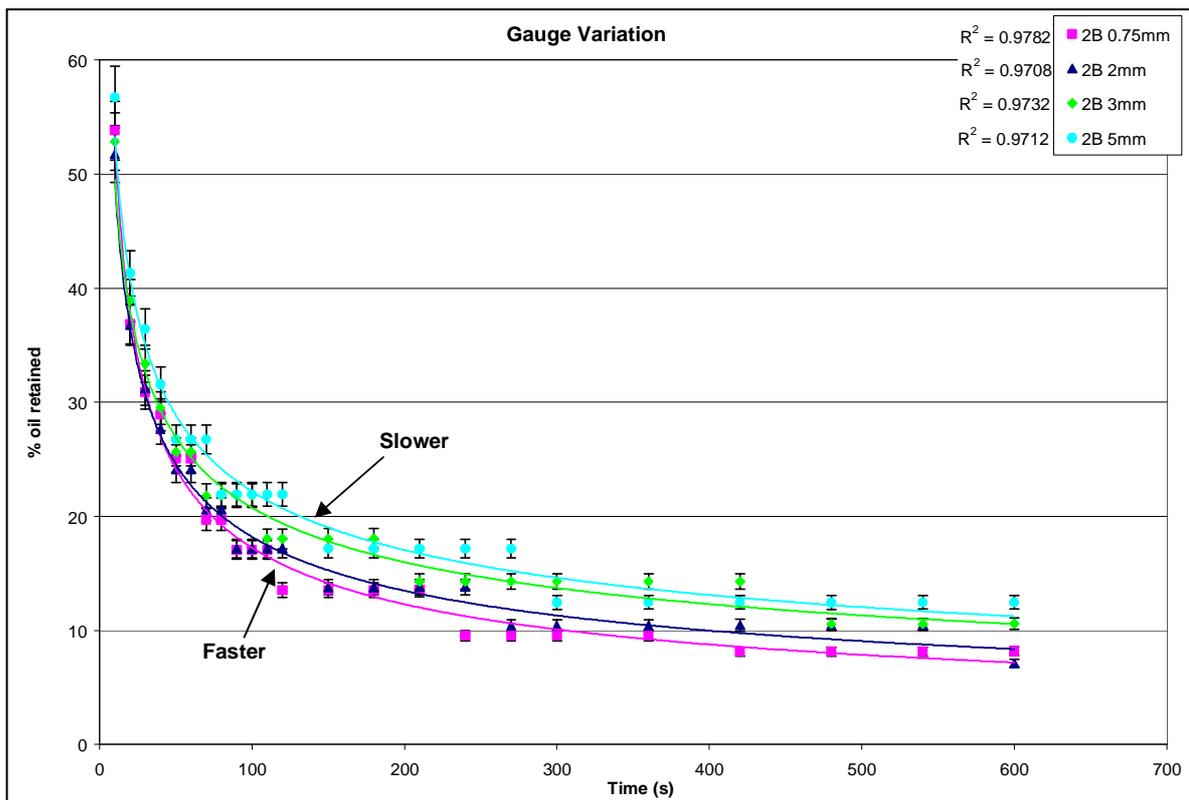
Figure 7.5: Graph showing variation of retained oil across four samples

Figure 7.6 shows the variation of the rolling direction on the material to the drip test direction (i.e. the drips run either with or against the rolling direction).
The lines are separate, indicating that this method is sensitive enough to determine whether the direction of rolling has an effect on the lubricant retention for the 2B finish and that retention is lower in the direction of rolling. Again the error bars interfere below around 80 seconds.

Note: the variation due to source of the sample is not studied due to a lack of sample availability.
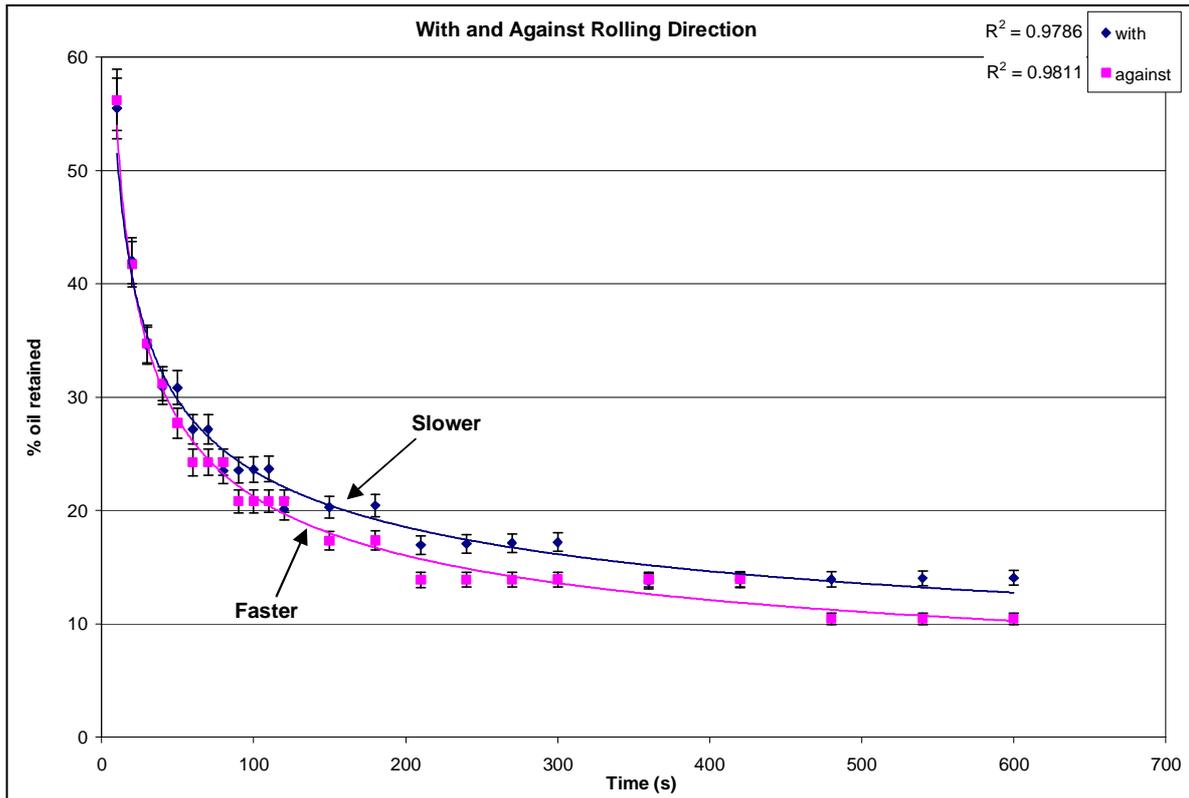
Figure 7.6: Graph showing variation of retained oil in relation to direction

7.5.2 Relationship of Lubricant Retention to 3D Topography Parameters

7.5.2.1 Results and Discussion

The following results show the correlation of the percentage lubricant retention to the 3D surface topography parameters of the features of the 2B finish. In order to assess the data, four time increments were chosen (60, 120, 240 and 480 seconds) and the percentage lubrication retention at these times was plotted against the topography parameters for the 4 samples shown in figure 7.5. Topography parameters were calculated using the whole of the data and also the separated plateau and valley data.

Sampling for all finishes was carried out in accordance with the test protocol (chapter 4). Y-error bars are ½ standard deviation of the 15 measurements made and X-error bars are ±4.8% (see section 7.4.1.1).

High R^2 values of correlation were found with many of the parameters (figure 7.8); although in some cases this is simply due to minimal variation in the parameter value. Additionally, many of the error bars on these graphs interfere, rendering the information generated ambiguous. Only a selection of the most interesting findings are presented graphically.

7.5.2.2 Amplitude Parameters

Good correlations were found between many of the amplitude related parameters and lubricant retention. Figure 7.7 shows the graphs of S_q (Root Mean Square Deviation) calculated for a) all the data and b) the separated valley data. The implication from these graphs is that as the roughness increases, the surface will retain a larger percentage of oil. The exception is for the time of 60 seconds, where it is thought that the excess oil is rapidly running off the surface and therefore is not affected by the roughness.

Similar results were found for the other amplitude parameters that are based on extreme data: S_v (Maximum Valley Height), S_z (Maximum Height of Texture surface), S_{5z} (Ten Point Height of surface) and also for S_a (Average Roughness).
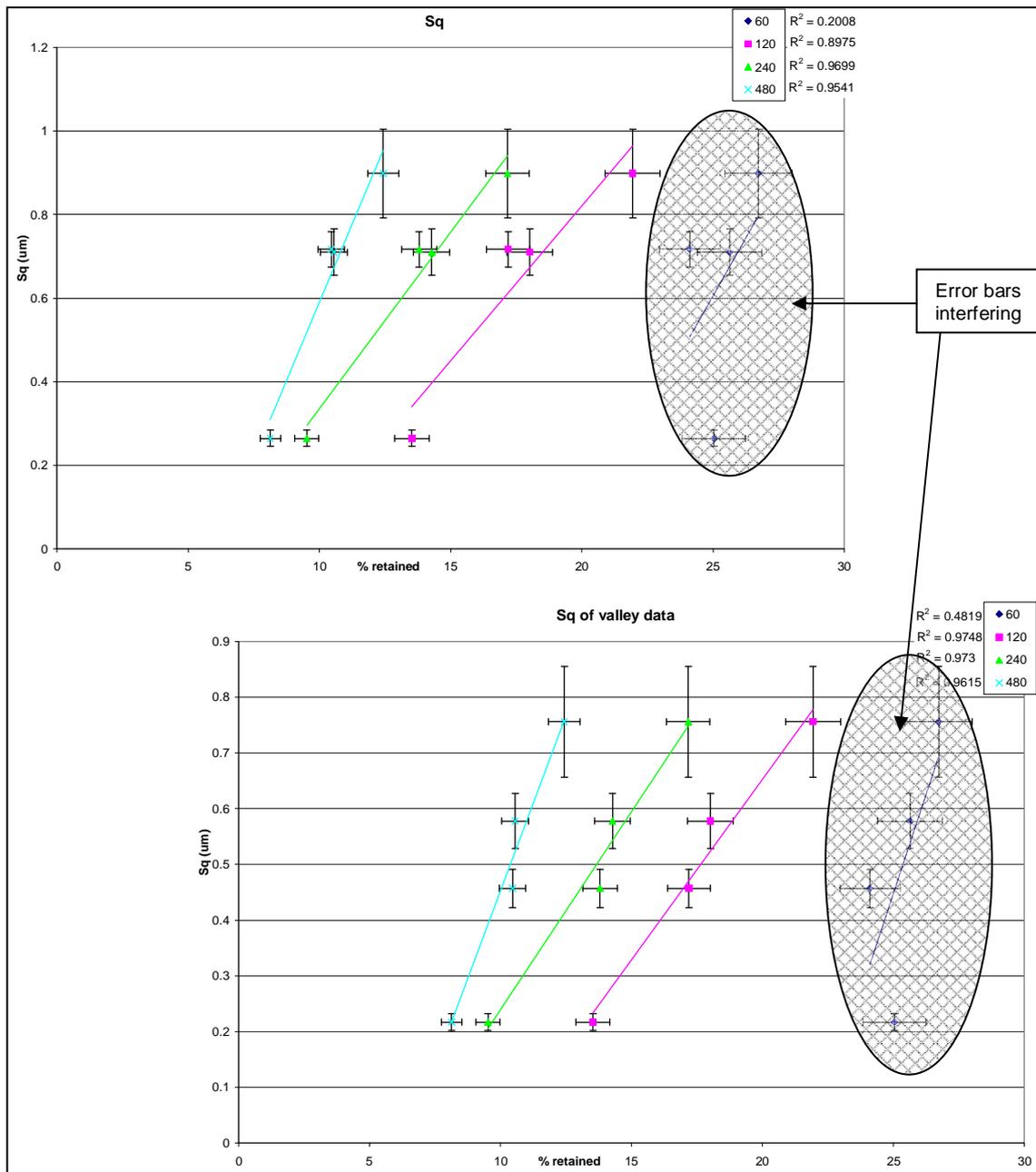
Figure 7.7: Graph of S_q (Root Mean Square Deviation) for a) all the data and b) the separated valley data against % of oil retained

Figure 7.8 shows the graph of S_p (Maximum Peak Height). This parameter only had a good correlation with the separated valley data, which is unexpected since it is peak related. The maximum peak height of the valley data gives an indication of the height of the transition plane (where the data is separated from the plateaus) above the mean plane of the surface. As this height increases, the percentage oil retained increases (or the flow of oil from the surface is slower for higher transition planes). Again, the data at 60 seconds has little meaning due to the interference of its error bars.
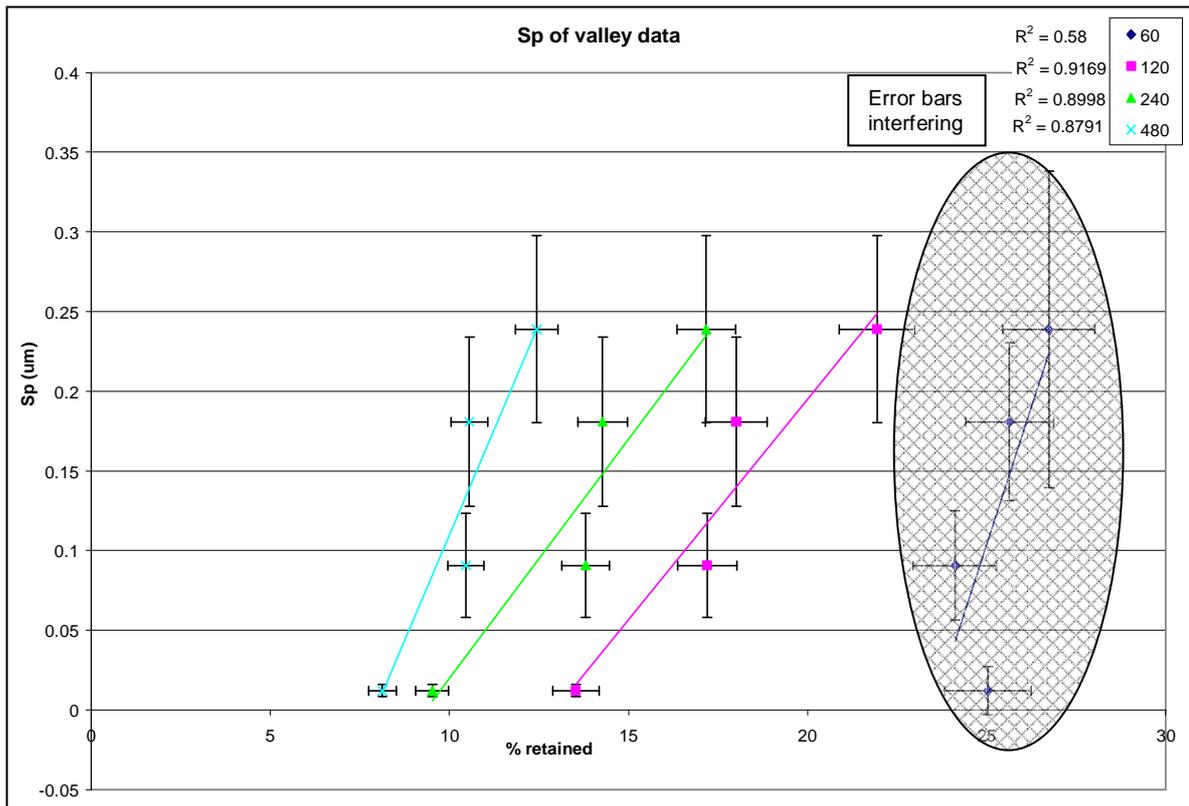
Figure 7.8: Graph of S_p (Maximum Peak Height) for the separated valley data against % of oil retained

7.5.2.3   Spacing Parameters

The only spatial parameter to be related to the lubricant retention was the S_{ds} (Density of Summits) for the separated data, although the error bars on the valley data sets interfere to an extent which renders the result ineffectual. Figure 7.9 shows the S_{ds} of the plateau data, with clear distinctions between the points. This graph implies that surfaces with higher summit densities (in the plateau micro-roughness regions) have lower oil retention. It follows that the runoff is faster for surfaces with more summits, which may indicate that the summits are affecting the surface tension properties of the oil (the cohesion of the droplet is lost due to summits). The data for 60 seconds is clearer with this parameter, implying that the rapid runoff at the beginning of the test is also affected by summit density.
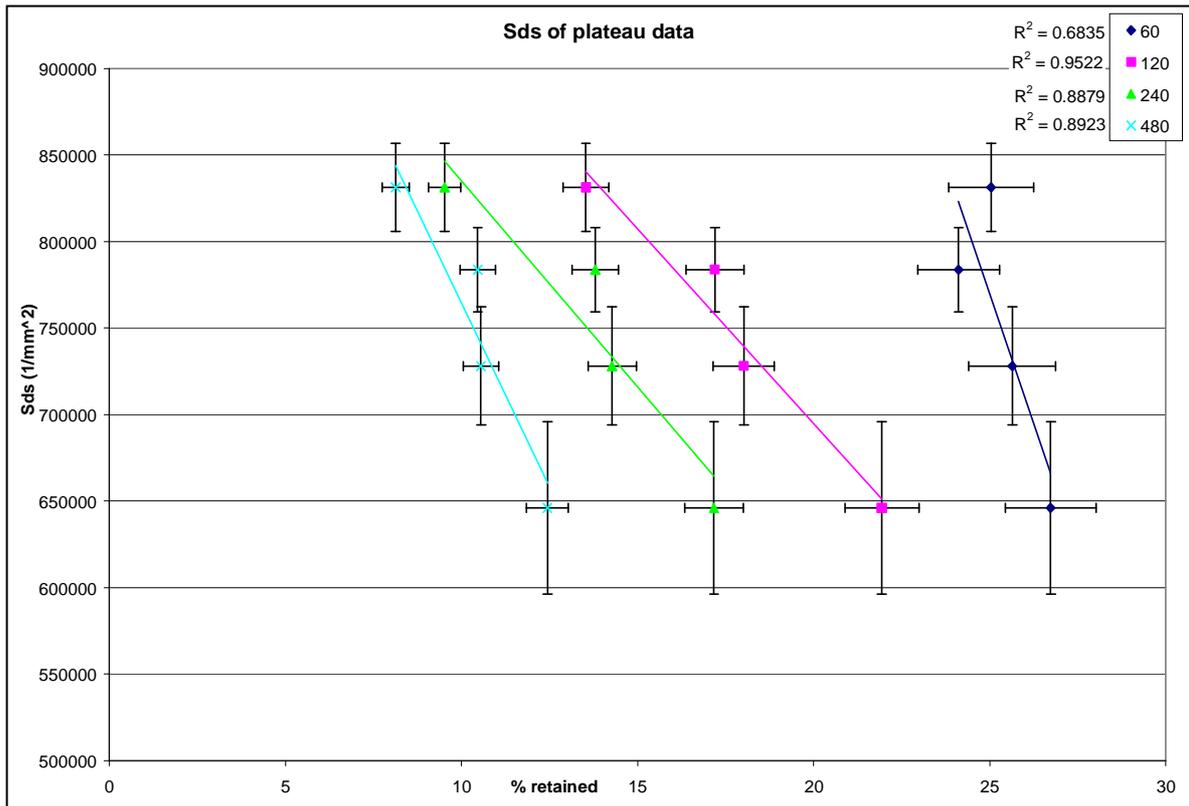
Figure 7.9: Graph of S_{ds} (Density of Summits) for the separated plateau data against % of oil retained

7.5.2.4   Hybrid Parameters

No correlation of hybrid surface topography parameters to lubricant retention was found. This may be due to the nature of the testing method (being vertically hung) since it is plausible that surface slope and peak curvature affect runoff rates.

7.5.2.5   Curve and Related Parameters

It was expected that the volume family parameters would have a relationship to the lubricant retention.

For the V_{mp} (Material Volume of the Texture surface) this was only true when it was calculated for the separated valley data, figure 7.10. This relates to the amount of material at the peak of the valley data, which links to the amount of plateau material. Alternatively, it could convey a characteristic of the shape of the valleys, since it is linked to a percentage height of the data (the top 10%). A larger V_{mp} could indicate a steeper valley wall or relatively thinner valleys. An increase in V_{mp} gave a larger retention (or slower runoff).
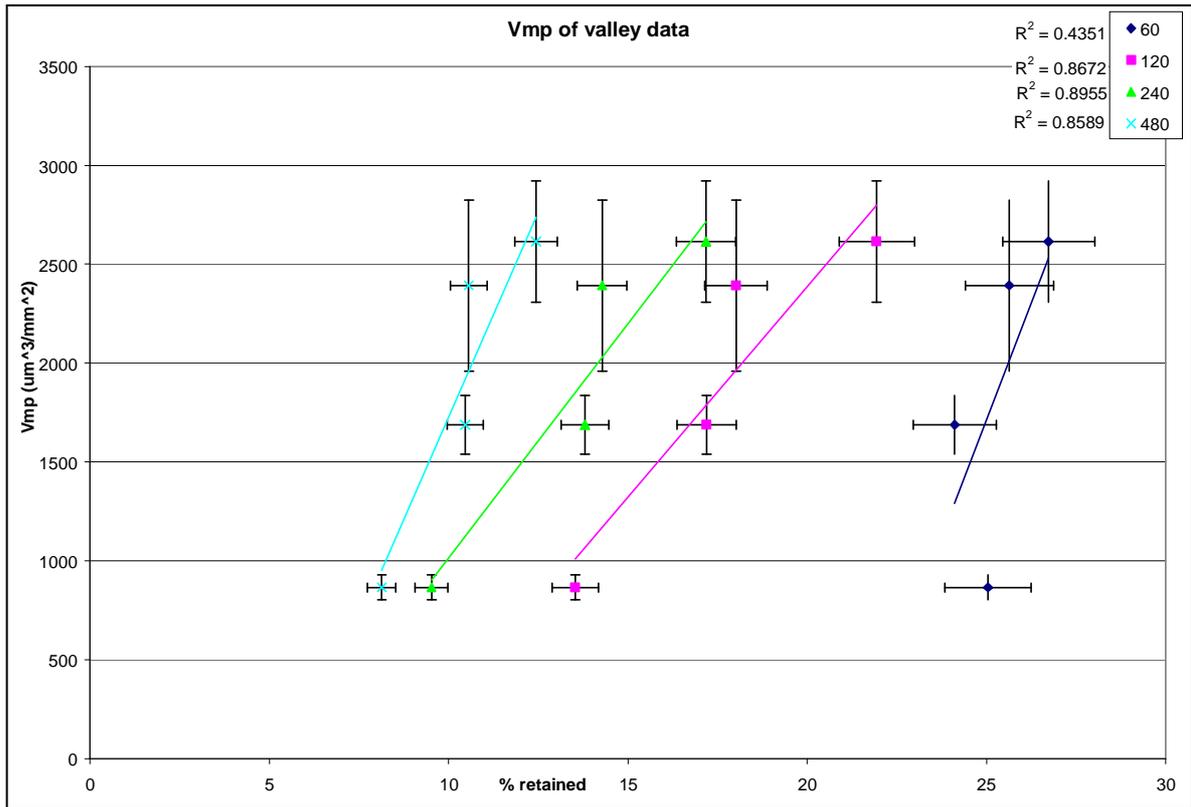
Figure 7.10: Graph of V_{mp} (Material Volume of the Texture surface) for the separated valley data against % of oil retained

The V_{mc} (Core Material Volume of the Texture surface) and V_{vc} (Core Void Volume of the Texture surface) related well to all the data sets, but better correlations were found in the two separated sets, since the data has a whole had much larger errors. As the core void volume of the data is increased the retention is increased, which would imply that the voids in the core trap the lubricant, figure 7.11.
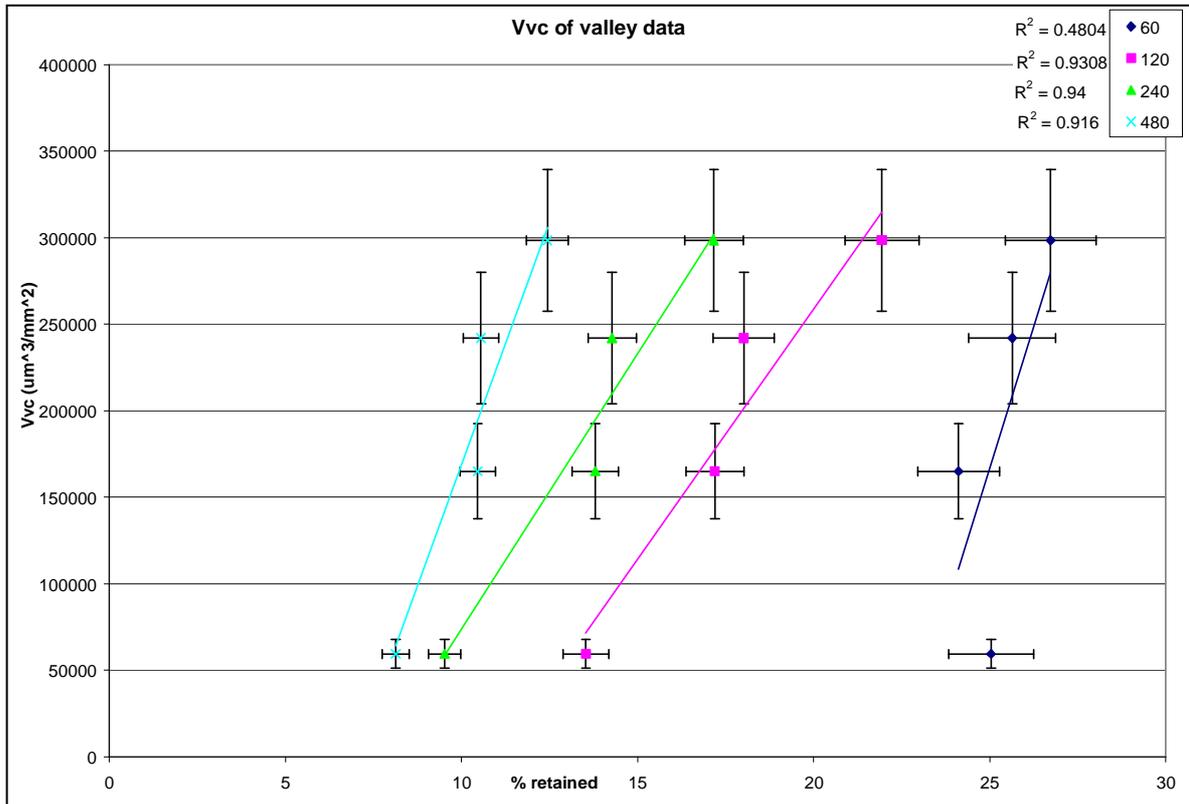
Figure 7.11: Graph of V_{mc} (Core Material Volume of the Texture surface) for the separated valley data against % of oil retained

Finally, the relationship of lubricant retention to the void volume of the valleys (V_{vv}) for the valley data set is shown in figure 7.12. The trend is similar to that of V_{vc}, which is to be expected since the oil can be trapped through out the valley volume (it is not dependant on the size of particles). There is an indication on the graph that the V_{vv} affects the rapid runoff at the beginning of the test, since a relationship can be seen between three of the points, whereby a greater volume of valley voids slows down the excess runoff.
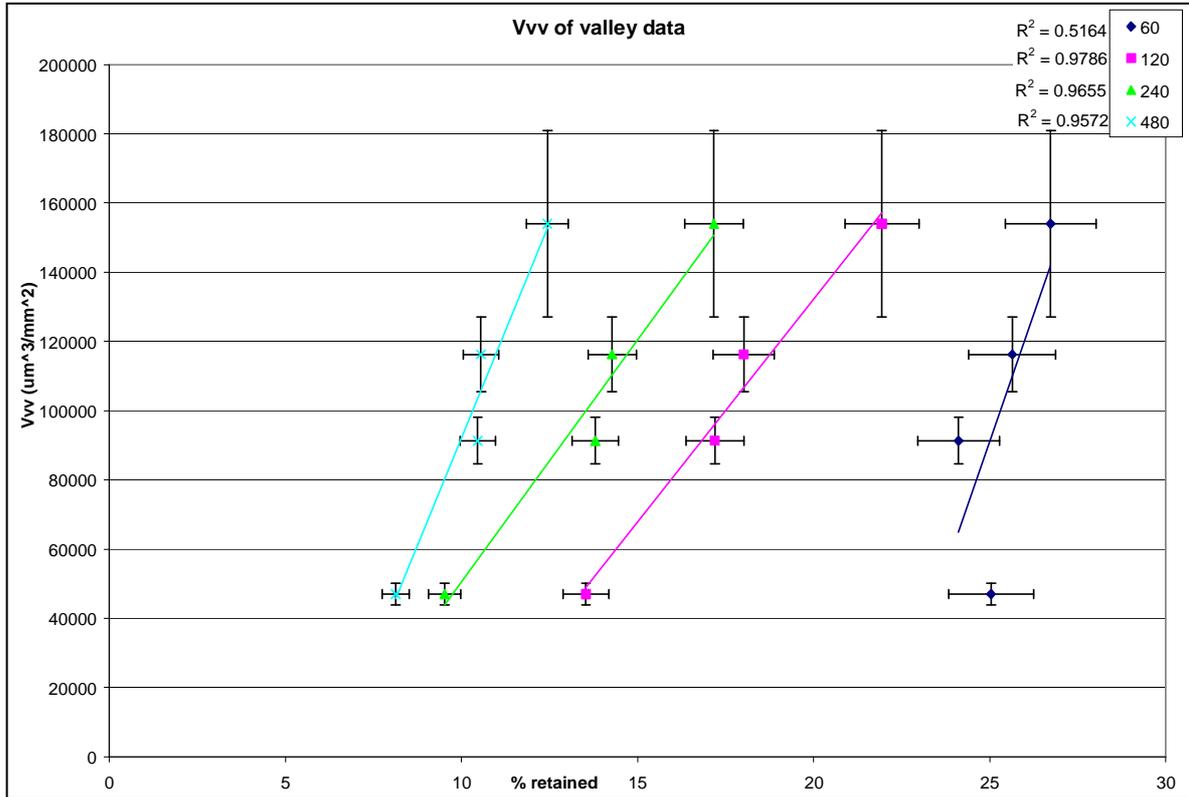
Figure 7.12: Graph of V_{vv} (Valley Void Volume of the Texture surface) for the separated valley data against % of oil retained

7.6. Conclusions

➢ The conclusion of the optimisation was that more oil gave better repeatability of results up to an optimum amount of 25 drops (before edge runoff occurred).

➢ The conclusion from the comparison of 2B and BA samples is that the test is sensitive enough to detect differences in the topographies of the samples. Also, as expected, the bright annealed surface has a faster run-off of oil than the 2B surface.

➢ In general the thinner gauge samples have a faster run off than the thicker gauges (for times above 80 seconds).

➢ Below around 80 seconds the data is unclear. The amount of oil dripped off is very rapid – it is simply surface runoff of excess oil and does not closely relate to the differences in the samples.

➢ This method is sensitive enough to determine that the direction of rolling has an effect on the lubricant retention for the 2B finish and that retention is lower in the direction of rolling.

➢ As the roughness increases, the surface retains a larger percentage of oil. The exception is for the time of 60 seconds, where the excess oil is rapidly running off the surface and therefore is not affected by the roughness.

➢ Surfaces with higher summit densities (in the plateau micro-roughness regions) have lower oil retention. The rapid runoff at the beginning of the test is also affected by summit density.

➢ An increase in the material volume of the texture surface (V_{mp}) gave a larger percentage retention (or slower runoff).

➢ As the core void volume (V_{vc}) of the data is increased the retention is increased, implying that the voids in the core trap the lubricant.

➢ The relationship of lubricant retention to the void volume of the valleys (V_v) for the valley data set has a similar trend to that of V_{vc}, which is to be expected since the oil can be trapped through out the valley volume (it is not dependant on the size of particles).

➢ The V_v affects the rapid runoff at the beginning of the test, whereby a greater volume of valley voids slows down the excess runoff.

Table 7.1: Suggested parameter set for lubricant retention

Surface Parameter

Parameter family	Whole of data	Plateaus	Valleys
Amplitude	S_q	S_q	S_q
Spatial		S_{ds}	
Volume			V_{mp}
			V_{vc}
			V_{vv}

145

Chapter 8   Corrosion

8.1. Summary of the Chapter

In collaboration with Birmingham University unidirectional finishes and brushed production finishes were assessed and rated on their corrosion resistance. New testing methods, developed at Birmingham University, are presented. Surface measurements were made in an effort to find the connection between certain surface characteristics and the susceptibility of a surface to pitting corrosion.

8.2. Introduction

Pitting proceeds by an autocatalytic process in which there is a local increase in chloride and acid concentrations due to corrosion product hydrolysis in cavities [26]. Areas on the surface which are depleted of chromium (such as the grain boundary valleys in the 2B finish) become anodes in the cell and the oxide film on the remaining surface forms the cathode.

8.3. Collaborative Research

In collaboration with Birmingham University several hand-polished unidirectional finishes and brushed production finishes were assessed and rated on their corrosion resistance. A new method was developed at Birmingham University, allowing faster evaluation than existing standard salt spray tests normally used by Outukumpu. Surface measurements were made in an effort to find the potential connection between certain surface characteristics and the susceptibility of a surface to pitting corrosion.

The initial objective of the work at Birmingham was to develop an appropriate technique to study the effect of surface roughness on pitting corrosion in order to provide an effective way of assessing and ranking pitting susceptibility of commercial surface finishes. Currently, a number of tests are used for ranking pit susceptibility for different surface finishes, for example salt spray testing [27] and critical pitting temperature measurements [28]. However, these can be quite slow. The work aimed to investigate electrochemical methods for assessing the pitting susceptibility of stainless steel with different surface finishes.

146

8.4. Developed Methods of Assessing Corrosion Susceptibility

Initially, four different electrochemical methods (Zero Resistance Ammeter (ZRA), Potentiostatic, Potentiodynamic and Galvanostatic) to measure forced corrosion were compared for hand-prepared samples (using 240, 400, 800, 1200 grit silicon carbide paper). Metastable pit current transients were found in both ZRA and potentiostatic measurements.
(Method descriptions in sections 8.4.1 and 8.4.2 are taken from [80]).

8.4.1   The ZRA Method

The ZRA method permits measurement of metastable pitting corrosion events in terms of current and voltage transients under realistic open circuit conditions. The theory is shown in figure 8.1.
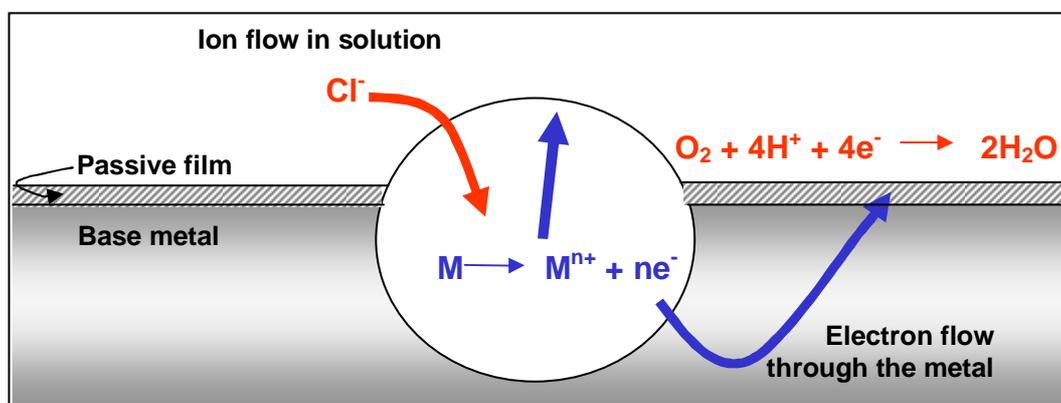
Figure 8.1: Theory of ZRA method

It is a relatively simple electrochemical technique, requiring two nominally identical working electrodes (steel samples) and a standard reference electrode, figure 8.2. Recording both current and voltage transients permits verification that current events are due to actual corrosion, and not to electrical noise. The magnitudes of these transients range from nanoamps to milliamps, and from microvolts to millivolts respectively. Measurements can detect metastable pits of less than 1 μm diameter, equivalent to the order of $5 \times 10^{-1}4$ grams of metal being released.
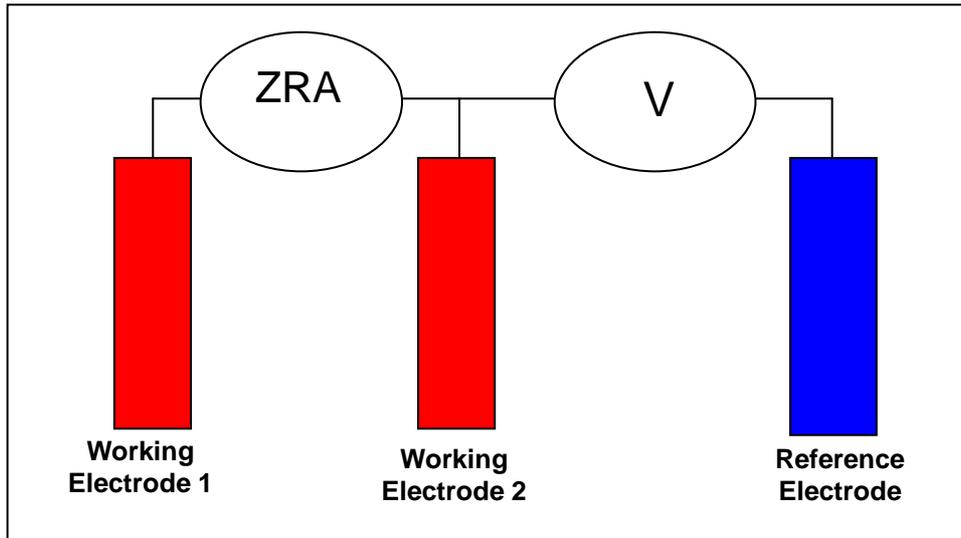
Figure 8.2: ZRA cell setup

Current peaks from metastable pitting events are recorded against time, figure 8.3. Integration of these gives the charge passed, which can then be converted into amount of metal loss using Faraday's Law, equation 8.1.

$$Q = nF\Delta m / M$$

Equation 8.1
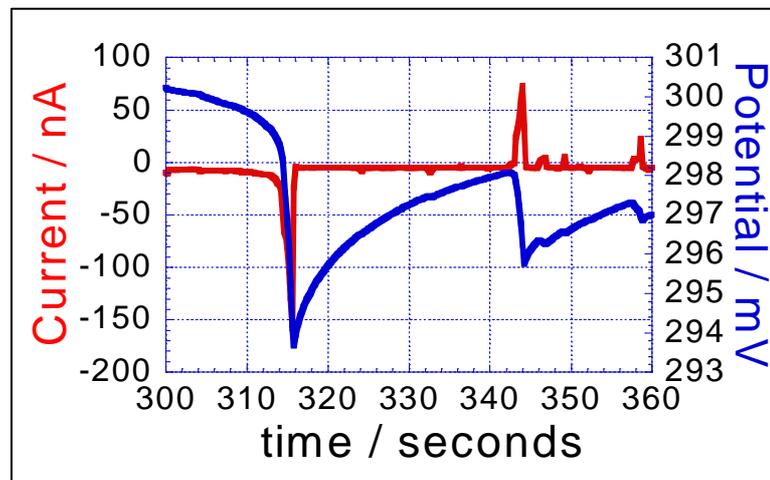
Figure 8.3: Recording of current peaks from metastable pitting

The ZRA measurements were carried out in 0.01M $FeCl_3$ and 0.03M NaCl at ambient temperature, exposed to lab air. Figure 8.4 shows current transient measured with ZRA for samples with different grit surface finishes. The number of metastable pit events in $FeCl_3$ is much higher than in NaCl due to the higher oxidizing power of $FeCl_3$. The number of pits also decreases in both solutions with increasing grit number (smoother surface) as show in Figure 8.5.

(a)

(b)
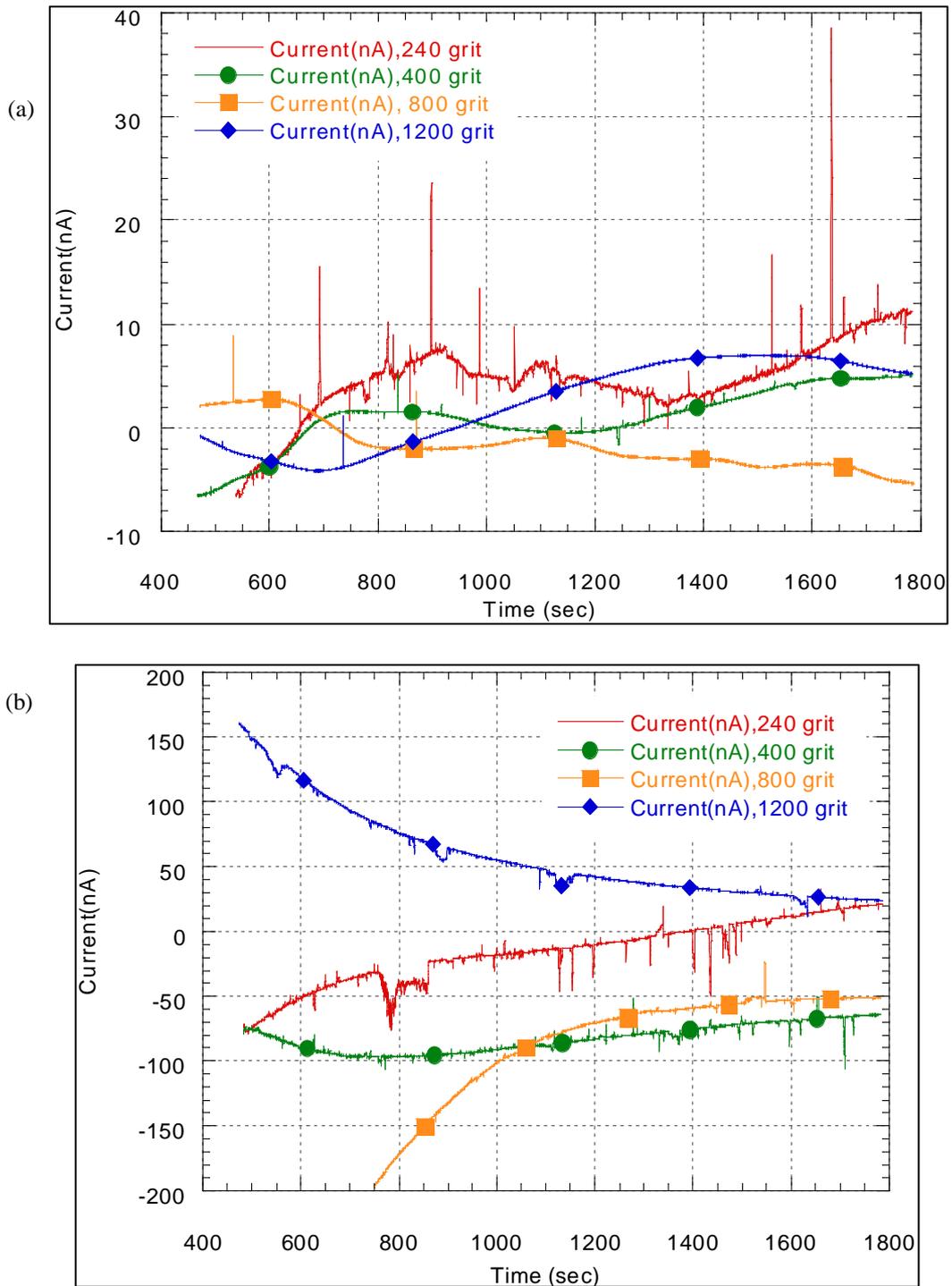
Figure 8.4: ZRA measurement for 304 SS with different surface finish: 240, 400, 800, 1200 in (a) 0.03M NaCl and (b) 0.01M FeCl$_3$
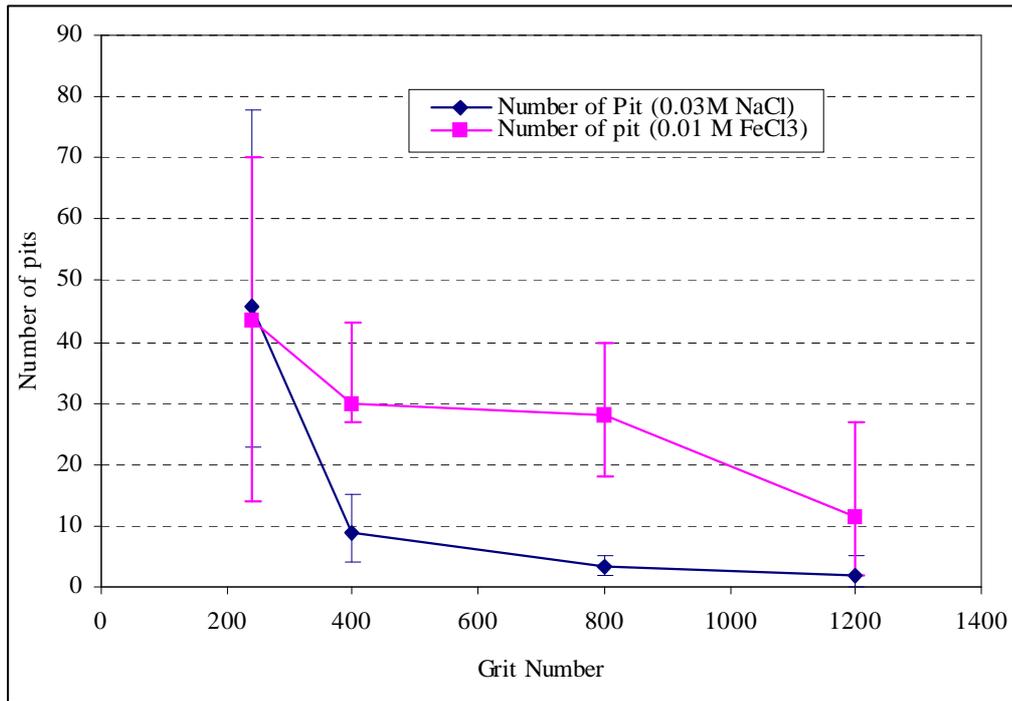
Figure 8.5: The relationship between number of pits on 304 SS in 0.03M NaCl and 0.01M FeCl$_3$ and grit number of surface finish

8.4.2 The Potentiostatic Method

The potentiostatic method has been used to measure the passive current density (due to passive film growth), and also show metastable pitting events. It has the benefit of having a smoother background than ZRA data because a constant potential is applied to the sample, figure 8.6. This permits easier data analysis.
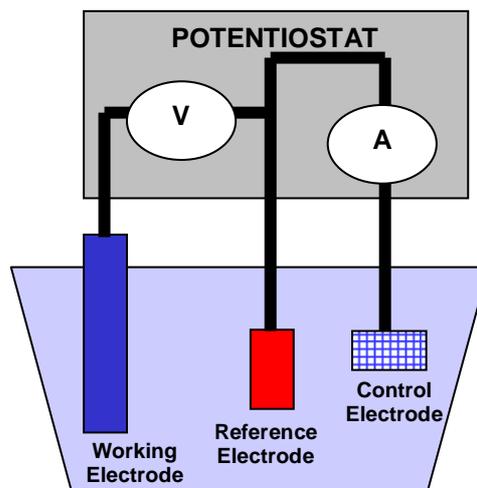
Figure 8.6: Potentiostatic method setup

Potentiostatic measurements were carried out in 0.03M NaCl at ambient temperature with constant potentials of −200, -100, 0, 100, 200 mV (SCE). Figure 8.7 shows an example of curves from a potentiostatic measurement at an applied potential of 100 mV/SCE with different surface finishes. The number of pits decreases for surfaces with higher grit numbers and also increases with applied potential as shown in figure 8.8.
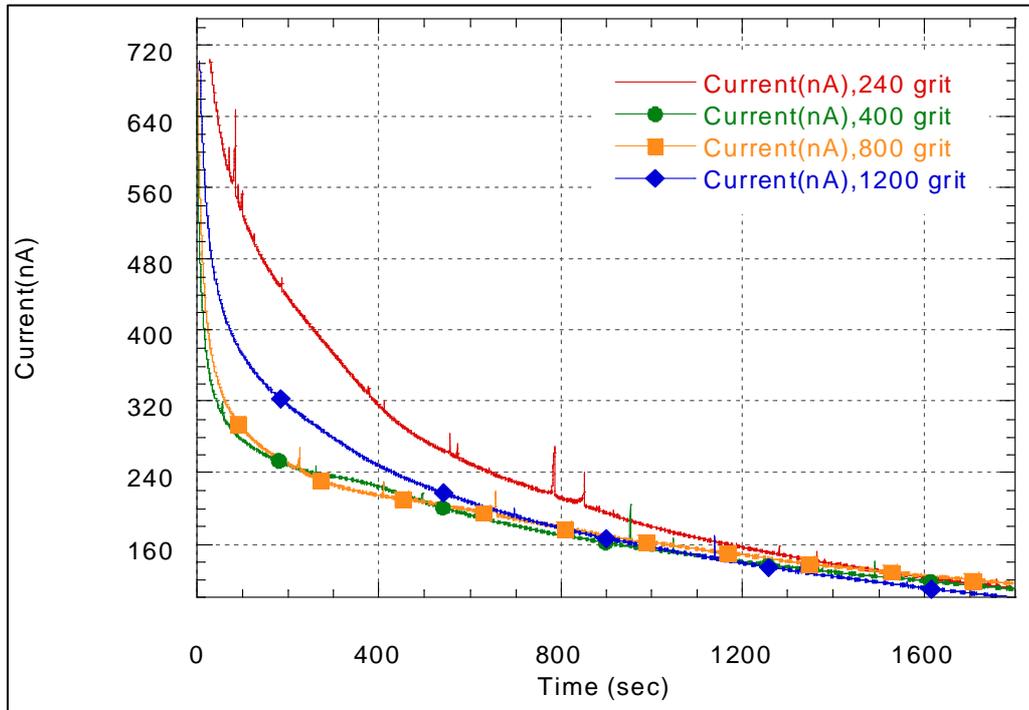
Figure 8.7: Examples of potentiostatic measurements showing metastable pits with an applied potential of 100 mV/SCE
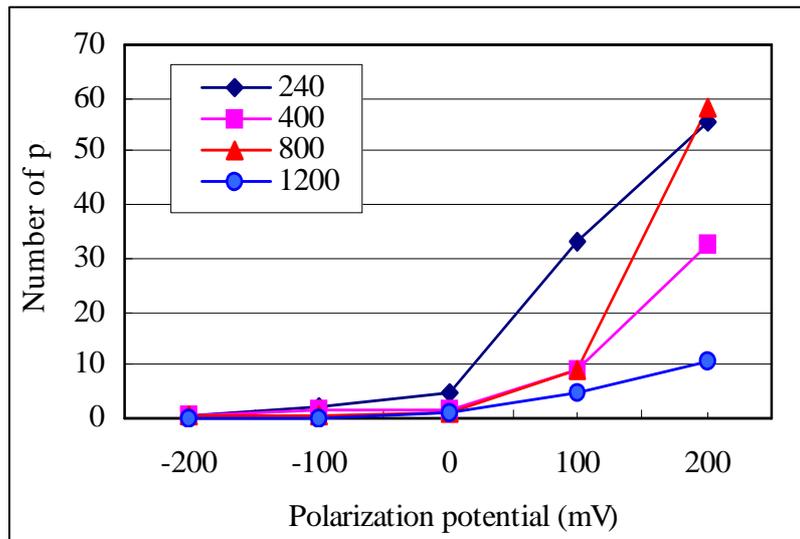
Figure 8.8: The relationship between the average number of pitting events for 304 SS in 0.03M NaCl solutions and applied potential

8.4.3   Discussion and Conclusions of Method Development

The initial work to investigate a suitable method for measuring metastable pitting activity using hand-produced finishes concluded that:

➤ ZRA and potentiostatic measurements are effective ways of monitoring metastable pitting activity on different surface roughnesses.

➤ The surface roughness, solution and potential affect the number of pitting events, which can be used to indicate pitting susceptibility.

8.5. Results

Further to the initial studies, tests were conducted on several commercially produced unidirectional finishes. The surface topography of these samples was measured following the relevant measurement protocol devised in Chapter 4. The following results show the corrosion ranking (given from the research carried out at Birmingham) against various 3D topography parameters for 6 samples, table 8.1. The error bars on the graphs are ±½ standard deviation of the 15 measurements taken.

Table 8.1: Unidirectional samples

Sample Name	Finish Reference	Ranking 1 = best corrosion resistance 6 = worst corrosion resistance
A	DPB	3
B	DP1	4
C	DPS	6
D	FP1	2
E	SP1	5
F	SB1	1

Figure 8.9 shows a graph of S_q (Root Mean Square Deviation) in relation to the corrosion susceptibility ranking (given by Birmingham University – note it is not a numerical result). The trend shows good linear correlation and as expected implies that smoother finishes are less susceptible to pitting corrosion.

S_z (Maximum Height of Texture surface) follows a similar trend to S_q, figure 8.10.
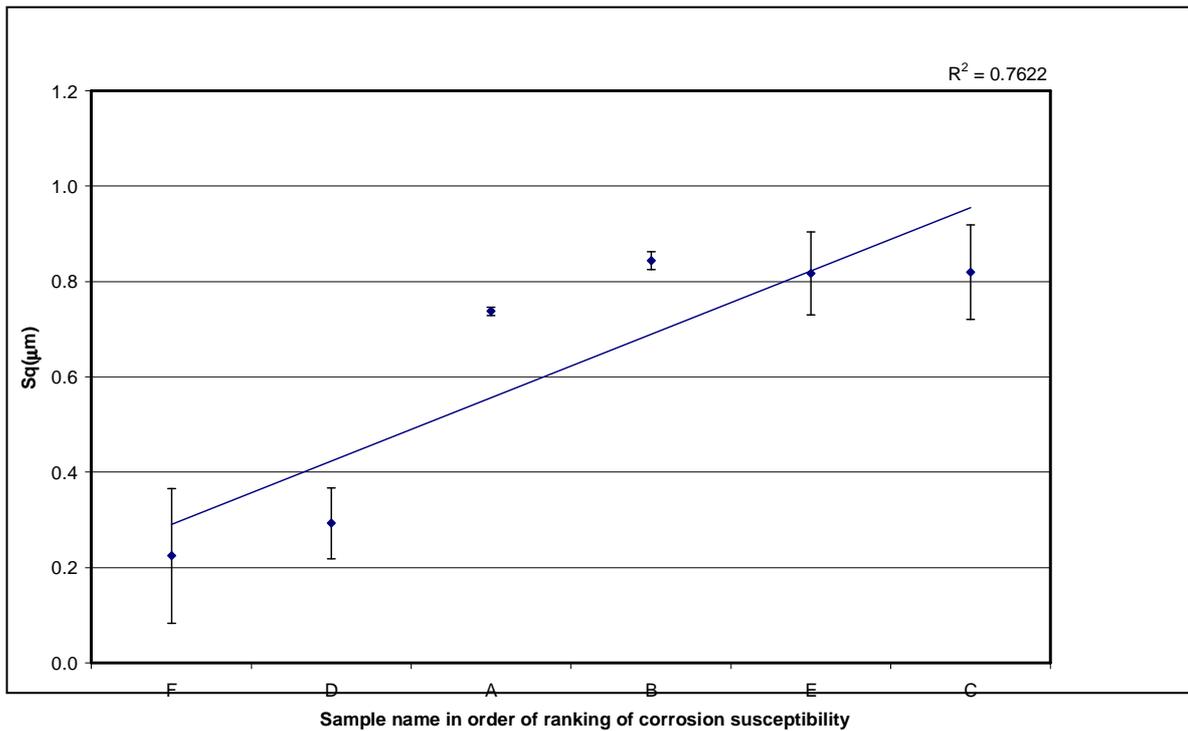
Figure 8.9: Graph of S_q (Root Mean Square Deviation) against corrosion susceptibility
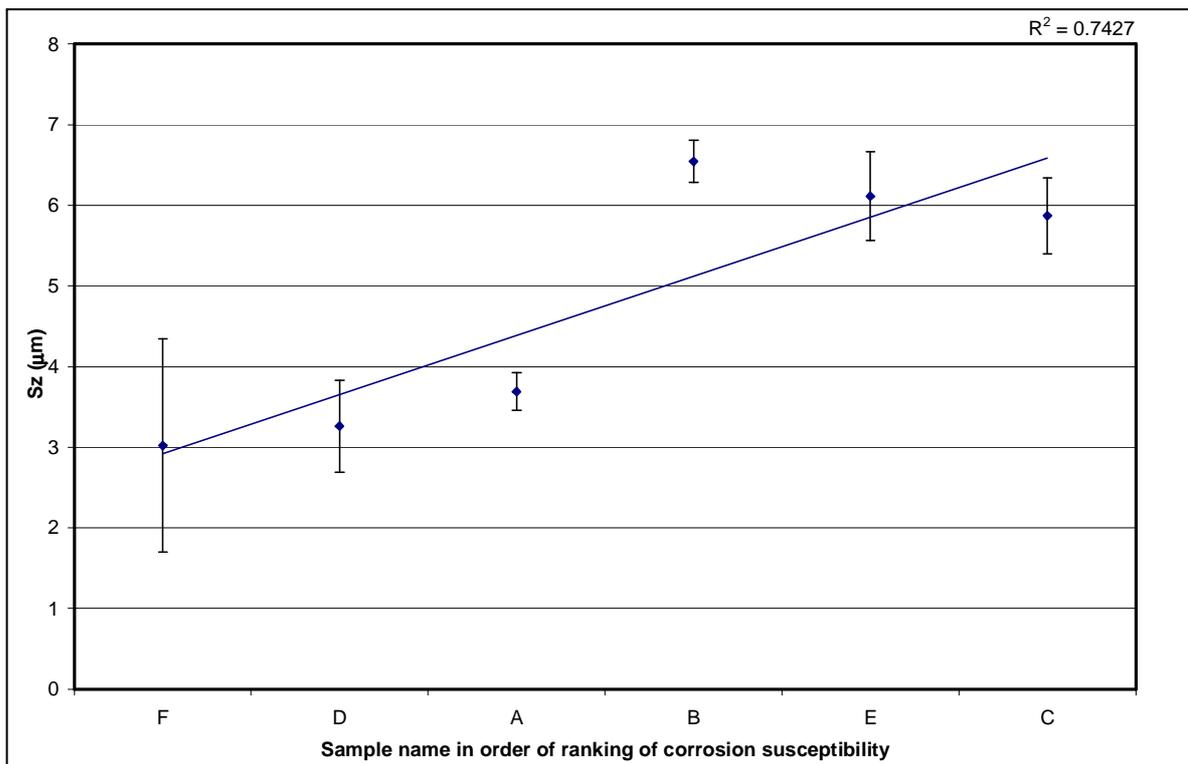
Figure 8.10: Graph of S_z (Maximum Height of Texture surface) against corrosion susceptibility

It was expected that a clear relationship between corrosion and the topographical properties of the valleys on the surface would be found. When studying the volume parameters, only V_{vc} (Core Void Volume of the Texture surface) showed good correlation, figure 8.11.
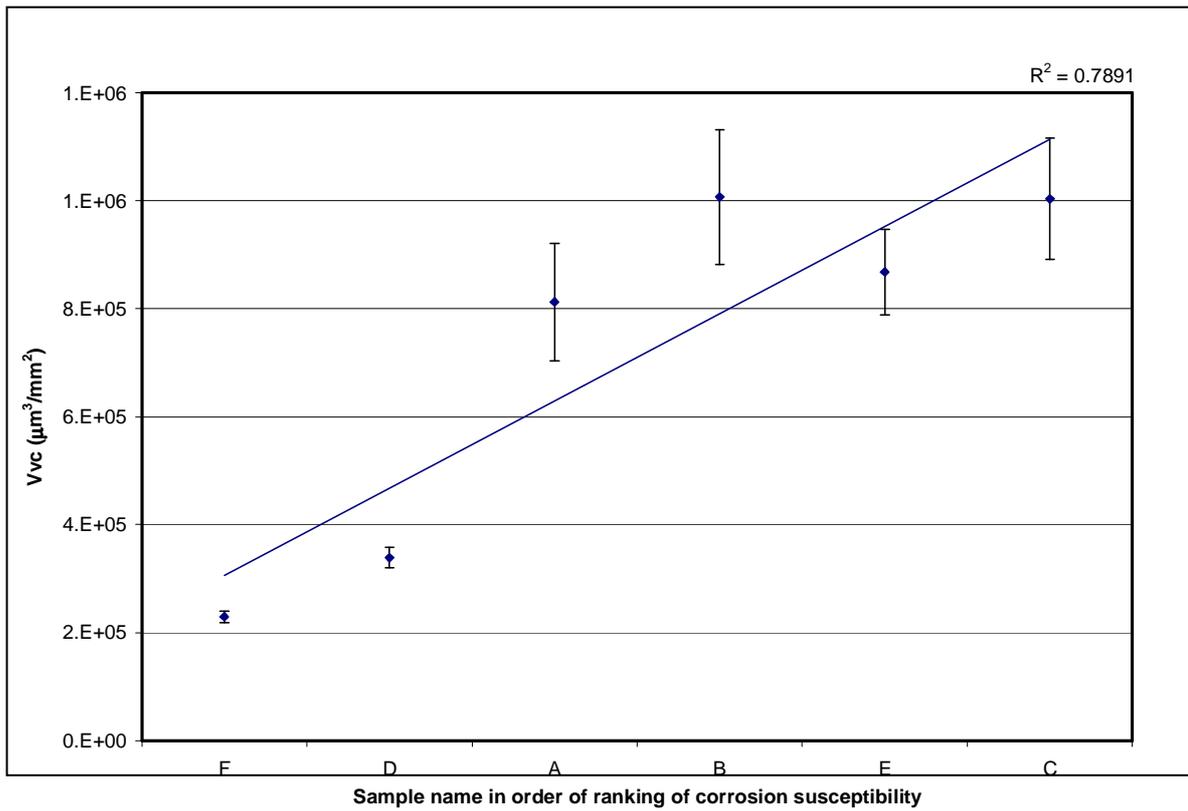
Figure 8.11: Graph of V_{vc} (Core Void Volume of the Texture surface) against corrosion susceptibility

8.6. Discussion

Due to the qualitative nature of the corrosion susceptibility ranking it is difficult to draw a quantitative assessment of the effects that surface topography have on these results. Figures 8.9 and 8.10 are related to the amplitude properties of the surface topography, S_q (Root Mean Square Deviation) and S_z (Maximum Height of Texture surface). The general trend implies that an increase in roughness causes an increase in the corrosion susceptibility. However, since some of the samples have very similar roughness this is only a tentative result.

Figure 8.11 implies that as the void volume in the core of the surface increases corrosion susceptibility also increase. This may be because an increase in core volume is due to more chromium depleted grain boundary valleys, which are the most likely sites for the initiation of pitting corrosion.

Further analysis of the results was carried out by researchers at Birmingham University to explain the differences between the preparations of the samples, table 8.2.

Table 8.2: Differences between sample preparation methods related to 3D surface topography parameters

Samples	Differences	Parameters used
B & D	Polishing media B = Aluminium Carbide D = Silicon Carbide	S_{sk} S_{ku} S_{ds} V_{mp}
B & E	Polishing Grit B = 240 E = 280	Amplitude Spatial V_{vv} S_{sk}
A & C	Brushing A = 180 grit silicon carbide followed by nylon brush polishing C = 180 grit silicon carbide	S_{ku} S_{ds} V_{mp} V_{vc} V_{vv}

Main findings from corrosion work done at Birmingham University (written by Chanada Watanatham, Outukumpu UK Foundation for Research and Development student):

<u>Polishing Media</u>

➢ S_{sk} of surface D was a positive value (+) while S_{sk} of surface B was a negative value (-). This indicated that both surfaces had an asymmetric height distribution and the surface D probably had more peaks than valleys, while surface B probably had more valleys than peaks.

- The S_{ku} value for surface D was larger than three while the S_{ku} value for surface B was smaller than 3. This indicated that surface D had a centrally distributed surface and surface B had a well spread distributed surfaces. This implied that surface D had many high peaks and surface B had few high peaks.

- The S_{ds} values of surface B and D were similar value. This indicated that both surfaces had a similar the number of summits on the surface. This was in agreement with SEM images.

- The V_{mp} value of surface B was higher than the V_{mp} value of surface D. This indicated that surface B had a plateau surface.

- The plateau surface shows a characteristically good the retention of solution in the valley zone. It was possible that the solutions therefore remained longer on the surface, which could be a cause of increased corrosion susceptibility.

Polishing Grit

- The amplitude and spatial parameters of surface E were similar value with surface B. Then, surface E had an asymmetric height distribution and a well distributed surface. This implied that surface E had more valleys than peaks overall but the surface still had many high peaks.

- The V_{vv} values of surface E were higher than the V_{vv} values of surface B. This indicated that the void volume of surface E was higher than surface that of B. The solution was therefore better maintained in the valley zone of the surface E than on surface B. This was possibly the reason why the surface E showed a higher corrosion susceptible.

Brushing

- S_{sk} and S_{ku} were used to characterise the amplitude characteristics of the surfaces. The S_{sk} values of surface A and C were negative. These showed that both of surfaces had asymmetric height distributions. They showed more valleys than peaks. The S_{ku} values of surface A and C were larger than three. This indicates that both surfaces had either a centrally distributed surface or many high peaks.

- The S_{ds} values of both surfaces were similar.

- The V_{mp} value of surface C was higher than the V_{mp} values of surface A. This was showed that surface C had more of a plateau morphology than surface A. The solution is better maintained with a plateau surface morphology than on a spiky surface.

- The V_{vc} value of surface C was higher than that of surface A. This indicated that on surface C the solution was better maintained in the core than on surface A.

- Inversely, the V_{vv} value for surface A was higher than the V_{vv} value for surface C. It was probable that the solution in the valley zone on the surface A was maintained better than on surface C. However, surface A had spiky surface morphology, so the solution was not maintained in the valley zone. This was possibly the reason why result surface A showed less corrosion susceptibility than surface C.

8.7. Conclusions

➢ ZRA and potentiostatic measurements are effective ways of monitoring metastable pitting activity on different surface roughnesses.

➢ The surface roughness, solution and potential affect the number of pitting events, which can be used to indicate pitting susceptibility.

➢ An increase in roughness causes an increase in the corrosion susceptibility.

➢ As the void volume in the core of the surface texture increases corrosion susceptibility also increases.

Chapter 9   Summary of Discussions

The overall aim of this research project was to characterise quantitatively the developed surface topography of some widely used finishes on stainless steel sheet using three-dimensional surface analysis techniques. Based on this surface characterisation an attempt has been made to identify 3D parameters for quantitative description of stainless steel sheet with respect to some aspects of their functional performance.

To effectively measure the topography it is important to first understand what the important features of the surface are. This is carried out in chapter 3 where initially, the functional topographical features of four finishes are determined and the predicted relevant parameters identified, giving respect to the process/es by which they were made. A model of 'normal' features is derived to aid in the development of the measurement strategy. For the 2B finish, which is linked to the functions of optical appearance and lubricant retention in chapters 6 and 7 respectively, the plateau regions with microroughness give the finish its distinctive reflectance and the interconnecting valleys can aid the spread and retention of lubricant. For a unidirectional finish, which is linked to the function of corrosion susceptibility in chapter 8, the model is mainly troughs and ridges with remnant 2B features.

A generalised measurement strategy is detailed in chapter 4, aiding the selection of measurement and instrument selection for any surface topography. The approach described could be used as a general guide for surface metrology of different surfaces. The strategy and its protocol have been demonstrated using three of the modelled surface finishes, produced by the sponsoring company. Once established this protocol is followed during further studies and additionally offers the potential to systematically approach the selection of variables for the measurement of other surface topographies. A flow chart of the generalised protocol is presented in figure 4.16 to aid in the visualisation of the steps involved for the sponsoring company (toward objective (iv)).

It is known by the sponsoring company that there is inherent variability in the surface topography produced due to differing process stages and grades of material. These variations are investigated using 3D topography parameters and a general relationship between surface roughness and gauge is expanded into an in-depth examination of what is happening to the features of the surface during cold rolling and how differences in the grade and process can affect the development of surface features. This initial study, chapter 5, showed that the characterisation using 3D surface topography parameters is viable and that variables in production can be explained in relation to them.

The sponsoring company is working towards a more quantitative assessment of the appearance of the main production finish, 2B. The ability to link the surface topography features to numerical optical property characteristics yields not only a better understanding of the effects of

topography on appearance but also enable manufacturers to quantify their pass/fail criteria and remove the subjectivity of human perception, eventually increasing consumer confidence.

In chapter 6, initial trials were used to confirm the available instruments suitability for measuring the optical properties of the 2B finish. Further to this a wide range of 2B finish samples were measured in an attempt to correlate the optical properties with the 3D topography parameters. A new method of analysing the data enabling separation of the important features of the topography was developed. The effect of rolling direction to appearance measurement direction, angle of appearance measurement and sample grade variation was studied. The relationships of two of the four optical descriptors to 3D topography parameters were found.

It has long been believed that rougher surfaces have lower values of these optical properties but this relationship was not clearly seen until the data was separated using the newly developed method. The results show that specular reflectance is influenced mostly by the microroughness of the plateaus and that light entering the valleys does not return to the detectors and therefore no correlation to valley data is evident. However, the same relationship is not found in relation to gloss, which may be due to the relatively low gloss of all the surfaces measured. The following results were also found: the light is scattered more by a surface with high arithmetic mean peak curvature; increases in the root-mean-square slope of the surface of the plateaus decreased the gloss and specular reflectance due to diffuse scattering; as the density of summits in the valleys increases, the specular reflectance decreases indicating that these summits have an influence of whether the light is reflected back to the detector or diffused.

In chapter 7, a simple drip test method is employed to assess the lubricant retention properties of topography. The development of the methodology included proof of the equipment repeatability and approach suitability for testing the 2B finish. Optimisation implied that more oil gave better repeatability of results up to an optimum amount of 25 drops (before edge runoff occurred).The average error in repeatability of the test was calculated as ±4.8% and used as the standard error of the percentage of oil retained in further studies.

Good correlations were found between many of the amplitude and volume related parameters and lubricant retention. The implication is that as the roughness increases, the surface will retain a larger percentage of oil and that the voids in the core and valley areas trap the lubricant. The exception is for the time of 60 seconds, where it is thought that the excess oil is rapidly running off the surface and therefore is not affected by the roughness.

It was found that surfaces with higher summit densities (in the plateau micro-roughness regions) have lower oil retention possibly due to surface tension effects. The rapid runoff at the beginning of the test is also affected by summit density and the valley void volume.

In collaboration with Birmingham University several hand-polished unidirectional finishes and brushed production finishes were assessed and rated on their corrosion resistance. Two new methods (developed at Birmingham University) which allow faster evaluation than existing methods are used to find the connection between certain surface characteristics and the susceptibility of a surface to pitting. This connection was only briefly discussed due to the difficulty in comparing quantitative 3D topography data with a qualitative corrosion susceptibility

ranking. The two main (tentative) findings were in line with expected results: increases in the average roughness and the void volume in the core of the surface texture causes an increase in the corrosion susceptibility possibly due to an increase in pit initiation sites.

Chapter 10   Conclusion

10.1. Conclusions

The overall aim of this research project was to characterise quantitatively the developed surface topography of some widely used finishes on stainless steel sheet using three-dimensional surface analysis techniques. Then, based on this surface characterisation attempt to identify the 3D parameters that give a quantitative description of common stainless steel sheet finishes with respect to some aspects of their production and functional performance.

The major objectives were outlined as:

➢ Using the 3D techniques available, define a measurement strategy and protocol to effectively measure stainless steel sheet topography.
➢ Investigate the differences in topography across a range of grades and gauges of stainless steel using 3D topography parameters.
➢ Investigate the ability of 3D topography parameters to correlate with functional requirements of optical appearance, lubricant retention and corrosion.
➢ Develop a set of written procedures for industrial application to effectively characterise stainless steel sheet surface roughness.

A number of studies were developed and completed in order to fulfil these aims and objectives.

The main conclusions towards objective (i) are:

➢ Using the correct measurement strategy is imperative to avoid misleading data. A generalised measurement strategy is detailed in chapter 4. A flow chart of the protocol is presented in figure 4.16 to aid in the visualisation of the steps involved for the sponsoring company (toward objective (iv)).
➢ To effectively measure the topography it is important to first understand what the important features of the surface are.
➢ For the 2B finish, which is linked to the functions of optical appearance and lubricant retention in chapters 6 and 7 respectively, the plateau regions with microroughness give the finish its distinctive reflectance and the interconnecting valleys can aid the spread and retention of lubricant.
➢ For a unidirectional finish, which is linked to the function of corrosion susceptibility in chapter 8, the model is mainly troughs and ridges with remnant 2B features.

The main conclusions towards objective (ii), for the 2B finish, are:

➢ The thinner gauges have a smoother finish.
➢ Although the scale of the topography is getting smaller, the shape of the features on the surface and their relationship to each other is unchanged.
➢ There are very few peaks left on the surface and the valleys dominate the topography.
➢ On average, 304 materials have slightly higher surface roughness than 316 materials of the same thickness.
➢ The spread of the data for 316 grade materials is much greater than that of 304 grade materials.
➢ The peaks on 304 grade materials are not necessarily higher but do take up more volume than those on 316 grade materials.
➢ The skin pass method of final finishing (used on Source 1 samples) gives a smoother and more consolidated topography, having better defined edges than those that have undergone tension stretching (used on Source 2 samples).

The main conclusions, correlating the functional requirements of optical appearance to 3D topography parameters of a 2B finish, towards objective (iii) are:

➢ The glossmeter is a suitable instrument to measure two of the optical parameters of the 2B finish, gloss and specular reflectance.
➢ The haze and DOI cannot be accurately determined using this arrangement.
➢ The results are in general agreement with past research which established that smoother surfaces have higher gloss and specular reflectance.
➢ The gloss can be related to the curvature and slope of the surface, where an increase in either gives a decrease in the gloss.
➢ The specular reflectance is influenced by both the plateau and valley data regions and is closely related to the average roughness, curvature and slope of the plateau data and the average roughness and density of summits within the valley areas.

The main conclusions, correlating the functional requirements of lubricant retention to 3D topography parameters of a 2B finish, towards objective (iii) are:

➢ A drip test method can be used to assess the lubricant retention of a surface.
➢ The repeatability of results is affected by the initial amount of oil applied.
➢ The bright annealed surface has a faster run-off of oil than the 2B surface.
➢ In general the thinner gauge samples have a faster run off than the thicker gauges (for times above 80 seconds).
➢ Below around 80 seconds the data is unclear. The amount of oil dripped off is very rapid – it is simply surface runoff of excess oil and does not closely relate to the differences in the samples.

- This method is sensitive enough to determine that the direction of rolling has an effect on the lubricant retention for the 2B finish and that retention is lower in the direction of rolling.
- As the roughness of the surface increases, it retains a larger percentage of oil. The exception is for before 60 seconds, where the excess oil is rapidly running off the surface and therefore is not affected by the roughness.
- Surfaces with higher summit densities (in the plateau micro-roughness regions) have lower oil retention. The rapid runoff at the beginning of the test is also affected by summit density.
- An increase in the material volume of the texture surface gave a larger percentage retention (or slower runoff).
- As the core void volume of the data is increased the retention is increased, implying that the voids in the core trap the lubricant.
- The relationship of lubricant retention to the void volume of the valleys for the valley data set has a similar trend to that of void volume of the core, which is to be expected since the oil can be trapped throughout the valley volume (it is not dependant on the size of particles).
- The void volume of the valleys affects the rapid runoff at the beginning of the test, whereby a greater volume of valley voids slows down the excess runoff.

The main conclusions, correlating the functional requirements of corrosion susceptibility to 3D topography parameters of a unidirectional finish, towards objective (iii) are:

- ZRA and potentiostatic measurements are effective ways of monitoring metastable pitting activity on different surface roughnesses.
- The surface roughness, solution and potential affect the number of pitting events, which can be used to indicate pitting susceptibility.
- An increase in average roughness causes an increase in the corrosion susceptibility.
- As the void volume in the core of the surface texture increases corrosion susceptibility also increases.

The above conclusions lead to the suggested parameter set, table 10.1, for the characterisation of the 2B finish.

Table 10.1: Suggested parameter set

Parameter	Symbol	Finish				General
		2B			Unidirectional	
		Processing Variations	Appearance	Lubricant Retention	Corrosion	General
Root mean square deviation	Sq	**W**	**P**	**W & P**	**W**	**W & P**
Maximum peak height	Sp			**V**		
Maximum valley height	Sv	**W**				
Maximum height of texture surface	Sz	**W**				
Density of Summits	Sds		**V**	**P**		**P & V**
Root mean square slope of the surface	Sdq		**P**			**P**
Arithmetic mean peak curvature	Ssc		**P**			**P**
Material volume of the texture surface	Vmp	**W**		**V**		**V**
Core void volume of the texture surface	Vvc	**W**		**V**	**W**	**V**
Valley void volume of the texture surface	Vvv	**W**		**V**		**V**
Ten point height of surface	S5z	**W**				
Average Roughness	Sa		**V**			

W   = Whole data

P   = Plateau data

V   = Valley data

10.2. Contributions to Knowledge

➤ The company had very limited knowledge of the effects of processing and process variations on the stainless steel topography. They now have an in depth understanding of these effects and maybe able to better control any detrimental outcomes in addition to being able to give their customers an expanded specification.

➤ The protocol gives a uniform method to measure important surface features instilling confidence in the results.

➤ The relatively new 3D surface topography parameters have proven useful in linking topography data to functional aspects and a novel data separation technique has been developed and proven to give enhanced analysis capabilities for the 2B finish on stainless steel sheet.

10.3. Suggestions for Further Work

- Extension/confirmation of the protocol for new instruments, methods and different surface topographies.
- Further work on different types of surfaces and materials in respect of functionality.
- More comprehensive work on lubricant retention properties using improved equipment such as a bending under tension or draw bead simulation rig.
- Development of a standard tool pack for surface measurement and analysis (industry specific).
- Further investigation of enhanced data analysis (data separation) for characterisation of functional surfaces.

References

[1] Whitehouse D.J., Bowen D.K., Venkatesh V.C., Leonardo P., & Brown C.A., 'Gloss and Surface Topography', Annals of the CIRP, vol. 2, 1-9, 1994

[2] Duieu D., Private Communication, 2003

[3] BSEN 10088-2:1995, 'Technical delivery conditions for sheet/plate and strip for general purposes', 1995

[4] Freeman P. F., Hargate N., Barrett R. L., 'Finger Print Resistant Stainless Steel', 4th European Stainless Steel Science and Market Congress, Paris, 2002

[5] Crookes R., 'Materials and Applications Series, Volume 4 - Pickling and Passivating Stainless Steel', Published online at http://www.worldstainless.org/articles/ss_passivate.pdf, 2004

[6] Stout K.J. & Davis E.J., 'Surface topography of cylinder bores – the relationship between manufacture, characterisation and function', Wear, 95, pp. 111-125, 1984

[7] Pawlus P. and Chetwynd D.G., 'Efficient Characterisation of Surface Topography in Cylinder Bores', Precision Engineering, Vol. 19, pp. 164-174, 1996

[8] Whitehouse D.J., 'Handbook of Surface Metrology', Institute of Physics Publishing, 1994

[9] Sullivan P.J., Poroshin V. & Hooke C.J., 'An Application of a Three Dimensional Surface Analysis System to the Prediction of Asperity Interaction in Metallic Contacts', 5th International Conference on the Metrology and Properties of Engineering Surfaces, 1991

[10] Vermeulen M., De Boeck A., Claessens S., Antonissen J., Scheers J., 'Sheet Metal Processing, Texturing and Coating Methods in view of Application Manufacturing Steps', Proceedings of the 9th International Conference on Sheet Metal, Belgium, pp 3-26, 2001.

[11] Faraq M.M., 'Materials Selection for Engineering', Prentice Hall. 1997

[12] Smith K.B., 'A Sharper Look at Gloss', Surface Coatings International, Journal of the Oil and Colour Chemits' Association, Vol. 80, pp. 573-576, December 1997

[13] Adelson E. H., 'Lightness perception and lightness illusions', The Cognitive Neurosciences, pages 339–351, 1999

[14] Hunter R.S. & Harold R.W., 'The measurement of appearance', 2nd edition, John Wiley & Sons, 1987

[15] Ingersoll L.R., 'A means to measure the glare of paper', Electronics World, Vol. 60, pp. 645-647, 1914

[16] Thomas T.R.,'Rough Surfaces', Longman Press, London, 1982

[17] F Sacerdotti, B J Griffiths, C Butler, F Benati, 'Surface topography in autobody manufacture—the state of the art', Proceedings of the Institution of Mechanical Engineers, Part B: Journal of Engineering Manufacture, Vol. 214, No. 9, pp. 811 – 820, 2000

[18] Steinhoff K., Rasp W., Pawelski O., 'Development of deterministic–stochastic surface structures to improve the tribological conditions of sheet forming processes', Journal of Material Process Technology, Vol. 60, No. 1-4, pp 355–61, 1996

[19] Jonasson M., Wihlborg A., Gunnarsson L., 'Analysis of surface topography changes in steel sheet strips during bending under tension friction test', Int. J. Mach. tools Manufact., Vol. 38, No. 5-6, pp. 459-467, 1998

[20] Wihlborg A., Crafoord R., 'Frictional study of uncoated steel sheets', Proceedings of International Conference on Technology of Plasticity, 1999

[21] Meiler M., Pfestorf M., Geiger M., Merklein M., 'The use of dry film lubricants in aluminum sheet metal forming', Wear, Vol. 255, pp. 1455–1462, 2003

[22] Blunt L., 'The Development of a Basis for 3D Surface Roughness Standards – Surfstand Final Report', not published, Commission of the European Communities Project Number 3374/1/0/170/90/2, 2001

[23] Vermeulen M., De Boeck A., Claessens S., Antonissen J., Scheers J., 'Sheet Metal Processing, Texturing and Coating Methods in view of Application Manufacturing Steps', Proceedings of the 9th International Conference on Sheet Metal, Belgium, pp 3-26, 2001

[24] Jonasson M., Wihlborg A., Gunnarsson L., 'Analysis of surface topography changes in steel sheet strips during bending under tension friction test', Int. J. Mach. tools Manufact., Vol. 38, No. 5-6, pp. 459-467, 1998

[25] Leslie W.C., 'The physical metallurgy of steels', Hemisphere Publishing Corporation, 1981

[26] Trethewey K.R. & Chamberlain J., 'Corrosion for science and engineering', 2nd edition, Longman Scientific and Technical, 1995.

[27] Freeman P., Private communication, 2002

[28] Moayed M.H., Laycock N.J., Newman R.C., 'Dependence of the Critical Pitting Temperature on surface roughness', Corrosion Science, Vol. 45 , pp. 1203–1216, 2003

[29] Schmaltz G., 'Technische Oberflächenkunde', Springer-Verlag, Berlin, 1936

[30] Abbott E., Bousky S. and Williamson D.E., 'The Profilometer', Mechanical Engineering, Vol.60, pp. 205-216, 1938

[31] Reason R.E., Hopkins M.R. and Garrod R.I., 'Report on the Measurement of Surface Finish by Stylus Methods‚', Taylor-Hobson, Leicester, 1944

[32] Williamson J.B.P., 'Microtopography of Surfaces‚', Proceedings of the Institution of Mechanical Engineers, Vol. 182, Part 3K, pp. 21-30, 1967-8

[33] Peklenik J. and Kubo M.,'A Basic Study of a Three Dimensional Assessment of the Surface Generated in a Manufacturing Process', Annals of the CIRP, Vol. 16, pp. 257-265, 1967-8

[34] Sayles R.S. and Thomas T.R.,'Mapping a Small Area of a Surface', Journal of Physics E: Scientific Instruments, Vol. 9, pp. 855-861, 1976

[35] Stout K.J., 'Three Dimensional Surface Topography; Measurement, Interpretation and Applications', Penton Press, 1994, ISBN 1-85718-004-6

[36] Mummery L., 'Surface Texture Analysis – The Handbook', Hommelwerke GmbH, 1992

[37] Peklenik J. and Kubo M.,'A Basic Study of a Three Dimensional Assessment of the Surface Generated in a Manufacturing Process', Annals of the CIRP, Vol. 16, pp. 257-265, 1967-8

[38] Dagnall H., 'Exploring surface texture (2nd edition)', Rank Taylor Hobson Limited, 1986

[39] Thomas, T.R., Rough Surfaces, 2nd ed., Imperial College Press, London (1999).

[40] Lippold S. and Podlesny J., 'WYKO Surface Profilers - Technical Reference Manual', © Wyko Corporation, May 1996

[41] Stout K.J., Sullivan P.J., Dong W.P., Mainsah E., Luo N., Mathia T., Zahouani H., 'The Development of Methods for the Characterisation of Roughness in Three Dimensions', published on behalf of the Commission of the European Communities, Number 3374/1/0/170/90/2, ISBN 0 7044 1313 2, 1993.

[42] Baselt D., 'The Tip-Sample Interaction in Atomic Force Microscopy and its Implications for Biological Applications', Ph.D. thesis for California Institute of Technology, published on http://stm2.nrl.navy.mil/how-afm/how-afm.html, Copyright © David Baselt, 1993

[43] ThermoMicroscopes, 'A Practical Guide to Scanning Probe Microscopy ', for Park Scientific Instruments and TopoMetrix (Thermo Electron), published on http://www.thermomicro.com/, 1997

[44] DME, 'DME-DualScope / RasterScope 5000 General Installation Manual', Version 1.1 © DME (Danish Micro Engineering), 1998

[45] Binnig G., Quate C.F. and Gerber C., 'Atomic Force Microscope', Physical review letters, Vol. 56, No. 9, pp. 930-933, 1986

[46] Iowa State University Materials Science and Engineering Department, SEM images published on http://mse.iastate.edu/microscopy/path.html, accessed 2004

[47] Goldstein J.I., 'Scanning Electron Microscopy and X-ray Microanalysis', 3rd edition, Kluewer Press, 2003

[48] Steadman M., 'Basis for Comparing the Performance of Surface-Measuring Instruments', Precision Engineering, Vol. 9 (3), pp.149-152, 1987

[49] Thomas T.R., Private communication, 1999

[50] Bendat J.S. and Piersol A.G., 'Random Data: Analysis and Measurment Procedures', Wiley-Interscience, 1971, ISBN 0-471-06470-X

[51] Kubo M. and Peklenik J., 'An Analysis of Micro-geometrical Isotropy for Random Surface Structures', Annals of the CIRP, Vol. 16, pp. 235-242, 1968

[52] Lin T.Y., Blunt L. and Stout K.J., 'Determination of Proper Frequency Banwidth for 3D Topography Measurement using Spectral Analysis. Part 1: Isotropic Surfaces', Wear, Vol. 166, pp. 221-232, 1993

[53] Tsukada T. and Sasajima K., 'An Optimum Sampling Interval for Digitising Surface Asperity Profiles', 2nd International Conference on the Metrology and Properties of Engineering Surfaces, 1982

[54] Tsukada T. and Kanada T., 'Evaluation of Two and Three Dimensional Surface Roughness Profile and their Confidence', Wear, Vol. 109 (1-4), pp. 69-78, 1986

[55] Pawlus P. and Chetwynd D.G., 'Efficient Characterisation of Surface Topography in Cylinder Bores', Precision Engineering, Vol. 19, pp. 164-174, 1996

[56] Pfestorf M., Engel U., Geiger M., '3D-Surface parameters and their application on deterministic textured metal sheets', Proc. 7th Int. Conf. on Metrology and Properties of Engineering Surfaces, 1997

[57] Anamalay R.V., Kirk T.B., Panzera D., ‚Numerical descriptors for the analysis of wear surfaces using scanning confocal microscopy', Wear, Vol. 181-183, pp.771-776, 1995

[58] Sullivan P., Poroshin V., Hooke C., 'Application of a three-dimensional surface analysis system to the prediction of asperity interaction in metallic contacts', International Journal of Machne Tools and Manufacture, Vol. 32, No. ½, pp. 157-169, 1992

[59] Dobbin E., 'Quantitative Characterisation of 2B Surface Finishes on Stainless Steels using 3D Surface Topography Analysis', not published, 1998.

[60] Whitehouse D.J., 'Parameter Rash – Is there a Cure?', Wear 83 (pp. 75-78), 1982.

[61] Brooker K., 'Manual of British Standards in Engineering Metrology', British Standards Institution, London, 1984

[62] Blunt L. A., Jiang X., 'Advanced techniques for assessment surface topography: development of a basis for 3D surface texture standards "surfstand"', Kogan Page Science, 2003

[63] Von Weingraber H., 'Suitability of the Envelope Line as a Reference Standard for Measuring Roughness', Microtecnic, Vol. 11, pp.6-17, 1957

[64] DIN 4776, 'Measurement of Surface Roughness; Parameters Rk, Rpk, Rvk, Mr1, Mr2 for the Description of the Material Portion in the Roughness', German Standard Din 4776, 1990

[65] Blunt L., 'The Development of a Basis for 3D Surface Roughness Standards – Surfstand 2nd Year Progress Report', not published, Commission of the European Communities Project Number 3374/1/0/170/90/2, 2000

[66] Blunt L., Jiang X. and Stout K.J.,'Developments in 3D Surface Metrology', Proc. Int. Conf. Lambdamap, Southampton, July 1999

[67] Lin T.Y., Blunt L. and Stout K.J., 'Determination of Proper Frequency Banwidth for 3D Topography Measurement using Spectral Analysis. Part 1: Isotropic Surfaces', Wear, Vol. 166, pp. 221-232, 1993

[68] Lin T.Y., 'Characterisation, Sampling and Measurement Variation of Surface Topography: A Viewpoint from Standardisation', Ph.D. thesis for School of Manufacturing and Mechanical Engineering, University of Birmingham, U.K., not published, 1993

[69] Wihlborg A.H., 'The Influence of Steel Sheet Surface Topography on Friction in Stamping', Ph.D. thesis for Department of Production Engineering, Chalmers University, Sweden, published © Anders H. Wihlborg, 2000, ISBN 91-7197-885-2

[70] DIN, 'Measurement of Surface Roughness; Parameters Rk, Rpk, Rvk, Mr1, Mr2 for the Description of the Material Portion in the Roughness', German Standard Din 4776, 1990

[71] Scott P.J., 'The Mathematics of Motif Combination and their use for Functional Simulation', International Journal of Machine tools and Manufacture, Vol. 32 (1/2), pp. 203-209, 1992

[72] Bodenschwinna S.U., Mikro-Emo H. and Mikro-Emo S.U., 'Funktionsgerechte Rauhheitskennwerte Durch Auswerten der Abbott-Kurve', Teil 1-4. Z. Antriebstechnik, Vol. 26, 1987

[73] Fahl C.F., 'Motif Combination – A New Approach to Surface Profile Analysis', Wear, Vol. 83, pp. 165-179, 1982

[75] ASTM E112-96e1, 'Standard Test Methods for Determining Average Grain Size', American Society for Testing and Materials, 2000

[76] BS 1134-2:1990, 'Assessment of Surface Texture', 1990

[77] Waterworth A. and Blunt L., 'The Effects of a Variation in Modulation Threshold on Surface Measurements of 2B Stainless Steel', Proceedings 8th International Conference on Metrology and Properties of Engineering Surfaces, 2000

[78] BS EN 13565-3:2000, 'Geometrical product specifications (GPS) – Surface texture: Profile method; surfaces having stratified functional properties – Part 3: Height characterisation using the material probability curve', 2000

[79] Cao L., Vorburger T.V., Lieberman G., Lettieri T.R., 'Light-scattering measurement of the rms slopes of rough surfaces', International Journal for Applied Optics, Vol.30, pp. 3221-3227, 1991

[80] Wihlborg A., Gunnarsson L., Crafoord R., 'A factorial design study of coated steel sheets in a bending-under-tension test', Proceedings of the 5th International Tribology Conference, pp537-542, 1998

[81] Chanada Watanatham, Private Communication, 2003

[82] Michigan Metrology, 'Glossary of Surface Texture Parameters', www.michiganmetrology.com.

Appendix 1

"The Effects of a Variation in Modulation Threshold on Surface Measurements of 2B Stainless Steel"

By A. Waterworth and L. Blunt

Published in the Proceedings of the 8th International Conference on Metrology and Properties of Engineering Surfaces

2000

Quantitative Characterisation of Surface Finishes on Stainless Steel Sheet using 3D Surface Topography Analysis

A. Waterworth[*], L. Blunt, X. Jiang

Centre for Precision Technologies, University of Huddersfield, UK

Abstract

Since the growth and improvement of digital computers there have been significant changes in the way that surfaces can be measured and viewed. The 'parameter rash' that occurred in two-dimensional measurements [1] is being avoided by standardising 3 dimensional parameters before the techniques have wide spread use. Huddersfield University is heading much of this standardisation work, with the support of the Commission of the European Communities [2].

As the usage of stainless steel increases quantitative surface characterisation of the products assumes greater importance. There is a demand for an expanded range of surface finishes for aesthetic reasons and also for a deeper understanding of tribological factors in sheet metal forming and processing. To enhance further the degree of control over end product performance which can be exerted during strip processing, it would be advantageous to have a means of specifying and checking the surface properties by selecting parameters that are relevant to the end functions.

When the surface characteristics are determined, by means of parametric descriptors, the functional performance of the surface should be related to them. A measurement strategy for the correct acquisition of data and an optimised sampling methodology is presented. Then the use of the primary three dimensional parameter set [2] for characterising surface features on cold rolled stainless steel sheet is investigated.

Keywords: Three dimensional measurement, surface characterisation, stainless steel sheet

1 Introduction

The use of 3D techniques for measuring surface topographies is becoming more popular, as the equipment and methods improve and the advantages are realised. The correct use of these techniques can yield a better understanding of the processes by which surfaces are formed and the ability to control the development of the finish to give the desired functional performance.

For this project the aspects of sampling are studied and consideration is given to the use of the data collected to aid functional characterisation.

An established stainless steel designation, the finish produced by the 2B process route, has been chosen to demonstrate the primary parameter set [2]. The designation 2B is described in BSEN 10088-2:1995 [3] as a surface produced by the process of cold rolling, annealing, removing the scale formed on annealing and skin passing. Scale removal methods, mechanical and chemical, cause microscale attack of both the grains on the surface of the strip and at the grain boundaries. The final strip surface roughness depends upon the prior strip history and the nature and extent of the surface attack on descaling. To smooth and brighten the surface, as well as improve strip shape, a light cold rolling pass is applied to the annealed strip as part of the process route. This pass has the effect of flattening the grain regions (or plateaus), but leaves them surrounded by a network of valleys formed partly by the etched grain boundaries, see figure 1. These features have functional significance. Stainless steel sheet is usually formed using a combination of drawing, bending and stretching processes. It is also employed as the most frequent starting point for a range of other surfaces either developed within the process route, i.e. roll patterning or coil polishing, or during and after fabrication as a result of shot and bead blasting, directional or non-directional mechanical polishing or electrochemical polishing.

Figure 1: Optical interferometer images showing grain boundaries in 2B stainless steel
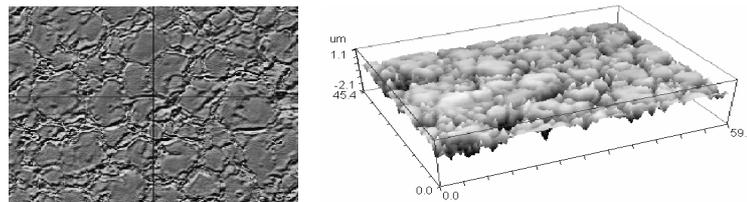
Initially a set of parametric descriptors is required to measure the surface features and relate them to the section of the manufacturing route where they were created. This can be used to reduce or control the variations in the topography of the common finishes. The solution lies in measuring the surface in the correct manner to gain information about the features of the surface that are relevant and describing those features mathematically and statistically using parameters that can be related to the functions.

The bulk of the work in this study is concentrated on the sampling conditions for measurement, specifically the evaluation of the sampling interval. This will be employed to legitimately acquire data with the appropriate instrument. The relevance of the primary set of 3D parameters is examined and their application in characterising the 2B finish is discussed. Conclusions will be drawn relating to both the sampling interval found, the methods of determining it and the extent to which the existing 3D parameters characterise the surface.

2   Sampling Methodology

When measuring a surface using a modern instrument a signal representing the surface roughness is converted from an analogue to a digital signal. This signal must be sampled and quantised. Digital sampling is normally performed at equal intervals of time on a signal and it is this interval that is the important variable. If the interval is unnecessarily small, redundant data will be collected and the correlation of points would

yield misleading results. If the interval is too large a phenomenon called aliasing will occur, where the high and low frequency components of the signal (the surface roughness) become confused.

There are a number of methods to decide on the correct sampling interval required for a particular surface topography, measuring instrument or functional interest, but initially the important features of the surface must be identified. Obviously, it is desirable to measure the largest area possible, to get as many of the variations possible. By increasing the area resolution is sacrificed, so there is a trade off from being able to measure at a high enough resolution to observe the critical features and having a large enough sample area to include all the critical points. The frequency of the features is needed to ensure that the demands of the Nyquist theorem [4] are met. It states that for a periodic signal, the sampling interval should be smaller than half of the wavelength of the signal. If this theorem is not satisfied then aliasing will occur. The result is the normal value of the short wavelength limit for the sampling interval, but this is for periodic signals, which surface topography data is not.

2.1   SEM Analysis

To decide on the critical sampling interval work has been done to establish and measure the major features of the 2B finish. By viewing a range of 2B product surfaces using a scanning electron microscope the features of the surface were recognised as plateau regions and a network of interconnecting valleys. These images reveal that the plateaus and valleys are of various sizes and the plateau regions are not totally smooth but have surface roughness in the form of small pits and shallow 'troughs' (relative to the deeper valleys). These small features must be resolvable using the chosen sampling interval so the average and minimum dimensions of both the plateaus and valleys are needed.

A scanning electron microscope (SEM) was employed to depict the areal geometry of the surface features and images as in figure 2 were collected from different samples, in several areas and at varying degrees of magnification. The images were manually examined and analysis (based on intercept methods in ASTM E112 [5]) used to collect the data in table 1.

Table 1: Data collected from SEM study

	Average	Maximum	Minimum
Plateau Diameter (μm)	9.1	12.3	4.5
Valley Width (nm)	700	1000	400
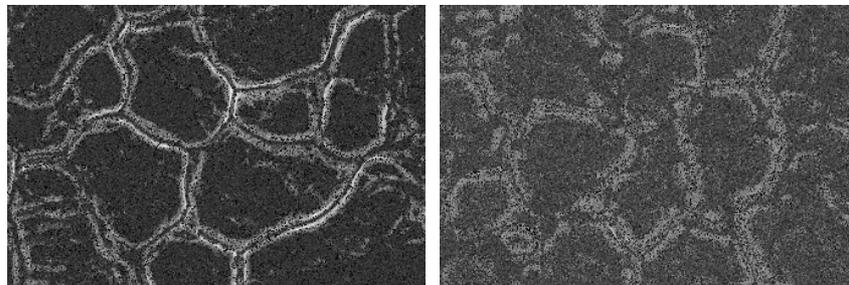
Figure 2: SEM images showing plateaus and valleys on 2B at x5k & x10k magnifications

The initial estimate of required sampling interval for 2B finish was calculated, based on the Nyquist theorem, mentioned previously. The smallest feature on the surface is

the minimum valley width, 400nm, so the initial estimate of sampling interval is half this, 200nm.

2.2 Frequency Spectrum Analysis

Frequency Spectrum analysis (using Fast Fourier Transforms, FFT's) has been used to determine the frequencies of the surface features. The frequency of the valleys of a 2B surface show up dominantly on a Power Spectral Density (PSD) plot and this can be used to find the correct sampling interval to accurately reconstruct the 3D surface data. Firstly surface data files from a non-contacting optical interferometer (Wyko NT 2000) were studied. The surfaces were measured with a lateral sampling interval of 160nm. From these 3D maps (see example map in figure 1) the PSD plot is found for numerous 2D profiles, using a real time FFT, see right-hand graph of figure 3. It can be seen that the important frequencies lie below about 1500mm^{-1}. This equates to a required sampling interval of approximately 330nm. The actual reconstructed surface at this interval can be viewed by entering the high frequency cut-off at this level and running an inverse FFT. The reconstructed surface on the left profile image in figure 3 is so closely matched to the actual measured surface; the difference is only noticeable on the outlying data. The estimation of sampling interval from the SEM study (200nm) relates to a frequency of 2500mm^{-1} and the Wyko minimum interval of 160nm relates to a frequency of 3125mm^{-1}. The reconstructed surfaces at these intervals reveal a very high correlation with the original measured surface.
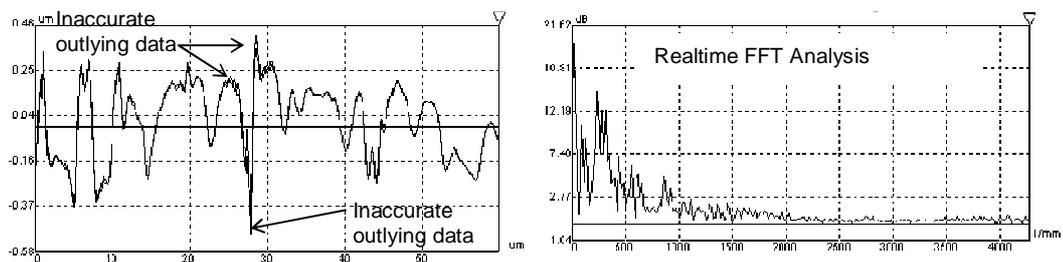
Figure 3: *Profile of surface with reconstruction at high frequency cut-off of 1500mm^{-1} and PSD plot for surface frequencies*

The significant frequencies were checked using higher resolution surface maps measured on an Atomic Force Microscope, AFM. The lateral sampling interval for the AFM measurements was approximately 40nm. In this case the important frequencies lie below 2000mm^{-1} (an interval of 250nm) and the initial estimate of a suitable frequency of 1500mm^{-1} is too low to accurately reconstruct the detailed valley bottom and fine plateau roughness data, figure 4.

High frequency cut-off = 1500 mm^{-1} High frequency cut-off = 2000 mm^{-1}

— Reconstructed surface
— Measured surface
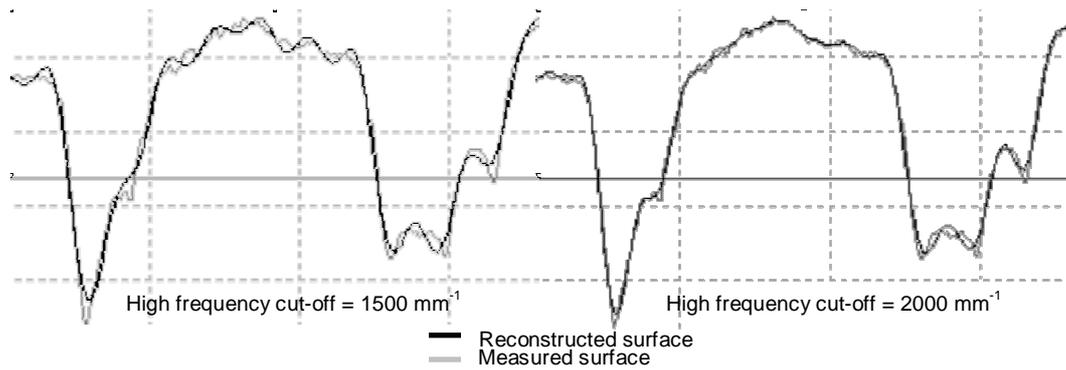
Figure 4: *Comparison of high cut-offs and their effect on accuracy of profile reconstruction*

2.3 Comparison

The results of the practical and mathematical analyses on the determination of sampling interval are very similar. From the SEM investigations a 200nm interval is suggested. Using the frequency spectrum analysis, a frequency of 2000mm^{-1} is recommended, equating to an interval of 250nm. The Wyko interferometer at 100 times magnification has a sampling interval of 160nm, indicating its suitability for measuring the 2B surface.

3 Functional Requirements

3.1 Functional Relevance

The requirements of characterisation are numerous and dependant on the functional specifications for the surface in post-processing. A surface can be either functional or non-functional. Functional surfaces are those where the properties of the surface influence the quality of the component. A control loop was suggested by Stout & Davis [6], figure 5, showing the interdependence between the required functional behaviour of the surface, its manufacture and the characterisation of its topography.
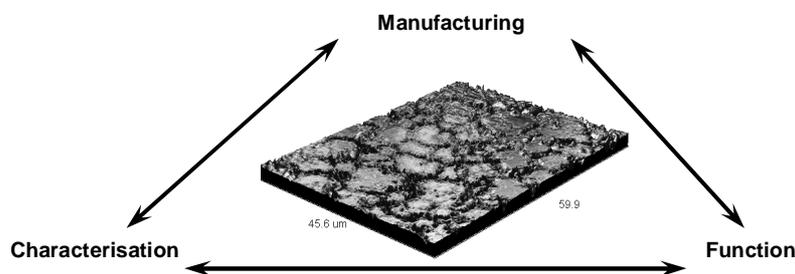
Figure 5: *Simplified control loop showing interdependencies [original from 7]*

If the function requires the surface to react in a certain manner the surface characteristics can be specified and a suitable manufacturing process chosen. This theory also works in the reverse direction; if a surface is manufactured with particular properties then the behaviour of the material under further processing can be predicted

and controlled. The quality of functional surfaces can be optimised by understanding the relationship between the surface features and component application.

Appearance can be thought of in many different ways and so parameters need to incorporate considerations for reflectivity, image clarity, degree of greyness or brightness and even hue. Optical properties like these are considered on a nano-scale, Thomas has stated, [8], 'When surface irregularities are present at wavelengths comparable with those of visible light the appearance of the surface will alter, e.g. a painted surface such as a car body may appear dull instead of glossy (amplitude 0 – 10 nm)'. Conceivably the features that affect optical properties are plateau roughness and the area fraction of plateaus to valleys. These dictate such aspects as the reflectivity and brightness of the surface.

For tribological concerns like how much lubricant the surface can retain or the extent of tool friction in forming operations different features are important. Lubricant retention is related to the valley characteristics like depth, slope, void volume and interconnectability. In some instances, like on plateau honed surfaces for cylinder bores, it is important that the surface possesses a certain amount of interconnectability (so that oil can be distributed around the whole of the surface) and have a specific lubricant reservoir volume (these parameters are currently under investigation for the second year EC project, number 3374/1/0/170/90/2, [9]). The size, density and slopes of asperities on the surface can also affect tool friction and the final appearance of a formed component.

Cleansibility characteristics and adhesive bonding factors are a combination of plateau and valley features. They could be related to the areas occupied by plateaus and valleys, the slope of asperities and valley sides and the plateau micro-roughness.

Pitting phenomena and localised corrosion behaviour with respect to variations in surface topography is currently under investigation. Particular interest lies in the shape and relative depth of existing pits on plateaus or in valleys and whether certain topographies promote the initiation of pitting corrosion or crack initiation. It is thought that a combination of valley depth and aspect ratio (crevice acuity) parameters will be required for functional use.

3.2   What can 3D do now?

Some of the standard 2D parameters have been developed for use with 3D topography data. A comprehensive survey of academic and industrial research trends on this subject was carried out in 1992. This resulted in the modification of a draft proposal for 3D parameters [2], for which a primary set of 14 parameters was proposed. An 'S' (for surface) instead of the conventional 'R' (for roughness in their 2D counterparts) denotes all of these new parameters. The most thorough description of the primary set can be found in [2], a brief summary table is presented below (table 2).

Table 2: Standardised 3-D parameter set, [2]

Family	Nomenclature	Parameter
Amplitude	S_q	Root-mean-square deviation of the surface
	S_z	Ten point height of the surface
	S_{sk}	Skewness of topography height distribution
	S_{ku}	Kurtosis of topography height distribution
Spatial	S_{ds}	Density of the summits of the surface
	S_{tr}	Texture aspect ratio of the surface
	S_{al}	The fastest decay autocorrelation length
	S_{td}	Texture direction of the surface
Hybrid	$S_{\Delta q}$	Root-mean-square slope of the surface
	S_{sc}	Arithmetic mean summit curvature of the surface
	S_{dr}	Developed interfacial area ratio
Functional Index	S_{bi}	Surface bearing Index
	S_{ci}	Core fluid retention
	S_{vi}	Valley fluid retention

Of this set of 14 parameters, the amplitude family should have consistent values for repeated measurements of the 2B surface provided that the sampling interval and area sizes are the same. S_z is an extreme parameter, the average height of the five highest peaks and five deepest valleys or pits. Since the surface topography contains few large peaks it is the depth of the valleys that will have a major influence on variations in this parameter.

The value of S_{sk} for a 2B finish is large and negative, as it has outliers (the valleys) and good bearing properties, because of the relatively flat plateau regions. The value of S_{ku} is very large, which is also due to the outliers. These two parameters should be used in conjunction with each other to identify surfaces that have relatively flat tops and deep valleys, like 2B, from other surface topographies with similar values for the other parameters.

The spatial and hybrid families are not particularly useful for functionally characterising the 2B surface, as it has no particular texture or lay. The functional indexes are good for the comparison of similar surfaces, but not as useful when only one surface is under examination.

Absolute values for volumes are calculated using the functional volume family of parameters. These three extra parameters, in table 3, were suggested in the initial study [2] and have since been formalised. The second EC report [9] deemed them useful for distinguishing between the functional zones of two bearing surfaces.

Table 3: Additional functional volume family of parameters

Family	Nomenclature	Parameter
Functional Volume	S_m	Material volume of the surface
	S_c	Core void volume of the surface
	S_v	Valley void volume of the surface

The existing parameters do cover a range of the roughness aspects that are required for characterisation but it has been decided that further, more specific parameters are needed for a full, functional characterisation of the surface finish of stainless steel.

3.3 Future

Further to the relevant parameters in the primary set and to make the set explicit, it is necessary to develop some new parameters to give functional significance. The first investigation into this matter was carried out by Dobbin, [10], who, because of the topography of the 2B finish, decided that meaningful parameters would be found by truncating the data to separate the plateau regions from the valleys. The chosen

truncation level was at S_q from the mean plane. A set of six parameters was devised for analysing the data, summarised in table 4.

Table 4: Summary of 'Truncated parameters'

'Zone'	Nomenclature	Parameter	Description	Functionality
Plateau	'S_q'	Average roughness	Calculated as Sq but on the top section of the truncated data	Appearance, friction and wear, adhesion, etc.
Valley	'S_t'	Maximum valley depth	Maximum vertical distance, from the truncation level	Brightness, lubrication & dirt retention
	'S_{vm}'	Average maximum valley depth	The average of successive values of the maximum valley depths over a sampling length	As above & sealing, adhesion
	'S_q'	Average valley depth	Calculated as Sq but on the lower section of the truncated data	As above
	Not given	Area fraction ratio	Ration of the total contacting area over the sampling area	Appearance, bearing properties, forming, etc.
	Not given	Volume of voids	The air volume enclosed between the truncation plane and the material beneath that plane	Lubricant retention, wetting/cleansibility
Other Plateau params.		Heights of asperities	Calculated as Sz but on the top section of the truncated data	Appearance, tool friction/wear, bearing area, forming, sealing
		Density of asperities	Calculated as Sds but on the top section of the truncated data	As above
		Size and distribution of plateau regions	Using edge detection on truncated data	As above & adhesion/surface wetting
		Isolated pits	Number/size etc of isolated pits on plateaus	Appearance, tribology, especially local corrosion/pitting
Other Valley params.		Interconnectability	Using 'motif' combination	Lubricant retention, forming, wetting
		Aspect ratio	Depth to width of valley	As above & crack initiation/local corrosion

These parameters would certainly be functionally relevant to the 2B surface but the study carried out by Dobbin was inconclusive due to a deficiency in the sampling used. Research into a more functional choice of truncation level is in progress and the application of these parameters and other 'truncated' parameters (see table 4) are under investigation.

4. Conclusions

- Certain parameters from the primary set could be used to describe some of the sheets' characteristics. It is thought that the truncated parameters outlined in tables 4 and 5 provide a functionally relevant set for characterisation of the 2B surface.
- The characterisation by statistical methods is useful as long as the sampling conditions are properly defined. In this case, for the 2B finish the recommended sampling interval is 200nm. An interval of 160nm is appropriate and is achieved using the Wyko NT 2000 interferometer with a magnification of x100.
- Both the practical and mathematical methods of determining the correct sampling interval gave similar results for the 2B surface finish. This may not be the case for all surface topographies, so it is suggested that for functional applications a combination of approaches like the ones presented here be employed.

5.   References

[1]   D.J. Whitehouse, *Parameter Rash – Is there a Cure?*, Wear 83, 1982, pp. 75-78

[2]   K.J. Stout, P.J. Sullivan, W.P. Dong, E. Mainsah, N. Luo, T. Mathia, H. Zahouani, *The Development of Methods for the Characterisation of Roughness in Three Dimensions*, published on behalf of the Commission of the European Communities, 1993, Number 3374/1/0/170/90/2, ISBN 0 7044 1313 2

[3]   BSEN 10088-2:1995, *Stainless Steels. Technical Delivery Conditions for Sheet/Plate and Strip for General Purposes,* 15 November 1995, ISBN 0 580 24672 8

[4]   J.S. Bendat and A.G. Piersol, *Random Data: Analysis and Measurment Procedures*, Wiley-Interscience, 1971, ISBN 0-471-06470-X

[5]   ASTM E112-96e1, *Standard Test Methods for Determining Average Grain Size*, American Society for Testing and Materials, 2000

[6]   K.J. Stout & E.J. Davis, *Surface Topography of Cylinder Bores – The Relationship between Manufacture, Characterisation and Function*, Wear 95, 1984, pp. 111-125

[7]   D.J.Whitehouse, *Handbook of Surface Metrology*, Institute of Physics Publishing, 1994, ISBN 0-7503-0039-6

[8]   T.R. Thomas, *Rough Surfaces*, Longman Press, London, 1982

[9]   L. Blunt (Editor), *The Development of a Basis for 3D Surface Roughness Standards – Surfstand*, 2nd Year Progress Report, not published, Commission of the European Communities Project Number 3374/1/0/170/90/2, 2000

[10]   E. Dobbin, *Quantitative Characterisation of 2B Surface Finishes on Stainless Steels using 3D Surface Topography Analysis*, not published, 1998

Appendix 2

2D R_a Values

2D R$_a$ values for the 2B finish, provided by D.Dulieu, Outukumpu.

Ra
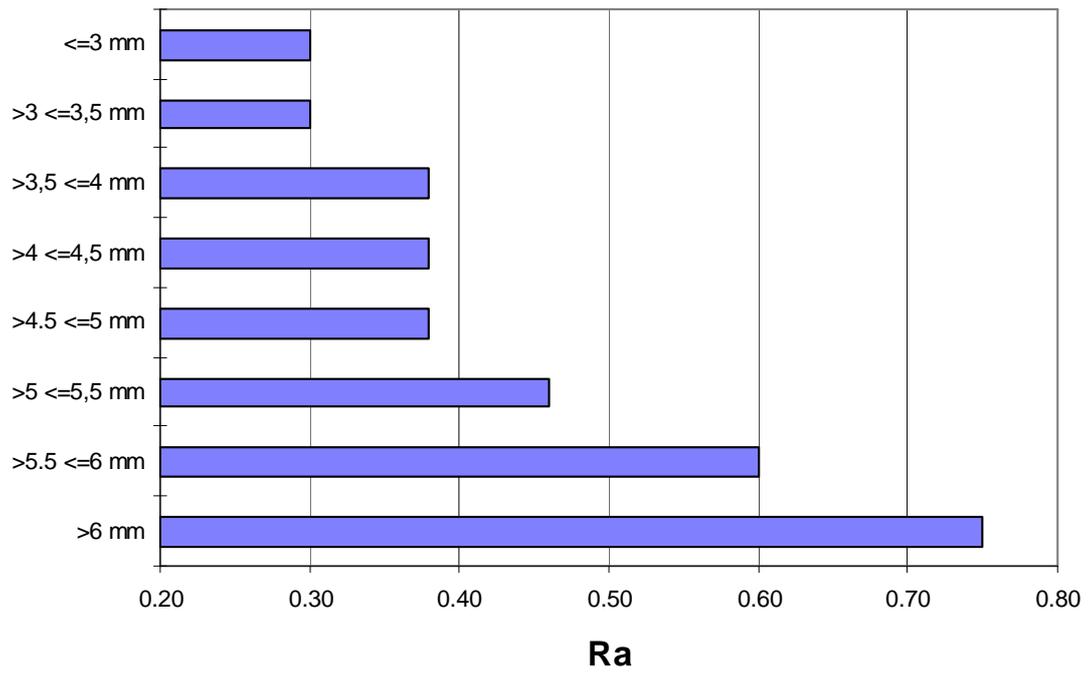
Appendix 3

Distinctness of Image and Haze Graphs

Sq to haze

Sq to DOI

Sq of plateaus to DOI

Vmp of valleys to haze
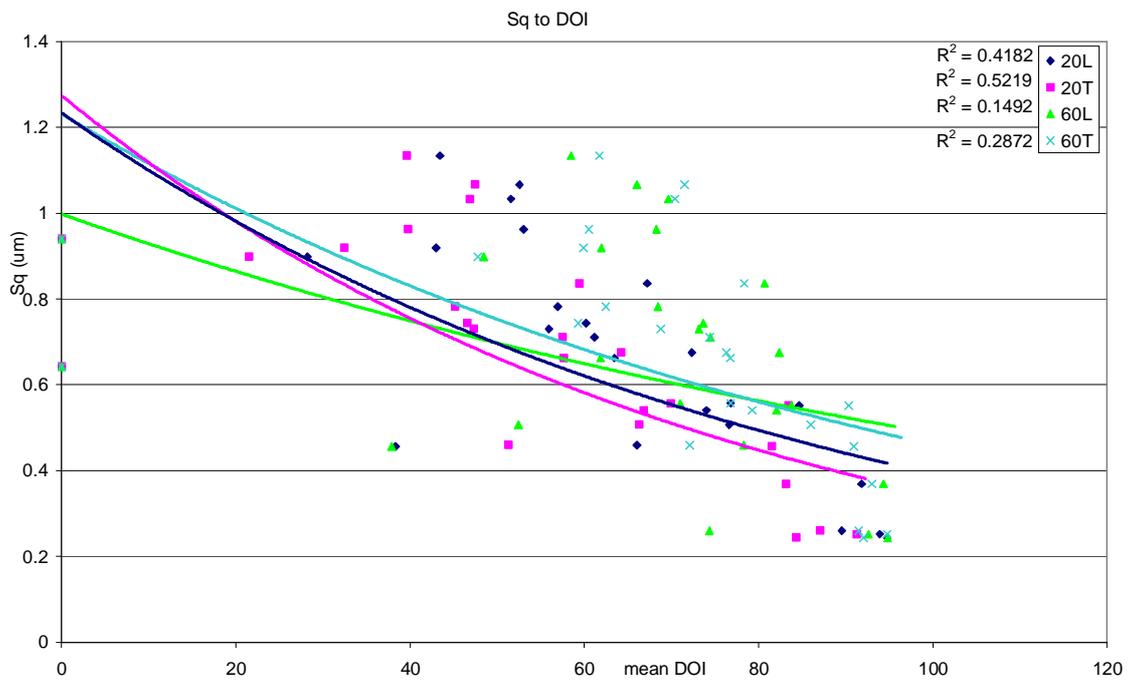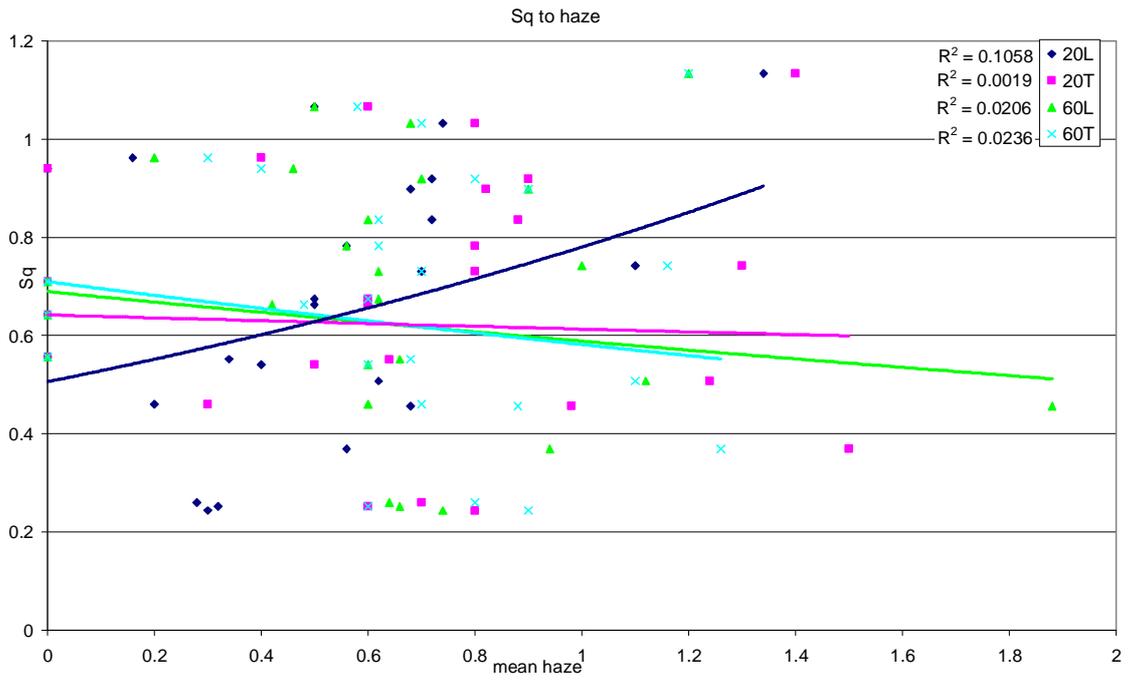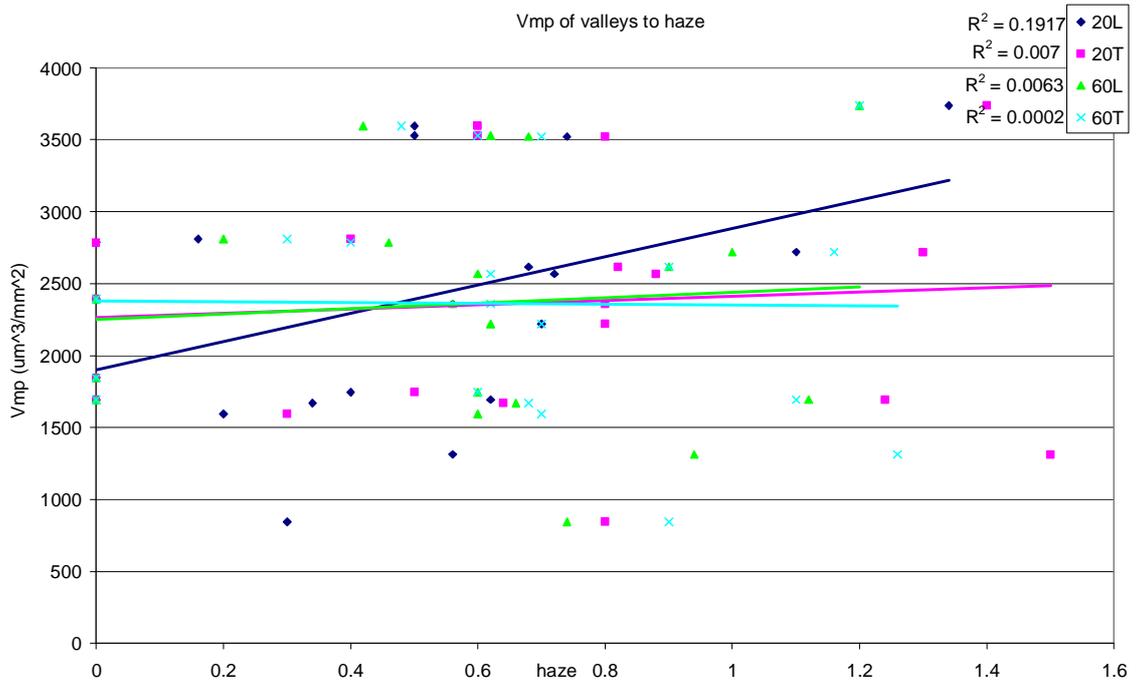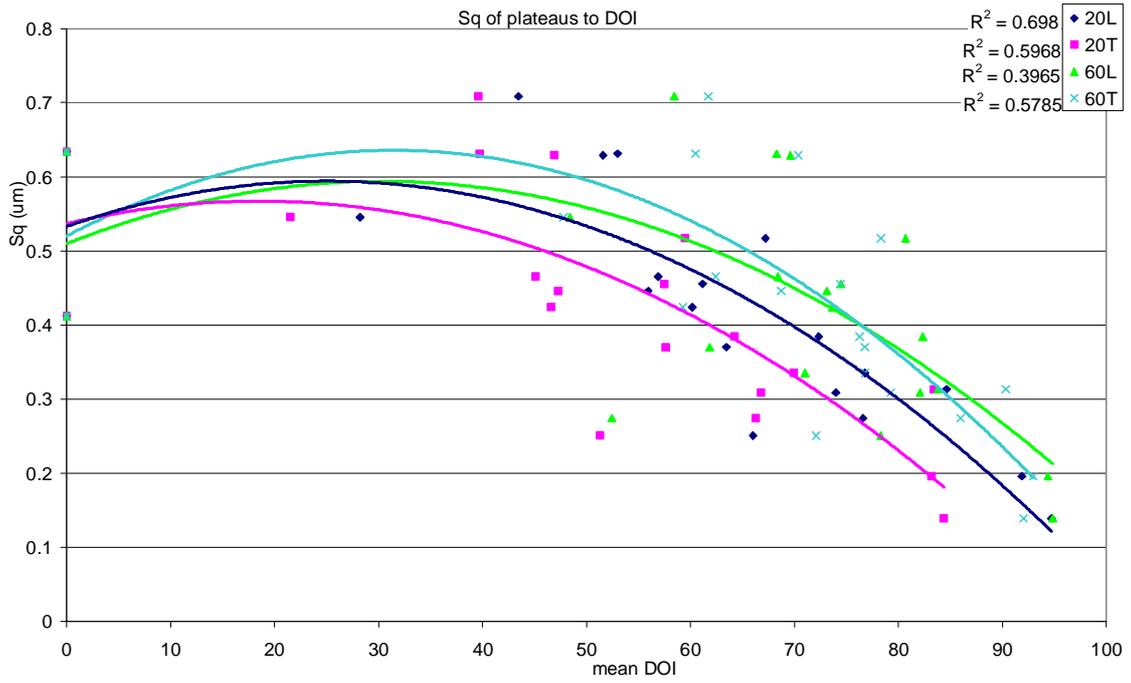
Appendix 4

2D Parameters

Glossary of Surface Texture Parameters by Michigan Metrology [82]

R_a{ XE "Ra" }, the roughness average, is the arithmetic average of the absolute values of the surface height deviations measured from the best fitting plane, cylinder or sphere. R_a is described by:

$$R_a = \iint_a |Z(x, y)| \, dxdy$$
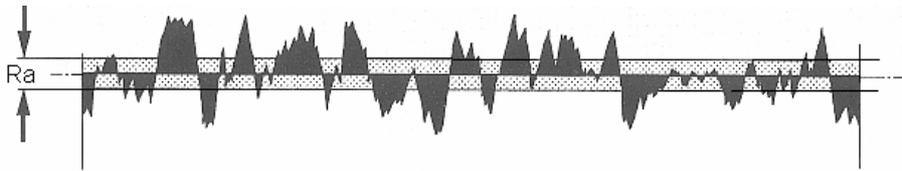
R_q{ XE "Rq" }, the root mean square (rms) roughness is the rms (standard deviation) or "first moment" of the height distribution, as described by:

$$R_q = \sqrt{\iint_a (Z(x, y))^2 \, dxdy}$$
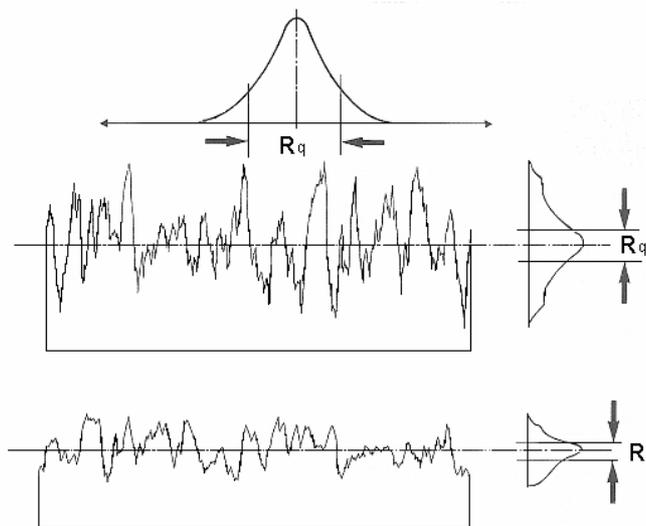
R_{sk}{ XE "Rsk" }, the skewness, is the 'second moment" of the height distribution.

$$R_{sk} = \frac{1}{R_q^3} \iint_a (Z(x, y))^3 \, dxdy$$
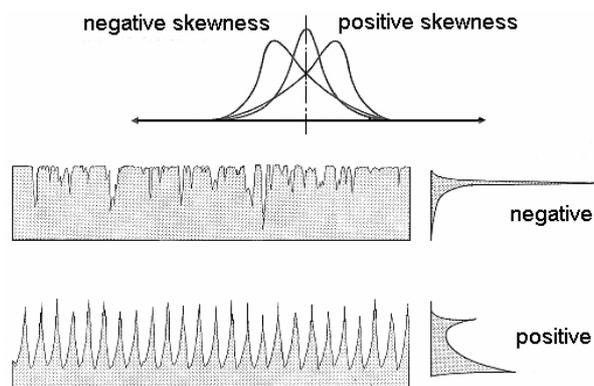
R_{ku}{ XE "Rku" }, the kurtosis, is the "third moment" of the height distribution, described by:

$$R_{ku} = \frac{1}{R_q^4} \iint_a (Z(x, y))^4 \, dxdy$$

R_p, R_v, and R_t are parameters evaluated from the absolute highest and lowest points found on the surface. R_p{ XE "Rp" }, the maximum peak height, is the height of the highest point, R_v{ XE "Rv" }, the maximum valley depth, is the depth of the lowest point and R_t{ XE "Rt" } the maximum height of the surface, is found from $R_p – R_v$.

The parameters R_{pk}, R_k, R_{vk}, M_{r1}, and M_{r2} are all derived from the bearing ratio curve based on the ISO 13565-2:1996 standard. The bearing area curve is a measure of the relative cross-sectional area of a plane, passing through the measured surface, from the highest peak to the lowest valley. R_{pk}{ XE "Rpk" }, the reduced peak height is a measure of the peak height above the nominal/core roughness. R_k{ XE "Rk" }, the core roughness depth is a measure of the nominal or "core" roughness (peak-to-valley) of the surface with the predominant peaks and valleys removed. R_{vk}{ XE "Rvk" }, the reduced valley depth, is a measure of the valley depth below the nominal /core roughness. M_{r1}{ XE "Mr1" }, the peak material portion, indicates the percentage of material that comprises the peak structures associate with R_{pk}. M_{r2}{ XE "Mr2" }, the valley material portion, relates to the percentage of the measurement area that comprises the deeper valley structures given by 100%-M_{r2}.

Appendix 5

3D Parameters

Areal Surface Parameters [41, 82]

AMPLITUDE PARAMETERS

Six parameters are used for characterising the amplitude property of surfaces. They are classified into four categories, i.e. (i) dispersion, (ii) asymmetry of the height distribution, (iii) sharpness of the height distribution and (iv) extreme.

(1) Root Mean Square Deviation of the Surface S_q

This is a dispersion parameter defined as the root mean square value of the surface departures within the sampling area.

$$S_q = \sqrt{\frac{1}{MN}\sum_{j=1}^{N}\sum_{i=1}^{M}\eta^2(x_i, y_j)} \tag{1}$$

Where M is the number of points per profile and N is the number of profiles.

S_q is a very general and widely used parameter. In statistics, it is the sample standard deviation.

Application

The S_q parameter represents an overall measure of the texture comprising the surface. S_q is insensitive in differentiating peaks, valleys and the spacing of the various texture features. The figure below demonstrates two very different surfaces with identical S_a and S_q values, indicating the insensitivity of these parameters. Nonetheless, once a surface type has been established, they may be used to indicate significant deviations in the texture characteristics.

Plateau-like surface -Sa = 16.03nm   Sq= 25.4nm   *Surface with Peaks -Sa = 16.03nm   Sq= 25.4nm*
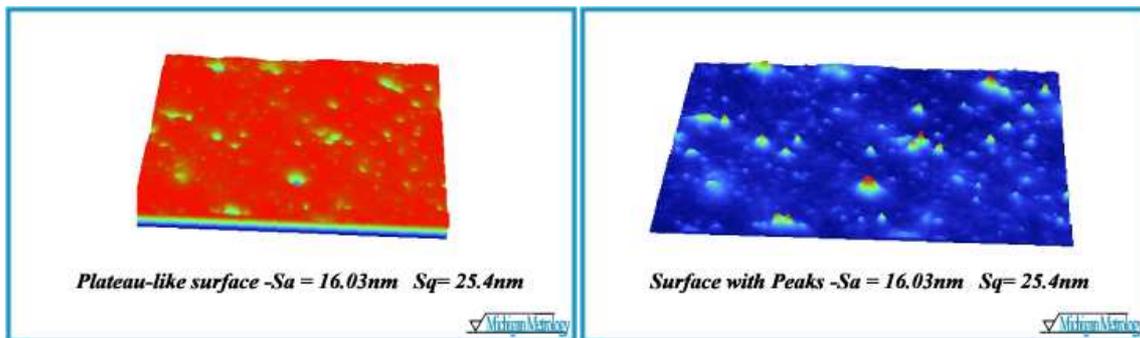
S_{sk} and S_{ku}{ XE "Ssk and Sku" } are the Skewness and Kurtosis of the 3D surface texture respectively. Figuratively, a histogram of the heights of all measured points is established and the symmetry and deviation from an ideal Normal (i.e. bell curve) distribution is represented by S_{sk} and S_{ku}. Mathematically, the S_{sk} and S_{ku} are evaluated as follows:

(2) Skewness of Topography Height Distribution S_{sk}

This is the measure of asymmetry of surface deviations about the mean plane.

$$S_{sk} = \frac{1}{MNS_q^3} \sum_{j=1}^{N} \sum_{i=1}^{M} \eta^3(x_{i,} y_j) \qquad (2)$$

This parameter can effectively be used to describe the shape of the topography height distribution. For a Gaussian surface that has a symmetrical shape for the surface height distribution, the skewness is zero. For an asymmetric distribution of surface heights, the skewness may be negative if the distribution has a longer tail at the lower side of the mean plane or positive if the distribution has a longer tail at the upper side of the mean plane. This parameter can give some indication of the existence of "spiky" features.

(3) Kurtosis of Topography Height Distribution S_{ku}

This is a measure of the peakedness or sharpness of the surface height distribution.

$$S_{ku} = \frac{1}{MNS_q^4} \sum_{j=1}^{N} \sum_{i=1}^{M} \eta^4(x_{i,} y_j) \qquad (3)$$

This parameter characterises the spread of the height distribution. A Gaussian surface has a kurtosis value of 3. A centrally distributed surface has a kurtosis value larger than 3 whereas the kurtosis of a well spread distribution is smaller than 3. By a combination of the skewness and the kurtosis, it may be possible to identify surfaces that have a relatively flat top and deep valleys.
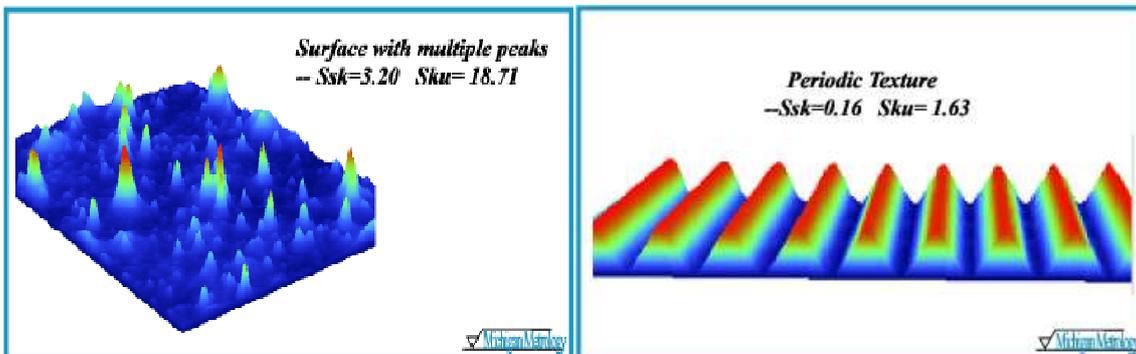
Application

S_{sk} represents the degree of symmetry of the surface heights about the mean plane. The sign of S_{sk} indicates the preponderance of peaks (i.e. $S_{sk}>0$) or valley structures ($S_{sk}<0$) comprising the surface. S_{ku} indicates the presence of inordinately high peaks/ deep valleys ($S_{ku}>3$) or lack thereof ($S_{ku}<3$) making up the texture. If the surface heights are normally distributed (i.e. bell curve) then S_{sk} is 0 and S_{ku} is 3. Surfaces described as gradually varying, free of extreme peaks or valley features, will tend to have $S_{ku} <3$. S_{sk} is useful in specifying honed surfaces and monitoring for different types of wear conditions. S_{ku} is useful for indicating the presence of either peak or valley defects which may occur on a surface.

(4) The Highest Peak of the Surface S$_p$

This is an extreme parameter defined as the height of the highest peak from the mean surface plane within the sampling area.

$$S_p = MAX(\eta_p) \qquad \text{with} \quad \eta_{p>0} \tag{4}$$

Where η_p are the highest surface summits on the surface, which relies on the eight nearest neighbour summits definition, i.e. a peak is defined if it is higher than its 8 nearest neighbours.

(5) The Lowest Valley of the Surface S$_v$

This is an extreme parameter defined as the height of the lowest valley from the mean surface plane within the sampling area.

$$S_v = MIN(\eta_v) \qquad \text{with} \quad \eta_{v<0} \tag{5}$$

Where η_v are the lowest surface valleys on the surface, which relies on the eight nearest neighbour summits definition.

(6) Height Deviation between the Lowest and Highest Points of the Surface S$_z$

This is an extreme parameter defined as the maximum of the absolute heights of the highest peaks and the depths of the deepest pits or valleys within the sampling area.

$$S_z = (\left| S_p \right| + \left| S_v \right|) \tag{6}$$

Where S_p and S_v are the highest surface summits and lowest surface valleys on the surface respectively, which relies on the eight nearest neighbour summits definition.

Application

S_z is useful in characterising the "envelope" that contains most of the surface heights, particularly when S_a or S_q is dominated by general texture features. The texture of sheet steel is typically specified with S_z as well as shaft surfaces when considering sealing applications. S_z may demonstrate a change sooner than S_a or S_q as a surface is modified such as when studying a wear mechanism.

A predominantly low roughness (Sa= 0.12mm) surface with deep valleys detected by Sz --- Sz = 2.36mm
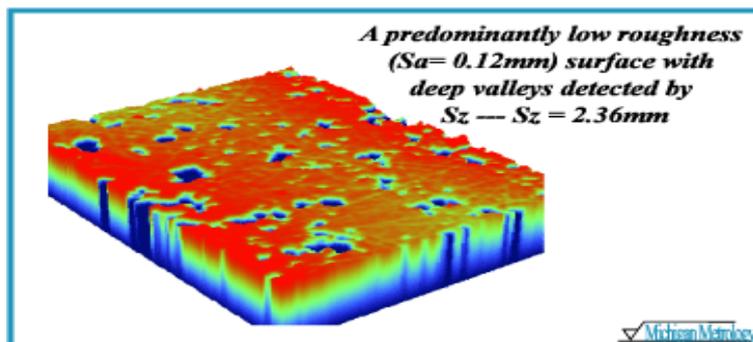
SPATIAL PARAMETERS

Introduction: Autocorrelation Function{ XE "Autocorrelation Function" } (ACF)

The development of the spatial parameters involves the use of the mathematical technique of the Autocorrelation Function (ACF). This section will review the basic concepts behind the ACF, necessary to understand the various spatial parameters.

The ACF is found by taking a duplicate surface (Z(x-□x,y-□y)) of the measured surface ((Z (x, y)) and mathematically multiplying the two surfaces together, with a relative lateral displacement (□x,□y) between the two surfaces. Once multiplied together, the resulting function is integrated and normalized to S_q, to yield a measure of the area of overlap between the two functions. If the shifted version of the surface is identical to the original surface then the ACF is 1. If the shifted surface is such that all peaks align with corresponding valleys then the ACF will approach –1. Thus the ACF**{ XE "ACF" }** is a measure of how similar the texture is at a given distance from the original location. If the ACF stays near 1 for a given amount of shift, we conclude that the texture is similar along that direction. If the ACF falls rapidly to zero along a given direction, then we conclude that the surface is different and thus "uncorrelated" with the original measurement location.
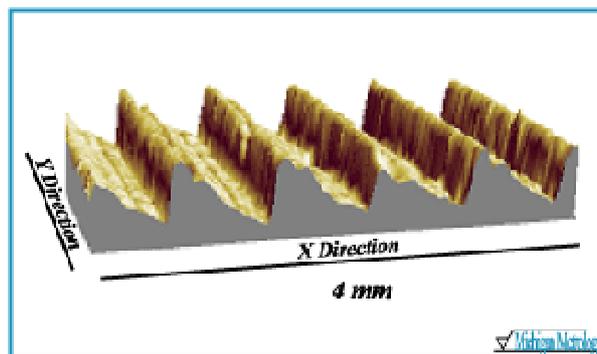
For the turned surface above, the ACF in the X direction falls to zero quickly as the peaks of the shifted surface align with the mean plane. The ACF along X becomes negative as the peaks of the surface align with the valleys of the shifted surface. Shifting along the Y direction, the surface is near identical to the original resulting in the ACF in the Y direction remaining near 1.
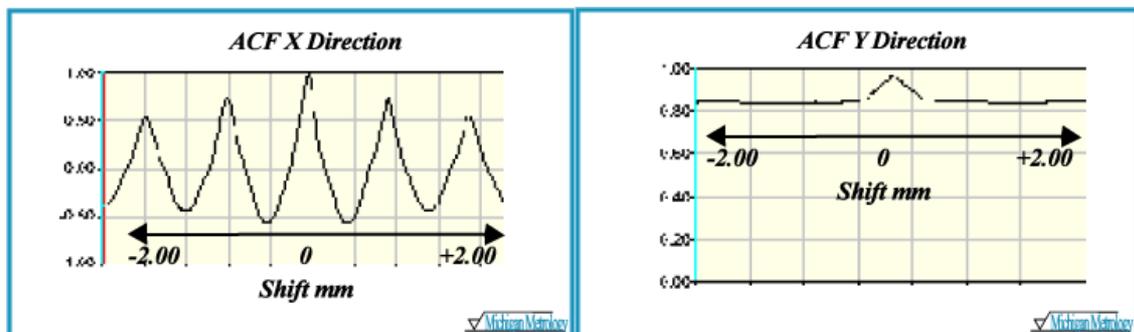
Four parameters are used to characterise spatial properties, density of summits, texture aspect ratio, fastest decay autocorrelation length and directionality of surface lay.

(7) Density of Summits of the Surface S$_{ds}$

This is the number of summits of a unit sampling area, which relies on the eight nearest neighbour summits definition.

$$S_{ds} = \frac{\text{Number of summits}}{(M-1)(N-1) \cdot \Delta x \cdot \Delta y} \tag{7}$$

Application

S$_{ds}$ is a key parameter when considering surfaces used in applications such as bearings, seals and electronic contacts. The manner in which the summits elastically and plastically deform under load is related to the S$_{ds}$ parameter. Depending on the application, a low S$_{ds}$ may result in high-localised contact stresses resulting in possible pitting and debris generation. In applications involving sliding components, a number of summits are needed to prevent optical contacting while maintaining a reasonable load distribution. Summit density may also be related to the cosmetic appearance of a surface once painted.

(8) Texture Aspect Ratio of the Surface S$_{tr}$

S$_{tr}$**{ XE "Str" }**, the texture aspect ratio, is a measure of the spatial isotropy or directionality of the surface texture. This is a parameter used to identify texture strength, i.e. uniformity of texture aspect. For a surface with a dominant lay, the parameter will tend towards 0, whereas a spatially isotropic texture will result in a S$_{tr}$ of 1. It is defined by the Areal Autocorrelation Function (AACF). S$_{tr}$ can be defined as the ratio of the fastest to slowest decay to correlation length, 0.2, of the AACF function.

Where

$$S_{tr} = \frac{\min\ (\sqrt{\tau_x^2 + \tau_y^2}\ )}{\max\ (\sqrt{\tau_x^2 + \tau_y^2}\ )} \Bigg|_{\tilde{R}(\tau_x,\tau_y)\leq 0.2} \qquad 0 \prec S_{tr} \leq 1 \tag{8}$$

$$R(\tau_x,\tau_y) = \frac{1}{(M-1)(N-1)} \sum\sum \eta(x_k, y_l)\eta(x_{k+i}, y_{l+j})$$

$$i = 0, 1, ..., m \prec M, \quad j = 0, 1, ..., n \prec N, \quad \tau_i = i \cdot \Delta x, \quad \tau_j = j \cdot \Delta y$$

In principle, the texture aspect ratio has a value between 0 and 1. Larger values, say S$_{tr}$>0.5, of the ratio indicates uniform texture in all directions, i.e. no defined lay. Smaller values, say S$_{tr}$<0.3, indicates an increasingly strong directional structure or lay. Since the size of the sampling area is finite, it is possible that the slowest decay of the AACFs of some anisotropic surfaces never reaches 0.2 within the sampling area. In this case the longest distance of the AACF along the slowest decay direction can be used instead.

Application

S$_{tr}$ is useful in determining the presence of lay in any direction. For applications where a surface is produced by multiple processes, S$_{tr}$ may be used to detect the presence of underlying surface

modifications. S_{tr} may find application in finding subtle directionality on an otherwise isotropic texture.

(9) The Fastest Decay Autocorrelation Length S_{al}

S_{al}{ XE "Sal" }, the auto-correlation length, is a measure of the distance over the surface in an optimum direction such that the new location will have minimal correlation with the original location. This is a parameter in length dimension used to describe the autocorrelation character of the AACF. It is defined as the horizontal distance of the AACF that has the fastest decay to 0.2. In other words S_{al} is the shortest autocorrelation length that the AACF decays to 0.2 in any possible direction.

$$S_{al} = \min(\sqrt{\tau_x^2 + \tau_y^2}) \quad \tilde{R}(\tau_x, \tau_y) \le 0.2 \tag{9}$$

For an anisotropic surface S_{al} is in a direction perpendicular to the surface lay. A large value of S_{al} denotes that the surface is dominated by low frequency (or long wavelength) components, whilst a small value of S_{al} denotes the opposite situation.

Application

S_{al} is a quantitative measure as to the distance along the surface by which one would find a texture that is statistically different from the original location. S_{al} is useful in establishing the distance between multiple measurements made on the surface to adequately determine the general texture specification of the surface.

Highly Directional Surface with Str of 0.11 and Sal of 37mm

Highly istropic surface with Str of 0.88 with a Sal of 21mm
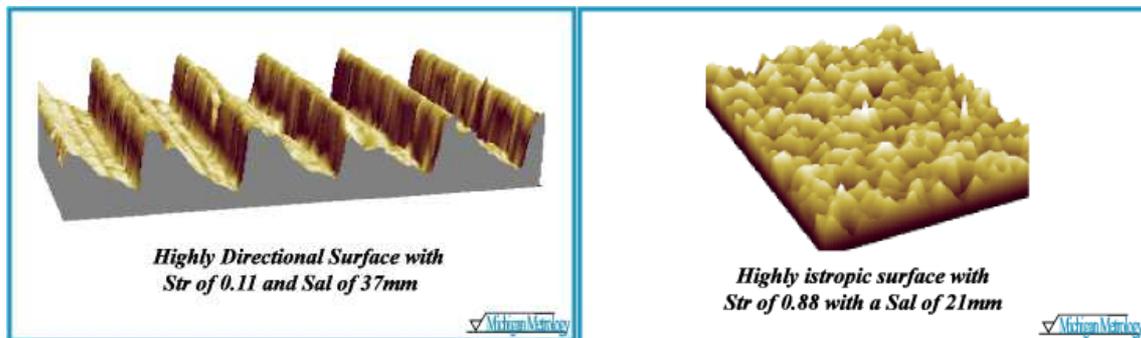
Introduction: Angular Power Spectral Density Function (APSDF)

The development of the spatial parameters involves the use of the advanced mathematical technique of the Angular Power Spectral Density Function{ XE "Angular Power Spectral Density Function" } (APSDF{ XE "APSDF" }). This section will review the basic concepts behind the APSDF necessary to understand the S_{td} spatial parameter.

Based on Fourier analysis, we can consider the surface texture to be composed of a series of sine waves in all directions with different frequencies and amplitudes. The power spectrum is a measure of the amplitude of each sine wave for a particular frequency, along a given direction. Thus for a 3D surface, the power spectrum would be displayed as a "3D" function in which the X and Y axes represent the various spatial frequencies for a given direction. The amplitude of the power spectrum (displayed on the Z axis) represents the amplitude of the sine wave at a particular spatial frequency direction. The angular power spectrum is found by integrating the

amplitudes of each component sine wave as a function of angle. The table below demonstrates a crosshatched surface, the power spectral density of the surface and the angular power spectral density function.

Crosshatched Surface

The bright regions of the power spectrum for the crosshatched surface correspond to higher amplitude sine waves at a given combination of spatial frequencies along the X / Y directions. The two dominant bright lines are thus along a direction perpendicular to the two lay patterns of the crosshatched surface.

The APSDF is found by integrating the power spectrum from the centre out radially and displaying the relative magnitude vs. angle. The two peaks in the APSDF correspond to the large sine wave amplitudes found along directions perpendicular to the two lay patterns of the crosshatched surface.

Power Spectrum

Angular Power Spectrum Density Function (APSDF)
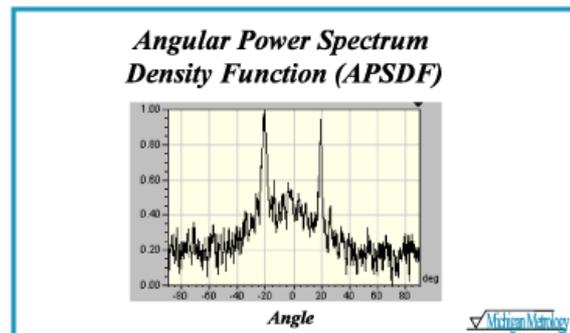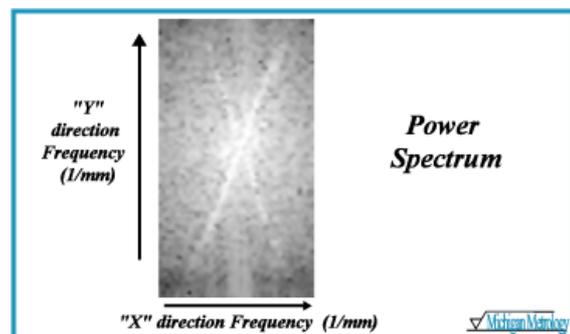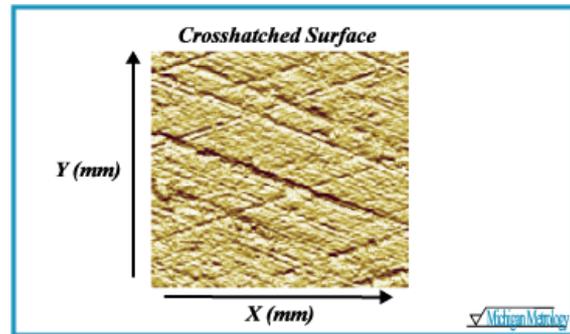
(10) The Texture Direction S_{td}

S_{td}{ XE "Std" }, the texture direction, is determined by the APSDF and is a measure of the angular direction of the dominant lay comprising a surface. S_{td} is defined relative to the Y axis. Thus a surface with a lay along the Y axis will return a S_{td} of 0 deg.

Std = -17.0 deg

Std = N/A deg

This surface is spatially isotropic there is no lay, thus Std is indeterminate
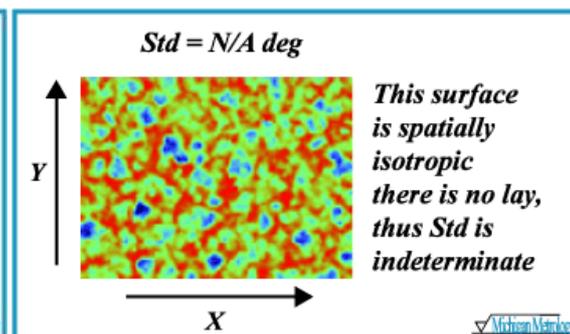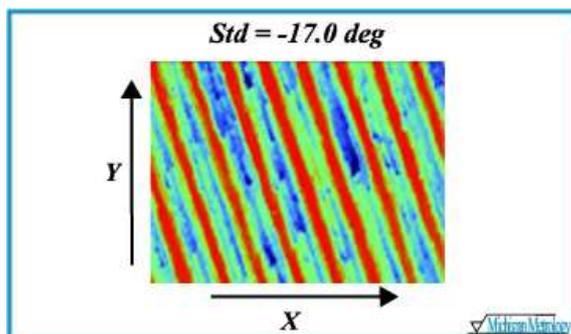
Application

S_{td} is useful in determining the lay direction of a surface relative to a datum by positioning the part in the instrument in a known orientation. In some applications such as sealing, a subtle change in the surface texture direction may lead to adverse conditions. S_{td} may also be used to detect the presence of a preliminary surface modification process (e.g. turning), which is to be removed by a subsequent operation (e.g. grinding).

HYBRID PARAMETERS

The hybrid properties of a surface are a combination of both amplitude and spacing. Any changes that occur in either amplitude or spacing may have an effect on the hybrid property. Three hybrid parameters are calculated here.

(11) Root-Mean-Square Slope of the Surface $S_{\Delta q}$

This is the root-mean-square value of the surface slope within the sampling area.

$$S_{dq} = \sqrt{\frac{1}{(M-1)(N-1)}\sum_{j=2}^{N}\sum_{i=2}^{M}\rho_{i,j}^2} \tag{11}$$

Where

$$\rho_{i,j} = \left[\left(\frac{\partial\eta(x,y)}{\partial x}\right)^2 + \left(\frac{\partial\eta(x,y)}{\partial y}\right)^2\right]^{1/2}\Bigg|_{x\,=\,x_i,\,y\,=\,y_j}$$

$$\approx \left[\left(\frac{\eta(x_i,y_j)-\eta(x_{i-1},y_j)}{\Delta x}\right)^2 + \left(\frac{\eta(x_i,y_j)-\eta(x_{i,}y_{j-1})}{\Delta x}\right)^2\right]^{1/2}$$

Application

$S_{\Delta q}$ is a general measurement of the slopes, which comprise the surface and may be used to differentiate surface with similar average roughness, S_a as demonstrated below. $S_{\Delta q}$ may find application for sealing applications and surface cosmetic appearance.

Sa = 17nm, Sdq=0.2 deg   *Sa = 16nm, Sdq=0.6 deg*
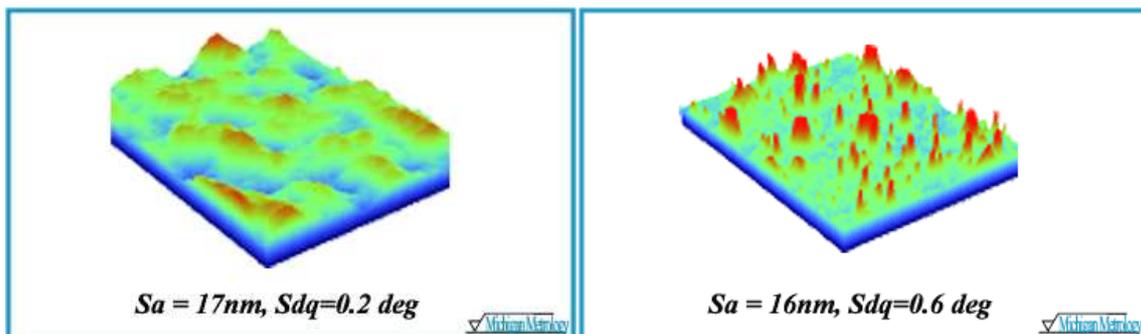
(12) Arithmetic Mean Summit Curvature of the Surface S$_{sc}$

This is defined as the average of the principal curvatures of the summits within the sampling area. Since the sum of the curvatures of a surface at a point along any two orthogonal directions is equal to the sum of the principal curvatures.

$$S_{sc} = -\frac{1}{2} \cdot \frac{1}{n} \sum_{k=1}^{n} \left(\frac{\partial \eta^2(x,y)}{\partial x} + \frac{\partial \eta^2(x,y)}{\partial y} \right) \Bigg|_{\text{for any summit}} \tag{12}$$

$$\approx -\frac{1}{2} \cdot \frac{1}{n} \sum_{k=1}^{n} \left(\frac{\eta(x_{p+1}, y_q) + \eta(x_{p-1}, y_q) - 2\eta(x_p, y_q)}{\Delta x^2} + \frac{\eta(x_p, y_{q+1}) + \eta(x_p, y_{q-1}) - 2\eta(x_p, y_q)}{\Delta y^2} \right)$$

$$\Bigg|_{\text{for any summit located by } x_p, y_q}$$

This parameter can only be calculated after the summits.

Application

S$_{sc}$ is useful in predicting the degree of elastic and plastic deformation of a surface under different loading conditions and thus may be used in predicting friction and wear characteristics of a system.

Clutch Surface for which Ssc = 37 mm-1 (i.e. mean radius of curvature is 27µm)
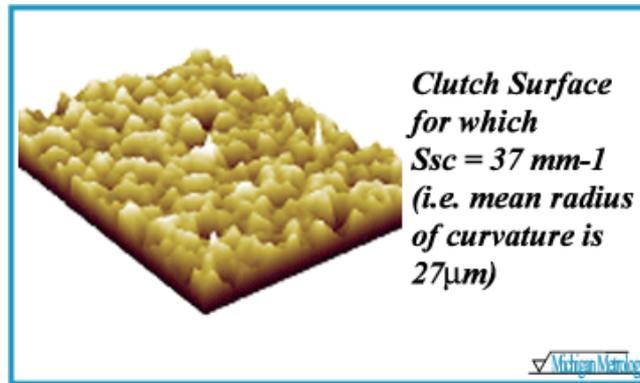
(13) Developed Interfacial Area Ratio S$_{dr}$

This is the ratio of the increment of the interfacial area of a surface over the sampling area.

$$S_{dr} = \frac{\sum_{j=1}^{N-1} \sum_{i=1}^{M-1} A_{i,j} - (M-1)(N-1)\Delta x \cdot \Delta y}{(M-1)(N-1)\Delta x \cdot \Delta y} \cdot 100\% \tag{13}$$

Where the interfacial area of the quadrilateral is defined as:

$$A_{i,j} = \frac{1}{4} \Big\{ \left[\Delta y^2 + (\eta(x_i, y_j) - \eta(x_i, y_{j+1}))^2 \right]^{1/2} + \left[\Delta y^2 + (\eta(x_{i+1}, y_{j+1}) - \eta(x_{i+1}, y_j))^2 \right]^{1/2} \cdot$$
$$\left[\Delta x^2 + (\eta(x_i, y_j) - \eta(x_{i+1}, y_j))^2 \right]^{1/2} + \left[\Delta y^2 + (\eta(x_i, y_{j+1}) - \eta(x_{i+1}, y_{j+1}))^2 \right]^{1/2} \Big) \Big\}$$

The developed interfacial area ratio reflects the hybrid property of surfaces. A large value of the parameter indicates the significance of either the amplitude or the spacing or both.

Application

S_{dr} may further differentiate surfaces of similar amplitudes and average roughness. Typically S_{dr} will increase with the spatial intricacy of the texture whether or not S_a changes. S_{dr} is useful in applications involving surface coatings and adhesion. S_{dr} and may also find relevance when considering surfaces used with lubricants and other fluids. S_{dr} may be related to the surface slopes and thus may also find application related to the manner in which light is scattered from a surface.

Sa=994nm, Sdr= 1.6%   Sa=1173nm, Sdr= 0.5%
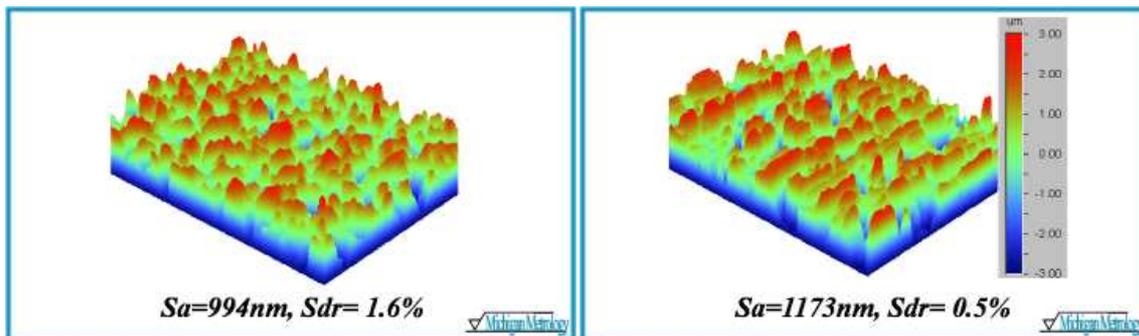
FUNCTIONAL PARAMETERS

S_k Parameters

The S_k parameters are a simple approach where the knee-shaped bearing area curve is approximated by a set of straight lines. The S_k construction is designed to divide the bearing ratio curve into three sections: the small peaks above the main plateaus, the plateaus themselves and the deep valleys between plateaus. The first step is to slide a "window" across the bearing ratio curve looking for the minimum secant slope. The window is 40% tp wide. As the window slides across the curve it intersects two points on the curve. The goal is to find the position where the slope between the two points is minimised, or since the window has constant width, where the height Htp between the two points is minimised.

Once the window with minimum secant slope is found, the S_k parameters can be calculated out from the intercept of this slowest decay line and the bearing curve and its X and Y axes.

(14) Reduced Peak Height S_{pk}

S_{pk} is an estimate of the small peaks above the main plateau of the surface. These peaks will typically be worn off (or down) during the run-in period for a part. Generally, it would be desirable to have a fairly small S_{pk}.

(15) Core Roughness Depth S_k

The parameter S_k is the vertical height between the left and right intercepts of the line through the ends of the minimum Htp 40% window.

S_k correlates with the depth of the working part of the surface, the flat part of the bearing area curve. After the initial running in period (i.e. after the peaks represented by S_{pk} are worn down), this part of the surface carries the load and most closely contacts the mating surface. Sometimes this part of the surface is called the "core roughness" or the "kernel" (hence the k subscript).

(16) Reduced Valley Height S_{vk}

S_{vk} is an estimate of the depth of valleys that will retain lubricant in a functioning part.

(17) Peak Material Component S_{mr1}

S_{mr1} is the fraction of the surface that consists of small peaks above the main plateau.

(18) Peak Material Component S_{mr2}

S_{mr2} is the fraction of the surface that will carry load during the practical lifetime of the part. Alternatively, 100%- S_{mr2} is the fraction of the surface that consists of deeper valleys that will retain lubricant.

(19) Material Filled Surface Peak Area S_{a1}

S_{a1} denotes the "area" of the peak portion of the bearing ratio curve. It is related to S_{pk} and S_{mr1}.

(20) Lubricant Filled Surface Valley Area S_{a2}

S_{a2} denotes the "area" of the valleys in the S_k construction. It is related to S_{vk} and S_{mr2}. S_{a2} is the oil retention "volume" of the surface.

Functional Volume Family

Four improved functional parameters derived from the volume information of a bearing ratio curve are proposed. This parameter set is the so-called volume family, which is based on an assumption that the peak material embraces 0~10% of the bearing area whilst the core and valley ranges cover 10~80% and 80~100% of the bearing area respectively. The volume family addresses the disadvantages of the index family and develops the R_k family advantages. These functional parameters can characterise not only the common functional properties of surfaces, for instance, area and volume geometrical properties, but also interpret wear and tribological properties in a running-in procedure. The volume family has enormous practical significance and can be used to numerically evaluate the bearing area ratio of surfaces.

(21) Peak Materiel Volume of the Surface V_{mp}

Firstly, the peak material volume is defined as the material portion enclosed in the 10% bearing area and normalised to unity.

$$V_{mp} = \frac{V_m(h_{0.10})}{(M-1)(N-1)\Delta x \Delta y} \tag{17}$$

Where

$$V_m(h_{0.10}) = \frac{\Delta x \cdot \Delta y}{9} \left\{ 16 \sum_{j=1}^{\frac{N}{2}-1} \sum_{i=1}^{\frac{M}{2}-1} \eta(x_{2i}, y_{2j}) + 8 \left[\sum_{j=1}^{\frac{N}{2}-1} \sum_{i=2}^{\frac{M}{2}-1} \eta(x_{2i-1}, y_{2j}) + \sum_{j=2}^{\frac{N}{2}-1} \sum_{i=1}^{\frac{M}{2}-1} \eta(x_{2i}, y_{2j-1}) \right] \right.$$

$$+ 4 \left[\sum_{j=2}^{\frac{N}{2}-1} \sum_{i=2}^{\frac{M}{2}-1} \eta(x_{2i-1}, y_{2j-1}) + \sum_{i=1}^{\frac{M}{2}-1} [\ \eta(x_{2i}, y_1) + \eta(x_{2i}, y_{n-1})\ ] + \sum_{j=1}^{\frac{N}{2}-1} [\ \eta(x_1, y_{2j}) + \eta(x_{m-1}, y_{2j})\ ] \right]$$

$$+ 2 \left[\sum_{i=2}^{\frac{M}{2}-1} [\ \eta(x_{2i-1}, y_1) + \eta(x_{2i-1}, y_{n-1})\ ] + \sum_{j=2}^{\frac{N}{2}-1} [\ \eta(x_1, y_{2j-1}) + \eta(x_{m-1}, y_{2j-1})\ ] \right]$$

$$\left. + [\eta(x_1, y_1) + \eta(x_1, y_{n-1}) + \eta(x_{m-1}, y_1) + \eta(x_{m-1}, y_{n-1})] \right\} \quad , \qquad \eta(x,y) \geq h_{0.10}$$

The peak material volume is not only a geometrical descriptor of the surface, but also has significant functional implications. The peak material volume may reflect wear and the running-in properties. A plateaued surface, such as an automotive bearing surface which needs a good load bearing capability and good lubrication retention, will have a high peak material volume; whereas a spiked surface, such as a bored surface, will have a low peak material volume.

(22) Core Material Volume of the Surface V_{mc}

The core material volume is the material portion enclosed from 10% to 80% of surface bearing area and normalised to the unit sampling area.

$$V_{mc} = \frac{V_m(h_{0.8}) - V_m(h_{0.10})}{(M-1)(N-1) \cdot \Delta x \Delta y} \qquad (18)$$

(23) Core Void Volume of the Surface V_{vc}

The core void volume is the void portion enclosed from 10% to 80% of surface bearing area and normalised to the unit sampling area.

$$V_{vc} = \frac{V_v(h_{0.10}) - V_v(h_{0.8})}{(M-1)(N-1) \cdot \Delta x \Delta y} \qquad (19)$$

Where

$$V_v(h) = V_v(h_{max}) - (M-1)(N-1)\Delta x\ \Delta y(h_{max} - h) + V_m(h) \qquad (20)$$

(24) Valley Void Volume of the Surface V_{vv}

The valley void volume of the unit sampling area is defined as a void volume at the valley zone from 80% to 100% of surface bearing area.

$$V_{vv} = \frac{V_v(h_{0.8})}{(M-1)(N-1) \cdot \Delta x \Delta y}$$ (21)

The void volume is proposed here to provide a direct inspection of lubrication and fluid retention of surfaces. It represents the fluid retention ability of a highly worn surface. For the same reason a plateaued surface will give a high valley volume whereas a spiked surface will give a large core volume.

OTHER PARAMETERS

The S_a parameter for characterising the amplitude property of surfaces is given here due to the wide use of its equivalent parameter in 2D and the fact it has been adopted by some instrument manufacturers.

(25) Arithmetical Average of the Surface S_a

This is the average value of the absolute heights over the entire surface. It may be obtained by adding individual height values without regard to sign and dividing the sum by the number of the data matrix.

$$S_a = \frac{1}{MN} \sum_{j=1}^{N} \sum_{i=1}^{M} \left| \eta(x_i, y_j) \right|$$ (22)

Where M is the number of points per profile and N is the number of profiles. S_a is a very general and widely used parameter.